Present Status of Transistor Development

By J. A. MORTON

The invention of the transistor provided a simple, apparently rugged device that could amplify—an ability in which the vacuum tube had long held a monopoly. As with most new electron devices, however, a number of extremely practical limitations had to be overcome before the transistor could be regarded as a practical circuit element. In particular: the reproducibility of units was poor—units intended to be alike were not interchangeable in circuits; the reliability was poor—in an uncomfortably large fraction of units made, the characteristics changed suddenly and inexplicably; and the "designability" was poor—it was difficult to make devices to the wide range of desirable characteristics needed in modern communications functions. This paper describes the progress that has been made in reducing these limitations and extending the range of performance and usefulness of transistors in communications systems. The conclusion is drawn that for some system functions, particularly those requiring extreme miniaturization in space and power as well as reliability with respect to life and ruggedness, transistors promise important advantages.

INTRODUCTION

When the transistor was announced not quite four years ago, it was felt that a new departure in communication techniques had come into view. Here was a mechanically simple device which could perform many of the amplification functions over which the electron tube had long held a near monopoly. The device was small, required no heater power, and was potentially very rugged; moreover, it consisted of materials which might be expected to last indefinitely long, and it did not appear to be too complicated to make.

However, as might be expected for a newly invented electron device, the practical realization of these promises still required the overcoming

411

of a number of obstacles. While the operation of the first devices was well understood in a general way, several items were limiting and puzzling, for example:

a—Units intended to be alike varied considerably from each other—*the reproducibility was bad.*

b—In an uncomfortably large fraction of the exploratory devices, the properties changed suddenly and inexplicably with time and temperature, whereas other units exhibited extremely stable characteristics with regard to time—*the reliability was poor.*

c—It was difficult to use the theory and then existing undeveloped technology to develop and design devices to a varied range of electrical characteristics needed for different circuit functions. Performance characteristics were limited with respect to gain, noise figure, frequency range and power—*the designability was poor.*

Before the transistor could be regarded as a practical circuit element, it was necessary to find out the causes of these limitations, to understand the theory and develop the technology further in order to produce and control more desirable characteristics.

Over the past two years measurable progress has been made in reducing, *but not eliminating*, the three listed limitations.

These advances have been obtained through an improved understanding, improved processes and very importantly through improved germanium materials. As a result:

a—the beginnings of method have evolved in the use of the theory to explain and predict the electrical network characteristics of transistors in terms of physical structure and material properties.

b—It is now possible to evaluate some of the effects and physical meaning of empirically derived processes and thereby to devise better methods subject to control. Previously, inhomogeneities in the material properties masked the dependence of the transistor electrical properties even on bulk properties (such as resistivity) as well as on processing effects.

c—As a result, on an exploratory development level, it is now possible to make transistors in the laboratory to several sets of prescribed characteristics with usable tolerances and satisfactory yields.

d—Such transistors are greatly improved over the old ones in so far as life and ruggedness are concerned, and some reduction in temperature dependence has been achieved. However, it is not to be inferred that all reliability problems are solved.

e—It has become possible in the laboratory to explore experimentally some of the consequences of the theory with the result that point con-

tact devices with new ranges of performance are indicated. Even more importantly, new *p-n* junction devices have been built in the laboratory and these junction devices have indicated an extension in several performance characteristics.

f—By having interchangeable and reliable devices with a wider range of characteristics, it has become possible to carry on exploratory circuit and system applications on a more realistic basis. Such applications effort is, in turn, stimulating the development of new devices towards new characteristics needed by these circuit and system studies.

It is the purpose of the remainder of this paper to give an over all but brief summary of recent progress made at Bell Telephone Laboratories in reducing the above-mentioned limitations on reproducibility, reliability and performance. Since a fair number of types of devices are currently under development, each with different characteristics to be optimized, the data will be presented as a sort of montage of characteristics of several different types of devices. It is not to be inferred that any one type of transistor combines all of the virtues any more than such a situation exists in the electron tube art. Moreover, it will be impossible in a paper of practical length to present complete detailed characteristics on all or even several of these devices under development; nor would it be appropriate since most of these data are on devices currently under development. Rather, what is desired, is a summary of progress across the board to give the reader an integrated and up-to-date picture of the current state of transistor electronics.

REPRODUCIBILITY STATUS

Description of Transistors

Before quantitative data comparing the characteristics of past with present transistors are presented, it will be useful to briefly review physical descriptions of the various types of transistors to be discussed. Fig. 1 shows a cutaway view of the now familiar point-contact cartridge type transistor. All of the early transistors were of this general construction and the characteristics of a particular one, called the Type A[1], will be used as a reference against which to measure results now obtainable with new types under current development. Fig. 2 is a semi-schematic picture of the physical operation of such a device. Pressing down upon the surface of a small die of *n*-type germanium are two rectifying metal electrodes, one labelled E for emitter, the other C for collector. A third electrode, the base, is a large area ohmic contact to the underside of the die of germanium. The emitter and collector electrodes obtain their
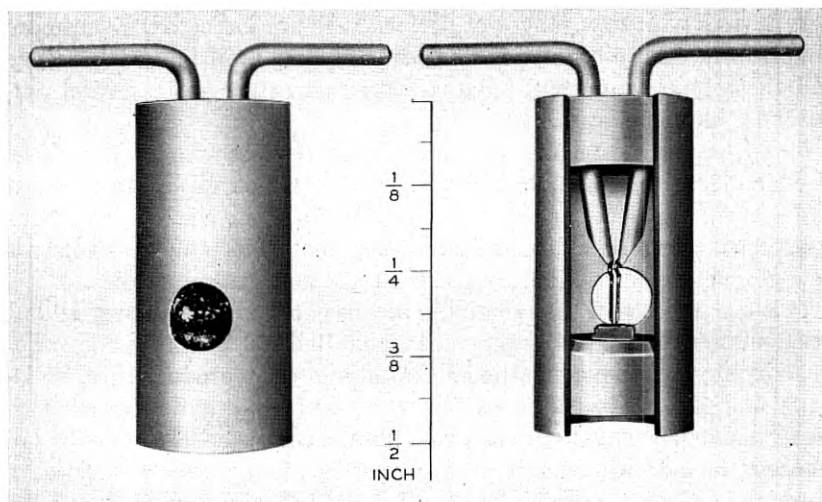
Fig. 1—The type A transistor structure.

rectifying properties as a result of the *p-n* barrier (indicated by the dotted lines) existing at the interface between the *n*-type bulk material and small *p*-type inserts under each point. When the collector is biased with a moderately large negative voltage (in the reverse direction) so that the collector barrier has relatively high impedance, a small amount of reverse current flows from the collector to the base in the form of electrons as indicated by the small black circles. Now, if the emitter is biased a few tenths of a volt positively in the forward direction, a current of holes (indicated by the small open circles) is injected from the
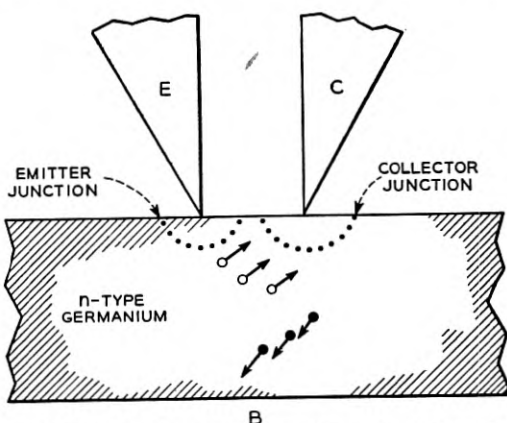

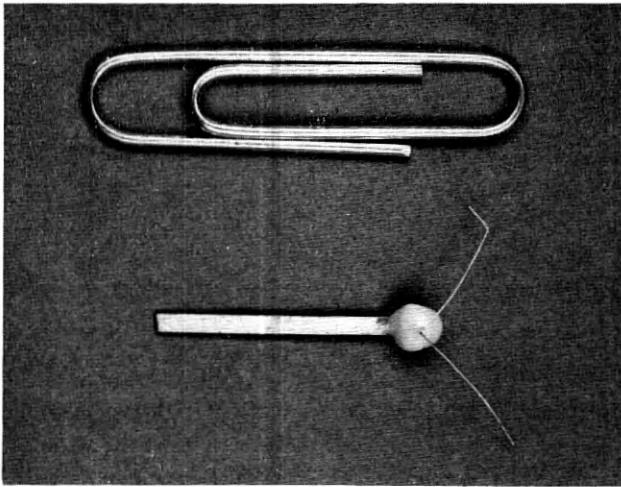Fig. 2—Schematic diagram of a point-contact transistor.

Fig. 3—The M1689 point-contact transistor is typical of those used in minia-ture packaged circuit functions.

emitter region into the n-type material. These holes are swept along to the collector under the influence of the field initially set up by the original collector electron current—thus adding a controlled increment of collector current. Because of their positive charge these holes can lower the potential barrier to electron flow from collector to base and thus allow several electrons to flow in the collector circuit for every hole entering the collector barrier region. This ratio of collector current change to emitter current change for fixed collector voltage is called alpha, the current gain. In point-contact transistors alpha may be larger than unity. Since the collector current flows through a high impedance when the emitter current is injected through a low impedance, voltage amplification is obtained as well.

Some of the new transistors are point-contact transistors similar in physical appearance to the type A. However, their electrical character-istics will be shown to be significantly improved not over the old type A only insofar as reproducibility and reliability are concerned, but also as to range of performance.

For use in miniature packaged circuit functions, the point contact transistor has been miniaturized to contain only its bare essentials. Fig. 3 is a photograph of a so-called "bead" transistor (compared to a paper clip for size) and several of the current development types are being made in this form.

In Fig. 4 is shown the family of static characteristics representative of the M1689 bead type transistor. Note in particular the collector
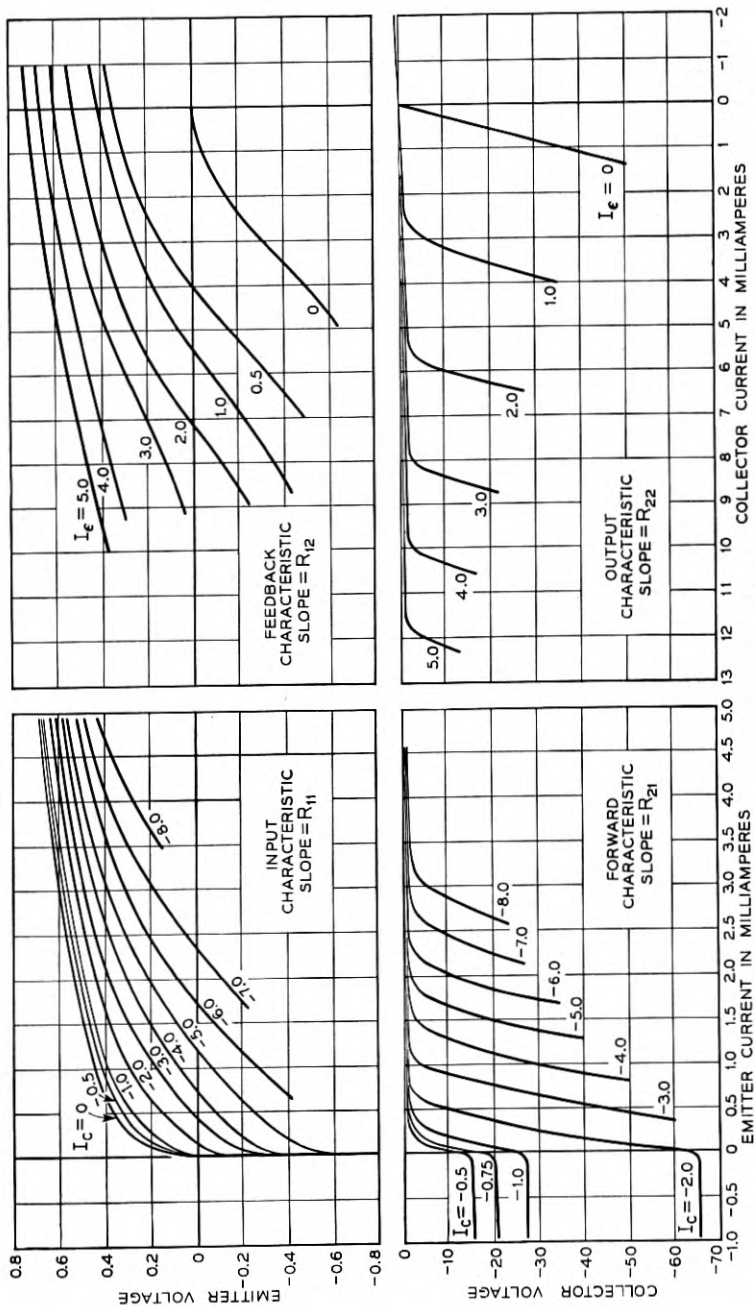
Fig. 4—Static characteristics of the M1689 transistor.

family which gives the dependence of collector voltage upon collector current with emitter current as parameter. These characteristics may be thought of as the dual to the plate family of a triode.[2] The slope of these curves is very nearly the small-signal ac collector impedance of the transistor.* For a fixed collector voltage of -20 volts, when the emitter current is changed from zero to one milliampere, note that the collector current correspondingly changes slightly more than two milliamperes, indicating a current gain, alpha, of slightly more than two.

Newest member of the transistor family recently described by Shockley, Sparks, Teal, Wallace and Pietenpol is the n-p-n junction transistor.[3, 4] Fig. 5 is a schematic diagram of such a structure. In the center of a bar of single crystal n-type germanium there is formed a thin layer
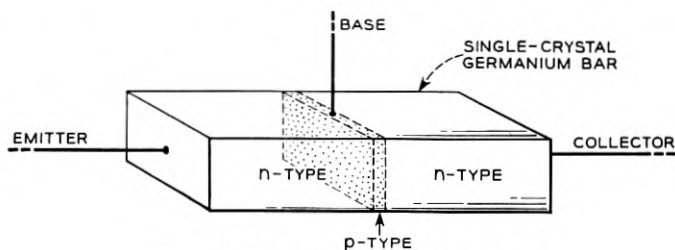

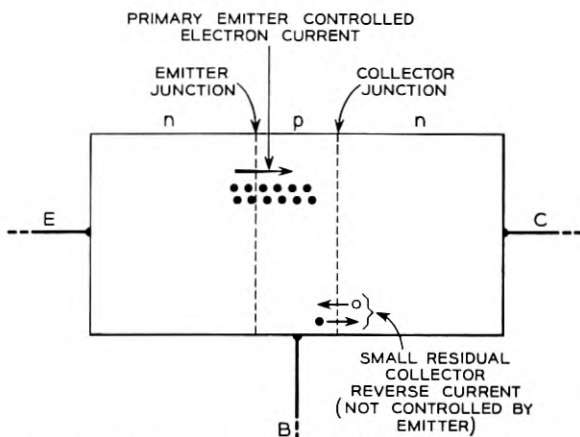Fig. 5—The n-p-n junction transistor

Fig. 6—Schematic diagram of a junction transistor.

* As shown by Ryder and Kircher,[1] the ac collector impedance, $r_c = R_{22} - R_{12}$, where R_{22} is the open-circuited output impedance and R_{12} is the open-circuit feedback impedance. Usually, $R_{22} \gg R_{12}$.

of p-type germanium as part of the same single crystal. Ohmic non-rectifying contacts are securely fastened to the three regions as shown, one being labelled emitter, one base and one collector. In many simple respects, except for change in conductivity type from p-n-p in the point-contact (see Fig. 2) to n-p-n in the junction type, the essential behavior is similar.

As shown in Fig. 6, if the collector junction is biased in the reverse direction, i.e., electrode C biased positively with respect to electrode B, only a small residual back current of holes and electrons will diffuse across the collector barrier as indicated. However, unlike the point-contact device, this reverse current will be very much smaller and relatively independent of the collector voltage because the reverse impedance of such bulk barriers is so many times higher than that of the barriers produced near the surface in point-contact transistors. Now again, if the emitter barrier is biased in the forward direction, a few tenths of a volt negative with respect to the base is adequate, then a relatively large forward current of electrons will diffuse from the electron-rich n-type emitter body across the reduced emitter barrier into the base region. If the base region is adequately thin so that the injected electrons do not recombine in the p-type base region (either in bulk or on the surface), practically all of the injected emitter current can diffuse to the collector barrier; there they are swept through the collector barrier field and collected as an increment of controlled collector current. Hence, again, since the electrons were injected through the low forward impedance and collected through the very high reverse impedance of bulk type p-n barriers, very high voltage amplification will result. No current gain is possible in such a simple bulk structure and the maximum attainable value of alpha is unity. However, because the bulk barriers are so much better rectifiers than the point surface barriers, the ratio of collector reverse impedance to emitter forward impedance is many times greater, more than enough to offset the point-contact higher alpha; thus, the junction unit may have much larger gain per stage.[1, 3, 4] Fig. 7 is a photograph of a developmental model of such a junction transistor called the M1752.

The upper part of Fig. 8 is a collector family of static characteristics for the M1752 n-p-n junction transistor. By way of comparison to those of the point contact family, note the much higher reverse impedance of the collector barrier (relatively independent of collector voltage) and the correspondingly smaller collector currents when the emitter current is zero. In fact, Fig. 9 is an expanded plot of the lower left rectangle of the collector family of Fig. 8.   The almost ideal straight-line character
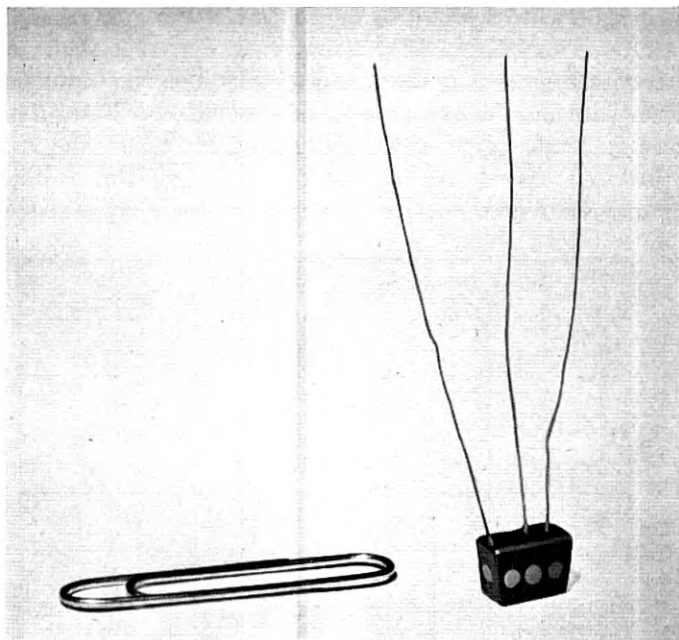
Fig. 7—The M1752 junction transistor.

and regular spacing of these curves persists down to voltages as low as 0.1 volt and currents of a few microamperes. Thus, essentially linear Class A amplification is possible for as little collector power as a few microwatts. Constant collector power dissipation curves of 10, 50 and 100 microwatts are shown dotted for reference.

Reproducibility of Linear Characteristics

In describing progress in the reproducibility of those transistor characteristics pertinent to small-signal linear applications, one possible method is to give the statistical averages and dispersions in the linear open-circuit impedances of the transistor as defined by Messrs. Ryder and Kircher.[1] Such a procedure, of course, implies a state of statistical control in the processes leading to a reasonably well behaved normal distribution for which averages and control limits can be defined. This situation can be said to be in effect for most transistors under current development.

However, for the old type A unit, control simply was not in evidence; so that in quoting figures on type A's, ranges for commensurate fractions of the total family will be given. In order that symbols and terminology

will be clear, it will be useful to review briefly the method of defining the linear characteristics of all transistors. In Fig. 10 is shown a generalized network representing the transistor in which the input terminals are emitter-base and the output terminals are collector-base. Then, over a sufficiently small region of the static characteristics, the linear relations between the incremental emitter and collector voltages and currents may be represented by the pair of linear equations shown.[1]
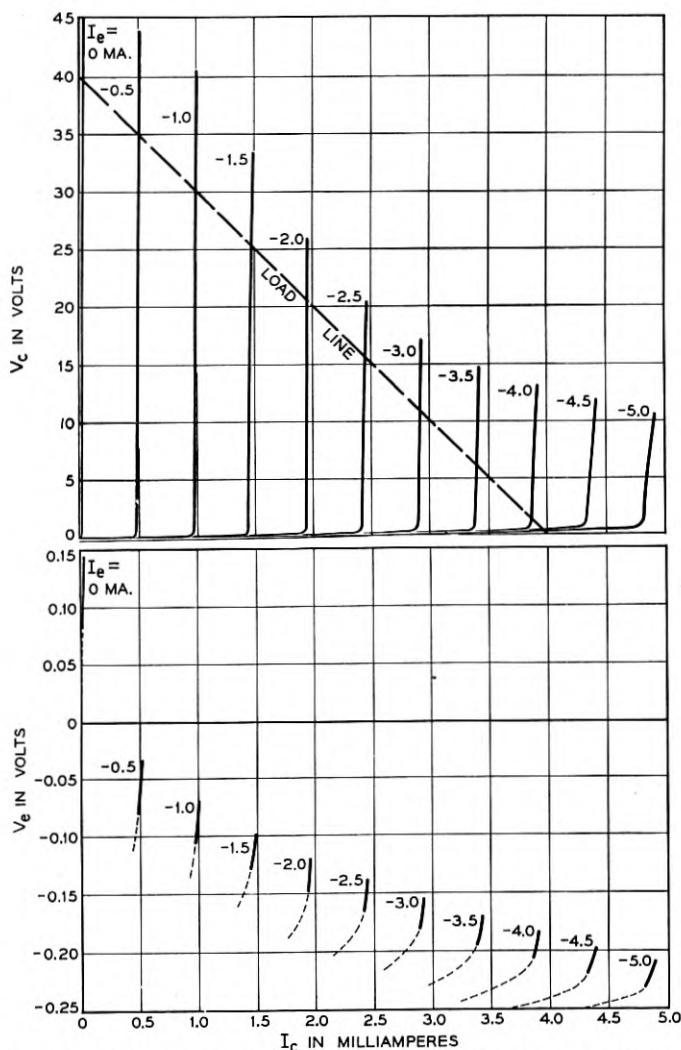

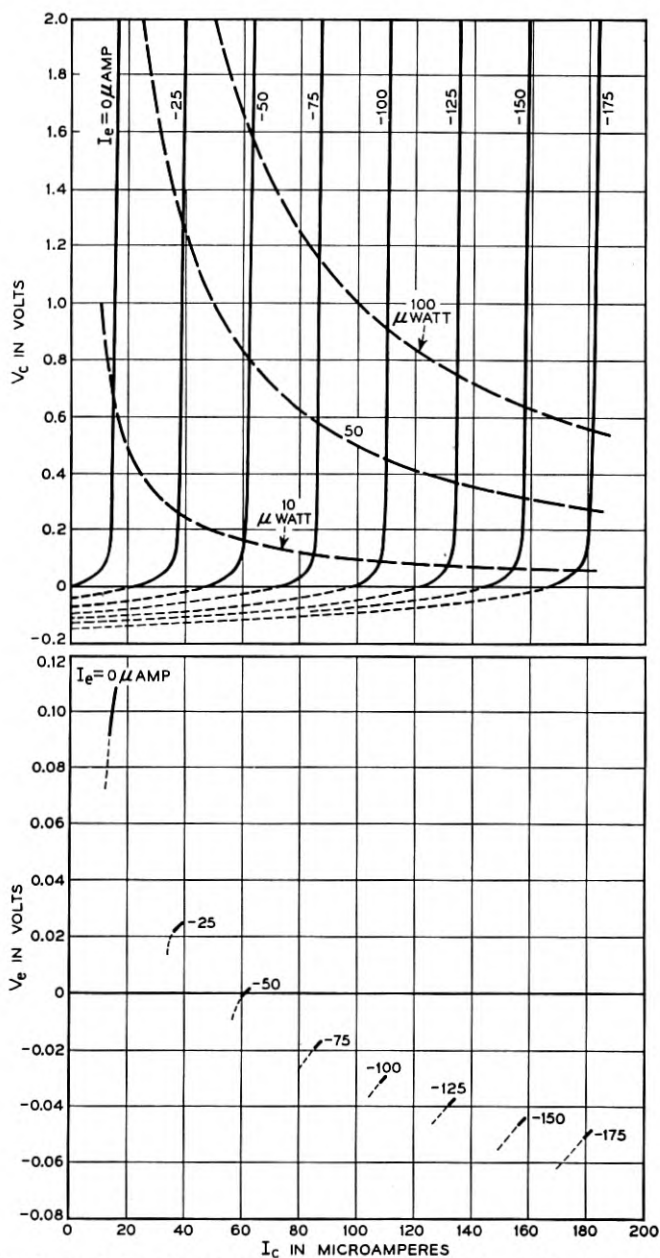Fig. 8—Static characteristics of the M1752 junction transistor.

Fig. 9—Expanded plot of the microwatt region of the static characteristics of the M1752 transistor.

The coefficients are simply the open-circuit driving point and transfer impedances of the transistor, or the slopes of the appropriate static characteristics at fixed dc operating currents. These equations may be represented by any one of a large number of equivalent circuits of which the one shown in Fig. 11 is perhaps currently most useful. In this circuit r_e is very nearly the ac forward impedance of the emitter barrier, r_c is very nearly the ac reverse impedance of the collector barrier, r_b is the feedback impedance of the bulk germanium common to both, and a is the circuit current gain representing carrier collection and multiplication if any. It turns out this is very nearly equal to the current multiplication factor a of the collector barrier mentioned before. Average values of these elements for the type A transistor are given in Fig. 11. In Fig. 12 are given the ranges of these parameters for the type A as of September, 1949, and the control limits* for the same characteristics for new point-contact transistors now under development. For September, 1949, the ranges are taken about the average values shown in Fig. 11 for the type A transistor. The control limits given for the present situation apply to a number of different types of point contact transistors so that the present average values of these

$$v_\epsilon = i_\epsilon z_{11} + i_c z_{12}$$
$$v_c = i_\epsilon z_{21} + i_c z_{22}$$
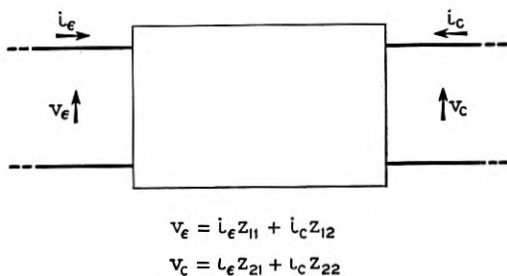
Fig. 10—The general linear transistor.

equivalent circuit elements depend upon the type of transistor considered. In Fig. 13 are given the average values of the characteristics of the M1729 point-contact video amplifier transistor which bears the closest resemblance to the older type A transistor. By way of contrast are given some typical values of the elements for the M1752 junction transistor which is not yet far enough along in its development to have design centers fixed nor reliable dispersion figures available.

As Ryder and Kircher have shown,[1] transistors in the grounded-base connection may be short-circuit unstable if $a > 1$ and r_b is too large,

---

* A.S.T.M. Manual, "Quality Control of Materials," Jan. 1951, Part III, pp. 55–114.

since r_b appears as a positive feedback element. The curve in Fig. 14 is a plot of the short-circuit stability contour when r_e and r_c have the nominal values of 700 and 20,000 ohms. Transistors having a and r_b sufficiently large to place their representative points above this contour will be short-circuit unstable, i.e., they will oscillate when short-circuited. Those having an $a - r_b$ point below the stability contour will be unconditionally stable under any termination conditions. The large unshaded rectangle bounds those values of a and r_b, which were repre-

$\overline{r_e} = 250$ OHMS $\overline{r_c} = 20,000$ OHMS
$\overline{r_b} = 250$ OHMS $\overline{a} = 2$
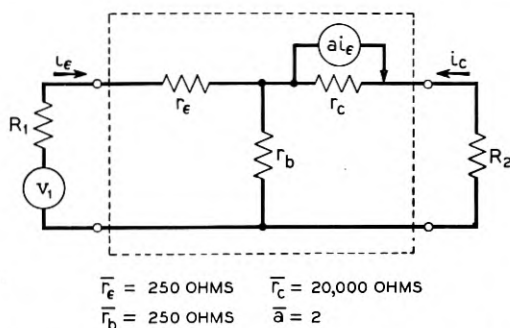
Fig. 11—Equivalent circuit and average element values of the type A transistor.

ELEMENT	RANGE SEPTEMBER 1949	RANGE JANUARY 1952
a	4 : 1	±20%
r_c	7 : 1	±30%
r_e	3 : 1	±20%
r_b	7 : 1	±25%

Fig. 12—Reproducibility of point-contact linear characteristics.

TYPE	M 1729	M 1752
r_e	120	25
r_b	75	250
r_c	15,000	5×10^6
a	2.5	0.95

Fig. 13—Average characteristics of the M1729 and typical characteristics of the M1752 transistors.

sentative of the type A transistor in September, 1949. It is apparent that the circuit user of type A units had approximately a 50 per cent chance of obtaining a short-circuit unstable unit from a large family of type A units. The smaller shaded rectangle bounds the values of a and r_b now realized in the M1729 transistor presently under development. Not only has the spread in characteristics been greatly reduced as shown, but also the design centers have been moved to a region for which all members of the M1729 family are unconditionally stable.

It is of interest to note that spreads of the order of ± 20 to ± 25 per cent are of the same magnitude as those dispersions now existing amongst the characteristics of presently available well-controlled electron tubes. These kinds of data on reproducibility of the linear equivalent circuit element values hold for practically all classes of point-contact devices
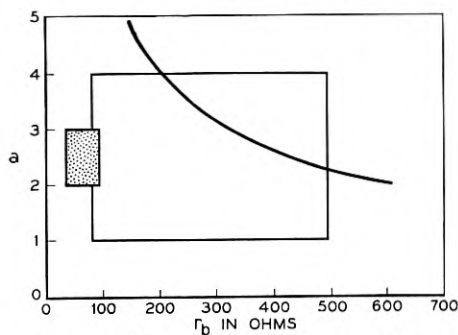
Fig. 14—Stability contour and ranges of a and r_b.

now under development for cw transmission service. While it is too early to prove that such a situation pertains as well to junction transistors, there is every reason to expect similar results after a suitable development period.

Reproducibility of Large-Signal Characteristics for Pulse Application

When electron devices are employed for large-signal applications, particularly those of switching and computing, it is well known that the characteristics must be controlled over a very broad range of variables from cutoff to saturation. In September, 1949, very little attempt was made to control such pulse use characteristics. In the intervening time, transistor circuit studies have proceeded to the point where it is possible to define certain necessary large scale transistor characteristics which, if met, permit such transistors to be used interchangeably and reproducibly in a variety of pulse circuit functions such as binary counters,

bit registers, regenerative pulse amplifiers, pulse delay amplifiers, gated amplifiers and pulse generators. Moreover, it has been possible to meet these requirements on a developmental level with good yields in at least three types of point-contact switching transistors. The scope of this paper will not permit a detailed accounting of the technical features of this situation and such an account will be forthcoming in future papers on these particular studies. However, a brief description of some of the more important pulse characteristics and their tolerances is certainly pertinent.

In practically all of the transistor pulse handling circuits examined to date, one characteristic common to all is the ability of the transistor, by virtue of its current gain, to present various types of two-state negative resistance characteristics at any one or all of its pairs of terminals. A typical simple circuit and corresponding characteristic is shown in Fig. 15 for the emitter-ground terminals when a sufficiently large value of resistance is inserted in the base to make the circuit unstable. In region I where the emitter is negative, the input resistance is essentially the reverse characteristic of the emitter as a simple diode. In region II as the emitter goes positive, alpha, the current gain rises rapidly above unity. If R_b is sufficiently large and alpha, the current gain, is greater
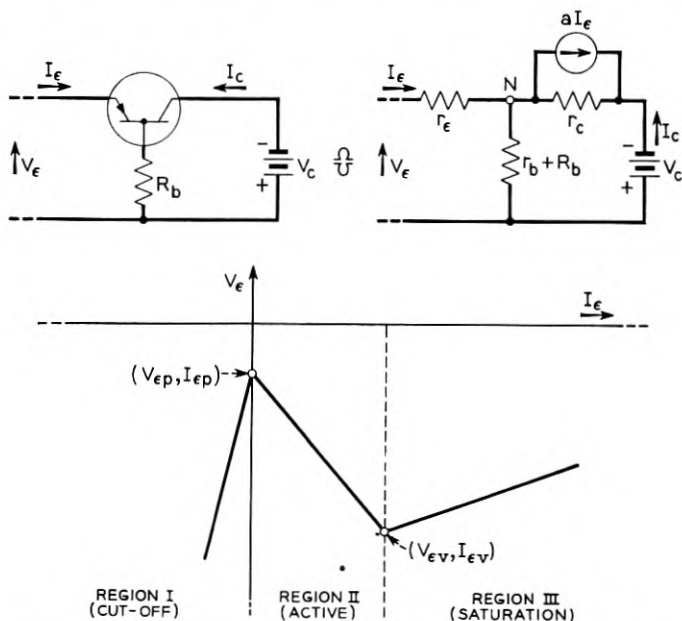

Fig. 15—Emitter-ground negative resistance circuit and characteristic.

than unity the emitter to ground voltage will begin to fall because of the larger collector current increments driving the voltage of the node N negative more rapidly than the emitter current drop through r_e would normally carry it. This transition point is called the peak point. If then $\alpha(r_b + R_b)$ is sufficiently large, in this sense, the input resistance may be negative in this region II. When the internal node voltage has fallen to a value near that of the collector terminal the "valley point" has been reached. At this point, the emitted hole current has reduced the collector impedance to a minimum value beyond which a is essentially zero; the transistor is said to be saturated. From this point on the input impedance again becomes positive and is determined almost entirely by the base and emitter impedances. By terminating the emitter-ground terminals in various ways with resistor-capacitor-bias combinations, such a network can be made to perform monostable, astable or bistable functions. Under such conditions, the emitter current and correspondingly the collector current switch back and forth between cutoff and saturation values. For example, in Fig. 16 is shown a value of emitter bias and load resistance such that there are three possible equilibrium values of emitter current and voltage. It may be shown that the two intersections in regions I and III are stable whereas that in region II is unstable. Hence, if the stable equilibrium is originally in I, a small positive pulse Δ_p applied to the emitter will be enough to switch from stable point I to stable point II and conversely, $-\Delta_v$ will carry it from the high current point to the low current point. The circuit designer is interested in reproducing in a given circuit (with different transistors of the same type) the following points of the characteristic:

a—The off impedance of the emitter—he desires that this be greater than a certain minimum.

b—The peak point V_{ep}—he desires that this be smaller than a certain maximum.

c—The value of the negative resistance—he desires that this be greater than a certain minimum.

d—The valley point V_{es}, I_{es}—he desires that these be greater than certain minima, and

e—The slope in region III—he desires that this be smaller than a certain maximum so that he may control it by external means.

It may be shown that these conditions can be satisfied for useful circuits by specifying certain maximum and minimum boundaries on the static characteristics. Fig. 17 is an idealized set of input or emitter characteristics. By specifying a minimum value for the reverse resistance

in region I, condition (a) above is satisfied. By specifying a maximum slope in region II and III, condition (e) is satisfied. Now refer to the idealized collector family in Fig. 18; by specifying a maximum value to V_{C3}, it is possible to insure condition (d) and by specifying a minimum value for r_{co}, condition (b) can be satisfied. Finally, in Fig. 19 by de-
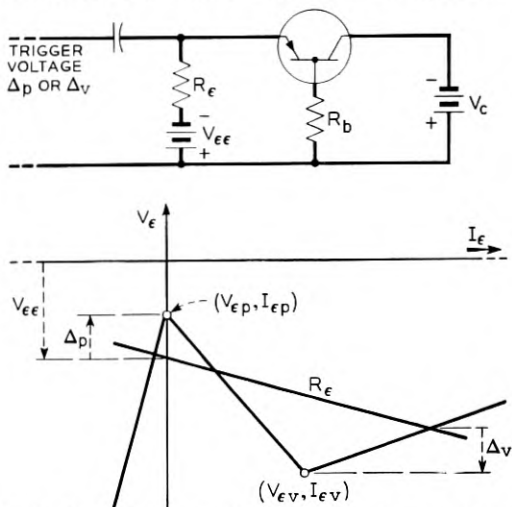
Fig. 16—Bistable circuit and characteristics showing trigger voltage requirements.
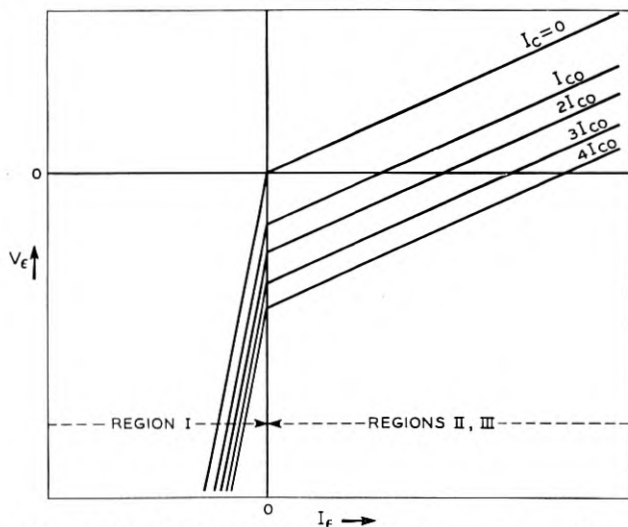
Fig. 17—Idealized emitter characteristics − slope = R_{11}.

manding that alpha, as a function of I_e, go through a transition from a negligible value (at small negative I_e) to a value well in excess of unity (at a correspondingly small positive value of I_e) and maintain its value well in excess of unity at large values of I_e, conditions (b) and (c) can be met.

In Fig. 20 are given the characteristic specifications which must be met by the M1689 bead type switching transistor now under development. With these kinds of limits, circuit users find it possible to interchange such M1689 units in various pulse circuits and obtain overall circuit behavior reproducible to the order of about ±2 db.

Fig. 18—Idealized collector characteristics.
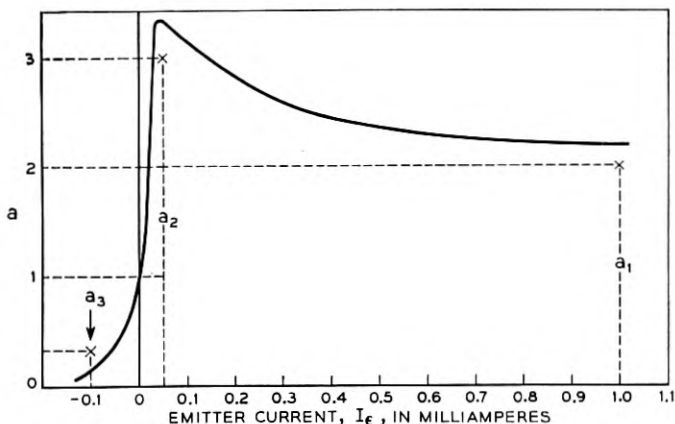
Fig. 19— Effective alpha characteristic.

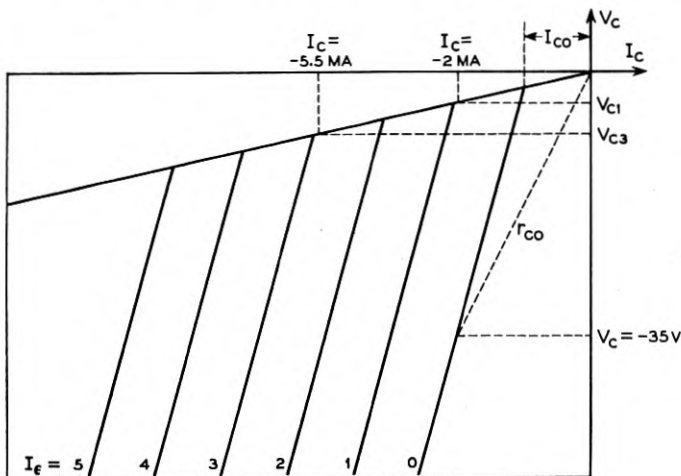| TEST	CONDITIONS	MINIMUM	MAXIMUM
r_{CO} – OFF COLLECTOR DC RESISTANCE	$V_C = -35$ V DC $I_\epsilon = 0$ MA DC	17,500 OHMS	——
V_{C1} – ON COLLECTOR VOLTAGE	$I_C = -2$ MA DC $I_\epsilon = 1$ MA DC	——	-3 V DC
V_{C3} – ON COLLECTOR VOLTAGE	$I_C = -5.5$ MA DC $I_\epsilon = 3$ MA DC	——	-4 V DC
OFF EMITTER RESISTANCE	$V_C = -10$ V DC	50,000 OHMS	——
ON EMITTER RESISTANCE R_{11}	$V_C = -10$ V DC $I_\epsilon = 1$ MA DC	——	800 OHMS
a_1	$V_C = -30$ V DC $I_\epsilon = 1.0$ MA DC	1.5	——
a_2	$V_C = -30$ V DC $I_\epsilon = +0.05$ MA DC	2.0	——
a_3	$V_C = -30$ V DC $I_\epsilon = -0.1$ MA DC	——	0.3
R_{12} – OPEN CIRCUIT FEEDBACK RESISTANCE	$V_C = -10$ V DC $I_\epsilon = +1$ MA DC	——	500 OHMS
R_{21} – OPEN CIRCUIT FORWARD RESISTANCE	$V_C = -10$ V DC $I_\epsilon = +1$ MA DC	15,000 OHMS	——
R_{22} – OPEN CIRCUIT OUTPUT RESISTANCE	$V_C = -10$ V DC $I_\epsilon = +1$ MA DC	10,000 OHMS	——

Fig. 20—Tentative characteristics for the M1689 switching transistor.

RELIABILITY FIGURE OF MERIT	SEPTEMBER 1949	JANUARY 1952
AVERAGE LIFE	$\doteq$ 10,000 HOURS	> 70,000 HOURS
EQUIVALENT TEMPERATURE COEFFICIENT OF r_C	-1% PER DEG C	$-1/4\%$ PER DEG C
SHOCK	?	> 20,000 G
VIBRATION	?	20 – 5000 CPS NEGLIGIBLE TO 100 G

Fig. 21—Reliability status.

RELIABILITY STATUS

Life

Reliability figures of merit are not too well defined for electron tubes and the same situation certainly holds at present for transistors. However, insofar as these quantities can be presently defined, Fig. 21 shows

a comparison between the present status and that in September, 1949. Estimates of the half-life of a statistical family of devices are at best arbitrary and necessarily amount to extrapolations of survival curves assuming that a known survival law will continue to hold.* In September, 1949, life tests on type A units had been in effect some 4000 hours. With the assumption of an exponential survival law, it was not possible, on the basis of a 4000 hour test, to estimate the slope sufficiently accurately to warrant a half-life estimate in excess of 10,000 hours. These same type A units have now run on life test for approximately 20,000 hours. With the more reliable estimate of survival slope now possible, the half-life is now estimated to be somewhat in excess of 70,000 hours. It should be emphasized, however, that these are type A units of more than two years ago made with inferior materials and processes. It is believed that those units under current development, being made with new materials and processes, are superior; but, of course, life tests are only a few thousand hours old. Although these new data are encouraging, it is still too early to extrapolate the data such a long way.

Temperature Effects

Transistors like other semiconductor devices are more sensitive to temperature variations than electron tubes. In terms of the linear equivalent circuit elements, the collector impedance, r_c, and the current gain, a are the most sensitive. Over the range from $-40°C$ to $80°C$ the other elements are relatively much less sensitive. For type A transistors these temperature variations in r_c and a are shown in Fig. 22. While these curves are definitely not linear, an average temperature coefficient for r_c of about -1 per cent per degree was estimated for the purpose of easy tabulation and comparison in Fig. 21.

Thus, for the early type A, r_c fell off to about 20 to 30 per cent of its room temperature value when the temperature was raised to $+80°$ C; at the same time a increased from 20 to 30 per cent over the same temperature range. Today, this variation has been reduced by a factor of about four for r_c in most point-contact types, the variations in the current gain being relatively unchanged. Fig. 23 illustrates the temperature dependence of r_c and a for the M1729 transistor now under development. Again, for purposes of easy comparison in Fig. 21, the actual dependence of Fig. 23 was approximated by a linear variation and

---

* Estimates of life, of course, depend upon definitions of "death". For these experiments, the transistors were operated as Class A amplifiers. A transistor is said to have failed when its Class A gain has fallen 3 db or more below its starting value.

only the slope given in Fig. 21. For linear applications such as the grounded base amplifier, the Class A power gain is approximately proportional to $a^2 r_c$; hence the gain of such an amplifier will stay essentially constant within a db or two over the temperature range from $-40°C$ to $+80°C$. For pulse applications, and of importance to dc biasing with point-contact transistors, is the fact that the dc collector current (for fixed emitter current and collector voltage) will change at about the
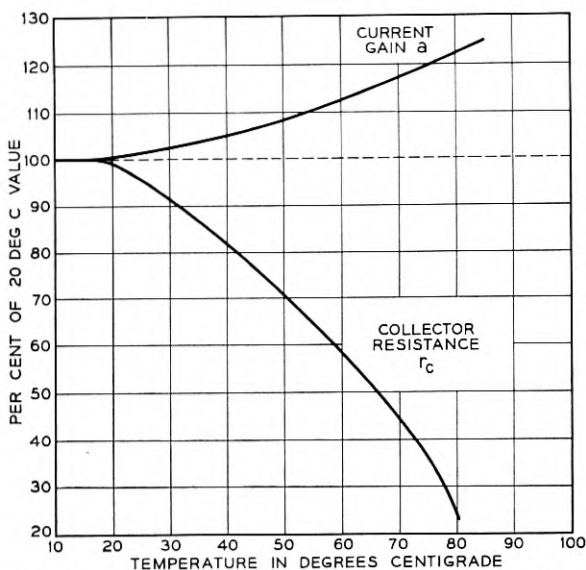

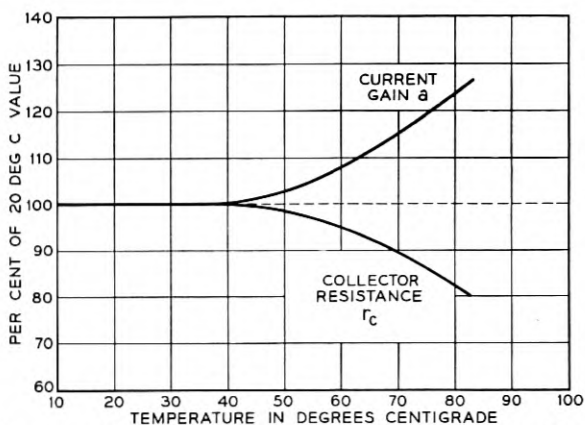Fig. 22—Collector resistance and a versus temperature for type A transistor

Fig. 23—Collector resistance and a versus temperature for type M1729 transistor.

same rate as does r_c, the small signal collector impedance. Similar improvements have been made in these variations for switching transistors and Fig. 24 is a series of graphs showing how the M1689 bead type switching transistor changes the pulse characteristics defined in Fig. 20 with respect to temperature. For those switching functions examined to date, it is believed that these data mean reliable operation to as high as $+70°C$ in most applications and perhaps as high as $+80°C$ in others.
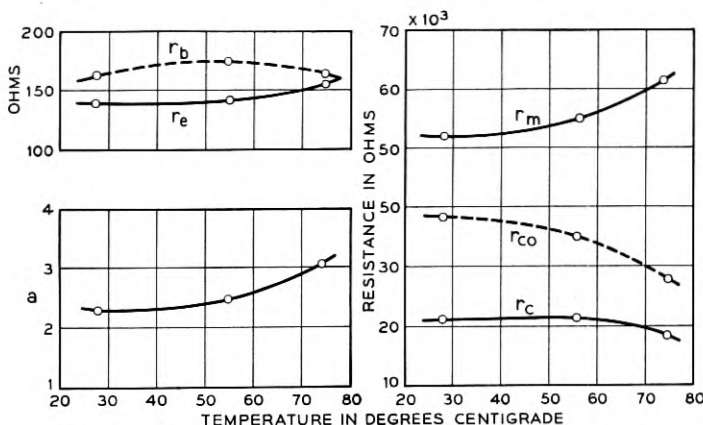
Fig. 24—Temperature behavior of the M1689 transistor.

In junction transistors the laws of temperature variation are not so well established, the device being in a much earlier stage of development. Preliminary data indicate smaller variations in the small signal parameters such as a and r_c. On the other hand, variations in the dc current, particularly I_{co}, are many times greater, of the order of 10 per cent per degree centigrade.* The only saving grace here is the fact that I_{co} is normally very much less than the actual operating value of I_c.

In summary, it may be said that while significant improvements have been made in temperature dependence to the point where many applications appear feasible, it is not to be inferred that the temperature limitation is completely overcome. Much more development work of device, circuit and system nature is required to bring this aspect of reliable operation to a completely satisfying solution.

Shock and Vibration

With regard to mechanical ruggedness, current point-contact transistors have been shock tested up to 20,000 g with no change in their

---

* I_{co} is the collector current at zero emitter current.

electrical characteristics. Vibration of point-contact and junction transistors over the frequency range from 20 to 5000 cps at accelerations of 100g produces no detectable modulation of any of the transistor electrical characteristics, i.e., such modulation, if it exists, is far below the inherent noise level. At a few spot frequencies in the audio range, vibration tests up to 1000g accelerations similarly failed to produce discernible modulation of the transistor characteristics.

MINIATURIZATION FIGURE OF MERIT	TYPE A SEPTEMBER 1949	JANUARY 1952	NEW DEVELOPMENT TYPE
VOLUME	$1/50$ IN^3	$1/2000$ IN^3	POINT – M1689
		$1/500$ IN^3	JUNCTION – M1752
MINIMUM COLLECTOR VOLTAGE FOR CLASS A OPERATION	30 V	2 V	POINT – M1768, M1734
		0.2 V	JUNCTION – M1752
MINIMUM COLLECTOR POWER FOR CLASS A OPERATION	50 MW	2 MW	POINT – M1768
		10 μ W	JUNCTION – M1752
CLASS A EFFICIENCY	20 %	35 %	POINT – M1768, M1729
		49 %	JUNCTION – M1752

Fig. 25—Miniaturization in space and power drain.

MINIATURIZATION STATUS

Space Requirements

In smallness of size, the transistor is entering new fields previously inaccessible to electron devices. The cartridge structure (see Fig. 25), such as the type A, has a volume of $\frac{1}{50}$ cubic inch, compared to about $\frac{1}{8}$ cubic inch for a sub-miniature tube and about 1 cubic inch for a miniature tube. Under current development, the M1689 bead point-contact transistor has substantially similar electrical characteristics to the M1698* cartridge switching unit but occupies only about $\frac{1}{2000}$ cubic inch. The M1752 junction bead transistor has a volume of approximately $\frac{1}{500}$ cubic inch but this may be reduced to the same order as the point-contact bead if necessary. For further substantial size reductions in equipment, the next move must comprise the passive components. It should be pointed out that the low voltages, low power drain, and correspondingly lower equipment temperatures should make possible further reductions in passive component size.

---

* The M1698 transistor is a cartridge type point-contact transistor with electrical characteristics designed for switching and pulse applications. This unit is proving useful in the laboratory development of new circuits or in cases where miniature packages are unnecessary.

Power Requirements

The transistor, of course, has the inherent advantage of requiring no heater power; moreover, significant advances have been made in the past two years in reducing the collector voltage and power required for practical operation. Consider the minimum collector voltage for which the small-signal Class A gain is still within 3 to 6 db of its full value. In September, 1949, the type A transistor could give useful gains at collector voltages as low as 30 volts. Today, several point-contact devices (M1768 and M1734) perform well with collector voltages as low as 2 to 6 volts even for relatively high-frequency operation. One junction transistor, the M1752, can deliver useful gains at collector voltages as low as 0.2 to 1.0 volt. Under these same conditions, the minimum collector power for useful gains may be as low as 2–10 mw for point-contact devices and as low as 10 to 100 μw in the case of the junction transistors.*

Class A efficiencies have been raised for the point-contact devices to as high as 30–35 per cent and for junction transistors this may be as high as 49 per cent out of a maximum possible 50 per cent. Class B and C efficiencies are correspondingly close to their theoretical limiting values.

PERFORMANCE STATUS

Exact electrical performance specifications for the transistor depend, of course, upon the intended applications and the type of transistor being developed for such an application. These types are beginning to be specified; and in fact, they are already so numerous that mention of only a few salient features of some of them will be attempted. Bear in mind, as was pointed out before, that no one transistor combines all the virtues any more than does any one tube type. Fig. 26 attempts to compare the progress made in several important performance merit figures by development of several point-contact and junction types during the last two years. Again the reference performance is that of the type A as of September, 1949.

Some switching and transmission applications need transistors having high current gain. By going to a point-junction structure, useful values of alpha as high as 50 are now possible with laboratory models.

For straight transmission applications, the single stage gain of point-contact types (M1768, M1729) has been increased to 20–24 db, whereas for the M1752 junction type the single stage gain may be as high as 45–50 db.

---

* In some special cases, depending upon the application, practical operation may be obtained for as little as 0.1 to 1.0 microwatt.

PERFORMANCE FIGURE OF MERIT	TYPE A SEPTEMBER 1949	JANUARY 1952	NEW DEVELOPMENT TYPE
a – CURRENT GAIN	5 X	50 X	JUNCTION
SINGLE STAGE CLASS A GAIN	18 DB	22 DB	POINT – M 1729, M1768
		45 DB	JUNCTION – M 1752
NOISE FIGURE AT 1000 CPS	60 DB	45 DB	POINT – M 1768
		10 DB	JUNCTION – M 1752
FREQUENCY RESPONSE f_c	5 MC	7 – 10 MC	POINT – M 1729
		20 – 50 MC	POINT – M 1734
CLASS A POWER OUTPUT	0.5 WATT	2 WATTS	JUNCTION
SWITCHING CHARACTERISTICS	NONE	GOOD	POINT – M 1698, M1689 M 1734
FEEDBACK RESISTANCE r_b	250 OHMS	70 OHMS	POINT – M 1729
LIGHT/DARK PHOTOCURRENT RATIO	2 : 1	20 : 1	JUNCTION – M 1740

Fig. 26—Performance progress.

For high-sensitivity low-noise applications, the point-contact devices have been improved to have noise figures of only about 40–45 db, whereas the M1752 n-p-n transistor has been shown to have noise figures in the 10–20 db range. All such noise figures are specified at 1000 cps and it should be remembered that they vary inversely with frequency at the rate of about 11 db per decade change in frequency.

For video, I.F., and high-speed switching applications, measurable improvement has been attained in the frequency response. For video amplifiers up to about 7 mc, the M1729 point-contact transistor is capable of about 18-20 db gain per stage. For high-frequency oscillators and microsecond pulse switching, the M1734 point-contact transistor is under development. Preliminary models of 24 mc I.F. amplifiers using the M1734 have been constructed in the laboratory, these amplifiers having a gain of some 18–24 db per stage and a band-width of several megacycles. However, more work needs to be done on the M1734 to reduce its feedback resistance. For pulse-handling functions, such M1734 units work very nicely as pulse generators and amplifiers of $\frac{1}{2}$ microsecond pulses, requiring only 6–8 volts of collector voltage and 12–20 mw of collector power per stage. The amplified pulses can have ampli-

tudes as large as 4–5 volts out of a total collector voltage of 6 volts and rise times as little as 0.01–0.02 microsecond.

By increasing the thermal dissipation limits of junction transistors, the Class A power output has been raised to 2 watts in laboratory models. This, however, does not represent an intrinsic upper limit but rather a design objective for a particular application.

Characteristics suitable for switching are now available in the M1698, M1689 and M1734 point-contact types, as previously described, but this is a continually evolving process and more work certainly remains to be done. At present it is possible to operate telephone relays requiring as much as 50 to 100 ma with M1689 and M1698 point-contact transistors.

New junction-type phototransistors[5] represent a marked advance over the earlier point-contact type.[6] While their quantum efficiencies are not as high as those of the point-contact types, nevertheless the light/dark current ratios are greatly improved and the collector impedance has been raised 10–100 times thus making possible much greater output voltages for the same light flux.

SOME SELECTED APPLICATIONS

Data Transmission Packages

To determine the feasibility of applying transistors in the form of miniature packaged circuit functions, several of the major system functions of a pulse code data transmission system have been studied. This investigation has been undertaken under the auspices of a joint services engineering contract administered by the Signal Corps.

It was desired that these studies should lead to the feasibility development of unitized functional packages combining features of miniaturization, reliability and lower power drain. Accordingly, it was necessary to carry on in an integrated fashion activities in the fields of system, circuit and device development to achieve these ends. In particular, circuit and system means have been developed to perform with transistors the functions of encoding, translation, counting, registering and serial addition. The M1728 junction diode, M1740 junction photocell and M1689 bead switching transistor are direct outgrowths of this program and are the devices used in the circuit packages.

At this point, the major system functions shown in Fig. 27 have been achieved with interchangeable transistors. These major system functions are in turn built up of some seven types of smaller functional packages listed in Fig. 28. The end result of this exploratory development can be

said to have demonstrated the feasibility of such a data transmission
system in the sense that a workable (though not yet optimal) system
can be synthesized from reproducible transistor-circuit packages which
have been produced at reasonable yields and with reasonable (though
not yet complete) service reliability. Further development work would
be needed in all phases to make such a system of packages suitable for
field use. It is estimated that the present laboratory model requires
about one-tenth the space and power required to do the same job with
present tube art. Fig. 29 is a photograph of a transistor bit-register
package and Fig. 30 is another photograph of such packages showing
both sides of the various types employed.* Actual final packages would

1.   4 DIGIT REVERSIBLE BINARY COUNTER

2.   6 DIGIT ANGULAR POSITION ENCODER

3.   6 DIGIT GRAY - BINARY TRANSLATOR

4.   5 DIGIT SHIFT REGISTER

5.   2 WORD SERIAL ADDER

Fig. 27—System functions tested.

DEVELOPMENT PACKAGE TYPE	PACKAGE FUNCTION	DEVELOPMENT TRANSISTOR, DIODE TYPES USED
M 1731-1	REGENERATIVE GATE	M 1689 M 1727
M 1732-1 M 1736 M 1790	BIT REGISTER	M 1689 M 1727 M 1734
M 1733-1 M 1792	PULSE AMPLIFIER	M 1689
M 1735-1 M 1747-1 M 1748-1 M 1751-1 M 1751-2 M 1751-3	DIODE GATE	M 1727 400A
M 1745-1 M 1791	BINARY COUNTER	M 1689 400A
M 1749-1	PHOTOCELL READOUT	M 1740
M 1746-1	DELAY AMPLIFIER	M 1689

Fig. 28—Development transistor—circuit packages.

* The Auto-Assembly Process used in the construction of these packages is a
Signal Corps Development.
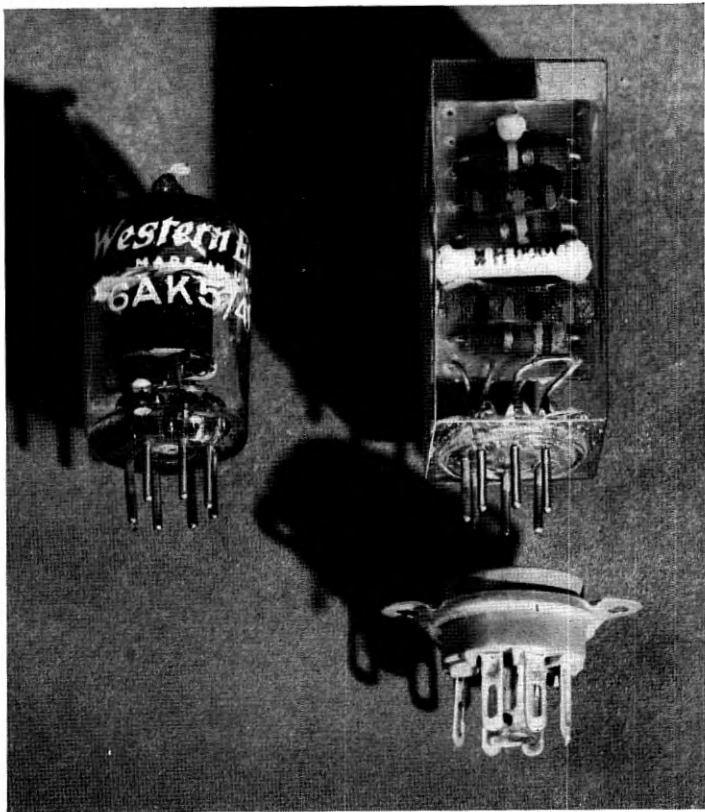
Fig. 29—Bit register package.

probably not use such clear plastics and Fig. 31 shows some packages in which the plastic has been loaded with silica to increase its strength and thermal conductivity. The assembly in Fig. 31 consists of a six-digit position encoder at the left, followed by six regenerative pulse amplifiers which in turn feed a six-digit combined translator-shift register.

N-P-N *Transistor Audio Amplifier and Oscillator**

To the right in Fig. 32 is shown a transformer-coupled audio amplifier employing two M1752 junction transistors. This amplifier has a pass band from 100–20,000 cps and a power gain of approximately 90 db. Its gain is relatively independent of collector voltage from 1–20 volts,

---

* The material of this section represents a summary of some work by Wallace and Pietenpol described more completely in Ref. 4.

Fig. 30—Package construction illustrated.

Fig. 31—Laboratory model of encoder-transistor-register using transistor packages.
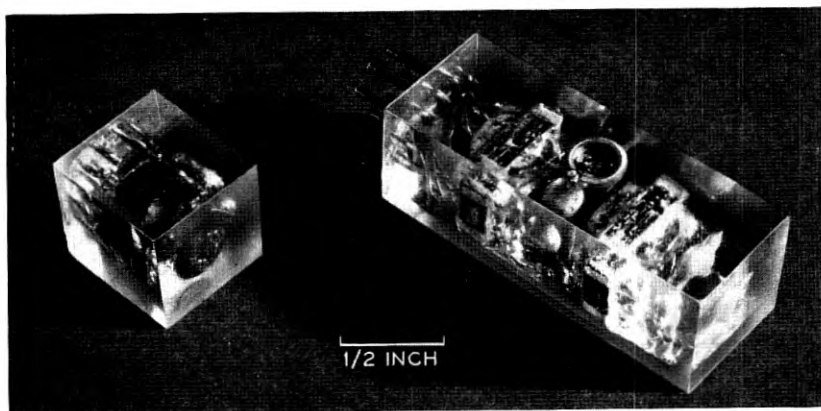
Fig. 32—Packaged oscillator and amplifier using junction transistors.

only the available undistorted power output increasing as the voltage is increased. At a collector voltage of 1.5 volts it draws a collector current of approximately 0.5 ma per unit for a total power drain of 1.5 milliw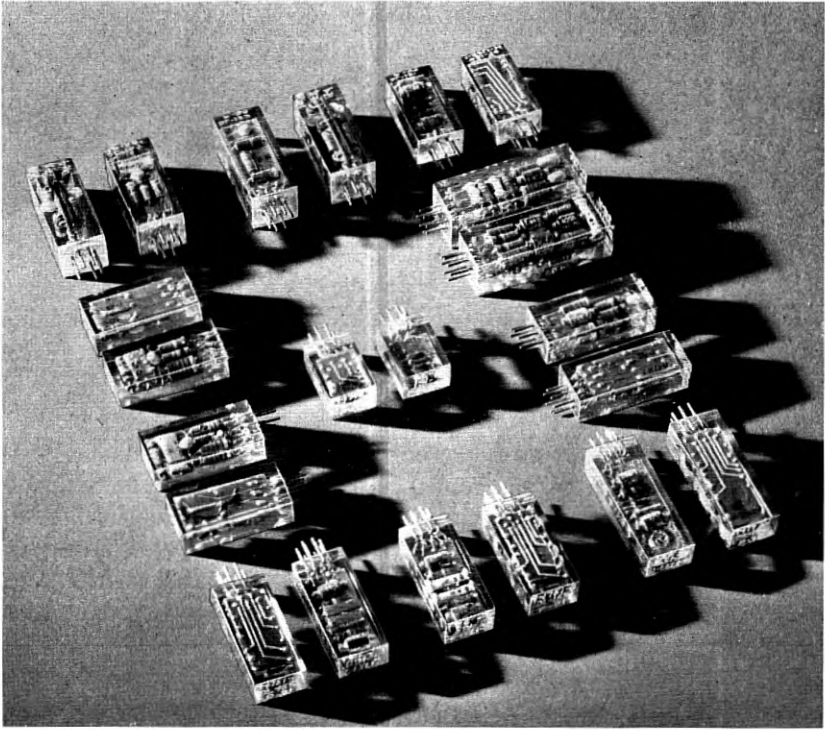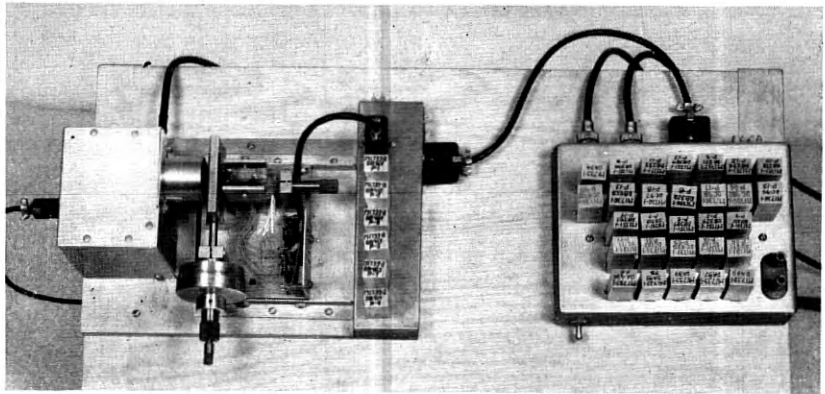atts. Under these conditions it will deliver Class A power output of about 0.7 milliwatt. The noise figure of such an amplifier has been measured to be in the range from 10–15 db at 1000 cps depending upon the operating biases.

To the left of Fig. 32 is shown a small transistor audio oscillator having a single M1752 transistor, a transformer and one condenser. To see just how little power was the minimum necessary to produce stable oscillations such an oscillator was tried at increasingly lower collector supply voltages. It was found that stable oscillations could be maintained down to collector supply voltages as low as 55 millivolts and collector current as low as 1.5 microamperes for a total drain of 0.09 microwatt.

SUMMARY

With respect to reproducibility and interchangeability, transistors now under development appear to be the equal of commercial vacuum tubes.

With regard to reliability, transistors apparently have longer life and greater mechanical ruggedness to withstand shock and vibration than most vacuum tubes. With regard to temperature effects, transistors are inferior to tubes and present upper limits of operation are 70–80°C for most applications. This restriction is often reduced in importance by the lower power consumption which results in low equipment self-heating. This, however, is the outstanding reliability defect of transistors.

With regard to miniaturization, the comparison figures are so great as to speak for themselves. Operation with a few milliwatts is always feasible and in some cases operation at a few microwatts is also possible.

With regard to performance range, it is believed that the above results imply the following tentative conclusions:

In pulse systems (up to 1–2 mc repetition rates) transistors should be considered seriously in comparison to tubes, since they provide essentially equal functional performance and have marked superiority in miniature space and power. Bear in mind that in some reliability figures they are superior whereas in the matter of temperature dependence they are inferior to tubes.

In CW transmission at low frequencies (<1 mc) essentially the same conclusions are indicated, primarily because of junction transistors. In the range from 1–100 mc, tubes are currently superior in every functional performance figure (except perhaps noise and bandwidth) so that for transistors to be considered for such applications, much greater premium must be placed on miniaturization and reliability than for the first two applications areas.

Thus, it might be assumed that, even though there are many outstanding development problems of a circuit and device nature to be solved, it is appropriate for circuit engineers to explore seriously the application possibilities of transistors—not only in the hope of building better systems, but also to influence transistor development towards those most important systems for which their intrinsic potentialities best fit them. It should not be inferred that all important limitations have been eliminated—nor, on the other hand, that the full range of performance possibilities have been explored.

If one remembers the history of engineering research and development in older related fields, it seems apparent that a relatively short time has elapsed since the invention of the first point-contact transistor. Already, new properties and new types of devices are under study and some have been achieved in the laboratory. It therefore is possible, and certainly stimulating, to infer that more than a single new component is involved; that much more lies ahead than in the past; that, indeed we may be entering a new field of technology, i.e., "transistor electronics".

number of workers in physical research, chemical and metallurgical research and transistor development. In reality, these colleagues are the authors of this paper; and it is to them the writer owes full and appreciative credit for the material that has made possible this report of progress in transistor electronics.

REFERENCES

1. R. M. Ryder, R. J. Kircher, "Some Circuit Aspects of the Transistor", *Bell System Tech. J.*, **28**, p. 367, 1949.
2. R. L. Wallace, G. Raisbeck, "Duality as a Guide in Transistor Circuit Design", *Bell System Tech. J.*, **30**, p. 381, 1951.
3. W. Shockley, M. Sparks, G. K. Teal, "*p-n* Transistors", *Phys. Rev.*, **83**, p. 151, 1951.
4. R. L. Wallace, W. J. Pietenpol, "Some Circuit Properties and Applications of *n-p-n* Transistors", *Bell System Tech. J.*, **30**, p. 530, 1951.
5. W. J. Pietenpol, "*p-n* Junction Rectifier and Photocell", *Phys. Rev.*, **82**, No. 1, pp. 122–121, Apr. 1, 1951.
6. J. N. Shine, "The Phototransistor", *Bell Laboratories Record*, **28**, No. 8, pp. 337–342, 1950.

An Experimental Electronically Controlled Automatic Switching System

By W. A. MALTHANER AND H. EARLE VAUGHAN

(Manuscript received February 15, 1952)

An automatic telephone switching system, built as a laboratory experiment, is described in which electronic techniques, high speed relays and a subscriber telephone with a pre-set dialing mechanism were employed. One-at-a-time operation within the office was made possible by these fast tools; that is, only a single control circuit was provided for each function. This experimental system, although not commercially economical, showed that an advantageous reduction in the number of control and connector circuits is made possible by this method of operation.

INTRODUCTION

This paper describes a laboratory experiment in automatic telephone switching systems. The investigation was conducted at the research level to gather valuable information and circuit techniques from a laboratory trial and not to evolve a system economically competitive with existing systems since the area of investigation is always broader and the results more general in character when the work is unfettered by economic restraints. Indeed, the results are not economically competitive.

Purposes of the investigation were to determine what advantages may be derived from faster operation, largely through the use of electronic techniques, and to introduce and test some previously unexplored philosophies in switching and signaling. Some of the basic tools employed were dry-reed relays, mercury relays, multi-element cold cathode gas tubes, cold cathode gas diodes, and thermionic electron tubes. An experimental subscriber's telephone set, incorporating a preset dial mechanism with circuits for generating dialing signals of a new form, together with suitable signal receivers for the central office was designed as well as a novel type of switching network with its control circuits. A basic aim of the experiment was one-at-a-time operation within the central office.

BACKGROUND AND OBJECTIVES

In many recent designs of dial telephone central offices, especially those in use in large urban areas, the subscriber's dial does not control directly the setting of switches leading toward the desired destination as was the case in early dial systems. Instead the information is received first by a register circuit which is selected from a group of such register circuits and is connected to the calling subscriber's line on the origination of a call. The register cooperates with other complex circuits to ascertain the location of idle trunks to the called subscriber's office and possible routes through the switching network to these trunks, and to control the selection and use of one such path to this called office. In the called office another register circuit, frequently of a type different from that into which the subscriber originally dialed, is selected from a group of such circuits and the directory number of the called subscriber is transmitted to it from the register-sender circuit in the calling office. In the terminating office the procedure of locating and testing the called line and switching paths to it, and of establishing a connection over one of these paths is accomplished through the use of additional control circuits. These various circuits which are used in setting up a conversational path are called common control circuits.

Each type of common control circuit is provided in sufficient number to handle the expected traffic. The number required is, of course, related to speed of operation since the shorter the holding time of a circuit, i.e., the length of time a circuit takes to complete its functions for one call, the more calls such a circuit can complete in a given time. The holding time of a control circuit is, in turn, dependent upon the operating speed of the equipment controlled. Furthermore, control circuits of the same type, if more than one of a given type is required, will have added to their normal functioning time during busy traffic periods a delay time interval since they must not interfere with each other's actions in the controlled equipment. Common control circuits, such as dial pulse registers, which receive information directly from subscribers must be engineered on the basis of an average holding time which allows for the variable reaction times, hesitations, partial usages and other personal idiosyncrasies of subscribers. Present designs of automatic central offices require a number of each type of control circuit and auxiliary circuits for selecting and connecting the control circuits as required in the operation of the system. These control circuits and connectors embrace a considerable fraction of the space and cost of such an office.

Dr. T. C. Fry, at the time he was Director of Switching Research

at the Bell Telephone Laboratories, suggested that a program be started to explore the possibilities of a new system which would require only a single control circuit of each type. This would require that each group of functions assigned to a common control circuit be performed on a one-call-at-a-time basis. It might be accomplished in a fresh approach to system design employing recent developments in high speed components. High speed in the common control units alone would not be sufficient. It would also be necessary to have fast switches since the operating time of a switching network is part of the holding time of the control circuit which operates the network. Similarly, since the signaling time is part of the holding time of the control circuit which receives and registers the signals, some form of high speed signaling would also be required. Further, the subscribers should have no direct control of the holding time of any common control unit. It was hoped that a great reduction in the number of common control circuits and connectors would result in a reduction in the size and cost of a central office even if the individual control circuits were somewhat more expensive. Furthermore, a speed permitting one-at-a-time operation would result automatically in faster service for the subscriber.

Consideration of the various factors of one-at-a-time operation was undertaken by the members of the Switching Research Department and possible system components evolved. Primary elements of inherently high speed, such as cold cathode gas tubes, thermionic electron tubes, dry-reed relays and mercury relays, were immediately adopted for the system. A network of high-speed switches with its high-speed control circuits was designed. A pre-set dialing device in the subscriber telephone set with transmission of high-speed dialing signals to the central office under control of common equipment in the office was selected as a means of eliminating the direct influence of subscribers on control circuit holding time. A code of high-speed signals, suitable for transmission over all existing types of local telephone facilities, with means for the pre-selection and controlled generation of telephone numbers was designed into the subset. Such a subset is necessarily complex since it becomes a form of manually operated register with all digits of a number stored before transmission to the central office. Circuits to control the generation of subset signals from the central office and receiver circuits to decode and register the signals were constructed.

These parts were then combined in the design of the Electronically Controlled Automatic Switching System, ECASS. A skeletonized laboratory version was built and tested to investigate the feasibility of combining the circuit elements and techniques, and to prove the operability
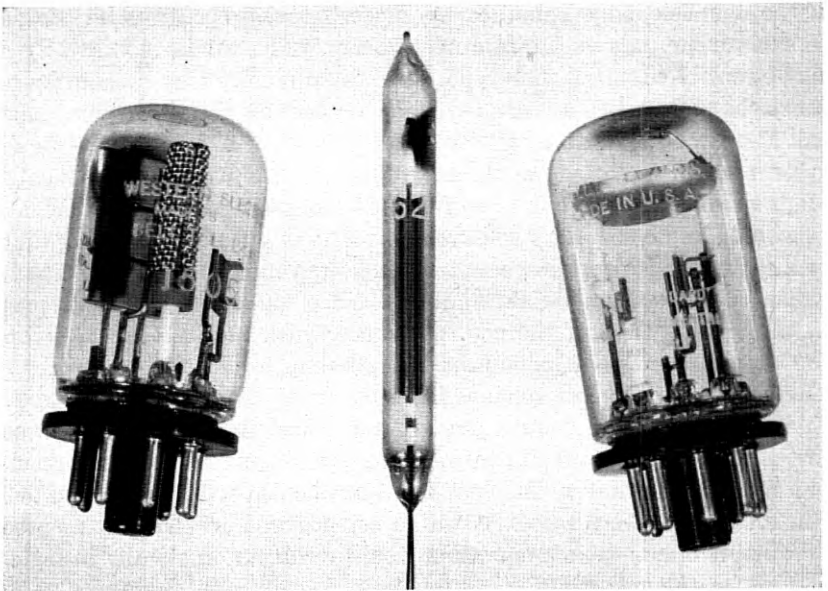
Fig. 1—Cold-cathode gas tubes—pentode, diode and octode.

of such a system. System operation is described in this paper after a more detailed discussion of the components mentioned above.

COMPONENTS

Cold cathode tubes, usually diode or triode types, have found widespread application in the past but the gas tubes used in the ECASS system were developed to have special characteristics for switching use. The three types of cold cathode gas tubes used were: a diode, a screen grid pentode and a multi-purpose octode. Fig. 1 shows a photograph of each type and Fig. 2 gives a schematic drawing of the internal elements. These tubes were developed by W. A. Depp and R. L. Vance. The diode
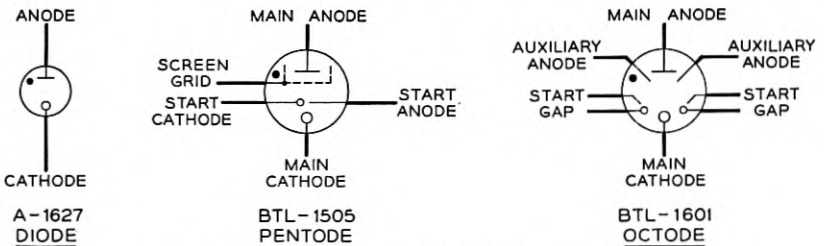
Fig. 2—Schematics of cold-cathode gas tubes.

is used at many points throughout the switching network, the screen-grid pentode in the path selection processes in the switching network, and the octode for miscellaneous purposes in the line, trunk, number group and other circuits.

The dry-reed switch, which is used as the contact element in many fast relays as well as in the metallic talking path through the office, is shown in Fig. 3. This switch consists of two permalloy rods sealed in opposite ends of a small glass tube which is filled with an inert gas. The over-lapping ends of the rods normally have a gap between them and the application of a magnetic field coaxial with the reeds will cause them to pull together and close a metallic path from one rod or reed to the other through rhodium plating at the contacting ends. The dry-reed switch has an extremely small operate and release time, and because of the gas sealed and permanently adjusted construction provides a highly reliable dirt-free contact for low current applications. The dry-reed switch and relays employing it were developed by W. B. Ellwood. Mercury contact relays, also of a sealed and permanently adjusted construction, are used where fast operation at heavier currents is required. A sectional drawing
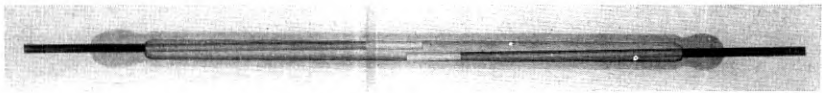
Fig. 3—Glass-sealed dry-reed switch.

of a mercury contact relay is shown in Fig. 4. These relays were developed by J. T. L. Brown and C. E. Pollard. Dry-reed relays and mercury relays are described in *Electrical Engineering*, Vol. 66, pp. 1104–1109, November, 1947, and in *Bell System Monograph*, 1516.

THE PRE-SET SUBSCRIBER'S TELEPHONE

In order to eliminate direct control of any common equipment by the subscriber and thereby to reduce the holding time of the dialed information receiving circuits and the associated subscriber-connecting circuits, the experimental pre-set dial telephone set shown in Fig. 5 was designed for this system by K. S. Dunlap, H. E. Hill and D. B. Parkinson. Eight selector finger wheels are grouped on a common shaft with only their edges visible across the front of the telephone housing. Each finger wheel is provided with ten indentations along its exposed periphery. Each indentation is designated by an engraved number or group of letters conforming to the telephone directory numbering system and each indentation is of suitable configuration to permit a subscriber's

finger to engage and move the wheel in either direction to one of ten detented positions. All of the wheels may be returned to their normal "zero" position simultaneously by depressing the release button on the front right corner of the housing. To place a call the subscriber positions each of the wheels so that the desired number may be read across the wheels on the line of indentations immediately above the lower edge of the enclosing frame. The first three wheels are set to the code of the called office and the next five to the called line directory number with the last of these being used for the party letter, if required. A number is preset in this manner before the handset is removed from its cradle across the back of the housing. With this method of operation the number may be rapidly and completely transmitted to the central office when its receiving circuit has been connected to the line.
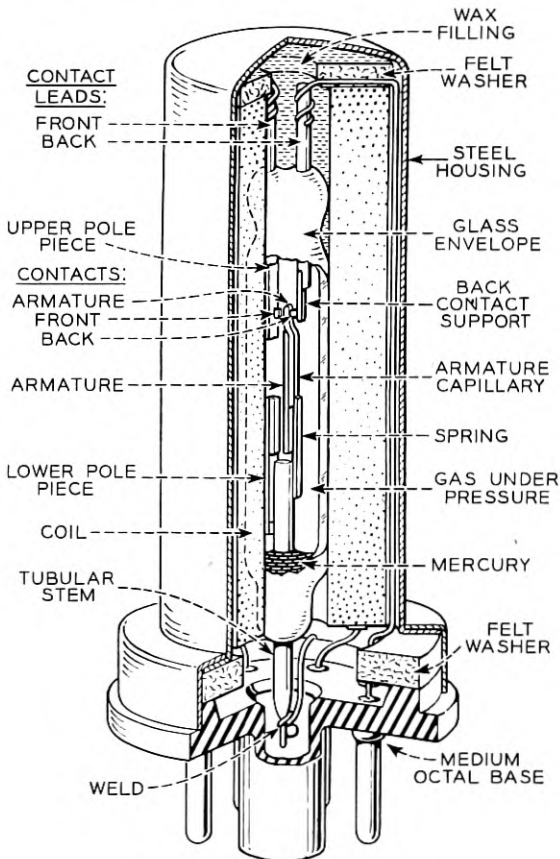
Fig. 4—Mercury contact relay.

Fig. 5—Pre-set pulse-position-dialing telephone set.

As shown in Fig. 6, which is a schematic of the mechanism and circuit of this telephone set, the handset when resting in its supporting cradle depresses the switchhook pins and causes two bell cranks to operate two sets of switchhook contact assemblies. One of these contact assemblies is controlled solely by the position of the handset while the other contacts are controlled jointly by the handset and by a magnetic locking device. This magnetic locking device consists of a permanent magnet yoke which holds the contacts in the position shown after the removal of the handset from its cradle until direct current of the correct polarity is allowed to flow in the windings of a latch magnet.

These two sets of switchhook contacts jointly control the connection of any of three subdivisions of the apparatus in the telephone set to the line to the central office. If the handset is removed from its cradle to originate a call, the free set of switchhook contacts releases to complete a circuit through the latched set of contacts to the signaling equipment of the station. In this signaling condition the voice transmission equipment remains disconnected from the circuit; thus, interference and transmission losses caused by voice transmission equipment are avoided during signaling. Upon completion of signaling direct current is provided from the central office to trip the latched switchhook contacts.
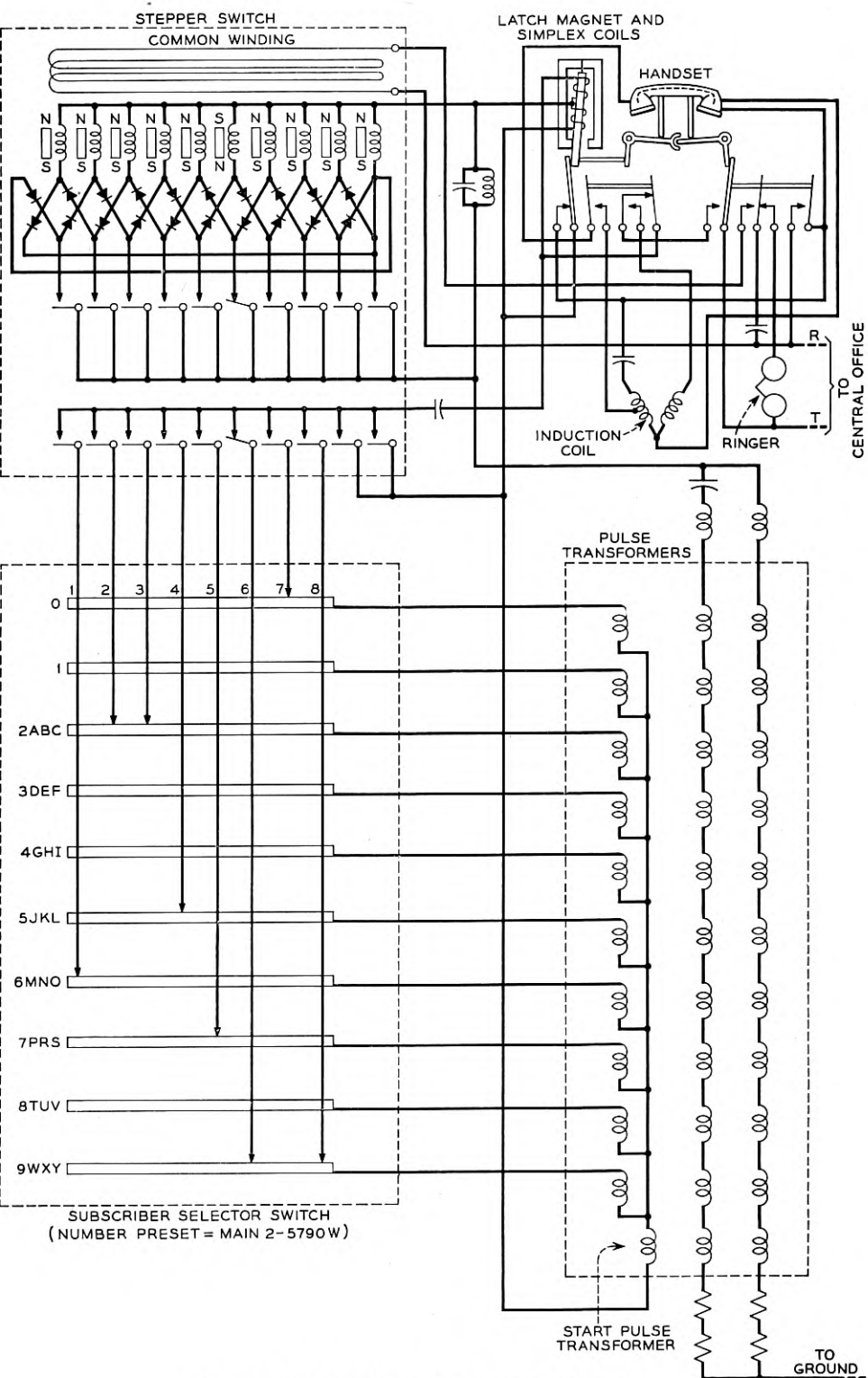
Fig. 6—Pulse-position-dialing subset schematic.

450

With both sets of switchhook contacts now released the usual transmitter, receiver and induction coil arrangement for transmission of voice currents is connected to the telephone line and all of the station signaling equipment, including the tripping windings of the latch magnet, is disconnected from the circuit. Interference and transmission losses caused by signaling equipment are thus avoided during conversation. When the handset is resting on its cradle between calls with both sets of switchhook contacts operated, the usual ringer and ringer condenser are connected across the line for responding to incoming calls. Upon removal of the handset in answer to such an incoming call, direct current is provided from the central office to trip the latched switchhook contacts and thereby the set is placed immediately in the talking condition.

PULSE POSITION DIALING SIGNALS

Before describing further the operation of this telephone set, it will be necessary to explain briefly the dialing signals generated by it and used in the system.

From the subscriber's telephone set eight digits are transmitted for a complete local area directory number and the transmission is repeated as many times as necessary for the functioning of the central office equipment. In order to indicate the starting point of the transmission of a complete called number, a time interval of two digits duration during which no signals are transmitted is provided at the beginning of each transmission. Each digit interval is 0.01 seconds; therefore, a time interval of 0.1 second is required for the no-signal or blank period and the eight digit number.

These signals, as shown in the wave form-time diagrams of Fig. 7, consist of two pulses per digit: a start pulse of 1 millisecond duration and a stop pulse of 1 millisecond duration, each pulse approximately a single cycle of a 1,000-cycle per second sine wave. The time interval between a start pulse and its following stop pulse is the measure of the associated digit value. The start pulses are generated at intervals of 0.01 seconds, or 10 milliseconds, and one stop pulse is generated some time during the 3.2 to 6.8 millisecond interval after each start pulse. In order to provide sufficient margins to permit reliable signaling over a wide variety of transmission facilities 3.2 milliseconds are allowed for the decay of each pulse and the pulses themselves occupy a section of the voice-frequency spectrum transmitted by practically all communication facilities. The possible starting times of stop pulses representing
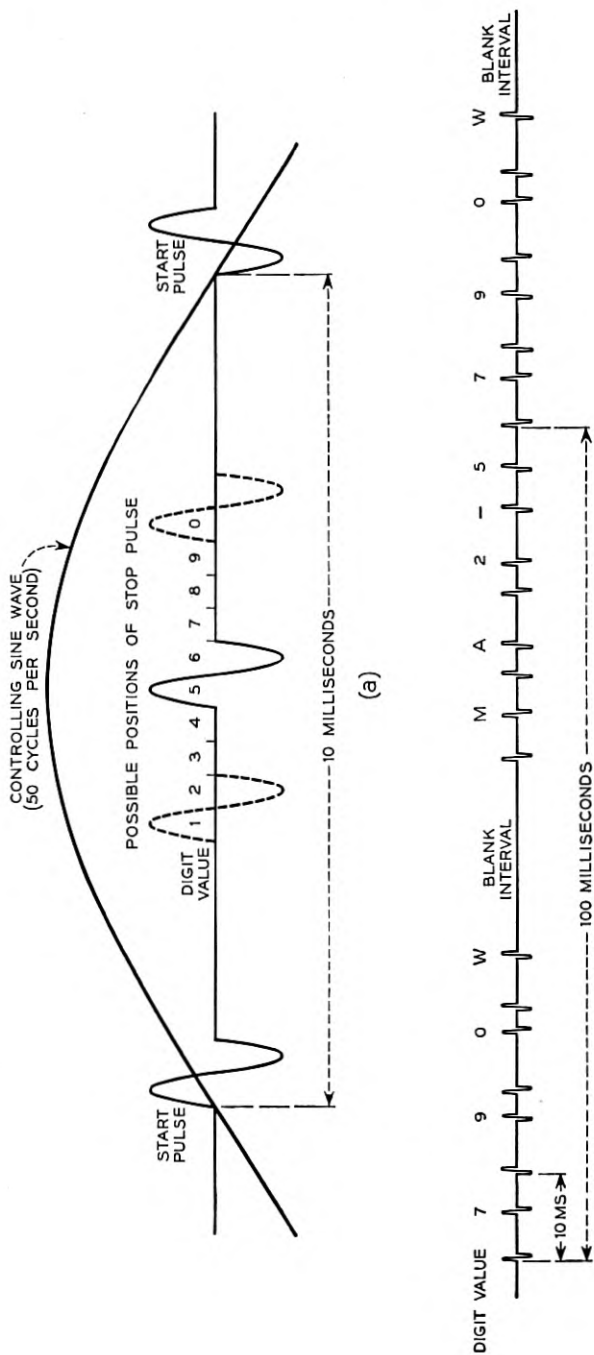
Fig. 7—Pulse-position-dialing signals.

digits of successive magnitudes differ by 0.4 milliseconds. Thus, digit 1 is represented by a start pulse followed by a stop pulse 3.2 milliseconds later; digit 2 is represented by a start pulse followed by a stop pulse 3.6 milliseconds later; and so on. It will be observed that the stop pulse for the digit 0 is 6.8 milliseconds after its start pulse and 3.2 milliseconds before the next succeeding start pulse. Thus, there is provided an increment of time of 3.2 milliseconds for the decay of the start pulse, increments of 0.4 milliseconds each for the generation of a pulse at any one of the ten times necessary to represent the various digits, and a last increment of 3.2 milliseconds to permit a stop pulse to decay should it occur at the end of the ninth increment of time.

Referring again to Figure 6, the signaling pulses are generated by the eleven pulse transformers shown. These saturation-type transformers are assigned, one for each of the numerals 0 to 9 and one for the start pulse. The excitation for the signaling apparatus is a constant amplitude 50-cycle current of sinusoidal wave form transmitted from the central office on a simplex circuit consisting of the two line wires to the set with ground return.* The currents from the line wires pass into the signaling apparatus through the windings of the latch magnet. These latch magnet windings thus serve also as a simplexing coil and since the excitation magneto-motive-forces in the two windings are mutually opposing there is no reaction on the latch itself.

From the simplex coil the excitation current flows through a stepper switch and its shunting phase shifter to a phase splitting network in which the current is converted to a two phase source with its two currents 90 degrees out of phase. Each of the pulse generating transformers has a single secondary and two primary windings. The primary windings of the transformers are serially interconnected and connected with the two phases of the excitation current so that one phase is applied to one primary winding of each transformer and so that the other phase is applied to the other primary winding of each transformer. The secondary windings are connected across the line through the pre-set selector, contacts of the stepping switch and a series capacitor. The secondary winding of the pulse transformer for the start pulse is in a lead common to all the stop pulse secondaries.

The magnetic core of each pulse transformer is designed to be saturated except for very small values of ampere-turns, and a voltage pulse

* The time interval spacings of signal pulses given in this section and in the following section on the signal receiver are based on a 50-cycle control current. The system operated satisfactorily on 50 cycles. However, in most of the laboratory tests a control current of 45 cycles per second was used since a stable source of this frequency is readily derived from commercial 60-cycle power sources.

is generated in the secondary winding of each transformer when the flux is changed from saturation at one polarity to saturation at the other polarity. The flux generated in the core of each transformer depends upon the number of turns in the two primary windings and upon the current flowing in each winding. In order to assure that all pulses be substantially alike as to wave form and amplitude it is necessary that the total maximum ampere-turns on each core be equal. In order to cause each transformer to generate a pulse at a suitable time during each half-cycle of the excitation current the total ampere-turns driving flux through the transformer cores must be controlled so that the flux in each transformer is zero at the time assigned to the pulse which that transformer serves to generate. These conditions determine the number of turns and the polarity of each winding when the angular position of the desired pulse is fixed in relation to each half-cycle of the basic excitation current.

Since the magnetic flux in each transformer is reduced to zero two times during each cycle of excitation current, it follows that a combination of two pulses representing a digit must occur during each half-cycle of the excitation current and that each combination of two pulses representing a digit is of opposite polarity to the preceeding two pulses. The capacitor through which the pulse generating transformer secondary windings are connected to the line is so proportioned to the impedances of these windings and to the impedance of the line that each half-cycle pulse as generated by a transformer is applied to the line as a single complete cycle of alternating current of about 1 millisecond duration.

A selector switch, which is the internal mechanism connected with the finger wheels pre-set by the subscriber, serves to interconnect the transformer pulse windings with the line through the stepper switch. Thus, pulses representing any of the digits 0 to 9 may be impressed across the telephone line as any desired part of a complete telephone number in accordance with the setting of the selector switch.

The stepper switch employs ten relays of the glass-sealed dry-reed type and each of the relays has an individual coil surrounding two normally open reed contacts. The reeds are polarized by a permanent magnet of sufficient strength to hold the reed contacts closed but not strong enough to close them until assisted by current of the correct polarity through the winding. A reverse current through the winding is required to release the contacts. In addition a common winding is provided which surrounds all of the reeds in such a manner that when a current of sufficient magnitude is passed through the winding the reeds of a predeter-

mined delay will be closed and the reeds of all the other relays will be opened. This action is produced by reversing the individual winding and bias magnet of the single relay which is to be operated by the current through the common stepper winding. The preliminary setting of the stepper to insure correct operation is provided on each origination of a call by the discharge current from the ringer capacitor through the common winding of the stepper. The ringer capacitor is charged from the central office between calls.

One reed in each of the relays is employed to connect successive brushes of the digit selector switch with the line while the other reed in each relay in conjunction with two diode rectifiers per relay winding is employed to control the operation of the stepper. The stepping operation may be explained by reference to Fig. 6 as follows: The stepper is shown with the reeds for the sixth step closed. When the 50-cycle excitation current makes the terminal common to the individual stepper coils positive with respect to the terminal common to the stepping control contacts, current flows through the upper reed contact of the sixth step, a diode rectifier and the winding of the seventh step relay causing its reeds to close. With the seventh set of reeds closed current flows through a diode rectifier and the winding of the sixth step relay causing its reeds to open. The stepper will remain in this position until the reversal of excitation current a half-cycle later at which time a circuit through an oppositely poled diode rectifier will cause the operation of the relay for the eighth step followed by the release of the relay for the seventh step. The phase of excitation current through the stepper is so adjusted by the shunt phase shifting network that the stepper relays operate and release during the 3.2-millisecond guard interval preceding a start pulse. This prevents mutilation of the signal pulses. The stepping circuit is made reentrant so that the pre-set number will be transmitted repeatedly so long as excitation current is provided.

With the chosen 50-cycle excitation the complete transmission of eight digits and a two-digit silent interval takes only 0.1 second. This results in a short holding time for the central office receiving circuit and the repetitive signaling feature permits repeated trials in case of signal mutilation as well as direct dialing from the subscriber's telephone set to distant offices rather than some form of relayed signaling from registers in the subscriber's own office.

SIGNAL RECEIVER

A simplified block diagram of an experimental receiver for the pulse-position signals used in this system is shown in Fig. 8. The receivers

were designed by N. D. Newby and the authors of this paper. The signals after passing through a bandpass filter are amplified to a standard level by a circuit incoporating backward acting automatic volume control. The arrival of each signal pulse is detected by a threshold device. Since the minimum time interval between the generation of a pulse and the next succeeding pulse is 3.2 milliseconds, the threshold device is arranged to disable itself upon the detection of a pulse for about 3 milliseconds. This prevents false operations of the detector either by tail transients resulting from distortion of a pulse in the transmission medium or by noise occuring in this interval.

When the silent or blank interval which exists between the complete transmission of a number and its next repetition is recognized by the
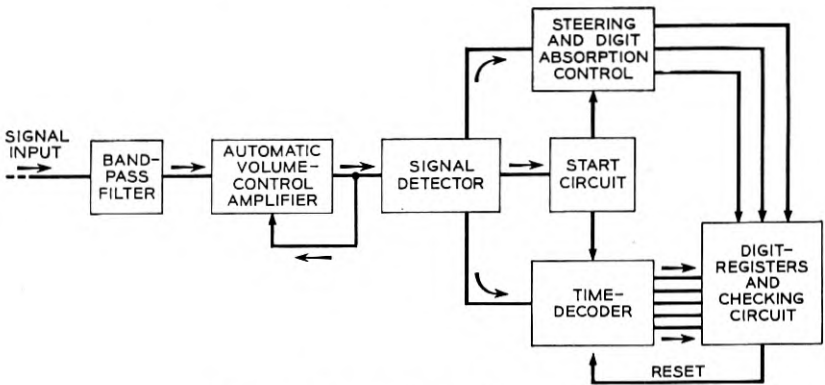
Fig. 8—Pulse-position-dialing receiver.

start circuit attached to the detector, the time-decoder circuit is enabled as well as the steering and digit absorbing circuit. The time decoder subsequently measures the length of time between each detected start pulse and the following detected stop pulse, and energizes the corresponding digit value leads into the registers. The steering circuit enables a separate set of register elements for the storage of each decoded digit which is to be used by its associated circuits and withholds such enablement through its digit absorbing features for digits which are not of immediate interest. The steering circuit also enables a check circuit associated with the registers.

Several features of the signaling code permit a check to be made that the received signals are in accordance with the code. The number transmission cycle has been already described but a brief restatement is made here to emphasize the checkable features: The first pulse following

the blank interval is a start pulse and eight start pulses at uniform 0.01-second time-interval spacing occur between blank intervals. One and only one stop pulse occurs between start pulses. The total number of signal pulses between blank intervals is sixteen. The check circuit utilizes one or more of these properties to insure that no signal pulses have been lost during transmission and that no extraneous pulses have been detected. If the actions of the check circuit indicate that an error in transmission has occurred, the receiver circuits are completely reset for another trial.

THE SWITCHING NETWORK

To meet the objective of a single common control circuit for the operation of the switching network, which provides the selectable paths between any subscriber and any trunk, it was necessary to have the switches in the network considerably faster than any of present commercial design. The laboratory model of the switching network and its associated path selecting equipment employing cold cathode gas tubes and dry-reed relays was developed by E. Bruce and S. T. Brewer. In addition to high operating speed this switching arrangement has certain other desirable properties: The idle path testing and selection functions are incorporated in the internal controls of the network. Busy sections of the network are automatically isolated from the sections tested for subsequent calls. Selection of a trunk within a trunk group, as well as path selection through the network, may be accomplished by the internal controls of the network if the trunks of a group are assigned one trunk per frame. Selection of an idle trunk and an idle switch path in combination reduces blocking. These internal selection controls eliminate many of the connector contacts that would otherwise be required between the switches and external common control circuits.

The switching network consists of line frames and trunk frames with each frame divided into primary and secondary switches. Each primary line and trunk switch has a number of vertical input columns across the switch to which are connected line or trunk circuits respectively and a number of horizontal output rows across the switch. At the intersection of each row and column of a switch is a relay consisting of an operating coil and three dry-reed make contacts. By analogy to the crossbar system which employs a somewhat similar rectangular array of rows and columns per switch and a similar primary-secondary path distribution, a switch intersection is called a crosspoint and a switch relay is called a crosspoint relay. In the crosspoint relay two of the contacts are used

to connect the talking conductors associated with the particular column to the talking conductors associated with the particular row. A cold-cathode gas diode is also associated with each crosspoint relay, and this diode in series with the winding of the relay is connected between the control lead of the particular column and the control lead of the particular row. The third contact of the crosspoint relay is used to short-circuit the associated gas diode. A typical crosspoint is shown schematically in Fig. 9. The use of these crosspoint gas diodes in the control leads facilitates the identification and selection of idle paths through the switching network and the short-circuiting of the diodes at operated crosspoints facilitates the holding of an established connection through the network at a lower power level than required for initial operation and the maintenance of a busy indication along an established connection during the path selection processes of subsequent calls. Dry-reed contact relays, rather than a more conventional type, are used in the crosspoints to provide the operating speed required for single control circuit operation.

Each secondary switch is a similar rectangular array except that the horizontal rows are used as input terminals and the vertical columns as switch outlets. Within a frame the horizontal outputs of the primary switches are interconnected with the horizontal inputs of the secondary
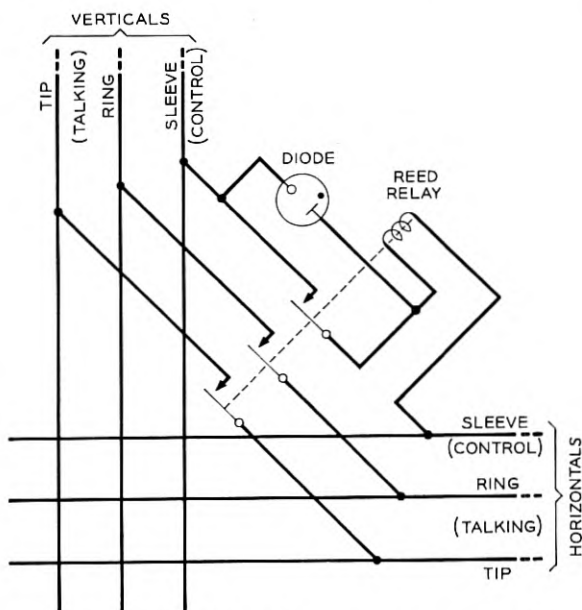

Fig. 9—Reed-diode switch—crosspoint connection.

switches so as to provide one path from each primary switch to each secondary switch.

Connections are made between the secondary line frame switches and the secondary trunk frame switches to provide talking paths between each line frame and each trunk frame. A direct metallic connection is made for the two talking conductors of each path but the control lead from each secondary line switch outlet is connected to an individual control circuit, called a junctor, and the control lead from a secondary trunk switch outlet associated with the same talking path is connected to the same control circuit or junctor. The size of the switches on each type of frame and the number of frames in each particular office will be determined by the number of subscribers and other offices connecting to this office and the calling habits of the subscribers served.

The operation of the switching network may be explained by reference to Fig. 10 which shows the control lead diagram of a skeletonized switching network of a large size office. This figure shows two line frames, each of which has two primary switches and two secondary switches. Three vertical inlets are provided on each primary switch and two vertical outlets on each secondary switch. The figure also shows two trunk frames, each of which has two primary switches and two secondary switches. The trunk switches provide two vertical trunk inlets on the primary switches and two vertical outlets on the secondary switches. Eight junctors are required as indicated. This switching network then serves to interconnect twelve subscribers with eight trunk appearances. This is the actual size built in the experimental model.

As shown in Fig. 10 each control lead path between a primary and a secondary switch on both the line and trunk frames is connected through a high value of resistance to a −45-volt power supply. In addition each control lead path from a secondary switch terminates in a similar resistor connected to a −105-volt power supply. In a junctor involved in an established connection, such as junctor 5 of Fig. 10, the control leads connect to a −24-volt source through low resistance relay windings. A talking path is shown as fully established between line C on line frame 2 and trunk D on trunk frame 2. This connection is held by the current flowing from the −24-volt source in junctor 5 through the operated reed crosspoints in the line frame to a ground in the line circuit and in the same manner through the operated reed crosspoints in the trunk frame to a ground in the trunk circuit. The −24-volt potential on the junctor leads and the resulting −12-volt potential on the primary-to-secondary switch link leads are effective path busy indications for subsequent path selection operations in the network.
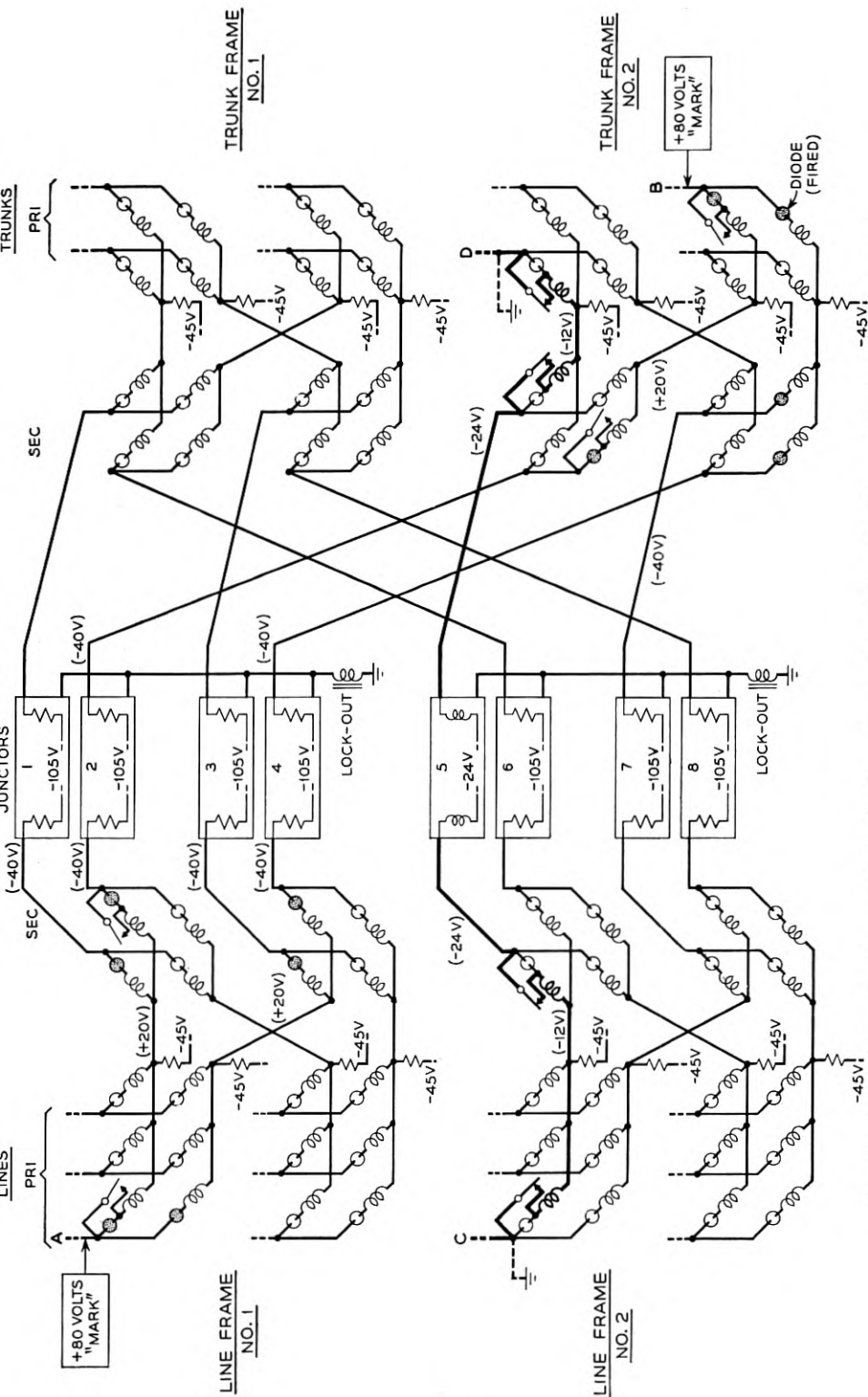
Fig. 10—Switching network control lead schematic—path marking, holding and busy voltage conditions.

460

If a talking path is now desired between line A on line frame 1 in Fig. 10 and trunk B on trunk frame 2, a +80-volt power source is connected to the control leads at these points. These applied voltages are called "marks" and originate in a number group circuit. The +80-volt mark at line A in conjunction with the −45-volts supplied to the primary-secondary switch links causes the cold cathode gas diodes of the line A vertical to fire and conduct at low current. The substantially constant voltage-drop characteristic of gas diodes causes the voltage on the two horizontal outlets of this primary switch to shift to +20 volts thereby "marking" one input lead on each secondary switch of this line frame. These +20-volt marks in conjunction with the −105 volts supplied from the junctors causes the gas diodes between the marked secondary switch inlets and the junctor outlets to fire, to conduct at low current and thereby to mark the associated junctors with −40 volts again by virtue of the gas diode characteristic. As indicated by the shaded diodes in Fig. 10 a mark on line A results in marks on junctors 1, 2, 3 & 4 and thus reveals all the idle paths from line A through the line frame.

In a similar manner the +80-volt mark applied to trunk B results in the firing of the diodes along the idle paths from this trunk to junctors 2, 4 and 7. The path to junctor 5, which is in use on the connection between line C and trunk D, is not marked in this case. The −24 volts presented by junctor 5 on its trunk control lead is not sufficient when combined with the +20-volt mark on the trunk primary-secondary link which leads to this junctor to fire the associated crosspoint diode.

For this desired connection there are two possible paths, either through junctor 2 or through junctor 4, as indicated by the −40-volt marks existing on both the line and trunk sides of these junctors. Selection between these paths is automatically accomplished by use of a lockout circuit which is common to all junctors serving the same line frame.

It is known that if a conduction path through a negative resistance gas tube is provided with a load impedance of proper value which is common to a similar conduction path through one or more other similar gas tubes, only one tube will ionize and remain ionized even if firing potentials are applied to several tubes either simultaneously or in sequence. Such a circuit employing two or more gas tubes with a common load impedance functions as a lockout circuit. The phenomenon is due to the region of negative resistance in the characteristics of the gas tube through which the tube current passes in the range between the breakdown and sustaining voltages. In this region as the current through a tube increases, the voltage across the tube decreases, tending to prevent other tubes with the common load from firing. To reduce the possibility that two

tubes fired simulatneously will then travel through this unstable region exactly together, an inductive element is used in the common load circuit. This increases the time interval required to traverse the unstable region thereby permitting differences between tubes to result in lockout.

In each junctor a five-element cold-cathode gas tube is used for path detection and selection. One control element of this tube is marked from the line side and other control element from the trunk side of the junctor if this junctor is usable in the call being set-up. The main anode is connected, together with those of the other junctors of the same line frame, in a lockout circuit so that only the gas tube in one junctor can conduct in its main gap. The junctor in which the gas tube does conduct in the main gap is the selected junctor and the switching network path associated with it is the selected path. Assume that junctor 2 is so selected. It first shorts out the resistors in its −105-volt supply leads. This permits a higher value of current to flow through the gas diodes along the selected path and causes the operation of the reed contacts associated with the crosspoint relay windings which are in series with the diodes. The control lead contact at each of these crosspoints, as shown along the selected path in Fig. 10, shorts out the gas diodes. With the diodes shorted out a further increase in the current operates relays in series with this control lead path in the line and junctor circuits. These relays cause the −105-volt supplies in the associated junctor, junctor 2 in this case, to be replaced by the −24-volt sources and the +80-volt marks on the line and trunk terminals to be replaced by ground. This shift of power sources permits gas diodes along paths marked but not selected for this call to extinguish but holds at a low power level the crosspoint relays along the selected path. With all diodes extinguished the switching network is ready for the next path selection operation. Removal of the ground at the trunk end of an established connection, at the end of conversation, results in complete release of the associated operated crosspoints and junctor.

With a central office traffic rate during busy hours of 50,000 calls per hour, 50 milliseconds is the maximum allowable holding time for a single common control ciruit at 70 per cent usage. A single control circuit, even during its busiest periods, should not be in use more than about 70 per cent of the time. If the usage is increased beyond this point the delays which other circuits encounter in attempting to use the common control circuit increase very rapidly. This produces the same effect as increased control circuit holding time.

The holding time of the control circuit for the switching network determines the traffic capacity of the switching arrangement if only a

single control circuit is provided. The control circuit holding time, in turn, consists of three parts: operate and release times of connector relays, line testing and "marking" times, and the operate time of the switches and junctors. The average holding time for the control circuit of the switching network for the system described was about 40 milliseconds. This is considerably shorter than the maximum 50 milliseconds permissible under the heavy traffic conditions of the preceding paragraph.

SYSTEM OPERATION

An experimental skeletonized ECASS constructed for laboratory tests is shown in Fig. 11. The equipment is located on these frames from left to right as follows: Frame No. 1, line and originating actuator circuits, switching network and controls; Frame No. 2, trunk, outward actuator and number group circuits; Frame No. 3, originating receiver circuits; Frame No. 4, power supplies; and Frame No. 5, terminating receiver circuits.

Without further detailed description of the various component circuits the successful placing of a call through the system may now be traced by reference to the block diagram of Fig. 12.
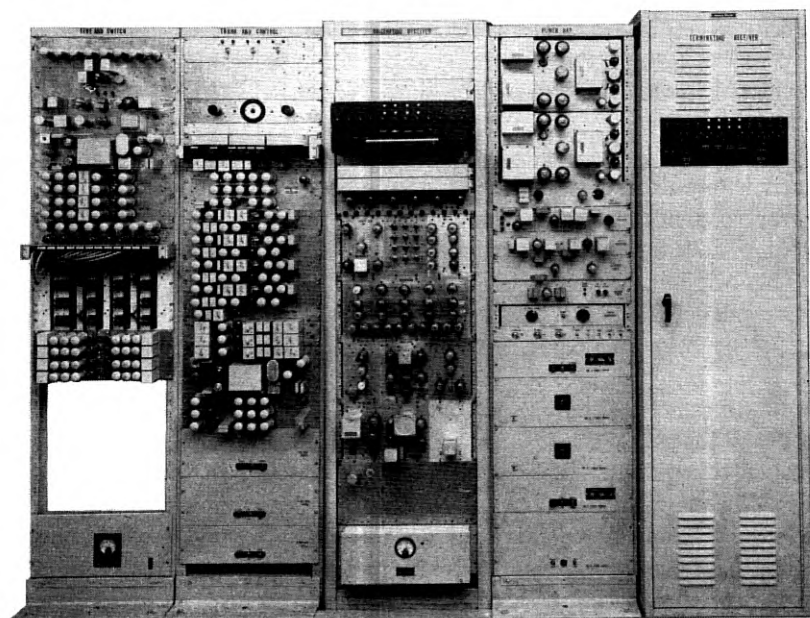

Fig. 11—Skeletonized laboratory model of ECASS.

A subscriber in originating a call first pre-sets the complete called line number on the finger wheels of his subset. The subset has been "latched" in the signaling condition by the mechanical reset on hanging up after the previous call. When the subscriber then removes the handset of his telephone from its cradle a line relay in the central office operates in recognition of a demand for service. The line relay in turn energizes a start gap of an associated cold-cathod gas tube. The gas tubes for a group of lines are connected in a lockout arrangement such that only one gas tube at a time can conduct in a main gap. When the tube does conduct in the main gap it operates a relay which connects the associated line directly to a common originating actuator and receiver circuit. During the short period that one line is attached to the receiver, originating service is withheld from all other lines in the same group but incoming calls may be terminated to any idle line.

The name, actuator, in this system refers to a circuit which includes an amplifier for transmitting 50-cycle current to a subscriber's subset over the simplex. This current is maintained at a constant amplitude despite the differences between various subscriber loops and the possible presence of earth potentials by the high output impedance of the amplifier. This high output impedance is obtained by the use of 35 db of feedback from the output of the amplifier. In addition, the actuator circuit also monitors its 50-cycle current flow when connected to a subscriber loop as the means of maintaining supervision since no direct current is permitted in the loop during the signaling period. The 50-cycle current in the subscriber's set causes the complete pre-set number to be generated repetitively as pulse position dialing signals which are returned to the receiver circuit in the central office over the loop. The use of simplex power to generate loop signals was adopted to simplify the filtering problem at the receiver circuits.

The originating receiver detects the dialing signals including the occurrence of the blank interval between repetitions of a complete number. It decodes the signals representing the first three digits following the blank interval, i.e., the called office code, and registers these digits unless the check circuit indicates that another trial is necessary. The action of the check circuit has been described in the Signal Receiver section of this paper. The receiver ignores the signals representing the called line number. Upon the successful registration of the called office code the originating receiver connects to the trunk number group circuit.

The name, number group circuit, in this system refers to a circuit through which a connection may be made to the switching network appearance of the control lead of any of a group of trunks or lines. In

the trunk number group a matrix of cold cathode gas tubes combines the three digits of an office code to establish a single lead control path to the equipment appearances of the trunks. This translator feature permits an arbitrary assignment between trunk locations and directory listed office codes. Another circuit, the subscriber number group, similarly includes translation of a called line directory number into the switching network line equipment number. Over such a control path a test is made of the idle, busy, or vacant condition of any designated trunk or line, and this same control path is used, together with other control leads to the switching network, to establish a connection through the switching network to this trunk or line.

If the test through the number group discloses an idle trunk, the control terminal of the trunk appearance on the reed-diode switches is "marked" with voltage over the same busy-testing path and the control lead of the calling line appearance is similarly "marked" over a path extending through the receiver-actuator connector. These marks from opposite ends of the switching network cause the selection of an idle junctor located in the connecting leads between line and trunk frames. The selected junctor in turn functions to make the marks effective in operating the switch crosspoints of all four switch stages as described
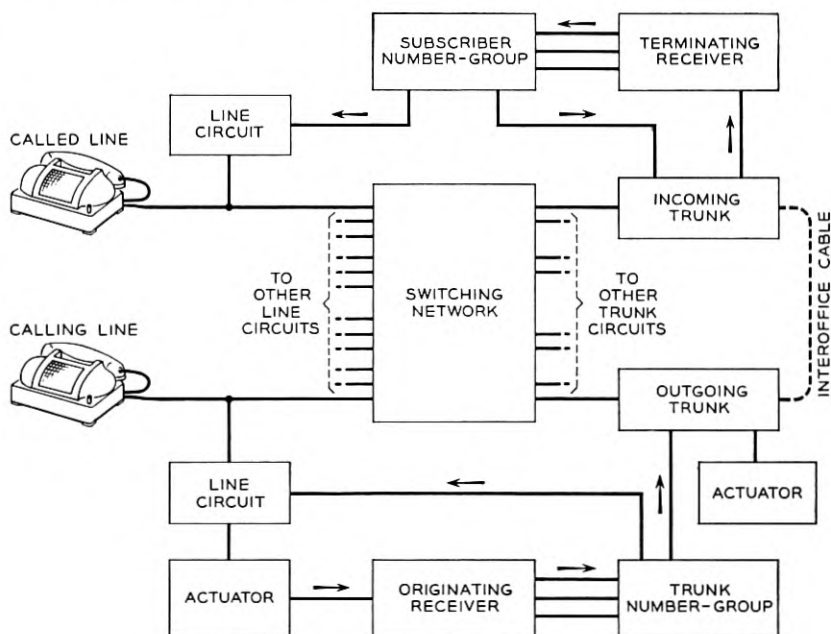

Fig. 12—Block diagram of ECASS.

in the section on Switching Network. The marking and switch operating voltage is applied to the line terminal of the switches through a line cut-off relay, which operates on the increased current which flows in this circuit immediately after the diodes in the switch crosspoints have been shorted out. The operation of the line cut-off relay releases the originating actuator and receiver which were connected through back contacts of this relay and, in turn causes the release of the trunk number group.

The next step is to send the called line number over the outgoing trunk so that the distant office may complete the connection to the called subscriber. An outward actuator is provided for this purpose. A relay in series with the marking path in the outgoing trunk circuit operates to connect the outward actuator directly to the trunk. The trunk-to-actuator connector circuits include gas tube lockout to insure that only one trunk is connected to the actuator at a time. During the short delay of awaiting an actuator that may occur during heavy traffic periods the established switching network connection is held under control of direct current supervision from the trunk circuit. The outward actuator, when connected, transmits 50-cycle current through the switching network to the calling subscriber's subset and maintains the connection by monitoring the 50-cycle current flow. This 50-cycle current causes the subscriber's set to transmit again the called number repetitively through the switches and outgoing trunk to the associated incoming trunk at the called office. In this paper it is assumed that all other offices connecting to this one are of the same type as this one or are arranged to transmit and receive, when required, the signaling pulse code used in this office. The arrangements in this office for completing incoming calls, including calls originating within this office itself, are shown in Fig. 12.

Operation of the connector relay which connects the outgoing trunk to an actuator signals the incoming trunk circuit in the terminating office to connect to an incoming receiver circuit for receiving the repetitive dialing signals. Connection between the incoming trunk and signal receiver is made through a lockout circuit which insures that only one trunk is connected to the receiver. When the incoming receiver has absorbed the office code, registered the called line number and checked the registration, it causes the incoming trunk to transmit a reverse battery pulse to the outgoing trunk as a number-received signal. This reversal causes the outgoing trunk to dismiss the outward actuator and to trip the latch in the subscriber's subset to the talking position with direct current talking and supervisory battery supplied from the outgoing trunk. At the same time the incoming receiver connects to the subscriber number group for making an idle-busy-vacant test of

TABLE I

Connecting Times	Milliseconds
1. Calling line off-hook to connection to outgoing trunk......	180
2. Incoming trunk seizure to ringing of called line...........	200
Total time to establish a call........................	380

Holding Times	Milliseconds
1. Originating receiver......................................	165
2. Trunk number group.....................................	38
3. Switching network control (each usage)...................	14
4. Outward actuator.......................................	291
5. Terminating receiver....................................	184
6. Subscriber number group................................	38

the called line and for "marking", if idle, the called line control terminal appearance on the reed-diode switches. At the time of this test, a voltage "mark" is applied to the incoming trunk control lead appearance also. As before, these two "marks" from opposite ends of the switching network cause the selection of an idle junctor and in turn the operation of the reed crosspoints in the four switching stages along the selected path. The "marking" voltage is applied to the incoming trunk terminal of the switches through the winding of a relay which, operating immediately after the crosspoints, causes the release of the incoming receiver and places the switching connection under joint supervision of the called and calling subscribers. The line cut-off relay whose winding is in series
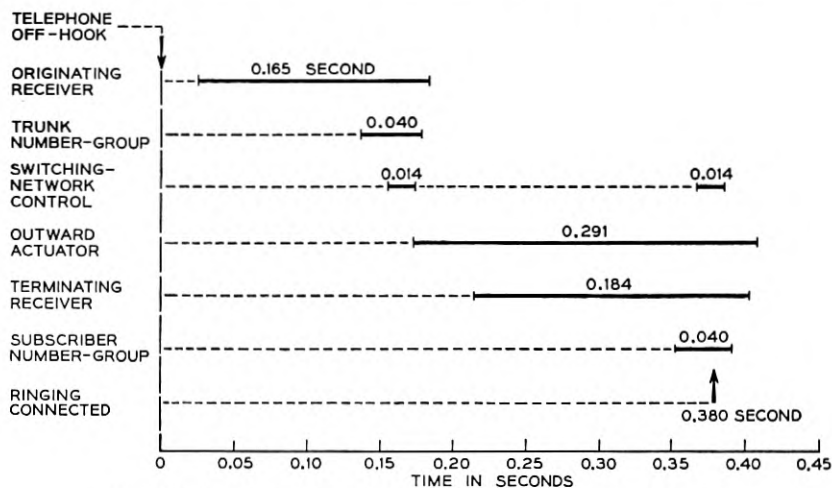
Fig. 13—Operating sequence based on average holding times.

with the marking path to the line appearance on the switches operates to remove the line relay and other originating apparatus from the called subscriber's line.

Based on the result of the idle-busy-vacant test of the called line, the incoming register circuit either sets the incoming trunk to provide ringing to the called subscriber upon closure of the crosspoints and ringing tone to the calling subscriber if the called line is idle, or sets the trunk to return busy tone to the calling subscriber if the called line is busy or vacant. In the latter case the incoming receiver is released immediately without setting up a terminating connection through the switches.

Since connections in the same reed-diode switching network are established through either of two number group circuits, lockout is provided between the originating receiver to trunk number group connector and the terminating receiver to subscriber number group connector so that only one number group circuit can be in operation at a time.

Some of the important average time intervals as measured in this system are given in Table I and shown graphically in Fig. 13.

CONCLUSION

The electronically controlled automatic switching system described in this paper was designed for large central offices and a skeletonized laboratory version has been built, tested and demonstrated. Successful operation at the speeds required was obtained. No failures of the gas tube lockout circuits were observed under the various combinations of possible simultaneous seizure. The experimental system shows that a large heavy traffic office could be made to operate on a one-at-a-time basis with advantageous reduction in the number of control and connector circuits. Many of the necessary components employed in this system for one-at-a-time operation are now available in a pre-development state and will probably be used in commercial systems. However, the commercial design and production of a complete office as described here is not economically competitive with existing systems since the subscriber subset and line circuit which are used in large numbers are too complex and expensive.

New Techniques for Measuring Forces and Wear in Telephone Switching Apparatus

By WARREN P. MASON AND SAMUEL D. WHITE

(Manuscript received February 15, 1952)

One of the main problems in obtaining long life in telephone switching equipment is the wear caused by large momentary forces. In order to investigate this problem several new techniques have been devised for measuring normal and tangential forces and for producing and controlling normal and tangential motions for wear studies. The forces are measured by inserting small barium titanate ceramics between the points of application of the forces and observing the voltages generated on a cathode ray oscillograph. Barium titanate ceramic is about fifty times as sensitive as quartz and has a high enough dielectric constant so that with conventional amplifiers time intervals as long as a tenth second can be measured. Both normal and tangential forces can be measured by using properly poled ceramics. By using weights on top of the crystals, normal and tangential accelerations can be measured. With these ceramics, forces have been measured for relays and for frictional sliding of a wire over a plastic. By employing a barium titanate transducer capable of a large amplitude at 18,000 cycles it has been shown that no wear occurs for normal forces, and that all the wear observed in a relay is due to tangential sliding. Quantitative measurements of wear have been made for a variety of materials, and it has been shown that materials with a large elastic strain limit will wear better than materials with a small elastic strain limit even though the latter have a higher yield stress; materials such as plastics and rubber will outwear materials such as metals or glasses.

As the length of slide is reduced there is a threshold of motion for which there is no gross slide and very little wear. This region is determined by the condition that the tangential force is smaller than the normal force times the coefficient of friction. Theoretical and experimental results are obtained for this region and an equation is derived which determines the possible displacement without gross slide. The stress strain curve occurs in the

*form of a hysteresis loop whose area varies approximately in proportion
to the square of the strain amplitude. This region is important for relays
for by introducing damping, long repeated vibrations—which are respon-
sible for considerable wear—are quickly brought down to the low wear, no
gross slide region with a corresponding reduction in wear. The mechan-
ical resistance associated with the stress strain loop is of the same type that
occurs in an assemblage of granular particles such as in a telephone trans-
mitter where the motion is small enough so that no gross slide occurs.*

I. INTRODUCTION

In obtaining long life in telephone equipment such as relays, switches,
selectors and other mechanical devices subject to large momentary
forces, one of the main problems is the wear encountered in various parts.
This is particularly true in such small motion devices as relays where
even a few mil inches of wear increases the distance that the armature
has to travel and may eventually cause the relay to fail to make contact.
To obtain a design objective of one billion operations requires a very
careful minimizing of deleterious forces and a careful selection of the
best wearing materials.

As a step toward investigating this problem several new techniques
have been devised for measuring normal and tangential forces and for
producing and controlling normal and tangential motions for wear
studies. These methods have been applied to relays and have given
considerable information on the types of motion to be avoided and on
the best types of materials to select for various parts of the relay to ob-
tain long life. Specifically they have shown that normal forces cause
very little wear and that tangential sliding of one part over another is
the principal cause of wear. Fortunately, by designing the motion of
the armature and contacts correctly, tangential sliding can be largely
eliminated with a corresponding reduction in wear.

To aid in the quantitative evaluation of wear produced by tangential
sliding two devices have been used. One is an electromechanical vibrator[1]
driven at 500 cycles per second which is capable of several mil inches
of motion and the other is a barium titanate longitudinal vibrator
coupled to a metal "horn"[2] which is capable of a two mil inch motion
at 18,000 cycles. Wires connected to these transducers are dragged over
materials whose wearing properties are to be tested. The normal forces
between the wire and material are varied as well as the length of the
stroke. The wear by both methods is comparable showing that the ac-
celerated wear testing method gives about the same wear as the slower

method. With the barium titanate transducer a billion cycles can be obtained in 17 hours and a very rapid wear test is obtained.

If lubrication is not used, wear tests show that materials having a large elastic strain limit will in general wear better than materials which have a smaller elastic strain limit even though the latter may have a higher yield stress; materials such as plastics and rubbers will outwear materials such as metals and glasses. The volume of wear for one billion operations is porportional to the product of static force times the length of the stroke. The initial rate of wear is several times as large as the final rate. Calculations show that only about one part in 10^9 of the energy goes into producing wear, the rest going into heat production.

As the length of slide is reduced, calculations and measurements show that there is a threshold of motion for which no gross slide occurs. This condition occurs when the tangential force is less than the product of the normal force times the coefficient of friction. The limiting displacement for no slide increases as the two-thirds power of the normal load and inversely as the two-thirds power of the shear stiffness. Hence a heavily loaded material with a small shear elastic constant—such as rubber—will have a large displacement for which no slide occurs, and hence will wear considerably better than a stiff material such as a metal. Wear tests in the region of no gross slide show that the rate of wear is considerably less in proportion to the energy dissipated than in regions of gross slide.

A quantitative experimental and theoretical study of the region of no gross slide has been made.[3] Experimentally the results have been obtained by moving a glass lens with a large radius of curvature on both surfaces between two glass lenses when the lenses are pressed together with known normal forces. It was shown theoretically that slip should occur between these lenses over a circular annulus and experiments verify this prediction quantitatively. Force-displacement curves have been measured and it has been shown that the relation is a hysteresis type loop whose area varies approximately as the square of the strain amplitude. The small wear observed is related to the wear found in ball bearings, where no gross slide occurs. This region is important in relays for by introducing damping, long repeated vibrations—which are responsible for considerable wear—are quickly brought down to the low wear, no gross slide region with a corresponding reduction in wear. The mechanical resistance associated with the stress strain hysteresis curve is of the same type that occurs in an assemblage of granular particles such as in a telephone transmitter, where the motion is small enough so that no gross slide occurs.

II. METHODS FOR MEASURING NORMAL AND TANGENTIAL FORCES

In order to investigate the performance of a mechanical device and the causes of wear in it, it is desirable to be able to measure the forces occurring in various parts of the device. To measure the complete performance it is necessary to measure not only the slowly applied forces but also the very short time dynamic forces that occur when various parts of the device impinge on each other.

The most common method for measuring such forces is by means of a piezoelectric crystal such as quartz. Quartz, however, has the disadvantage that it is not very sensitive and also that it has such a low dielectric constant that the input impedance of any amplifier associated with it has to be prohibitively high if forces varying as slowly as a one-tenth of a second are to be measured. Since the impedance of the oscillograph or amplifier is usually lower than that of the crystal, the crystal having the greatest sensitivity will be the one which generates the most charge for a given force, which corresponds to the crystal having the largest d piezoelectric constant. Table I shows a tabulation of the d constants for compression and shear for several of the most common piezoelectric crystals and for the ceramic barium titanate. The dielectric constants are also given.

Of these materials the only ones that have sufficient mechanical strength to withstand the mechanical shocks they are subjected to in the measurements of forces are quartz, tourmaline and barium titanate ceramic. The crushing strength of the ceramic has been found[4] to be from 60,000 to 80,000 pounds per square inch. From the values of the d piezoelectric constants it is seen that the barium titanate ceramic is about 50 times as sensitive as quartz or tourmaline and it is possible to use small pieces of the ceramic to work directly into cathode ray oscillo-

TABLE I

Crystal	Compression Constant in cgs units	Shear Constant in cgs units	Dielectric Constant
Quartz.......	$d_{11} = 6.76 \times 10^{-8}$ stat. coulombs/dyne	$d_{26} = 13.5 \times 10^{-8}$ stat. coulombs/dyne	4.55
Tourmaline..	$d_{33} = 5.5 \times 10^{-8}$	$d_{15} = 10.9 \times 10^{-8}$	8.0
ADP.........	$d_{31}' = 74 \times 10^{-8}$	$d_{36} = 148 \times 10^{-8}$	15.6
Rochelle Salt Y Cut......	$d_{21}' = 84.5 \times 10^{-8}$	$d_{25} = 169 \times 10^{-8}$	11.1
EDT.........	$d_{21} = 34 \times 10^{-8}$	$d_{36} = 50 \times 10^{-8}$	8.0
Barium Titanate Ceramic......	$d_{33} = 300$ to 400×10^{-8}	$d_{36} = 500$ to 650×10^{-8}	900 to 1500

graphs with the use of only the amplifiers that are included with such oscillographs. To work down to time intervals in the order of one-tenth second, the leakage resistance of the load across the polarized ceramic—which for small sizes may have a capacitance as low as 20-micro-micro-farads—has to be higher than is usually available in oscillographs. Fig. 1 shows a vacuum tube circuit[5] capable of giving a 750-megohm input resistance and when used with a barium titanate ceramic having a capacity of 20 $\mu\mu$f, allows measurements of forces for time intervals up to 0.015 seconds with no corrections. This time is usually sufficient to obtain all the force variations in a relay operation. The upper frequency limitation in the measurements of forces is caused by the setting up of natural vibrations in the ceramic block. The lowest frequency vibrations that can be set up in a ceramic block are the flexural vibrations. For a block 0.04 inch x 0.04 inch in cross section and 0.02 inch thick, such as have been used in relay force measurements, the lowest flexural frequencies are in the order of 1.6 x 10^6 cycles. The next lowest frequencies are the radial mode vibrations[6] which have frequencies above 4 megacycles for the block considered. Hence the measurements of force should be valid up to times in the order of a microsecond.

The properties of barium titanate and their stability with time and with large voltages applied in the opposite direction to the poling voltage depend to a large extent on the method of baking the ceramic and on
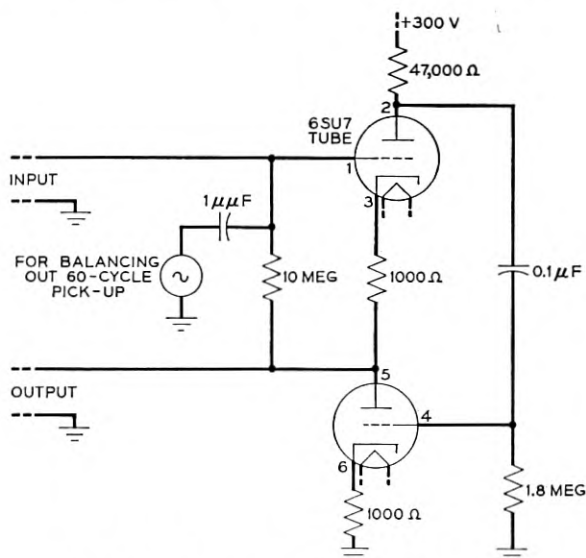
Fig. 1—High input resistance amplifier tube.
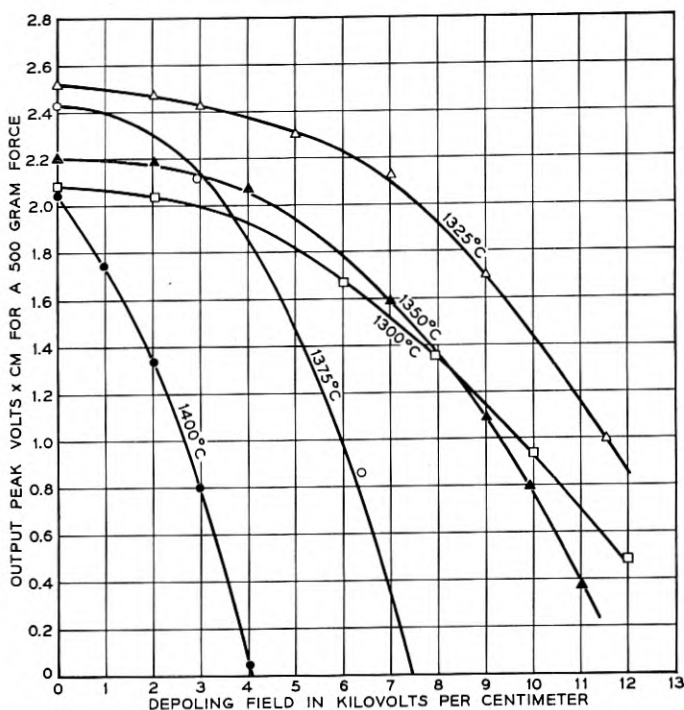
Fig. 2—Open circuit voltage for 500 grams force for normal barium titanate under depoling voltages.

the effect of additives. The data of Fig. 2 show[7] the effect of firing temperature on the initial open circuit voltage for sample disks 0.775 cm in diameter and approximately 0.15 cm thick. The variation of voltage with thickness and area was taken account of by multiplying the measured voltage by the area and dividing by the thickness.

The open circuit voltage was measured by using the circuit of Fig. 3. A barium titanate cylinder and metal horn described in a previous paper,[2] vibrating at 18,000 cycles, strikes the sample a blow at its central position. The voltage generated is applied to the input of a high resistance tube similar to the one shown by Fig. 1, and then actuates a cathode ray tube. The voltage corresponding to the height of the peak is calibrated by putting a known voltage in series with the ceramic across a small resistance R and hence the magnitude of the open circuit voltage can be quantitatively determined. The value of the mechanical blow applied to the polarized ceramic can be adjusted by controlling the drive on the ceramic cylinder. With the feed back circuit described in the

previous paper,[2] this value can be held very constant and can be controlled by controlling the bias on the limiting device. The magnitude of the force can be determined by comparing the voltage with that obtained by suddenly lifting a weight off the ceramic and has been adjusted to equal 500 grams. The voltages shown then correspond to the open circuit voltages generated by applying 500 grams to a point at the center of the ceramic.

As shown in the appendix, the effect of applying a force at a point in a ceramic is not the same as that caused by distributing the force uniformly over the surface due to the fact that radial strains are generated and these act through the radial piezoelectric constant to reduce the value generated by the thickness piezoelectric constant. It is shown that the point application of stress generates only 40 per cent as much as would
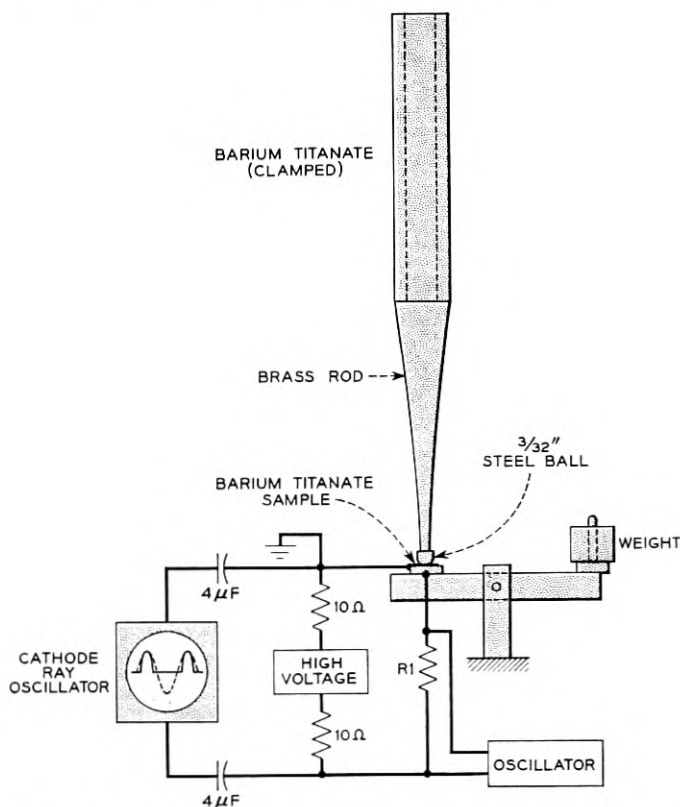
Fig. 3—Circuit used to measure open circuit voltages for barium titanate samples.

be generated in a disk with the stress applied uniformly. With this factor the open circuit voltage per unit of force—which determines the effective g_{33} piezoelectric constant of the ceramic—agrees well with that obtained by other methods of measurement. For the most desirable ceramic obtained for the 1325°C baking temperature the value of g_{33} equals

$$g_{33} = 3.25 \times 10^{-8} \frac{cm^2}{\text{stat-coulomb}} \text{ in c.g.s. units} = 0.98 \times 10^{-2}$$

$$\frac{\text{meters}}{\text{Newton}} \text{ in m.k.s. units} \qquad (1)$$

The dielectric constant ε of this material is about 1500 so that the d_{33} piezoelectric constant is

$$d_{33} = \frac{g_{33}\varepsilon}{4\pi} = 390 \times 10^{-8} \frac{\text{stat-coulombs}}{\text{dyne}} = 130 \times 10^{-12} \frac{\text{coulombs}}{\text{Newton}} \quad (2)$$

Since for some applications in this paper, high voltage gradients of opposite sign to the poling voltage are applied to the ceramic, it is a matter of importance to find out whether the ceramic will become depoled by the action of this voltage. To test out this feature the circuit of Fig. 3 is equipped with a high voltage generator, which is applied to the ceramic through 10-megohm resistors and the high voltage is kept out of the measuring circuit by 4-microfarad condensers. The procedure was to apply a negative voltage for 3 minutes, then to recalibrate the voltage due to impact. This was repeated with a higher voltage each time until the range was covered.

The curves of Fig. 2 show that there is an optimum baking temperature for a large coercive field. Above this temperature larger sized crystals grow in the ceramic and the coercive field decreases markedly. It is thought that the smaller crystal size corresponds to a more strained condition in the individual crystallites and it requires a higher field to overcome the mechanical bias and change the direction of the ferroelectric axis. A similar condition[8] has been found by x-ray techniques for single crystals where it has been found impossible to make a single domain out of a multidomain crystal by the application of a field, if the crystal is too highly strained.

The effects of additives are also very marked on the properties of the polarized ceramics. It has previously been reported[9] that the addition of 4 per cent of lead titanate to the commercial barium titanate increases the coercive field. This is confirmed by the curves of Fig. 4 which show

the open circuit voltage for a 4 per cent lead titanate barium titanate ceramic for various baking temperatures and negative biasing voltages. The optimum temperature for a small grain size structure is lowered about 50°C by the addition of the lead titanate. As can be seen the coercive field is considerably increased and it appears safe to use a negative field of 6000 volts per centimeter without any depolarization. In Section IV a system is described for which an ac voltage of this magnitude was successfully used for many days with no change in sensitivity of the ceramic. The open circuit piezoelectric constant for the optimum ceramic of Fig. 4 is

$$g_{33} = 3.82 \times 10^{-8} \frac{\text{stat-coulombs}}{\text{dyne}} = 1.15 \times 10^{-2} \frac{\text{meters}}{\text{Newton}} \qquad (3)$$

Since the dielectric constant is about 1000, the effective d_{33} piezoelectric constant is about

$$d_{33} = 310 \times 10^{-8} \frac{\text{stat coulombs}}{\text{dyne}} = 104 \times 10^{-12} \frac{\text{coulombs}}{\text{Newton}} \qquad (4)$$

Another property of interest is the stability of the piezoelectric properties of the ceramic over a long period of time. While no very good comparisons have been made between the various baking conditions and between barium titanate with and without additions, some long time measurements have been made on four samples of the optimum 4 per cent lead titanate used in the transducer of Fig. 3. Over a period of two years during which they have been continuously used in a calibrated oscillator, the calibration has not changed noticeably, i.e. less than 5 per cent. On account of the superior voltage and time stability of the lead titanate, barium titanate mixture, all of the elements used have had this composition.

Two types of units have been used for force measurements, one type that responds to normal forces and the other to tangential forces. The type responding to normal forces as shown by Fig. 5 is poled in the thickness direction which is also the direction in which the force is applied. The sensitivities for forces applied at points are given by the values of Fig. 4. For example for typical units having the dimensions 0.1 cm by 0.1 cm in cross section and 0.05-cm thick will produce an open circuit voltage of 2.7 volts for 100 grams applied to the ceramic. Such ceramics have been used in measuring the dynamic forces when various parts of the relay close or open. Fig. 6(a)[10] shows the voltage generated when the two relay contacts come together. The dynamic stress is somewhat higher than the static stress and varies with time due to mechanical
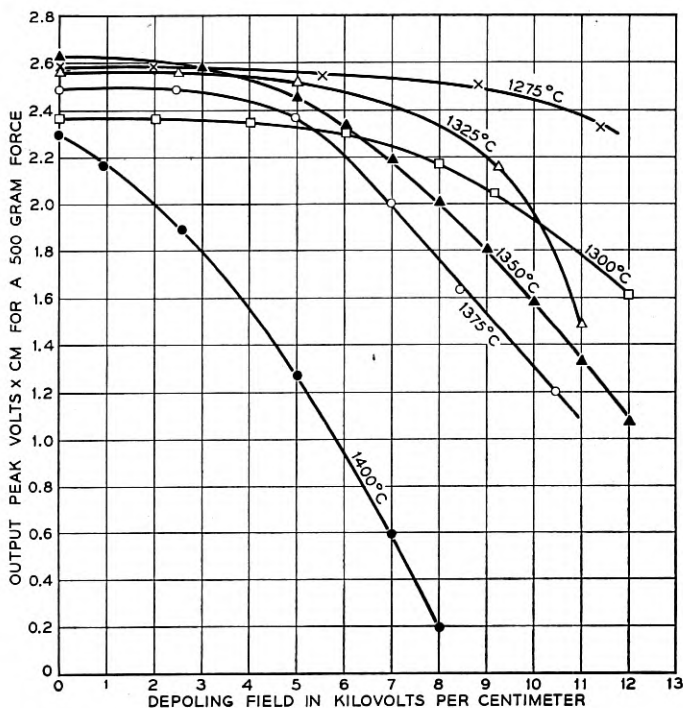
Fig. 4—Effect of 4 per cent lead titanate on the open circuit voltages generated for 500 grams force, and for depoling voltages.

vibrations of the relay structure. Fig. 6(b) shows the forces produced by opening the contacts. The large spikes are due to wire vibrations. By using such ceramics in various parts of the relay the points of high stress can be located.

The second type of structure which responds to tangential forces is poled as shown by Fig. 5 so that the poling direction lies along the direction for which the tangential force is applied and perpendicular to the
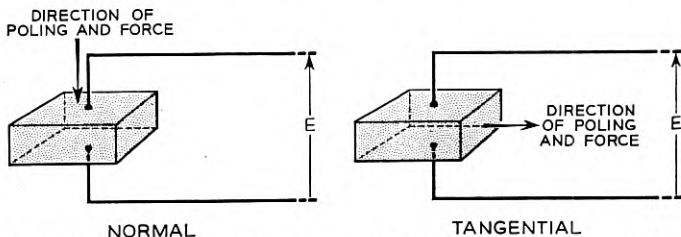
Fig. 5—Methods for polarizing barium titanate to respond to normal and tangential forces.
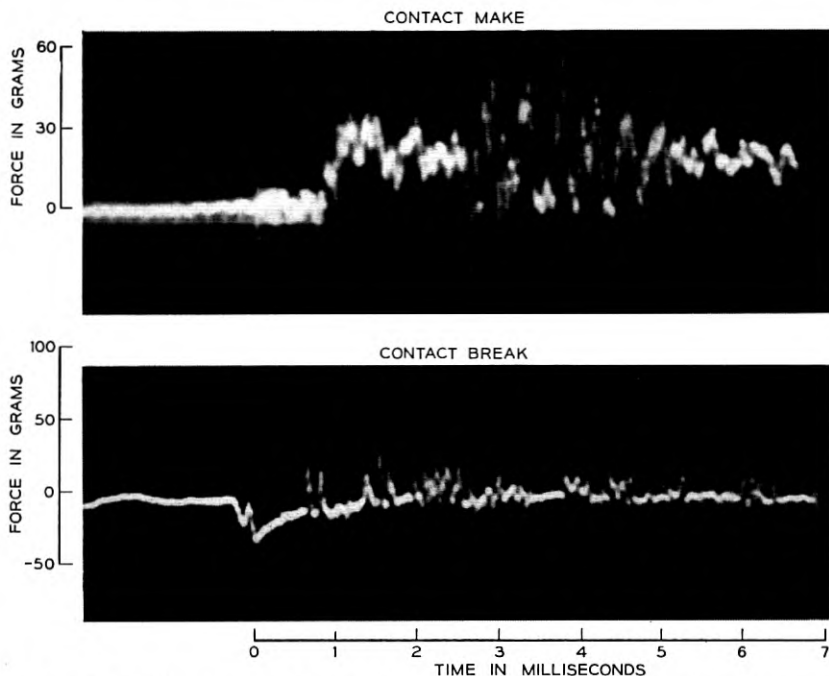
Fig. 6—Oscillograph tracings of forces generated in make and break operations.

direction of the electrodes. In this process, the crystal is first poled, after which the poling electrodes are ground or etched off and electrodes perpendicular to the poling direction are put on by using a polimerizing cement in which silver dust is mixed. The cement serves not only as an electrode but also holds the ceramic in the desired place. Fig. 7 shows an arrangement used for studying frictional forces. A small ceramic 0.1 by 0.1 cm in cross-sectional area is glued to a metal base while a thin specimen of the material whose frictional forces are to be studied is glued to the top surface. The forces caused by a wire drawn over the surface are transmitted to the crystal and generate a voltage which appears on the oscillograph. Pictures of such force generated voltages are

Fig. 7—Experimental arrangement for studying frictional forces.

shown by Fig. 9 of the next section and are discussed there. The sensitivity of this type of unit is higher than that for the normal force measuring unit. As shown in the appendix, the voltage generated is independent of the area of application and is about 9.7 volts for a unit the same size as discussed above which gave 2.7 volts for 100 grams applied at a point.

By placing weights on the upper surfaces both types of units can be used as accelerometers. They are cemented to the surface whose acceleration is to be measured and the force applied is equal to half the mass of the ceramic plus the added mass times the acceleration. By putting weights on the shear pickup ceramic types, tangential accelerations can be measured in the direction of the poling. By using three such accelerometers, the normal and two tangential components of acceleration of any surface can be measured.

III. METHODS FOR INVESTIGATING CAUSES OF WEAR

Wear in various parts of a relay is the limiting factor when a very large number of relay operations are desired. This wear opens up the spacing between contacts and causes the relay to lose its adjustment over a course of time.

A. *Force Measurements and Wear Caused by Normal Forces*

Since the forces operating on a material can be divided into normal and tangential forces, it appears desirable to separately determine the effects of each. Normal forces were produced by using the barium titanate, metal horn detail of Fig. 3. With a steel ball on the end of the metal horn, and a barium titanate specimen glued to the pivoted arm, the peak forces in grams are plotted against the volts used to drive the titanate unit for various static forces in Fig. 8. The pattern of voltage is approximately a rectified sine wave, since the ball is out of contact with the measuring titanate a part of each cycle. To observe the wear caused by normal forces a piece of material to be studied was glued to the pivoted arm on top of the barium titanate and the force was adjusted to the required value. For forces in the order of those measured in relays no wear at all was observed over a period of 18 hours which corresponds to a billion impacts, since the number per second is 18,000. For larger impulsive forces, it was found that the result of 60-million impacts against an insulator such as a phenolic was to produce a pit only a few tenths of a mil inch deep by a plastic flow. Since no wear of the type involved in relays was observed it was concluded that practically all of the wear was produced by tangential forces.
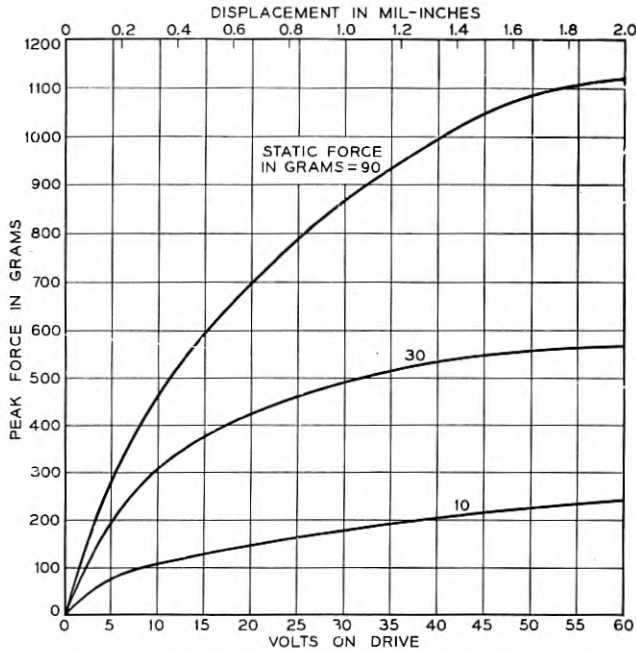
Fig. 8—Variation of normal impulse forces with drive voltages for three values of static force.

B. Tangential Force and Wear Measurements

To study the effect of tangential forces in producing wear, the transducer was mounted horizontally and the steel ball was replaced by a wire such as are used in some relays. The length of the wire was made short enough so that no lateral vibrations were generated and the motion was strictly tangential. Samples to be studied as shown by Fig. 7 were mounted on top of shear type ceramics which were glued to the pivoted arm in such a way that they responded to tangential forces applied perpendicular to the arm.

When a piece of A phenolic (which is a paper filled phenolic) was placed on top of the ceramic a series of oscillograph pictures were taken when the total displacement of the wire varied from 0.05 mil inch to 2.0 mil inches and the steady weight on the wire was 40 grams (0.0885 pound). These pictures are shown in Fig. 9. For amplitudes under 0.075 mil inch, the force is a good sine wave which increases with amplitude until the maximum force equals the product of normal force times the coefficient of friction. The force in this region is essentially elastic as is shown by the fact that the maximum force occurs at the time when

the maximum displacement of the wire takes place. Above this amplitude the wire begins to slip on the plastic and for a travel of 0.3 mil inch there are indications that the point of contact between the wire and the plastic has changed from one position to another. This agrees with the idea that friction is due to a definite bonding between points of contact of the two materials which is broken by their relative motion. New points of contacts are then made and a stick-slip process occurs. At 0.5-mil-inch motion a number of small contacts occur during the

LENGTH OF TRAVEL
IN MIL INCHES

0.05

0.075

0.10

0.15

0.30

0.50

0.75

1.0

1.5

2.0
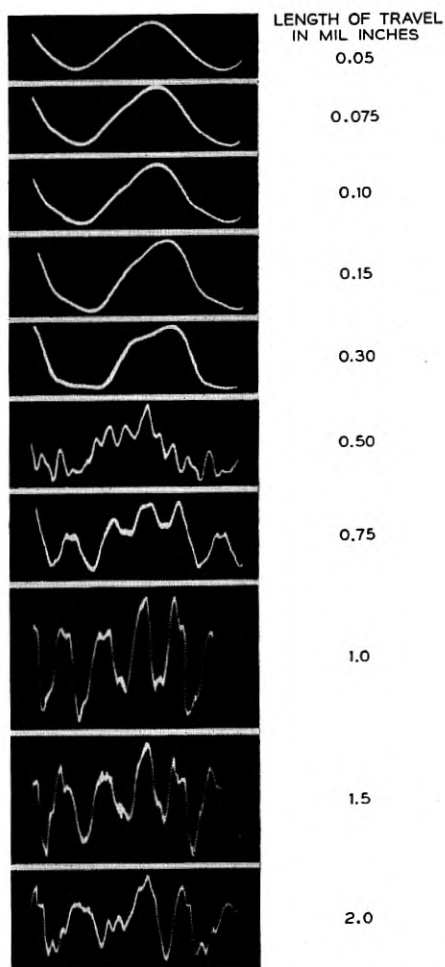
Fig. 9—Tangential forces measured for an 18,000 cycle oscillatory motion whose total displacements in mil inches are shown by the values given.
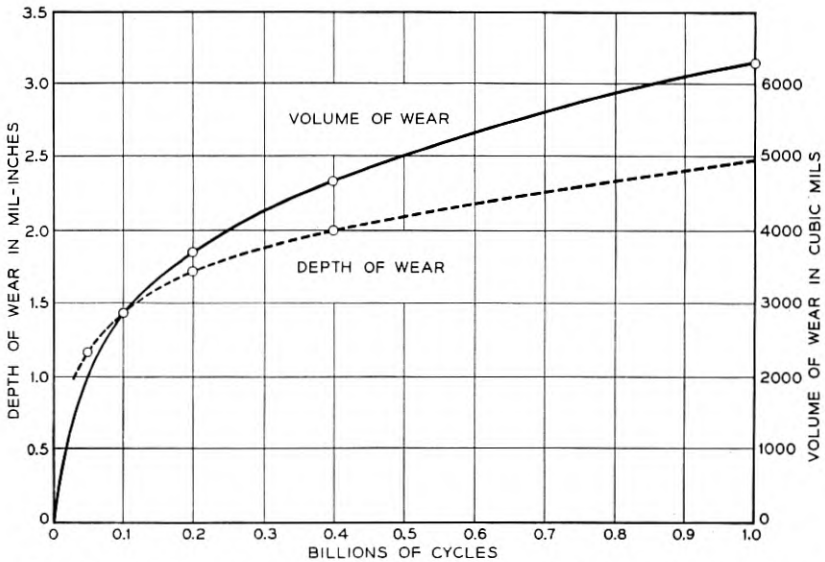
Fig. 10—Typical wear curve for A phenol fibre plotted as a function of the number of cycles.

travel. Since the picture is a trace of an oscillograph pattern which is being repeated 18,000 times a second and since a two second exposure is required to produce the picture it is obvious that the wire goes back and forth over the same points for a large number of times. Most of the energy is lost in producing elastic vibrations in the points of contact. These oscillations are produced by the bending of the areas of contact by the bonding force between them and by the motion. When the bond is broken the plastic forming the point is free to vibrate and the elastic energy goes into mechanical vibrations and eventually into heat. Since a pattern such as that for the 0.5-mil inch or the 0.75-mil inch displacement lasts unchanged for a number of minutes, it is obvious that very little of the energy goes into breaking the plastic points of contact and producing wear. This is confirmed by a rough calculation given later which shows that only about 1 part in 10^9 of the energy goes into producing wear. For displacements above a mil-inch motion it appears that groups of point contacts are broken at one time, and the pattern changes rather rapidly indicating that there is more wear at these amplitudes. Over a two-second interval the pattern is changing fast enough so that sharp pictures are not obtained.

Quantitative values of wear for various materials were obtained by running the barium titanate unit for various periods of time, different lengths of strokes and different normal forces. Fig. 10 shows a typical
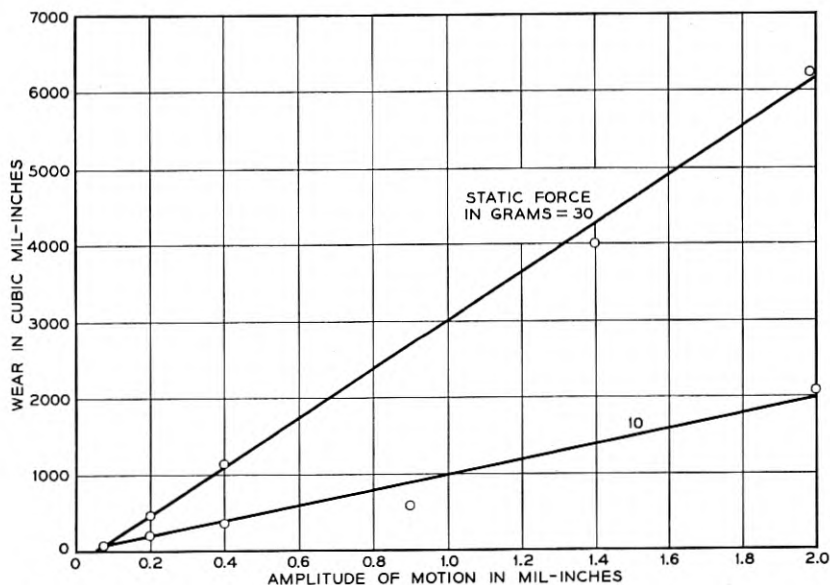
Fig. 11—Total wear for one billion cycles plotted against the length of stroke for two normal loads.

wear curve obtained for A phenolic (a paper filled phenolic) plotted as a function of the number of cycles. This wear was obtained by drawing a 0.025-inch nickel silver wire for a distance of 2.0 mil inches over the surface of the bar. The bar was $\frac{1}{4}$ inch wide. The normal force used was 30 grams (0.0665 pound). The wear was measured from the depth cut in the material and from this since the wire was round, the total volume of wear in cubic mil inches could be calculated. The rate of wear was faster at the start but approached a limiting rate with a large number of cycles.

A number of different lengths of stroke were employed and for the A phenolic the total wear for a billion operations is shown plotted by Fig. 11. The wear is approximately proportional to the slide but extrapolating down to small motions it appears that there is a threshold of motion below which the wear is very small. The values indicated are close to the no gross slide regions found from the force curves of Fig. 9 for both forces shown in Fig. 11. To check that the wear was definitely less in the no gross slide region an amplitude of motion of 0.075 mil inch for a normal force of 50 grams (0.11 pound) was run for a billion operations. The wear observed was so small that it could not be measured quantitatively, confirming the lower rate of wear in the elastic region.

Another type of wear measurement has also been employed. As shown by Fig. 12 the motor is a modification of the Western Electric 1A recorder, which was originally designed for cutting "hill and dale" phonograph records.[1] The moving system of this recorder consists of two coils (a drive coil and feedback coil) and a stylus, all rigidly coupled and coaxial. The drive coil is secured to the base of a cone shaped vibrating
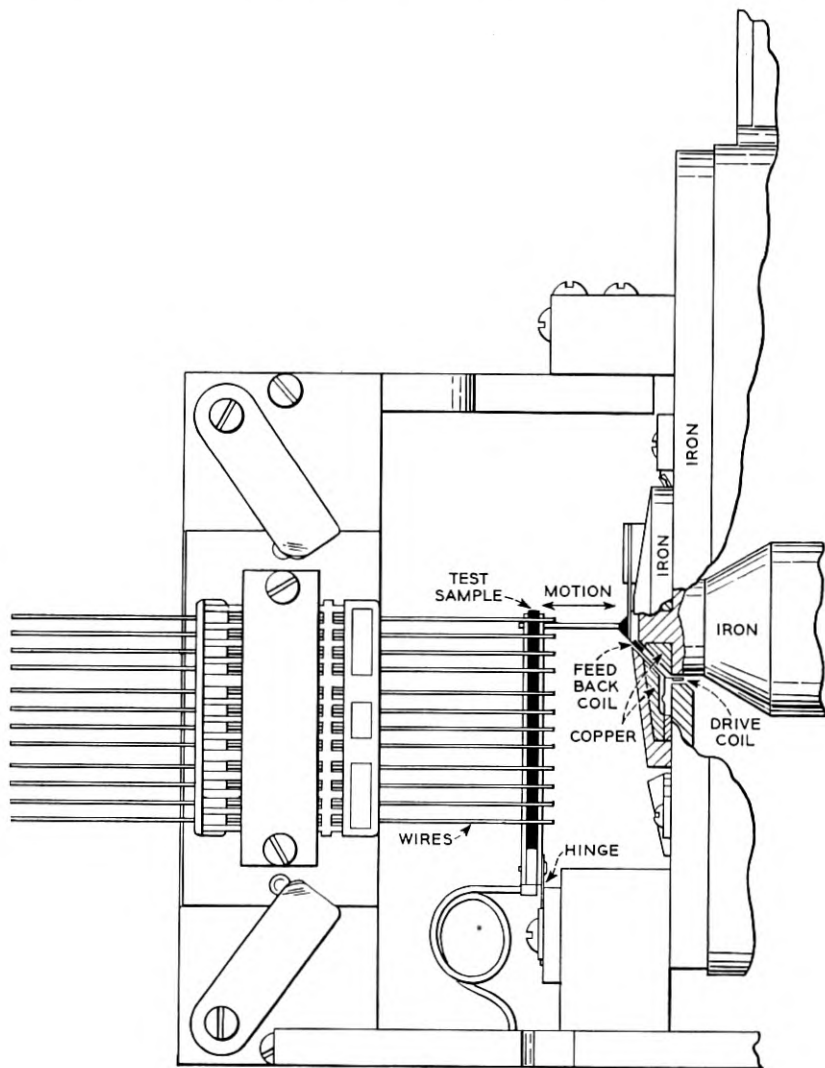
Fig. 12—Low frequency wear measuring device.

element which is carried at its base by a diaphragm and at its apex by cantilever springs. These furnish the restoring force and restrict the motion of the moving system to a single degree of freedom, motion parallel to the cone and coil axis. The second or feedback coil is secured to the cone near its apex, at which point the stylus or drive pin is attached. The coils move axially in annular air gaps polarized by a single magnet. In the space between the two coils, copper ring shielding (a shorted turn) is provided to minimize inductive coupling between them. The output of the driving amplifier is supplied to the drive coil, while the feedback coil is connected in proper (negative feedback) phase to the amplifier input.

The voltage generated in the feedback coil is proportional to the instantaneous velocity of the moving system, and by virtue of the negative feedback, the amplifier-recorder system becomes a high force, high mechanical impedance generator of mechanical motion, with the velocity very nearly proportional to the input voltage over a large range of frequency and mechanical load. Measurements of the voltage generated in the feedback coil provides a means of monitoring the velocity. Enough power capacity is present in the amplifier so that large changes in the load will not cause changes in the motion.

The samples of the materials to be tested for wear resistance are carried by a grooved aluminum beam, one end of which is hinged, the other being driven by the record stylus. The rubbing member, in this case 25-mil nickel silver wires, are tensioned against the test samples as they might be in switching apparatus. The wires can be removed for observation and measurements of the wear, and accurately replaced as the parts are dowelled together.

Fig. 13 shows a measurement of a number of materials for a normal force of 30 grams (0.0665 pounds) and a slide of 2 mil inches. The A phenolic, which is the same as that tested and recorded in Fig. 10 by the 18,000-cycle barium titanate transducer, produced essentially the same wear showing that the wear is approximately independent of the rapidity of motion for these materials. Nylon showed a rather erratic wear curve due to the fact that it has a low melting point and tends to ball up on the wires. This effect was considerably more pronounced at 18,000 cycles, where a very large indentation was found.

Only three materials show low wear at reasonably uniform rates out to a large number of cycles. These are C phenolic, a fabric filled phenolic, the B phenolic, a wood flour filled molding phenolic and the D phenolic, a cotton flock phenolic with graphite added. At lower forces and shorter slides the wear at 10^9 cycles is approximately proportional to the force
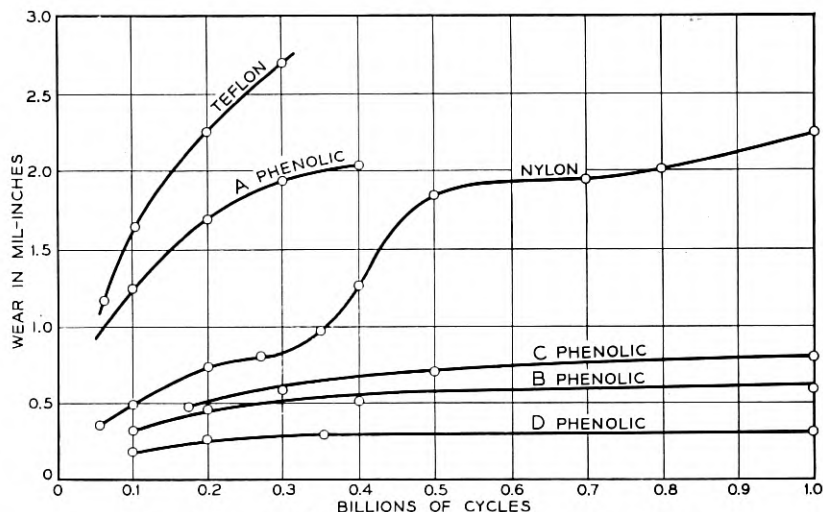
Fig. 13—Typical wear curves for a number of materials.

times the length of slide. Any of these three materials give sufficiently small wear to produce a long relay life, but the best performer under all conditions of force and slide appears to be the D cotton flock filled phenolic with graphite added.

In order to determine the causes of wear over a greater range of parameters a number of other materials were run by means of the barium titanate transducer. The wear for 2 mils motion, 30 grams (0.0665 pounds) force, and 10^9 cycles are shown by Table II.

C. Wearing Energy and Causes of Wear

A rough estimate of the energy required to break off pieces of the material shows that most of the energy goes into producing heat and very little into wear, i.e., into breaking pieces from the material. To show this let us consider a small cube fixed at one end and with a tangential force at the other. The force will cause the top surface to move with respect to the bottom surface as shown by Fig. 14, and a shearing strain S is set up in the material whose value is equal to

$$F = \mu S \, dx \, dy \tag{5}$$

where dx and dy are the cross section dimensions and μ the shear stiffness. In this displacement work is done by the sidewise displacement u equal to

$$W = \tfrac{1}{2} u F \tag{6}$$

But u the displacement is

$$u = \frac{\partial u}{\partial z} \, dz = S \, dz \tag{7}$$

and hence the total work done is

$$W = \tfrac{1}{2}\mu S^2 \, dx \, dy \, dz = \tfrac{1}{2}(\mu S^2) \times \text{volume of material} \tag{8}$$

If the force is increased, the shearing strain S increases until it reaches the limiting strain that the material can stand. This limiting strain depends on the material and whether the strain is long repeated so that the material becomes fatigued. For most plastics this limiting strain is in the order of 1 per cent and for most metals the value is less than this.
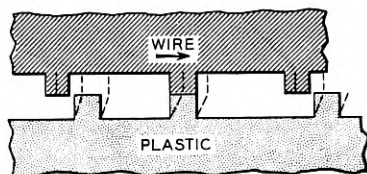
Fig. 14—Representation of points of contact and their displacements for plastic and wire.

Hence the energy to break up one cubic centimeter of material is

$$W = \tfrac{1}{2}\mu S_M^2 \tag{9}$$

where S_M is the breaking strain. For a plastic having a shear stiffness of $\mu = 2 \times 10^{10}$ dynes/cm^2 and a breaking strain of 0.01, the energy is 10^6 ergs per cubic centimeter.

This rough calculation and the amount of wear observed for various length strokes and forces allow a determination of the amount of energy going into wear production. The amount of work generated by a displacement of 0.002 inches or 0.005 cm with a normal force of 30 grams is

$$W = 0.005 \times 30 \times 980 \times f \text{ in ergs} \tag{10}$$

where f is the coefficient of friction. Since this is about 0.25 the work per stroke is 37 ergs. Twice this amount results from a complete cycle and for 10^9 cycles the work done is

$$W = 37 \times 2 \times 10^9 = 7.44 \times 10^{10} \text{ ergs} \tag{11}$$

The volume of wear observed for this condition is about 1×10^{-4} cubic cm for the A phenolic and hence we find that the part of the energy

that goes into producing wear is

$$\frac{1 \times 10^{-4} \times 10^{6}}{7.4 \times 10^{10}} = 1.35 \times 10^{-9} \tag{12}$$

or about 1 part in 10^9. This suggests that the wire goes back and forth over the same high points many millions of times until the material finally becomes fatigued and breaks off. This view is confirmed by the oscillograph pictures of Fig. 9 which are a stationary pattern for millions of oscillations.

According to this picture, the material that will wear the best is the one with the highest limiting shearing strain. If we assume that the limiting shearing strain is proportional to the limiting elongation strain under repeated vibrations—of which there are tables—the wear for various materials given in Table II agrees roughly with this concept. Table II shows the yield stresses, the Young's moduli, the per cent strains at the yield point and the relative wear at 10^9 cycles. It will be seen that the materials with the highest yield strain will in general wear longer than those with smaller yield strains.

An exception to this rule was nylon which had a large wear even though it has a large yield strain. However, nylon has a relatively low softening temperature and a low heat conductivity. Observations showed that the nylon was melted off rather than abraded off. According to this rule gum rubber should wear much better than any other material since it has such a high limiting shearing strain. A run was made with a two mil inch motion on a gum rubber specimen and no observable wear was found. The fact that a rubber tire will outwear a metal tire is also confirmation of this rule.

All the tests showed that the wear on the stainless steel or nickel silver

TABLE II

AMOUNT OF WEAR FOR VARIOUS MATERIALS CAUSED BY SLIDING A 0.025 INCH NICKEL SILVER WIRE FOR 2 MIL INCHES, 30 GRAMS NORMAL FORCE AND 10^9 CYCLES

Material	Yield Stress Dynes/Cm²	Youngs Modulus Dynes/Cm²	Per Cent Yield Strain	Wear, Cubic Cm, for 2-Mil Motion for 10^9 Cycles and 30-Gram Force
Lead Glass....	2.4 to 2.7 $\times$ 10^9	6.5 $\times$ 10^{11}	0.0037 to 0.0041	0.027
Brass..........	3.7 to 4.6 $\times$ 10^9	9 $\times$ 10^{11}	0.0041 to 0.0051	0.0075
Stainless Steel.	1.1 to 1.4 $\times$ 10^{10}	2 $\times$ 10^{12}	0.0055 to 0.007	0.00075
B Phenolic....	7.2 $\times$ 10^8	6.9 $\times$ 10^{10}	0.0105	0.000025

wire used to produce the wear on the plastic was always very much less than that of the plastic. The reason for this as seen from Fig. 14 is that since the displacement for a given force to break the bond between two high points is going to be inversely proportional to the shearing stiffnesses of the two materials, the displacement for stainless steel with a shear stiffness of 8 x 10^{11} dynes/cm^2 will be $\frac{1}{40}$ that of the plastic with a shear modulus of 2 x 10^{10} dynes/cm^2. Hence, the shearing strain for the stainless steel is much further below its limiting strain than is the shearing strain for the plastic. When the stainless steel wire was run against a bar of synthetic sapphire—which has a much higher shear constant—the stainless steel wire was soon worn through, while little wear occurred on the sapphire.

IV. THEORETICAL AND EXPERIMENTAL INVESTIGATION OF THE NO GROSS SLIDE REGION

Since in the no gross slide region, the shearing strain is less than in the gross slide region, the rate of wear should be considerably less. This is confirmed by direct tests of the wear as shown by Fig. 11, and by supplementary tests. Hence a further experimental and theoretical investigation has been made of this region which is defined by the condition that the tangential force is less than the product of the normal force by the coefficient of friction. If sliding motions can be kept small enough to be in this region, very little wear should occur.

Using a shear ceramic for measuring the tangential force, the static load was varied and the motion required to produce no gross slide was determined. Oscillograph figures of the type shown by Fig. 9 were used and when the figure was broadened out as shown by the third figure it was assumed that slide had occurred. Fig. 15, upper curve, shows the total motion in mil inches, plotted against the static force in grams, which will just cause gross slide. The bottom line shows the maximum shearing force in grams. This is slightly lower than the force determined by the coefficient of friction since the force becomes slightly larger as shown by the pictures of Fig. 9, when gross slide occurs. The total displacement for no slide increases as the two-thirds power of the static load.

Since neither the wire nor the plastic material is smooth, contact between the two is established at only a few points. To interpret the results obtained above, some calculations due to R. D. Mindlin[11] are used. These deal with the tangential forces and displacements of two balls pressed together, and are for conditions occurring before gross slide begins.
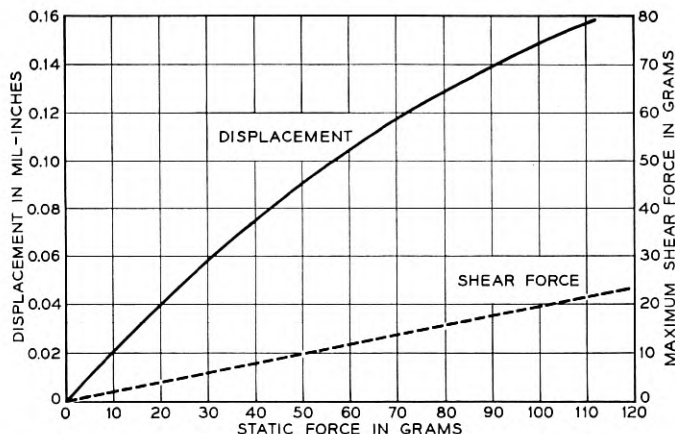
Fig. 15—Maximum total motion for no gross slide plotted against normal force. Low curve shows maximum tangential force.

From the Hertz theory of contacts,[12] the radius of contact a between two spheres is equal to

$$a = \sqrt[3]{\frac{3}{8} r N \left(\frac{1 - \sigma_1}{\mu_1} + \frac{1 - \sigma_2}{\mu_2} \right)} \tag{13}$$

where r is the radius of the spheres, N the normal force, μ_1 and σ_1 the shear elastic constant and Poisson's ratio for one sphere and μ_2 and σ_2 the same quantities for the second sphere. If now a tangential force T is applied to one of the spheres directed in the form of a couple, elastic theory shows that the tangential traction is everywhere parallel to the direction of the applied force and contours of constant tangential traction are concentric circles. The magnitude of the traction as shown by Fig. 16 rises from one half the average at the center to infinity at the edge of the circle of contact. The displacement of the circle of contact of one sphere with respect to its center is

$$\delta_x = \frac{2 - \sigma}{8 \mu a} T \tag{14}$$

where a is the radius of the contact area which is given in terms of the normal force by Equation (13).

A feature of this solution that requires further study is the infinite traction at the edge of the circle of contact. Presumably the tangential component of traction cannot exceed the product of the coefficient of friction f and the normal component of traction p, which from the Hertz
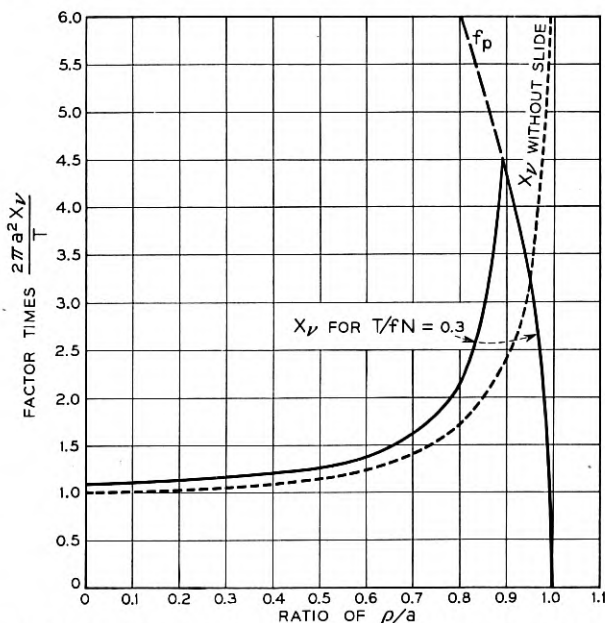
Fig. 16—Traction plotted against radius for elastic displacement and modification introduced by the effect of slip.

contact theory is

$$p = \frac{3N}{2\pi a^2} \sqrt{1 - \frac{r^2}{a^2}} \tag{15}$$

Mindlin assumes that slip takes place between the two surfaces until the tangential traction is equal to

$$X_v = \frac{3fN}{2\pi a^2} \sqrt{1 - \frac{\rho^2}{a^2}} \qquad \text{for } a' \gtreqqless \rho \gtreqqless a \tag{16}$$

and less than this for all interior points, where in this equation ρ is the radius vector and a' the inner radius for which slip stops. This corresponds to the introduction of a new system of forces and Mindlin has shown that equilibrium is reestablished when the surface tractions are given by Equation (16) when $a' \gtreqqless \rho \gtreqqless a$ and by

$$X_v = \frac{3fN}{2\pi a^2} \left[\sqrt{1 - \frac{\rho^2}{a^2}} - \frac{a'}{a} \sqrt{1 - \frac{\rho^2}{a'^2}} \right] \qquad \text{when } \rho \gtreqqless a' \tag{17}$$

Fig. 16 shows this distribution for the case $T/fN = 0.3$. The inner radius a' is given such a value that the integrated traction over the surface

equals T and its value is found to be

$$a' = a \sqrt[3]{1 - \frac{T}{fN}} \tag{18}$$

The added slip increases the displacement δ_x and it is shown that the total displacement is equal to

$$\delta_x = \frac{3fN\ (2 - \sigma)}{16\mu a}\left[1 - \left(1 - \frac{T}{fN}\right)^{2/3}\right] \tag{19}$$

A plot of this curve is shown by the line OPQ of Fig. 17 and it is evident that the displacement before gross slip occurs is 1.5 times larger than the elastic displacement calculated on the assumption of no slip.

These calculations have been extended in a recent paper[3] to include the case of a cylically varying force $T \lessgtr fN$ and it is shown that the force displacement curve is a hysteresis type loop whose end points lie
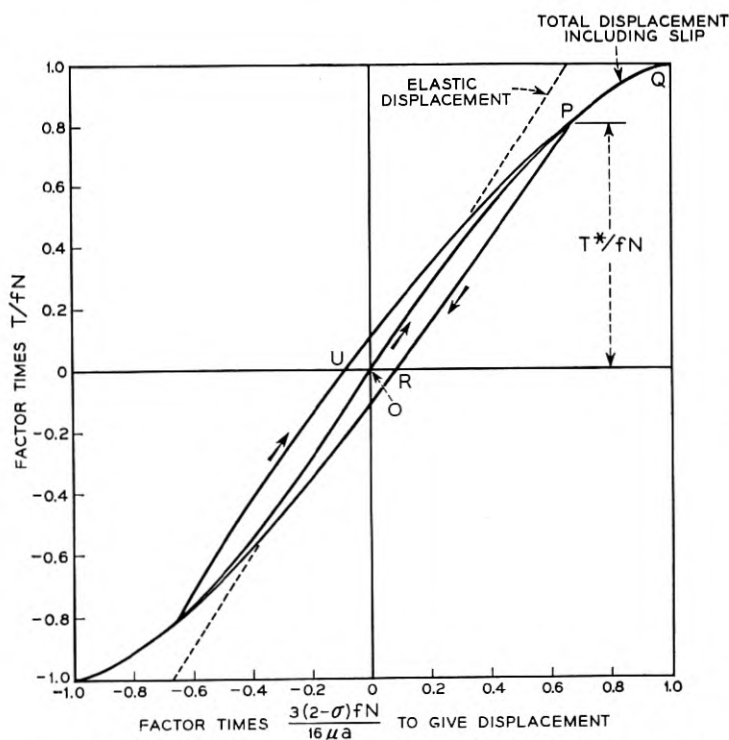
Fig. 17—Displacement versus force when slip is introduced. Hysteresis **curve** PRU shows displacement for an oscillating force.

on the OPQ curve of Fig. 17 and whose theoretical area W is

$$W = \frac{9(2 - \sigma) f^2 N^2}{10\mu a} \times$$
$$\left[1 - \left(1 - \frac{T^*}{fN} \right)^{5/3} - \frac{5T^*}{6fN} \left[1 + \left(1 - \frac{T^*}{fN} \right)^{2/3} \right] \right] \tag{20}$$

where during the oscillation the tangential force T varies between the limits $\pm T^*$. Slip takes place as before between the radii a and a' given by

$$a' = a \sqrt[3]{1 - \frac{T^*}{fN}} \quad \text{or conversely} \quad \frac{T^*}{fN} = 1 - \frac{a'^3}{a^3} \tag{21}$$

Since the distribution of traction over the surface cannot be uniquely derived from elastic theory, the introduction of the slip function is an assumption that has to be justified by experiment. This assumption has been shown to correspond with experiment by employing the experimental arrangement shown by the photograph of Fig. 18. A barium titanate driver shown in more detail in Fig. 19 drives the middle of three glass lenses that are pressed together by a static force applied to the lever system as shown by Fig. 19. The central glass lens has a radius of curvature of 4.85 inches on each side while the other two lenses have the same radius of curvature on the sides touching the middle lens, but are flat on the other two sides and are rigidly attached to the lower platform and upper hinged lever by cement. In order to get sufficiently large
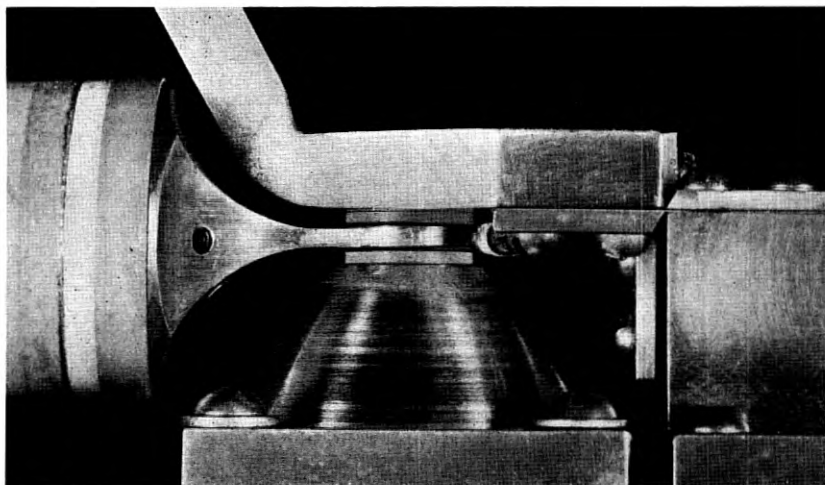
Fig. 18—Barium titanate driver, pick-up device and glass lenses.
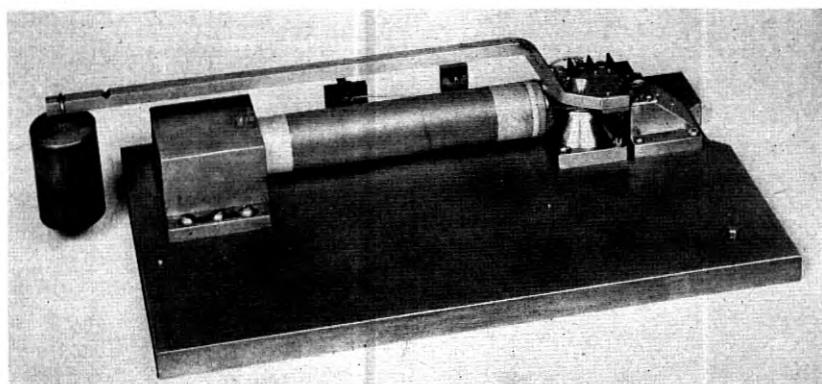
Fig. 19—The entire experimental arrangement.

circles of contact to be easily observed, normal loads on the lens system were 10 and 15 pounds which resulted in contact circles of 0.030 and 0.034 inches diameter.

With normal forces up to 15 pounds and two surfaces in contact, tangential forces up to 7.5 pounds are necessary in order to bring the central lens near the sliding point if the coefficient of friction is near one-quarter. This force was obtained by impressing voltages in the order of 3,000 rms volts on the barium titanate lead titanate hollow cylinder. This cylinder is $4\frac{3}{4}$ inches long, and has an outside diameter of 1 inch and an inside diameter of $\frac{1}{2}$ inch. The ceramic was poled in a radial direction and the constants of the material were such that a force of 167 pounds could be generated along the length for a clamped driver when a voltage of 3,000 volts (4,750 volts cm) was used. On the other hand if the driver works against no stress, the expansion in the plated length of 4 inches is 0.7×10^{-4} inches.

The actual force applied depends on how much the relative slip between the glass lenses amounts to. To measure this force, a poled lead titanate barium titanate disk is placed between the driver and the metallic bracket which clamps the middle lens as shown by Fig. 18. All the force exerted on the lens has to be exerted through the disk and hence the voltage generated by the disk is a measure of the force exerted on the middle lens. This voltage is calibrated by attaching a spring load of known constants and measuring the displacement of the load by means of a microscope.

Using a 60-cycle driving voltage, a number of sets of disks were run with varying tangential and normal loads and the wear patterns observed. Fig. 20 is a photograph (magnified 100 times) for a normal load
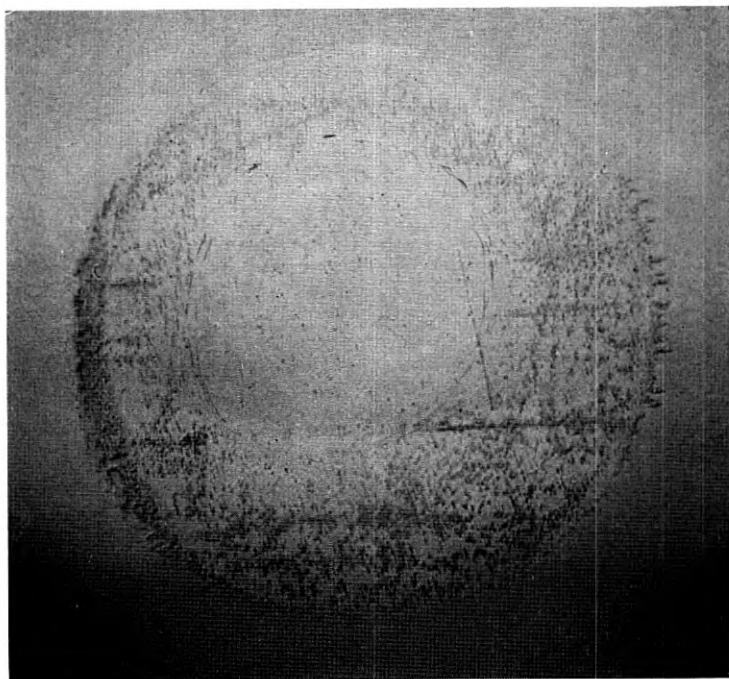
Fig. 20—Wear circles (magnified 100 times).

of 10 pounds and a maximum tangential load of 2.04 pounds per lens run for about 3 hours at 60 vibrations per second. The outer area of contact is seen to be 0.03 inches in diameter. The inner area of wear is a circle displaced slightly from a concentric form and has a diameter of 0.0175 inch. If we plot $1 - (a'/a)^3$ against the ratio of tangential to normal force, where a' is the inner radius and a the outer radius, as shown by Fig. 21, a point at 0.204 and 0.8 is obtained. A number of sets of lenses were run and as shown by Fig. 21 the results can be plotted on a straight line corresponding to a coefficient of friction of 0.25. This value agrees well with other determinations[13] of the coefficient of friction of glass on glass. Hence the assumption of slip between spheres under tangential forces appears to be verified. This type of slip may be responsible for some types of wear, such as in ball bearings, where no gross slide of one surface over another occurs.

An attempt was also made to check the area of the loop as determined theoretically by Equation (20). The applied force is measured directly by the barium titanate pickup and the displacement was measured by

attaching a velocity microphone pickup to the transducer. The force voltage was placed on one set of plates of an oscillograph while the integrated output from the velocity pickup was placed on the other set. A series of oscillographs were taken for various amplitudes of motion and the pictures are shown by Fig. 22. Since the force and displacement measurements were separately calibrated, the area of the curves in inch pounds could be evaluated and are shown by Fig. 23. For amplitudes of motion near the gross slip amplitude, the area agree well with that calculated from Equation (20) from which the dotted line is obtained. For lower amplitudes the measured area is larger than the calculated area. Possibly a stick-slip process is causing the displacement to lag behind the applied force. The measured areas are nearly proportional to the square of the amplitude. The mechanical resistance associated with the stress-strain hysteresis curves of this sort is of the same type that
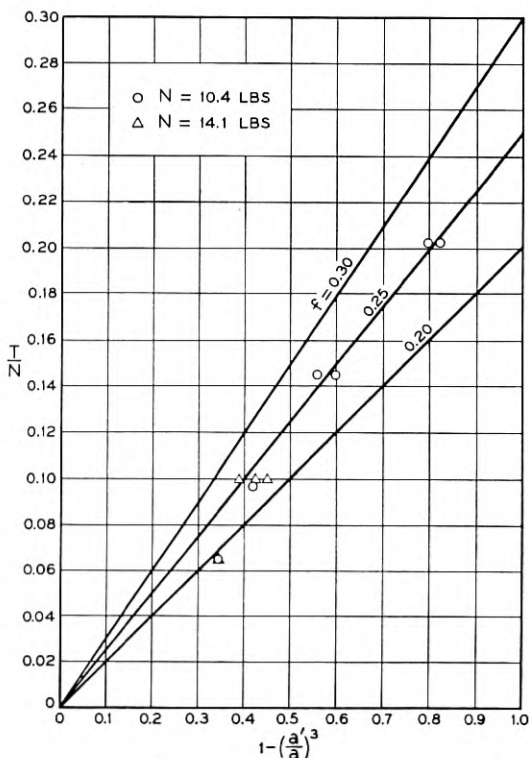
Fig. 21—Plot of $1 - (a'/a)^3$ against ratio of tangential and normal forces.

Fig. 22—Force displacement loops.

occurs in an assemblage of granular particles such as in a telephone transmitter for which the motion is so small that gross slide does not occur.

Since the theoretical displacement of Equation (19) has been verified by the glass lens experiment, we can use it to determine some of the quantities involved in the oscillographs of Fig. 9 and the displacement-normal force curve of Fig. 15. To obtain the relation between the total displacement δ_x and the normal force N, we have to eliminate a from Equation (17) since a is also a function of the normal force as shown by Equation (13). Introducing this equation, and neglecting $1/\mu_2$ as compared to $1/\mu_1$, since for the wire μ_2 is 40 times μ_1 of a plastic,

$$\delta_x = \frac{\left(\dfrac{3N}{\mu}\right)^{2/3}(2-\sigma)f}{8\sqrt[3]{r(1-\sigma)}}\left[1-\left(1-\frac{T^*}{fN}\right)^{2/3}\right] \tag{22}$$

Hence in agreement with the data of Fig. 15, the displacement for no gross slide should vary as the two-thirds power of the normal force.

Another deduction from Equation (22) is that the displacement for no slide should vary as the inverse two-thirds power of the shear stiffness constant μ. For example gum rubber with a shear stiffness of 2×10^7 dynes/cm^2 should give 100 times the displacement of a plastic with a shear stiffness of 2×10^{10} dynes/cm^2. A rough check of this deduction has been made by cementing a thin strip of gum rubber on the face of a shear responding ceramic and with a normal force of 30 grams (0.0665 pounds), vibrating the wire at its full amplitude of 2 mil inches. Over this range the voltage response was sinusoidal indicating that no gross slide took place. This is 33 times as large a motion as occurred for a plastic with an elastic stiffness 1,000 times that of the rubber and verifies the variation of δ_x with μ.

The other experimental quantity that can be obtained from Equation (22) is the radius r of the effective contact points of the plastic. If all
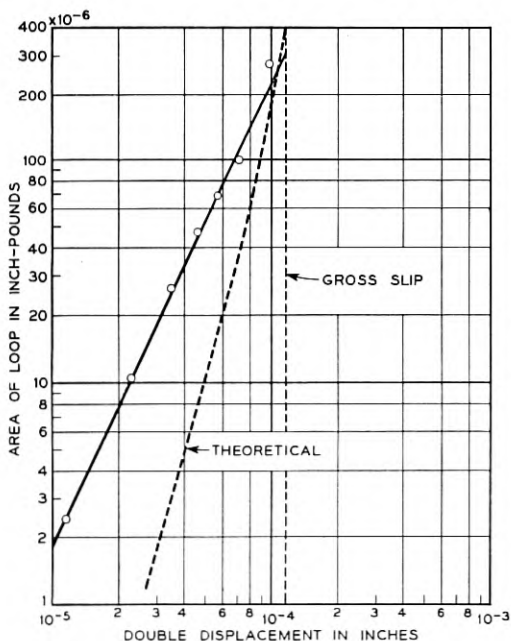
Fig. 23—Plot of area of force displacement loop against double displacement.

the force is supported by a single point at a time, then for

$$\delta_x = \pm 3 \times 10^{-5} \text{ inches} = \pm 7.5 \times 10^{-5} \text{ cm};$$

$$N = 30 \text{ grams} = 2.94 \times 10^4 \text{ dynes};$$

$$\mu = 2 \times 10^{10} \text{ dynes/cm}^2;$$

$$\sigma = 0.45$$

(23)

and the coefficient of friction $f = 0.25$, the value of r becomes 0.008 cm. If the weight were supported equally by n points the radius would be divided by n^2. Since the sidewise displacement would result in a strain of 0.009 for a single point and 0.036 for two points, the latter strain would be beyond the yield strain for the material. Hence the evidence seems to indicate that a single point supports the major part of the weight at any particular time.

While it is difficult to reduce the gross tangential slide of a relay to the values required for the low wear (no gross slide) region, the existence of such a region has considerable importance for other sources of wear in relays, namely long continued vibrations of component parts such as undamped wires. The tangential motions caused by such vibrations are small, but since they are repeated many times for each operation, the total integrated wear is considerable. By introducing damping so that the vibrations are quickly brought down to the low wear, no gross slide region, a considerable reduction in wear has been found for relays.

APPENDIX

VOLTAGE GENERATED BY COMPRESSIONAL AND TANGENTIAL CERAMICS BY FORCES APPLIED UNIFORMLY OR AT CONCENTRATED POINTS

When a stress is applied to a prepolarized barium titanate ceramic it has been shown[14] that the open circuit field generated along the Z axis is given by the equation

$$E_3 = -2[Q_{11}[\delta_{3_0}T_3 + \delta_{1_0}T_5 + \delta_{2_0}T_4] + Q_{12}[\delta_{3_0}(T_1 + T_2) \\ - (\delta_{1_0}T_5 + \delta_{2_0}T_4)]] \tag{24}$$

where δ_{1_0}, δ_{2_0}, δ_{3_0} are the remanent values of polarization introduced along the three axes by the poling process, T_1, T_2, T_3, T_4, T_5, T_6 the three extensional stresses and the three shearing stresses, and Q_{11} and Q_{12} are the two electrostrictive constants for the ceramic. From the "effective" piezoelectric constants measured for these ceramics we find

that

$$Q_{11}\delta_{3_0} = 2.2 \times 10^{-8}; \qquad Q_{12}\delta_{3_0} = -.8 \times 10^{-8} \text{ cgs units} \qquad (25)$$

for pure barium titanate and

$$Q_{11}\delta_{3_0} = 2.4 \times 10^{-8}; \qquad Q_{12}\delta_{3_0} = -.9 \times 10^{-8} \text{ cgs units} \qquad (26)$$

for 4 per cent lead titanate barium titanate ceramic.

If a force F is applied uniformly over the whole surface of a small barium titanate unit, then $T_3 = F/A$, where A is the area, and all the other stresses are zero. Under these circumstances when the permanent polarization δ_{3_0} is along the Z axis (normal poling), the open circuit potential is

$$E_3 = \frac{V_3}{l_t} = \frac{2Q_{11}\delta_{3_0}F}{l_w l} = \frac{2 \times 2.4 \times 10^{-8} \times F}{l_w l} \text{ cgs units} \qquad (27)$$

where l_t is the thickness and l_w and l the cross-sectional dimensions. To get the number of volts generated this factor is multiplied by 300 and

$$V_3 = \frac{1.44 \times 10^{-5} F}{l_w l} \text{ volts} \qquad (28)$$

where force F is expressed in dynes.

However for the data of Figs. 2 and 4, the voltage measured is that for a load applied at the center of the ceramic and for this case the stresses T_1 and T_2 of Equation (24) cannot be neglected. The solution[15] for the stresses occurring when a load F is applied at a point on the surface of a semi infinite solid is used to evaluate the corrections caused by the non-uniform load. In cylindrical coordinates the formulae for the three stresses T_{zz} and T_{rr} and $T_{\theta\theta}$ given by Timoshenko are

$$T_{rr} = \frac{F}{2\pi}\left[(1 - 2\sigma)\left[\frac{1}{r^2} - \frac{z}{r^2}(r^2 + z^2)^{-1/2}\right] - 3r^2 z(r^2 + z^2)^{-5/2}\right]$$

$$T_{\theta\theta} = \frac{F}{2\pi}(1 - 2\sigma)\left[-\frac{1}{r^2} + \frac{z}{r^2}(r^2 + z^2)^{-1/2} + z(r^2 + z^2)^{-3/2}\right] \qquad (29)$$

$$T_{zz} = \frac{-3F}{2\pi}z^3(r^2 + z^2)^{-5/2}$$

where r is the radial distance from the point of contact, z the distance below the surface and σ = Poisson's ratio.

The response of a barium titanate unit in terms of cylindrical coordinates has been shown[16] to be for a unit polarized along the z axis

$$E_z = -2\left[Q_{11}\delta_{3_0}T_{zz} + Q_{12}\delta_{3_0}(T_{rr} + T_{\theta\theta})\right] \qquad (30)$$

Now since the ceramic is plated, the major surface is an equipotential surface and hence E_z does not vary with r or θ. Hence integrating over the surface of the ceramic, we have for the open circuit field

$$E_z \int_0^\infty \int_0^{2\pi} r \, dr \, d\theta = -2 \left[Q_{11}\delta_{3_0} \int_0^\infty \int_0^{2\pi} T_{zz} r \, dr \, d\theta \right.$$
$$\left. + Q_{12}\delta_{3_0} \int_0^\infty \int_0^{2\pi} (T_{rr} + T_{\theta\theta}) r \, dr \, d\theta \right] \tag{31}$$

Introducing the values of T_{zz}, T_{rr} and $T_{\theta\theta}$ from Equation (29) and performing the integrations we find

$$E_z A = 2 \left[Q_{11}\delta_{3_0}F + Q_{12}\delta_{3_0} (1 + 2\sigma)F \right] \tag{32}$$

where A is the cross-sectional area of the ceramic. The first term agrees with that for a uniform stress, but the second term shows that we have a correction due to the radial and tangential stresses generated by the application of the force at a point.

The amount of correction can be calculated by putting in the values of Q_{12} and σ the Poisson ratio. Recent measurements of the thickness resonance and the resonance of a torsional ceramic have shown that the best values of the Lame elastic constants are

$$\lambda = 5.8 \times 10^{11} \text{ dynes/cm}^2; \quad \mu = 4 \times 10^{11} \text{ dynes/cm}^2 \tag{33}$$

With these values, Poisson's ratio becomes

$$\sigma = \frac{\lambda}{2(\lambda + \mu)} = \frac{5.8}{19.6} = 0.296 \tag{34}$$

For 4 per cent lead titanate barium titanate ceramic, introducing the values given above, the voltage generated by a force applied at a point is about 0.4 of that for a force applied uniformly, giving

$$V_z = \frac{0.575 \times 10^{-5} Fl_t}{l_w l} \text{ volts} \tag{35}$$

This value corresponds reasonably well with the data of Fig. 4.

When the remanent polarization is applied along the Y axis and the voltage measured along the Z axis, Equation (24) shows that the open circuit voltage will be

$$E_3 = -2 (Q_{11} - Q_{12})\delta_{2_0}T_4 \tag{36}$$

where $T_4 = Y_z$ is the stress in the direction of polarization (Y) applied to the surface of the ceramic. Since the single stress T_4 is involved, the

open circuit voltage will be independent of whether the force is applied uniformly over the surface or at a point. This follows from the fact that E_3 is independent of x and y and hence

$$E_3 \int_0^{lw} \int_0^l dx\,dy = -2(Q_{11} - Q_{12})\delta_{2_0} \int_0^{lw} \int_0^l T_4\,dx\,dy \qquad (37)$$

Integrating over the surface gives the total force F for the right side and hence

$$V_3 = \frac{2(Q_{11} - Q_{12})\delta_{2_0}l_t F}{l_w l} \text{ in cgs units} \qquad (38)$$

$$= \frac{1.98 \times 10^{-5} l_t F}{l_w l} \text{ in volts}$$

For a ceramic 0.1 cm by 0.1 cm in cross-section and 0.05 cm thick a tangential force of 100 grams should generate a voltage of 9.7 volts.

REFERENCES

1. L. Vieth and C. F. Wiebusch, "Recent Developments in Hill and Dale Recorders," *J. Soc. Motion Pictures Engrs.*, Jan., 1938.
2. W. P. Mason and R. F. Wick, "A Barium Titanate Transducer Capable of Large Motion at an Ultrasonic Frequency," *J. Acous. Soc. of A.*, **23**, pp. 209–214, Mar., 1951.
3. R. D. Mindlin, W. P. Mason, T. F. Osmer, and H. Deresiewicz, "Effects of an Oscillating Tangential Force on the Contact Surfaces of Elastic Spheres," presented before First National Congress of Applied Mechanics, June 14, 1951. The results of this paper are summarized here.
4. Measurements have been made by T. F. Osmer.
5. This circuit was devised by G. A. Head.
6. W. P. Mason, *Piezoelectric Crystals and Their Application to Ultrasonics*, D. Van Nostrand, Chapter XII, 1950.
7. The data of Figs. 2 and 4 were obtained by L. Egerton.
8. Elizabeth A. Wood, "Detwinning Ferroelectric Crystals," *Bell System Tech. J.*, **30**, No. 4, Part I, pp. 945–955, Oct., 1951.
9. W. P. Mason, *Piezoelectric Crystals and Their Application to Ultrasonics*, D. Van Nostrand, Chap. XII, 1950.
10. The photographs of Fig. 6 were obtained by T. E. Davis.
11. R. D. Mindlin, "Compliance of Elastic Bodies in Contact," *J. Appl. Mech.*, pp. 259–268, September, 1949.
12. A. E. H. Love, *Theory of Elasticity*, 4th Edition, page 198, Cambridge University Press.
13. I. Simon, O. McMahon and R. J. Bowen, "Dry Metallic Friction as a Function of Temperature Between 4.2°K and 600°K.," *J. App. Phys.*, **22**, pp. 170–184, Feb., 1951.
14. W. P. Mason, *Piezoelectric Crystals and Their Application to Ultrasonics*, D. Van Nostrand, Chap. XII, p. 300.
15. S. Timoshenko, *Theory of Elasticity*, McGraw-Hill Co., p. 311.
16. W. P. Mason, *Piezoelectric Crystals and Their Application to Ultrasonics*, D. Van Nostrand, Appendix A9, p. 490.

A Comparison of Signalling Alphabets

By E. N. GILBERT

Two channels are considered; a discrete channel which can transmit sequences of binary digits, and a continuous channel which can transmit band limited signals. The performance of a large number of simple signalling alphabets is computed and it is concluded that one cannot signal at rates near the channel capacity without using very complicated alphabets.

INTRODUCTION

C. E. Shannon's encoding theorems[1] associate with the channel of a communications system a capacity C. These theorems show that the output of a message source can be encoded for transmission over the channel in such a way that the rate at which errors are made at the receiving end of the system is arbitrarily small provided only that the message source produces information at a rate less than C bits per second. C is the largest rate with this property.

Although these theorems cover a wide class of channels there are two channels which can serve as models for most of the channels one meets in practice. These are:

1. The binary channel

This channel can transmit only sequences of binary digits 0 and 1 (which might represent hole and no hole in a punched tape; open-line and closed line; pulse and no pulse; etc.) at some definite rate, say one digit per second. There is a probability p (because of noise, or occasional equipment failure) that a transmitted 0 is received as 1 or that a transmitted 1 is received as 0. The noise is supposed to affect different digits independently. The cpacity of this channel is

$$C = 1 + p \log p + (1 - p) \log (1 - p) \tag{1}$$

bits per digit. The log appearing in Equation (1) is log to the base 2; this convention will be used throughout the rest of this paper.

---

[1] C. E. Shannon, "A Mathematical Theory of Communication," *Bell System Tech. J.*, **27**, p. 379–423 and pp. 623–656, 1948, theorems 9, 11, and 16 in particular.

2. The low-pass filter

The second channel is an ideal low-pass filter which attenuates completely all frequencies above a cutoff frequency W cycles per second and which passes frequencies below W without attenuation. The channel is supposed capable of handling only signals with average power P or less. Before the signal emerges from the channel, the channel adds to it a noise signal with average power N. The noise is supposed to be white Gaussian noise limited to the frequency band $|\nu| < W$. The capacity of this channel is

$$C = W \log\left(1 + \frac{P}{N}\right) \qquad (2)$$

bits per second.

Shannon's theorems prove that encoding schemes exist for signalling at rates near C with arbitrarily small rates of errors without actually giving a constructive method for performing the encoding. It is of some interest to compare encoding systems which can easily be devised with these ideal systems. In Part I of this paper some schemes for signalling over the binary channel will be compared with ideal systems. In Part II the same will be done for the low-pass filter channel.

PART I

THE BINARY CHANNEL

1. Error-Correcting Alphabets

Imagine the message source to produce messages which are sequences of letters drawn from an alphabet containing K letters. We suppose that the letters are equally likely and that the letters which the source produces at different times are independent of one another. (If the source given is a finite state source which does not fit this simple description, it can be converted into one which approximately does by a preliminary encoding of the type described in Shannon's Theorem 9.) To transmit the message over the binary channel we construct a new alphabet of K letters in which the letters are different sequences of binary digits of some fixed length, say D digits. Then the new alphabet is used as an encoding of the old one suitable for transmission over the channel. For example, if the source produced sequences of letters from an alphabet of 3 letters, a typical encoding with $D = 5$ might convert the message

into a binary sequence composed of repetitions of the three letters.

$$00000$$
$$11100$$
and 00111

If $K = 2^D$, the alphabet consists of all binary sequences of length D and hence if any of the digits of a letter is altered by noise the letter will be misinterpreted at the receiving end of the channel. If K is somewhat smaller than 2^D it is possible to choose the letters so that certain kinds of errors introduced by the noise do not cause a misinterpretation at the receiver. For example, in the three letter alphabet given above, if only one of the five digits is incorrect there will be just one letter (the correct one) which agrees with the received sequence in all but one place. More generally if the letters of the alphabet are selected so that each letter differs from every other in at least $2k + 1$ out of the D places, then when k or fewer errors are made the correct interpretation of the received sequence will be the (unique) letter of the alphabet which differs from the received sequence in no more than k places. An alphabet with this property will be called a k *error correcting alphabet*[2].

Error correcting alphabets have the advantage over the random alphabets which Shannon used to prove his encoding theorems that they are uniformly reliable whereas Shannon's alphabets are reliable only in an average sense. That is, Shannon proved that the probability that a letter *chosen at random* shall be received incorrectly can be made arbitrarily small. However, a certain small fraction of the letters of Shannon's alphabets are allowed a much higher probability of error than the average. This kind of alphabet would be undesirable in applications such as the signalling of telephone numbers; one would not want to give a few subscribers telephone numbers which are received incorrectly more often than most of the others. It is only conjectured that the rate C can be approached using error correcting alphabets. The alphabets which are to be considered here are all error correcting alphabets.

A geometric picture of an alphabet is obtained by regarding the D digits of a sequence as coordinates of a point in Euclidean D dimensional space. The possible received sequences are represented by vertices of the unit cube. A k error correcting alphabet is represented by a set of vertices, such that each pair of vertices is separated by a distance at least $\sqrt{2k + 1}$

Let $K_0(D, k)$ be the largest number of letters which a D dimensional

[2] R. W. Hamming, "Error Detecting and Error Correcting Codes," *Bell System Tech. J.*, **29**, pp. 147–160, 1950.

k error correcting alphabet can contain. Except when $k = 1$, there is no general method for constructing an alphabet with $K_0(D, k)$ letters, nor is $K_0(D, k)$ known as a function of D and k. Crude upper and lower bounds for $K_0(D, k)$ are given by the following theorem.

Theorem 1. The largest number of letters $K_0(D, k)$ satisfies

$$\frac{2^D}{N(D, 2k)} \leq K_0(D, k) \leq \frac{2^D}{N(D, k)} \tag{3}$$

where

$$N(D, k) = \sum_{r=0}^{k} C_{D, r}$$

is the number of sequences of D digits which differ from a given sequence in $0, 1, \cdots$, or k places.

Proof

The upper bound is due to R. W. Hamming and is proved by noting that for each letter S of a k error correcting alphabet there are $N(D, k)$ possible received sequences which will be interpreted as meaning S. Hence $N(D, k) K_0(D, k) \leq 2^D$, the total number of sequences.

The lower bound is proved by a random construction method. Pick any sequence S_1 for the first letter. There remain $2^D - N(D, 2k)$ sequences which differ from S_1 in $2k + 1$ or more places. Pick any one of these S_2 for the second letter. There remain at least $2^D - 2N(D, 2k)$ sequences which differ from both S_1 and S_2 in $2k + 1$ or more places. As the process is continued, there remain at least $2^D - rN(D, 2k)$ sequences, which differ in $2k + 1$ or more places from $S_1, \cdots, S_r$, from which S_{r+1} is chosen. If there are no choices available after choosing S_K, then $2^D - KN(D, 2k) \leq 0$ so the alphabet $(S_1, \cdots, S_K)$ has at least as many letters as the lower bound (3).

For all the simple cases (D and k not very large) investigated so far the upper bound is a better estimate of $K_0(D, k)$ than the lower bound. The upper and lower bounds differ greatly, as may be seen from a quick inspection of Table I. For example, in the case of a ten dimensional two error correcting alphabet, the bounds are 2.7 and 18.3.

2. Efficiency Graph

The first step in constructing an efficiency graph for comparing alphabets is to decide on what constitutes reliable transmission. The criterion used here is that on the average no more than one letter in 10^4 shall be misinterpreted.

TABLE I

TABLE OF $2^D/N(D, k)$

k =	1	2	3	4	5	6	7
D = 3	2						
4	3.2						
5	5.3	2					
6	9.1	2.9					
7	16	4.4	2.9				
8	28.4	6.9	2.8				
9	51.2	11.1	3.9	2			
10	93.1	18.3	5.8	2.7			
11	170.7	30.6	8.8	3.6	2		
12	315.8	51.8	13.7	5.2	2.6		
13	585.2	89.0	21.6	7.5	3.4	2	
14	1092.3	154.4	34.9	11.1	4.7	2.5	
15	2048	270.8	56.8	16.8	6.6	3.3	2

Missing entries are numbers between 1 and 2.

This sort of criterion might be appropriate for a channel transmitting English text. For other messages it is not always appropriate. For example, if the messages are telephone numbers, one would naturally require that the probability of mistaking a telephone number be small, say less than 10^{-4}. If the telephone numbers are L decimal digits long, and if the alphabet has K different letters in it (so that it takes about $L \log 10/\log K$ letters to make up a telephone number) the probability of making a mistake in a single letter should be required to be less than about

$$\frac{10^{-4} \log K}{L \log 10}$$

which gives alphabets with large K an advantage over alphabets with small K.

Since the probability that exactly r binary digits out of D shall be received incorrectly is $C_{D,r} p^r (1 - p)^{D-r}$, we achieve the required reliability with a D-dimensional k-error correcting alphabet provided p satisfies

$$\sum_{r=k+1}^{D} C_{D, r} p^r (1 - p)^{D-r} \leq 10^{-4}. \tag{4}$$

The value of p which makes the inequality hold with the equals sign determines the noisiest channel over which the alphabet can be used safely.

Let K be the number of different letters in the alphabet. Then the

rate in bits per digit at which information is being recieved is

$$R = \frac{\log K}{D}. \tag{5}$$

In Equation (5) we have neglected a term which takes account of the information lost due to channel noise. This is legitimate because all but 10^{-4} of the letters are received correctly.

The worst tolerable probability p of (4) and the rate R of Equation (5) determine the noise combating ability of an alphabet. To compare different alphabets one may represent them as points on an efficiency graph of R versus p. Fig. 1 is an efficiency graph on which the values (p, R) for a number of simple error correcting alphabets have been plotted. Each point on the graph is labelled with the two numbers k, D in that order. The alphabets represented were not found by any systematic process and are not all proved to be best possible (i.e., to have the largest K) for the stated values of k and D. Fortunately, R depends on K only logarithmically so that it is not likely the points representing the best possible alphabets lie far away from the plotted points.

The solid line represents the curve

$$R = C = 1 + p \log p + (1 - p) \log (1 - p).$$

According to Shannon's theorems, all alphabets are represented by points lying below this line.

The efficiency graph only partially orders the alphabets according to
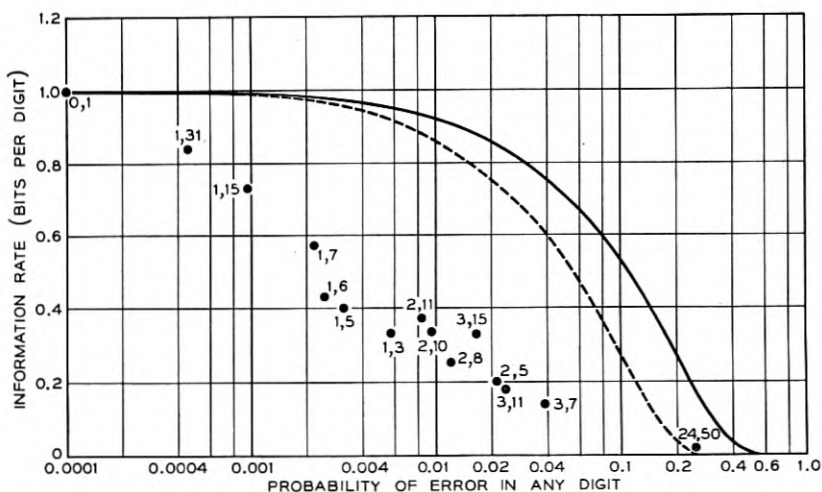
Fig. 1—Probability of error in a letter is 10^{-4}.

their invulnerability to noise. For example, it is clear that the alphabet 3, 15 is better than 2, 8. However, without further information about the channel, such as knowledge of p, there is no reasonable way of choosing between 3, 15 and 3, 7.

3. Large Alphabets

We have been unable to prove that there are error correcting alphabets which signal at rates arbitrarily close to C while maintaining an arbitrarily small probability of error for any letter. A result in this direction is the following theorem.

Theorem 2. Let any positive ϵ and δ be given. Given a channel with $p < \frac{1}{4}$ there exists an error correcting alphabet which can signal over the channel at a rate exceeding $R_0 - \epsilon$ where

$$R_0 = 1 + 2p \log 2p + (1 - 2p) \log (1 - 2p)$$

bits per digit and for which the probability of error in any letter is less than δ.

Proof

The probability of error in any letter is the sum on the left of (4). This is a sum of terms from a binomial distribution which, as is well known, tends to a Gaussian distribution with mean Dp and variance $Dp(1 - p)$ for large D. Hence there is a constant $A(\delta)$ such that all k error correcting alphabets with sufficiently large D have a letter error probability less than δ provided

$$k \geq Dp + A(\delta) \, (Dp(1 - p))^{1/2} \tag{6}$$

Let $k(D)$ be the smallest integer which satisfies (6) and consider an alphabet which corrects $k(D)$ errors and contains $K_0(D, k(D))$ letters. By Equation (5) and the lower bound of Theorem 1, this alphabet signals at a rate $R(D)$ satisfying

$$1 - \frac{1}{D} \log N(D, 2k(D)) \leq R(D).$$

Since $p < \frac{1}{4}$, $2k(D) < D/2$ for large D and hence

$$N(D, 2k(D)) < (2k(D) + 1)C_{D,2k(D)}.$$

Then an application of Stirling's approximation for factorials shows that as $D \to \infty$

$$1 - \frac{1}{D} \log N(D, 2k(D)) \to R_0.$$

Hence by taking D large enough one obtains an alphabet with rate exceeding $R_0 - \epsilon$ and letter error probability less than δ.

The rate R_0 appears on the efficiency graph as a dotted line.

It has not been shown that no error-correcting alphabet has a rate exceeding R_0. In fact, one alphabet which exceeds R_0 in rate is easy to construct. If the noise probability p is greater than $\frac{1}{4}$, then $R_0 = 0$. The alphabet with just two letters

$$0\ 0\ 0\ 0 \ldots 0$$

and

$$1\ 1\ 1\ 1 \ldots 1$$

will certainly transmit information at a (small) positive rate, and with a 10^{-4} probability of errors if D is large enough, as long as $p < \frac{1}{2}$.

Using a more refined lower bound for $K_0(D, k)$ it might be shown that there are error-correcting alphabets which signal with rates near C. If one repeats the calculation that led to R_0 using the upper bound (3) (which seems to be a better estimate of the true $K_0(D, k)$) instead of the lower bound (3), one is led to the rate C instead of R_0.

The condition (4) is more conservative than necessary. The structure of the alphabet may be such that a particular sequence of more than k errors may occur without causing any error in the final letter. This is illustrated by the following simple example due to Shannon: the alphabet with just two letters

$$0\ 0\ 0\ 0\ 0\ 0$$
$$1\ 1\ 1\ 0\ 0\ 0$$

corrects any single error but also corrects certain more serious errors such as receiving 0 0 1 1 1 1 for 0 0 0 0 0 0. An alphabet designed for practical use would make efficient enough use of the available sequences so that any sequence of much more than k errors causes an error in the final letter; the random alphabets constructed above probably do not. If this kind of error were properly accounted for, the rate R_0 could be improved, perhaps to C.

4. Other Discrete Channels

If instead of transmitting just 0's and 1's the channel can carry more digits

$$0, 1, 2, \cdots, n$$

a similar theory can be worked out. The simplest kind of noise in this channel changes a digit into any one of the n other possible numbers with probability p/n. Then the capacity of the channel is

$$C = \log (n + 1) + p \log \frac{p}{n} + (1 - p) \log (1 - p).$$

Error-correcting alphabets for this channel can also be constructed and the criterion (4) for good transmission remains unchanged. The proof of theorem 1 can be repeated with little change using

$$N(D, k) = \sum_{r=0}^{k} C_{D, r} n^r$$

as the number of sequences which can be reached after k or fewer errors [the terms 2^D in (1) and (3) are replaced by $(n + 1)^D$]. Once more, using the lower bound, one finds an expression for R_0 which is the same as the one for C but with p replaced by $2p$.

PART II

THE LOW PASS FILTER

1. Encoding and Detection

If $f(t)$ is a signal emerging from a low pass filter (so that its spectrum is confined to the frequency band $|\nu| < W$ cycles per second) then $f(t)$ has a special analytic form given by the sampling theorem[3]

$$f(t) = \sum_{m=-\infty}^{\infty} f\left(\frac{m}{2W}\right) \frac{\sin \pi (2Wt - m)}{\pi(2Wt - m)} \tag{7}$$

Thus the signal is completely determined by the sequence of sample values $f(m/2W)$. The average power of the signal $f(t)$ is measured by

$$P = \lim_{T \to \infty} \frac{1}{2T} \int_{-T}^{T} f^2(t) \, dt$$

which can be expressed in terms of the sample values as follows

$$P = \lim_{M \to \infty} \frac{1}{2M} \sum_{m=-M}^{M} f^2\left(\frac{m}{2W}\right). \tag{8}$$

As in Part I, consider a message source producing a sequence of letters from an alphabet of K equally likely letters. To transmit this information over the low pass filter we must encode the sequence into a function

[3] C. E. Shannon, "Communication in the Presence of Noise," Proc. I. R. E., **37**, pp. 10–21, Jan. 1949.

$f(t)$ of the form (7), or in other words into a sequence of sample values $f(m/2W)$. To do this, we construct a new alphabet containing K letters which are different sequences of real numbers of some fixed length, say D places. When we let the letters of the new alphabet correspond to letters of the old one the message is translated into a sequence of real numbers which we use for the sequence $f(m/2W)$.

If the K letters of the sequence alphabet are

$$S_1\colon\ a_{11},\ \cdots,\ a_{1D}$$
$$S_2\colon\ a_{21},\ \cdots,\ a_{2D}$$
$$\cdot\quad\cdot\qquad\quad\cdot$$
$$\cdot\quad\cdot\qquad\quad\cdot$$
$$\cdot\quad\cdot\qquad\quad\cdot$$
$$S_K\colon\ a_{K1},\ \cdots,\ a_{KD},$$

the expression (8) for the average power of the function $f(t)$ becomes

$$P = \frac{1}{DK}\,(d_1^2 + d_2^2 + \cdots + d_K^2) \tag{9}$$

where

$$d_i^2 = \sum_{j=1}^{D} a_{ij}^2.$$

If the D numbers in the sequence S_i are regarded as coordinates of a point in Euclidean D dimensional space, d_i^2 represents the square of the distance from the point representing S_i to the origin.

When $f(t)$ is transmitted, the received signal will be $f(t) + n(t)$ where $n(t)$ is some (unknown) white Gaussian noise signal. The noise signals $n(t)$ are characterized by the fact that their sample values $n(m/2W)$ are independently distributed according to Gaussian laws. That is,

$$\mathrm{Prob}\left(n\left(\frac{m}{2W}\right) \le X\right) = \frac{1}{\sqrt{2\pi}\sigma} \int_{-\infty}^{X} e^{-y^2/2\sigma^2}\,dy. \tag{10}$$

The variance σ^2 of the distribution of noise samples is, by an application of (8), the power of this ensemble of noise signals.

At the receiving end of the channel, there is a detector which observes each block of D sample values $f(m/2W) + n(m/2W)$ and tries to decide which one of the K letters $S_1,\ \cdots,\ S_K$ was sent. In terms of the geometric picture, the detector divides all of D dimensional space into K non-overlapping regions $U_1,\ \cdots,\ U_K$ with the property that, if the D received sample values are represented by a point in U_i, the detector

decides that S_i was sent. By Equation (10), the probability that the detector picks the wrong letter when S_i is sent is

$$p_i = \frac{1}{(2\pi)^{D/2}\sigma^D} \int \int_{\overline{U}_i} \cdots \int e^{-r_i{}^2/2\sigma^2} \, dy_1 \cdots dy_D \qquad (11)$$

where $\overline{U}_i$ is the set of all points not in U_i and r_i is the distance from $(y_1, \cdots, y_D)$ to the point representing S_i.

For any given alphabet the best possible detector (in the sense that it minimizes the average probability of making an error in guesssing a letter) is called a *maximum likelihood detector*. The region U_i for a maximum likelihood detector consists of all points $(y_1, \cdots, y_D)$ which are closer to the point S_i than to any other letter point $S_j (r_i < r_j$ for all $j \neq i)$. To prove that this choice of U_i is best possible consider any other detector such that U_i contains a set V of points in which $r_i > r_j$. A direct calculation shows that the detector obtained by removing V from U_i and making V part of U_j has a smaller probability of error per letter. The set of points equidistant from two given points is a hyperplane. The region U_i of a maximum likelihood detector is a convex region bounded by segments of the hyperplanes

$$r_i = r_1, \qquad r_i = r_2, \cdots.$$

To compare signalling alphabets under the most favorable possible circumstances, we always compute letter error probabilities assuming that the detector is a maximum likelihood detector.

2. Computation of error probabilities

Exact evaluation of the letter error probability integral (11) is impossible except in a few special cases. Fortunately we are only interested in (11) when σ is small enough in comparison to the size of U_i to make the integral small. Then fairly accurate approximate formulas can be derived.

Theorem 3. Let R_{ij} be the distance between letter points S_i and S_j. Then

$$1 - \prod_{j\neq i} (1 - Q_{ij}) \le p_i \le \sum_{j\neq i} Q_{ij} \qquad (12)$$

where

$$Q_{ij} = \frac{1}{\sqrt{2\pi}} \int_{R_{ij}/2\sigma}^{\infty} e^{-x^2/2} \, dx.$$

The proof of Theorem 3 follows from the fact that Q_{ij} is the probability that, when S_i is transmitted, the received sequence will be closer to S_j than to S_i.

In the cases to be computed Q_{ij} is a rapidly decreasing function of R_{ij} and the only terms worth keeping in (12) are the ones for which R_{ij} is the smallest of the numbers $R_{i1}, \cdots, R_{iK}$. Moreover since the Q_{ij} are all small enough so that the upper and lower bounds differ only by a few per cent, the upper bound is a good approximation to p_i. Then a simple approximate formula for the average letter error probability $p = (p_1 + \cdots + p_K)/K$ is

$$p = \frac{N}{\sqrt{2\pi}} \int_{r_0/\sigma}^{\infty} e^{-x^2/2} \, dx \tag{13}$$

where $2r_0$ is the smallest of the $K(K-1)/2$ distances R_{ij} and N is the average over all letters in the alphabet of the number of letter points which are a distance $2r_0$ away.

3. Efficiency graph

The efficiency graph to be described was constructed originally to compare alphabets for signalling telephone numbers of length equal to ten decimal digits. It was desired that on the average only one telephone number in 10^4 should be received incorrectly. As described in Part I section 2, if the telephone numbers are encoded into sequences of letters from an alphabet of K letters, we must require that the average probability of error in any letter be

$$p = 10^{-5} \log_{10} K \tag{14}$$

or smaller.

Given an alphabet, one can compute with the help of (13) and (14) and a table of the error integral the largest value of the noise power σ^2 which can be tolerated. The average power of the transmitted signal is P given by Equation (9). Hence we can compute the smallest signal to noise ratio

$$Y = P/\sigma^2 \tag{15}$$

which will be satisfactory.

A letter containing $\log K$ bits of information is transmitted during an interval of $D/2W$ seconds. Hence the rate at which information is received is

$$R = \frac{2W \log K}{D} \tag{16}$$

bits per second. Again Equation (16) ignores a term representing in-

formation lost due to channel noise which is negligible because the error probability is low.

The efficiency graph, Fig. 2, is a chart on which the signal to noise ratio Y in db [computed from Equation (15)] is plotted against the signalling rate per unit bandwidth $R/W = (2 \log K)/D$ for different alpha-
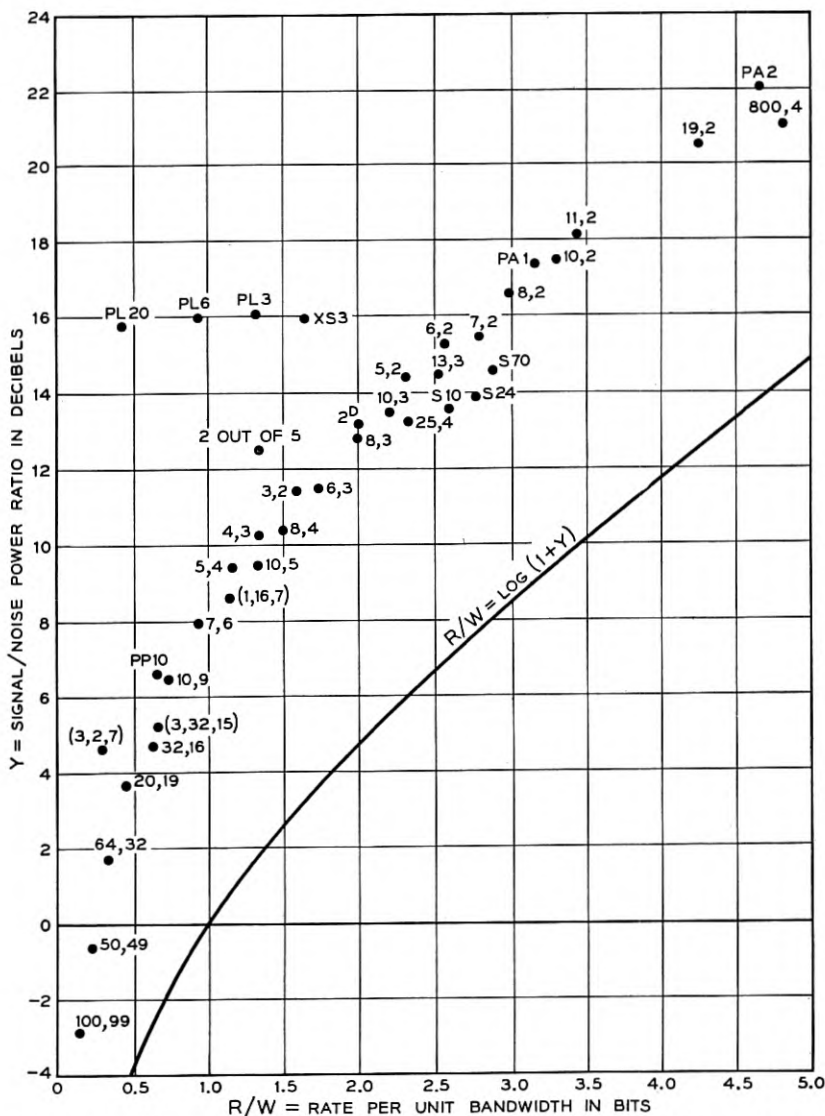
Fig. 2—Probability is 10^{-4} that an error is made in a 10 digit decimal number.

bets. An alphabet is considered poor if its point on the efficiency graph lies far above the ideal curve $R/W = C/W = \log (1 + Y)$.

4. The alphabets

The alphabets which appear on the efficiency graph are the following:

excess three (XS3): the ten sequences of 4 binary digits which represent 3, 4, $\cdots$, and 12 in binary notation;

two out of five: the ten sequences of five binary digits which contain exactly two ones;

pulse position (PP10): the ten sequences of ten binary digits which contain exactly one one;

2^D *binary*: all of 2^D sequences of D binary digits.

pulse amplitude (PAn): the $2n + 1$ sequences of length 1 consisting of $-n, -n + 1, \cdots , n$. This alphabet gives rise to a sort of quantized amplitude modulation.

pulse length (PLn): the $n + 1$ sequences of n binary digits of the form $11 \cdots 10 \cdots 0$, i.e., a run of ones followed by a run of zeros.

Minimizing alphabets (K, D): The above alphabets are taken from actual practice. They are convenient because, aside from PAn, they require a signal generator with only two amplitude levels. If we ignore ease of generating the signals as a factor, a great many geometric arrangements of points suggest themselves as possible good alphabets. The principle by which one arrives at good alphabets may be described as follows. When a D and K have been determined which give the desired information rate R [by Equation (16)] try to arrange the K letter points in D dimensional space in such a way that the distances between pairs of points are all greater than some fixed distance and that the average of the K squared distances to the origin is minimized. By Equations (9) and (13) it is seen that, apart from the small influence of the factor N, this process must minimize the signal to noise ratio Y required.

Ordinarily it is difficult to prove that a configuration is a minimizing one. Even to recognize a configuration which leads to a relative minimum (*i.e.* a minimum over all nearby configurations) is not always easy. The eight vertices of a cube, for example, do not give a relative minimum. Consequently, most of the alphabets to be described are only conjectured to be "best possible." Each of them satisfies one necessary requirement of minimizing alphabets that the centroid of the point configuration (assuming a unit mass at each letter point) lies at the origin. That this condition is necessary follows from the easily derived identity

$$r_2^2 = r_1^2 - R_0^2$$
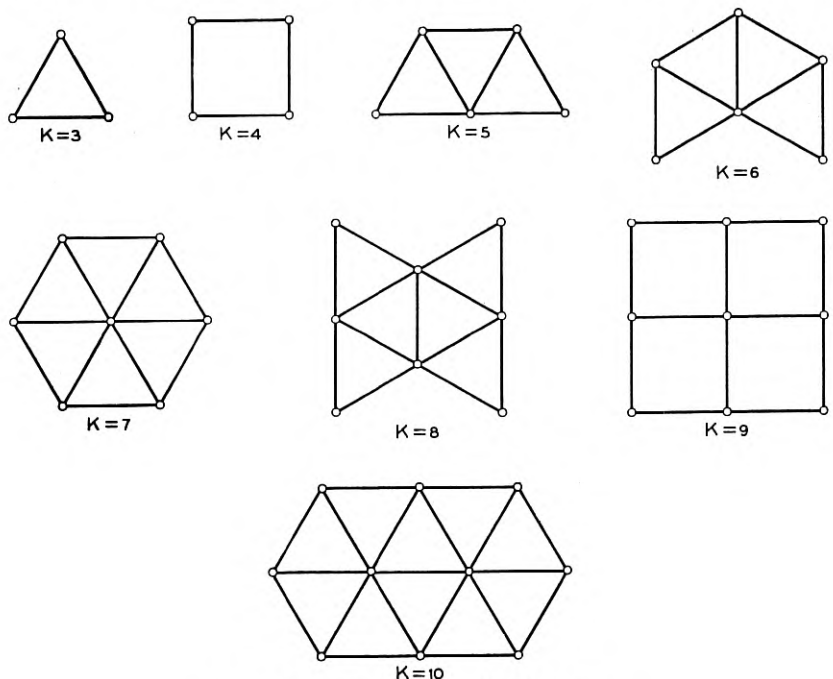
Fig. 3—Two dimensional alphabets.
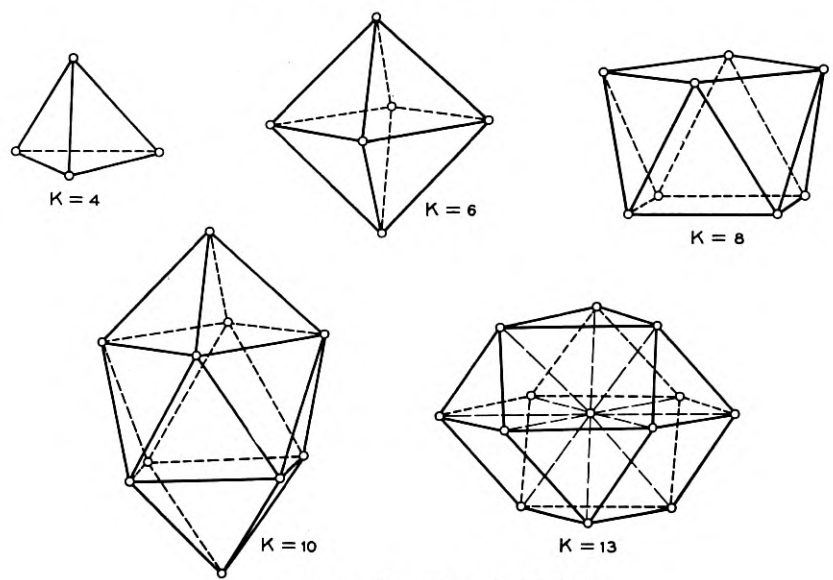
Fig. 4—Three dimensional alphabets.

where r_1 is the rms distance from the origin to the points of a configuration A, R_0 is the distance from the origin to the centroid of A, and r_2 is the rms distance from the points of A to the centroid of A.

In plotting points on the efficiency graph the notation K, D is used for the best K-letter D-dimensional alphabet which has been found. The arrangement of points for various $K, 2$ and $K, 3$ alphabets is given in Figs. 3 and 4. In these figures two points are joined by a straight line if the distance between them is 1 (which is the value we have adopted for the minimum allowed separation $2r_0$). Although not shown, the origin is always at the centroid of the figure. To aid interpretation of these diagrams we have included Fig. 5 which demonstrates how all the signals of a typical alphabet can be generated. The functions of time shown in
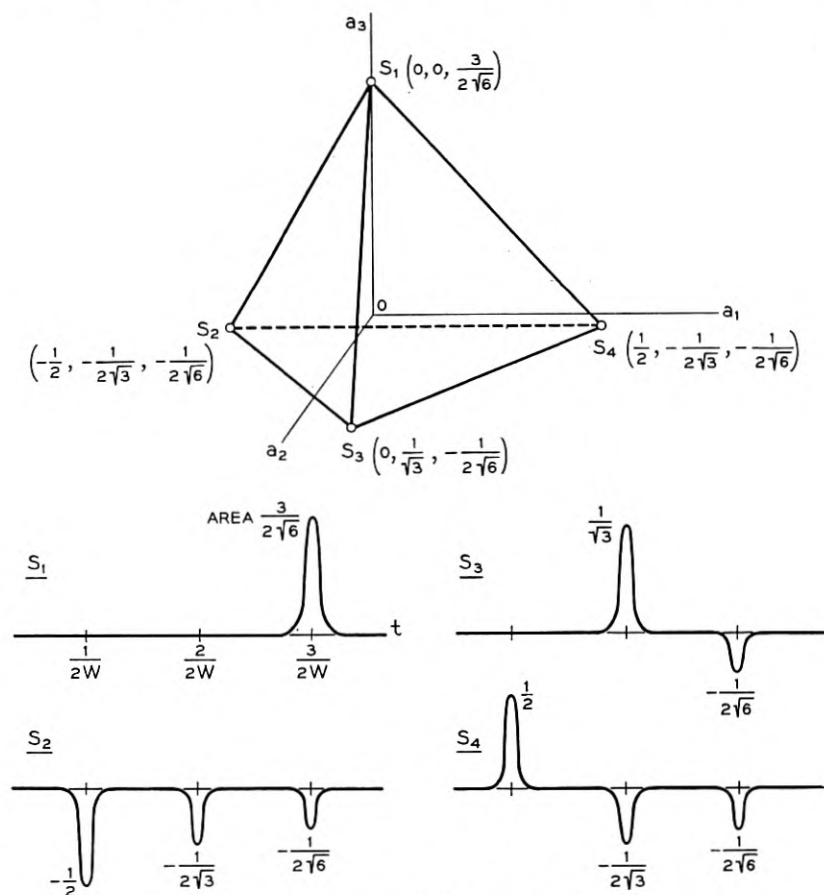
Fig. 5—Generation of the 4,3 code signals.

Fig. 5 are not the code signals themselves but impulse functions which are to be passed through a low pass filter with cutoff at W c.p.s. to form the code signals.

The best possible higher dimensional alphabets can be described more easily verbally than pictorially. In four dimensions we have found four alphabets.

The *25,4* alphabet consists of the origin and all 24 points in 4 dimensional space having two coordinates equal to zero and the remaining two equal to $1/\sqrt{2}$ or $-1/\sqrt{2}$. Each of the 24 points lies a unit distance away from the origin and its 10 other nearest neighbors; they are, in fact, the vertices of a regular solid. This alphabet has an advantage beyond its high efficiency. The code signals are composed entirely of positive and negative pulses of fixed energy and so should be easier to generate than most of the other codes which appear in this paper.

The *800, 4* alphabet is constructed in the following way: Consider a lattice of points throughout the entire 4-dimensional space formed by taking all the linear combinations with integer coefficients of a basic set of four vectors. That is, the lattice points are of the form $C_1v_1 + C_2v_2 + C_3v_3 + C_4v_4$ where $C_1, \cdots, C_4$ are integers and the v_i are the four given vectors. In connection with our problem it is of interest to know what lattice, (i.e. what choice of v_1, v_2, v_3, v_4) has all lattice points separated at least unit distance from one another and at the same time packs as many points as possible into the space per unit volume. When a solution to this "packing problem" is known, it is clear that a good alphabet can be obtained just by using all the lattice points which are contained inside a hypersphere about the origin as the letter points. Many of the two dimensional alphabets illustrated in the sketches are related in this way to the corresponding two dimensional packing problem (which is solved by letting v_1 and v_2 be a pair of unit vectors 60° apart). A solution to the four dimensional packing problem is afford by

$$v_1 = \frac{1}{\sqrt{2}}, \quad \frac{1}{\sqrt{2}}, \quad 0, \quad 0$$

$$v_2 = \frac{1}{\sqrt{2}}, \quad 0, \quad \frac{1}{\sqrt{2}}, \quad 0$$

$$v_3 = \frac{1}{\sqrt{2}}, \quad 0, \quad 0, \quad \frac{1}{\sqrt{2}}$$

$$v_4 = 0, \quad \frac{1}{\sqrt{2}}, \quad \frac{1}{\sqrt{2}}, \quad 0.$$

This lattice contains two points per unit volume (twice as dense as the cubic lattice in which $v_1, \cdots, v_4$ are orthogonal to one another) and each

point has 18 nearest neighbors. A hypersphere of radius 3 about the origin has a volume $(\pi^2/2)3^4$, about 400. Thus it contains about 800 lattice points. Take these as the code points of the 800, 4 code. Their average squared distances from the origin can be estimated as

$$\frac{\int_0^3 r^5\, dr}{\int_0^3 r^3\, dr} = \frac{2}{3}\,(3)^2 = 6.$$

N in Equation (13) may be estimated at 18; this is conservative because some lattice points outside the sphere are being counted.

The two remaining four dimensional alphabets belong to two families of D-dimensional alphabets.

The 4, 3; 5, 4; $\cdots$; $D + 1$, D $\cdots$ alphabets are the vertices of the simplest regular solid in D-dimensional space. For example, 4, 3 is a tetrahedron. Such a solid can be constructed from $D + 1$ vertices whose coordinates are the first $D + 1$ rows of the scheme

0	0	0	0	0	$\cdots$
1	0	0	0	0	$\cdots$
$\frac{1}{2}$	$\frac{3}{2\sqrt{3}}$	0	0	0	$\cdots$
$\frac{1}{2}$	$\frac{1}{2\sqrt{3}}$	$\frac{4}{2\sqrt{6}}$	0	0	$\cdots$
$\frac{1}{2}$	$\frac{1}{2\sqrt{3}}$	$\frac{1}{2\sqrt{6}}$	$\frac{5}{2\sqrt{10}}$	0	$\cdots$
$\frac{1}{2}$	$\frac{1}{2\sqrt{3}}$	$\frac{1}{2\sqrt{6}}$	$\frac{1}{2\sqrt{10}}$	$\frac{6}{2\sqrt{15}}$	$\cdots$
.	.	.	.	.	$\cdots$
.	.	.	.	.	$\cdots$
.	.	.	.	.	$\cdots$

The vertices all lie a distance $\sqrt{D/2(D + 1)}$ from the centroid of the figure.

6, 3; 8, 4; $\cdots$; $2D$, D, $\cdots$ are obtained by placing a point wherever any positive or negative coordinate axis intersects the sphere of radius

$1/\sqrt{2}$ about the origin. Thus it follows that 6, 3 consists of the vertices of an octohedron.

Error correcting alphabets $((k, K, D))$: The error correcting alphabets discussed in Part I can be converted into good alphabets for this channel by replacing all digits which equalled 0 by -1. Three error correcting alphabets appear on the chart; each is labelled by three numbers signifying (k, K, D).

Slepian alphabets (SD): Using group theoretic methods, D. Slepian has attempted to construct families of alphabets which signal at rates approaching C. Although this goal has not yet been reached, families of alphabets depending on the parameter D have been found which approach the ideal curve to within 6.2 db and then get worse as $D \to \infty$. In the simplest of these families of alphabets, $D = 2m$ is even and the letters consist of all the $2^m C_{2m, m}$ sequences containing m zeros, the remaining places being filled by ± 1. The best alphabet in this family is the one with $D = 24$. It lies 6.23 db away from the ideal curve and contains 1.1 x 10^{10} letters. The alphabets of this family for $D = 10, 24$, and 70 appear on the efficiency graph labelled $S10$, $S24$, and $S70$.

The conclusion to which one is forced as a result of this investigation is that one cannot signal over a channel with signal to noise level much less than 7 db above the ideal level of Equation (2) without using an unbelievably complicated alphabet. No ten digit alphabet tolerates less than 7.7 db more than the ideal signal to noise ratio.

It would be interesting to know more about good higher dimensional alphabets. They are very much more difficult to obtain. The regular solids, which provided some good alphabets in 3 and 4 dimensions, provide nothing new in 5 or more dimensions; there are only three of them and they correspond to our $D + 1, D; 2D, D$, and 2^D binary alphabets. Worse still, the packing problem also becomes unmanageable after dimension 5.

Principle Strains in Cable Sheaths and Other Buckled Surfaces

By I. L. HOPKINS

(Manuscript Received February 25, 1952)

Equations are developed for rigorous determination of magnitudes and directions of principal strains in plastic deformation, by means of measurements of rectangular strain rosettes. Application to the study of telephone cable sheath is described.

In the course of certain studies of the polyethylene used in the sheath of telephone cable, it was necessary to calculate the magnitudes and directions of the principal strains from data obtained by measurements of the distortion of a square grid which had previously been printed on the surface of the cable. The strains were large, rendering useless the usual expressions for analysis of strain rosette data[1]. Such large strains are characteristically sustained for a wide variety of high polymeric materials of increasing importance for wire and cable sheathing as well as other structural uses. In this article the requisite formulas are developed.

The basic assumptions are:

(1) The strains may be large.

(2) The strains are uniform over any square of the grid (equivalent to the condition that a square transforms into a parallelogram).

(3) The square may be regarded as plane.

(4) Two of the principal strains are parallel to the surface.

We shall first consider only the two principal strains in the plane of the surface of the cable. Suppose these two strains to be parallel with the x and y coordinate axes, respectively, and that one side of the square is aligned, before straining, at the angle ϕ with the x axis. This is illustrated in Fig. 1.

$$\text{Let } e_x = \text{maximum principal strain}$$
$$e_y = \text{minimum principal strain}$$
$$\lambda_x = 1 + e_x$$
$$\lambda_y = 1 + e_y$$

---

[1] Cf. for example, Max Frocht, "Photoelasticity," **1**, p. 37, 1941.

If primes are used to refer to the strained state,

$$\lambda_x = \frac{x_b' - x_a'}{x_b - x_a} = \frac{x_d' - x_c'}{x_d - x_c}$$

$$\lambda_y = \frac{y_b' - y_a'}{y_b - y_a} = \frac{y_d' - y_c'}{y_d - y_c}$$

If L_1 and L_2 are the lengths of the sides of the unstrained square, and L_3 and L_4 the diagonals,

$$(L_1 + \Delta L_1)^2 = \lambda_x^2(x_b - x_a)^2 + \lambda_y^2(y_b - y_a)^2 \tag{1a}$$

$$(L_2 + \Delta L_2)^2 = \lambda_x^2(x_d - x_c)^2 + \lambda_y^2(y_d - y_c)^2 \tag{1b}$$

$$(x_b - x_a)^2 = (y_d - y_c)^2 = L_1^2 \cos^2\phi_1 = L_2^2 \cos^2\phi_1 \tag{2a}$$

$$(y_b - y_a)^2 = (x_d - x_c)^2 = L_1^2 \sin^2\phi_1 = L_2^2 \sin^2\phi_1 \tag{2b}$$

whence, if

$$\frac{L_1 + \Delta L_1}{L_1} = L_1', \frac{L_2 + \Delta L_2}{L_2} = L_2', \text{etc.} \tag{2c}$$

$$L_1'^2 = \lambda_x^2 \cos^2 \phi_1 + \lambda_y^2 \sin^2 \phi_1 \tag{3a}$$

$$L_2'^2 = \lambda_x^2 \sin^2 \phi_1 + \lambda_y^2 \cos^2 \phi_1 \tag{3b}$$
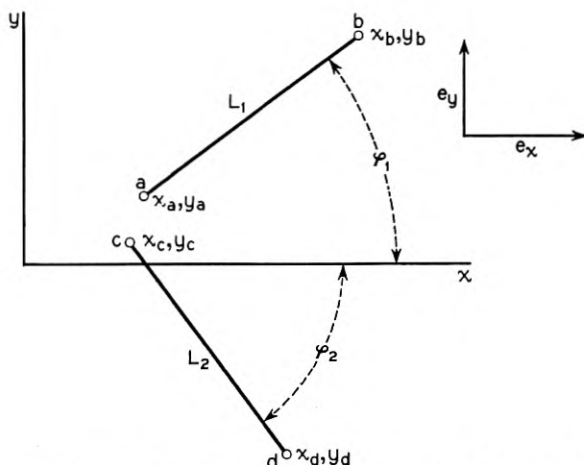
Fig. 1—Lines ab and cd, before the xy plane is strained by stretching (or compressing) in the x and y directions.

Henceforth, for clarity, suppose the subscript "1" to refer to the longer side of the parallelogram, "2" to the shorter side, "3" to the longer diagonal, and "4" to the shorter.

$$S_1 = \text{original slope of } L_1 = \tan \phi_1 = \frac{y_b - y_a}{x_b - x_a}$$

$$S_2 = \text{original slope of } L_2 = \tan \phi_2 = \frac{y_d - y_c}{x_d - x_c}$$

$$S_1' = \tan \phi_1' = \frac{\lambda_y}{\lambda_x} S_1 \tag{4a}$$

$$S_2' = \tan \phi_2' = \frac{\lambda_y}{\lambda_x} S_2 \tag{4b}$$

Since $\phi_1 - \phi_2 = 90°$,

$$S_2 = -\frac{1}{S_1} \tag{5a}$$

$$S_2' = -\lambda_y/\lambda_x S_1 \tag{5a}$$

By expansion and substitution from Equations (4) and (5),

$$\tan (\phi_1' - \phi_2') = \frac{\dfrac{\lambda_y}{\lambda_x} \left(S_1 + \dfrac{1}{S_1} \right)}{1 - \left(\dfrac{\lambda_y}{\lambda_x} \right)^2} \tag{6}$$

Let
$$\psi = 90° - (\phi_1' - \phi_2')$$

then

$$\tan (90° - (\phi_1' - \phi_2')) = \tan \psi = \frac{1 - \left(\dfrac{\lambda_y}{\lambda_x} \right)^2}{\dfrac{\lambda_y}{\lambda_x} \left(S_1 + \dfrac{1}{S_1} \right)} \tag{7}$$

which is the shear between L_1' and L_2'.

$$(S_1 + 1/S_1) = \tan \phi_1 + \cot \phi_1 = \frac{2}{\sin 2\phi_1} \tag{8}$$

and substituting this in equation (7),

$$\sin 2\phi_1 = \frac{2\lambda_x\lambda_y \tan \psi}{(\lambda_x^2 - \lambda_y^2)} \tag{9}$$

whence

$$\cos 2\phi_1 = \sqrt{1 - \frac{4\lambda_x^2 \lambda_y^2 \tan^2 \psi}{(\lambda_x^2 - \lambda_y^2)^2}} \tag{10}$$

Remembering that

$$\cos^2 \phi_1 = \frac{1 + \cos 2\phi_1}{2} \tag{11a}$$

and

$$\sin^2 \phi_1 = \frac{1 - \cos 2\phi_1}{2} \tag{11b}$$

and substituting Equation (10) in Equation (11), Equation (11) in Equation (3), and then solving the quadratic equation thus formed for λ_x and λ_y, we have

$$\lambda_x^2, \lambda_y^2 = \frac{(L_1'^2 + L_2'^2) \pm \sqrt{(L_1'^2 + L_2'^2)^2 - 4L_1'^2 L_2'^2 \cos^2 \psi}}{2} \tag{12}$$

Referring to Fig. 2, and using the law of cosines, and remembering that L_3' is the ratio of the strained to the unstrained length of the diagonal,

$$- \cos \theta = \sin \psi = \frac{2L_3'^2 - (L_1'^2 + L_2'^2)}{2L_1'L_2'} \tag{13a}$$

whence

$$\cos^2 \psi = \frac{4L_3'^2 (L_1'^2 + L_2'^2 - L_3'^2) - (L_1'^2 - L_2'^2)^2}{4L_1'^2 L_2'^2} \tag{13b}$$
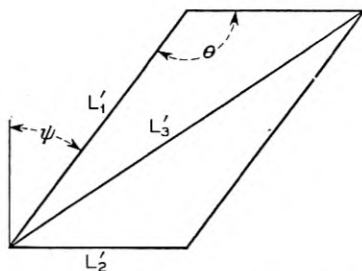
Fig. 2—A parallelogram formed by straining a square. L_1', L_2' and L_3' are the ratios of the lengths of the indicated lines to their original lengths.

This expression, substituted in Equation (12) and reduced, gives

$$\lambda_x^2, \lambda_y^2 = \frac{(L_1'^2 + L_2'^2) \pm \sqrt{2(L_1'^2 - L_3'^2)^2 + 2(L_2'^2 - L_3'^2)^2}}{2} \quad (14)$$

It may be noted here that a property of the parallelogram, namely, in the notation used here,

$$L_1'^2 + L_2'^2 = L_3'^2 + L_4'^2 \quad (15)$$

makes it immaterial which diagonal is used. This may be readily seen by substituting

$$L_3'^2 = L_1'^2 + L_2'^2 - L_4'^2$$

in Equation (14). The effect is merely that of substituting L_4 for L_3. In Equation (13a), however, the result is a change in the sign of ψ.

As an example of the application of these equations, the measurements of one specimen were:

$$L_1' = 2.1$$
$$L_2' = 1.2$$
$$L_3' = 2.0$$

From Equation (14),

$$\lambda_x^2 = 4.758, \quad \lambda_x = 2.181, \quad e_x = 1.181$$
$$\lambda_y^2 = 1.092 \quad \lambda_y = 1.045 \quad e_y = 0.045$$

From Equation (13a),

$$\sin \psi = 0.4266, \text{ whence}$$
$$\psi = 25.3°$$
$$\tan \psi = 0.472$$

From Equation (9),

$$\sin 2\phi_1 = 0.587$$
$$\phi_1 = 18.0°$$
$$\tan \phi_1 = 0.324$$

From Equation (4a),

$$\tan \phi_1' = 0.1554$$
$$\phi_1' = 8.83°$$

FromEquation (9), it is obvious that the maximum value of $\tan \psi$ occurs at $\phi_1 = 45°$, and is in this case equal to 0.804.

This example is illustrated in Fig. 3.

The question of direction of the x and y axes is simply settled by drawing a line through either of the acute angles of the parallelogram, crossing the parallelogram at an angle ϕ_1' with the longer side. This line will be parallel to the x direction, which is, according to the convention, that of greatest strain.

So far no mention has been made of strain in the third dimension; that is, a change in thickness of the sheath. In plastic deformation, the volume change is generally negligible. This requires that

$$\lambda_x \lambda_y \lambda_z = 1$$

whence

$$\lambda_z = \frac{1}{\lambda_x \lambda_y}$$
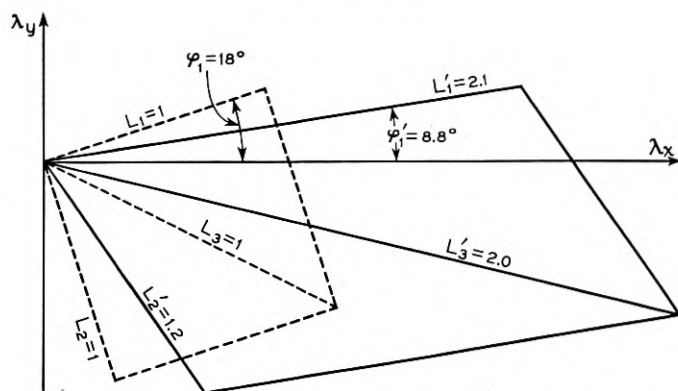
Fig. 3—A square and the parallelogram resulting from stretching to length ratios $\lambda_x = 2.181$ in the x-direction and $\lambda_y = 1.045$ in the y-direction.

TABLE I

Degrees of twist in 3 feet	Principal Strains, per cent		
	Parallel to Surface		Perpendicular to Surface
	Max.	Min.	
180	16	06	−19
270	26	09	−27
360	33	14	−34
450	36	20	−39
540	42	19	−41
630	43	22	−43
720	46	24	−45

In the example given,

$$\lambda_z = 0.439, \qquad e_z = -0.561$$

Polyethylene sheaths of cable specimens 3 feet long buckled severely over their entire length when the cables were twisted 720° and showed the strains given in Table I at steps up to the final twist[2].

The ratio of maximum to minimum strain parallel to the surface is about 2:1. Tests with a 1:1 ratio[3], a more severe condition, have shown that the principal strains at rupture will be of the order of 300 per cent. Therefore it is evident that the strains incidental to the most severe types of handling will not, of themselves, cause rupture of the sheaths.

---

[2] Unpublished memorandum by A. G. Hall.

[3] I. L. Hopkins, W. O. Baker and J. B. Howard, *J. Appl. Phys.*, **21**, No. 3, pp. 206–213, March, 1950.

A New Recording Medium For Transcribed Message Services

By JAMES Z. MENARD

A magnetic recording medium composed of rubber impregnated with magnetic oxide and lubricant is particularly suited to applications requiring the continuous repetition of short transcribed messages. It affords exceptional life, reliability, and economy in telephone applications, where it is utilized in the form of molded bands stretched over cylinders of the recording mechanisms.

In the Bell System there are several applications requiring the repetition of short voice announcements. Some of the existing applications are weather announcements, intercept of calls to vacant and unassigned numbers, quotations of delays on long-distance calls, and certain leased industrial services, such as stock price quotation. Most of these require continuous repetition of messages between 5 and 60 seconds in length. In some the message remains fixed but in others it is changed at frequent intervals.

Magnetic recorders offer particular advantages for services of this nature, because they require a minimum of equipment and operating skill to produce durable records which are instantly reproducible without processing. For several years the Bell System has used a magnetic recorder employing a loop of Vicalloy tape in the 3A announcement system to furnish weather announcements, and a similar type of recorder has been used in a leased industrial system at the *New York Times.*

Recently these Laboratories have undertaken the development of transcribed message facilities to meet additional service applications. It was required that the new facilities should provide satisfactory transmission quality and afford considerable flexibility in regard to message length, but the paramount requirement was for reliability and long life.

It did not appear practicable to extend the techniques of the Vicalloy tape machine to give the flexibility, convenience of operation and re-

liability desired in the new applications, and attention was therefore directed to two new classes of magnetic recording media which have been developed in recent years. These are the electroplated media and the powdered media.

In recent years magnetic recording media have been commercially produced by an electroplating process by the Brush Development Company of Cleveland, Ohio. Evaluation by Bell Telephone Laboratories shows that such a plating does not easily deteriorate, gives a relatively high signal output and is capable of excellent transmission characteristics. But in order to realize consistently satisfactory transmission, it is necessary to maintain intimate contact between the recording medium and the magnetic recording and reproducing heads. The expense of providing the relatively precise mechanisms necessary to obtain the desired performance objectives suggested the exploration of other media which might simplify this problem.

The powdered magnetic media have evolved from German work dating back to about 1932 and from American work since about 1941. In these media the active magnetic material is a finely divided ferro-magnetic powder, usually iron oxide. This is usually applied with a binder as a surface coating on a tape of plastic or paper, but the Germans at one time produced a tape which was a homogeneous mixture of oxide and plastic. In their present state of development, media of this type offer excellent transmission characteristics and are relatively economical. In the past four or five years they have found widespread commercial application in the form of coated tape in all fields of recording and transcription work.

Attempts were made to employ commercial types of these coated tapes in various forms of continuous-loop mechanisms, but none met the desired requirements in regard to life, reliability, and flexibility of operation. An analysis of the experimental results indicated that most failures were due to physical failure of the media as a result of the tension, flexion and abrasion to which they were subjected, but the magnetic records were substantially undeteriorated even when physical failure of the supporting base occurred.

It became apparent that a specialized recording medium would have to be developed to meet the Bell System requirements for transcribed message services. Development effort was concentrated on the field of powdered media, because these media offered attractive transmission properties and because the expanding commercial importance of this field promised a continuing industrial development and production program which would provide an economical source of high quality magnetic

materials. The following premises guided the development program:

(1) The recording medium should be subjected to the least possible physical manipulation in use to minimize failures. To accomplish this it was decided to develop the recording medium in a form suitable for use on the surface of a rotating cylinder and to use a helical recording track on this surface when the message length required more than one revolution of the cylinder. It was hoped that with this arrangement, physical failure of the recording medium would be eliminated, and the service life would be determined by the wear occurring between the medium and the magnetic pole pieces.

(2) The recording medium should exhibit some compliance to facilitate intimate contact with the magnetic pole-pieces.

(3) The transmission quality should meet present-day telephone standards for transmission of speech. The higher quality necessary for the recording of music, while desirable, should not be considered a requirement.

A number of experimental powdered media were prepared and tested. These all utilized commercially available iron oxide powder with a coercive force of approximately 250 oersteds, and the samples included coated media, made by dipping, spraying and doctoring the coating on various base materials, and impregnated media, prepared by mixing the oxide in the base material and forming the mixture.

A medium consisting primarily of an elastic rubber band impregnated with magnetic particles was found to be particularly suited to applications requiring long life in continuous service. A study of compounding and manufacturing processes for this medium was made by the rubber products group at these Laboratories under the direction of H. Peters, and the compound which evolved consists primarily of synthetic rubber loaded with magnetic iron oxide, and containing small amounts of lubricants, inhibitors and curing agents. The compound is decidedly rubberlike in character, and is utilized in the form of seamless bands about $\frac{1}{32}$ to $\frac{1}{8}$ inches thick, which are stretched over the surface of cylinders about 10 per cent larger than the bands.

The bands are prepared by thoroughly milling together the following:

> 100 Parts by weight type GN neoprene
>
> 100 Parts by weight magnetic iron oxide
>
> 5 Parts by weight zinc oxide
>
> 4 Parts by weight magnesium oxide
>
> 2 Parts by weight paraffin

and forming the compound into bands by conventional rubber molding and curing techniques. The resulting bands show a tensile strength of about 2500 pounds per square inch, and the elongation before breaking is about 700 per cent. No particularly difficult manufacturing problems are encountered, and present evidence indicates that satisfactory overall quality control can be achieved by carefully controlling the compounding constituents, the milling and the molding.

Several bands which are used in telephone services are shown in Fig. 1. These bands are utilized in recorder-reproducer mechanisms by stretching them over a cylinder, on which pivoted magnetic pole-pieces trace a cylindrical or a helical track as it rotates.

When the bands are first taken from the mold they exhibit a high coefficient of friction. After a few hours enough paraffin migrates to the surface to form a thin, slippery film. If the bands are then put into service the pole-pieces form a polished track and the continuing migration of paraffin maintains the lubricating film between the band and the pole-pieces.

If this recording medium is used intermittently, the self-lubrication may cause difficulty. The migration of lubricant to the recording surface is continuous, and the lubricant may accumulate on the surface in sufficient thickness to impair the contact with the magnetic head if the recording equipment is not operated for several weeks. It may then be
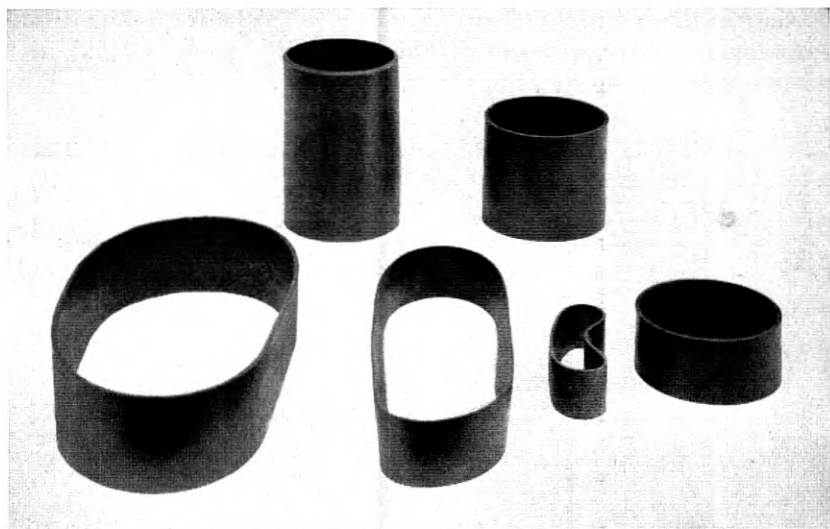
Fig. 1—Typical magnetic rubber bands used in telephone applications.

necessary to wipe the excess lubricant from the surface to obtain satis-
factory operation.

The lubricant in this particular recording medium was chosen for
operation in central offices and similar locations where temperature
ranges are moderate. If extreme temperatures are to be encountered the
lubricant problem will have to be re-examined. Continued research in this
field should result in improvement in this characteristic.

In life tests, five million message repetitions have been obtained with
insignificant wear of the band and the magnetic head, and with no
measurable deterioration in the level and quality of the recording after
an initial level drop of about 2 db which occurs during the first few
reproductions. The head pressure is a significant factor affecting the
life, and in these tests a head pressure of 25 grams was used with a
0.100 inch wide head.

This medium represents some compromise in the attainable trans-
mission properties to favor the physical properties desired for reliability
and long life, but the transmission is entirely adequate for the intended
applications.

A typical frequency response characteristic is shown in Fig. 2. This
is representative of the results obtained when the equipment is main-
tained by field personnel. The output level, also indicated by Fig. 2,
is from 8 to 12 db below that obtained from commercial coated magnetic
tape. This is largely because the concentration of magnetic oxide, on a
volume basis, cannot be made as high in the impregnated material as is
possible in the coating of conventional tape. This is not a serious dis-
advantage, however, as the level is high enough to permit amplification
without special precautions in regard to noise.
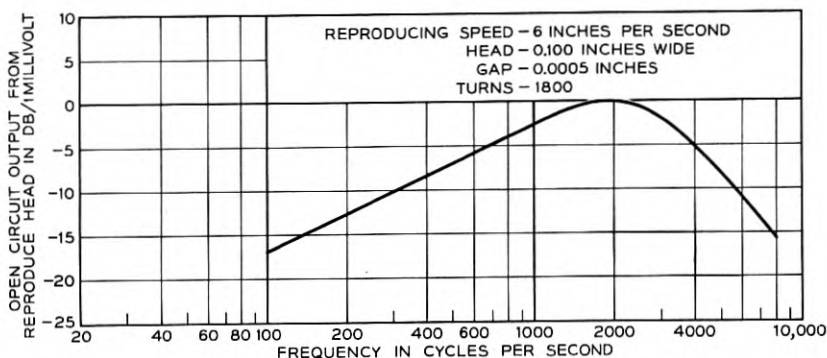
Fig. 2—Frequency response of magnetic recording equipment using iron oxide
impregnated molded neoprene bands.

When ring type magnetic heads are used for recording, these bands exhibit frequency response characteristics quite similar to coated tapes using the same magnetic oxides, although the bands are of homogeneous magnetic material up to $\frac{1}{8}$ inch thick and the tapes have magnetic coatings less than 0.001 inches thick. This is because the field from the recording gap becomes ineffective at a distance of about 0.001 inches, and the signal is recorded only on a thin surface layer of the medium, regardless of its total thickness.

The noise characteristic of this medium is somewhat unusual. It has been shown[*] that the reproducing process is not restricted to the surface layer of the medium, but that to a first approximation, when the medium has low permeability, the signal from a magnetized element at any depth in the recording medium will be attenuated with respect to the signal produced by the same element in intimate contact with the reproducing head by the factor:

$$\frac{55 \text{ decibels} \times S}{\lambda}$$

where S = distance between magnet and head
λ = "wavelength" of magnet

This indicates, for example, that the signal from a magnetized element at a depth of $\lambda/2.75$ will be attenuated by only about 20 db and may therefore make significant contribution to the total output.

In the Bell System telephone applications, where a transmission bandwidth of 100 to 4000 cycles per second is required, the belts are run at a speed of about 6 inches per second. The wavelength at 100 cycles per second is then 0.060 inches, and at this frequency significant output can be obtained from a layer about 0.02 inches thick. The desired recording is limited to a layer about 0.001 inches thick, but a layer of about twenty times this thickness may contribute to noise. As a consequence, at low frequencies this medium tends to exhibit higher background noise than do the coated tapes. The magnitude of the noise is appreciably affected by the method of erasure.

Two methods of erasing a magnetic record are known to the art. These are the saturation erase, in which the magnetic record is exposed to a unidirectional magnetic field of saturation intensity, and the neutralization erase in which the magnetic record is exposed to an alternating field which reaches saturation intensity and decreases cyclically to zero

* R. L. Wallace, Jr., "Reproduction of Magnetically Recorded Signals," *Bell System Tech. J.*, Oct., 1951.

over a period of several cycles. It is well known that a neutralization erase results in a residual background noise which may be as much as an order of magnitude below that produced by a saturation erase. The neutralization erase is therefore widely used in tape recording, and is obtained by energizing the erase head with alternating current of a frequency several times the highest signal frequency passed by the recording equipment.

With the impregnated recording medium, the recorded signal can be successfully erased by using a conventional ring-type erase head energized with high-frequency current. The field from this type of erasing effectively neutralizes the surface layer which contains the recorded signal, but does not penetrate appreciably beyond. Therefore, if precautions are not observed, the lower layers of this medium beyond the reach of the erase field may acquire a random cumulative magnetization from switching surges, accidental exposure to magnetized tools and strong fields, and this will be evidenced by a gradual deterioration in the signal to noise ratio at the low-frequency end of the transmission band. The quality, however, remains entirely adequate for commercial telephone use.

The foregoing limitations are minimized by an erasing method which has been developed at these Laboratories for applications where it is convenient to erase the entire message in one revolution of the recording cylinder, preparatory to recording a new message. This method employs an erasing structure in the form of an E-shaped stack of magnetic laminations, carrying on the center leg a coil which is energized by low-frequency (60 cycle) alternating current. The lamination stack is approximately the width of the recording medium, and the gaps between the center leg and each side leg are about $\frac{1}{4}$ inch wide. When this structure is spaced about $\frac{1}{16}$ inch from the surface of the recording medium traveling at 6 inches per second or less, and is energized by 60-cycle power to produce a maximum field of about 2000 gauss, the entire thickness of the recording medium is subjected to an alternating magnetic field which reaches saturation intensity and over a period of several cycles decreases progressively to zero. This effectively demagnetizes the full thickness of the recording medium. If the current is switched off with the erase structure in operating position, those elements of magnetic material within the field at that instant would be subjected to no further reversals and would consequently behave substantially as if they had been subjected to a direct-current magnetic field of the same intensity as the alternating-current field at the time it was interrupted. The section of record medium under the influence of the erase structure at the time it was de-energized would exhibit excessive noise in com-

parison with the remainder of the record-medium which was subjected to the normal alternating-current erase. This effect becomes negligible if the separation between the record medium and the erase structure is increased by $\frac{1}{2}$ inch before the current is interrupted. This is accomplished by using a solenoid-actuated mounting for the erase structure so arranged that the structure normally is retracted from the erasing position and holds open a switch in the circuit to its coil. When erasure is desired, the solenoid is actuated. This moves the erase structure into operating position and releases the switch to energize the coil. When the erase cycle is completed the solenoid is de-energized, and the erase structure retracts, opening the switch at the end of its travel. Fig. 3 is a sketch
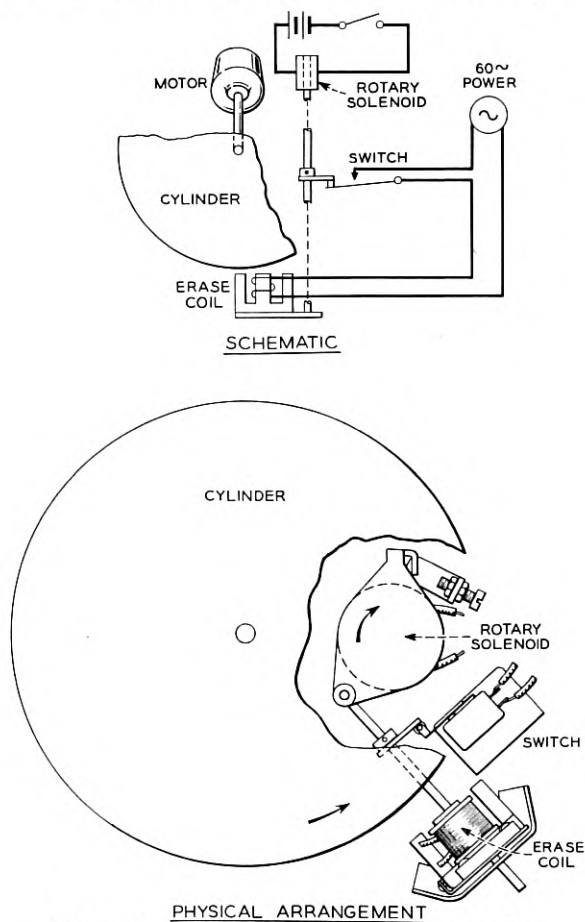
Fig. 3—Method of erasing magnetic recorder.
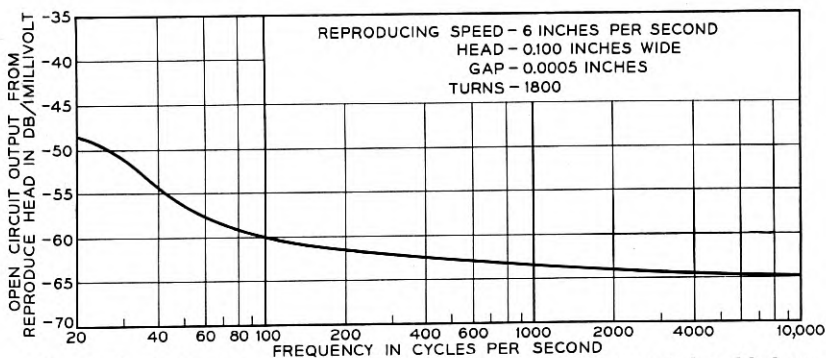
Fig. 4—Typical noise spectrum of $\frac{1}{8}$-inch iron oxide impregnated molded neoprene bands measured in 200 cycle bands after neutralization erase with 60-cycle ac field.

showing the application of this erase method to a cylinder-type machine. This method of erase results in a background noise level measured unweighted over a 4000-cycle band which is at least 45 db below a 1000-cycle signal recorded with 4 per cent total distortion. A typical background noise spectrum is shown in Fig. 4.
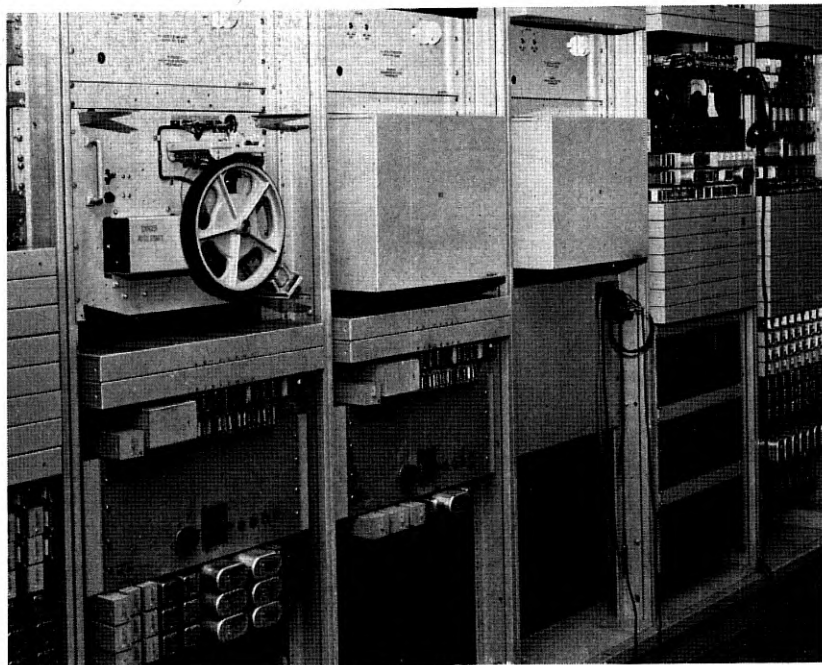
Fig. 5—General view of recording machines in 3A announcement system at Cleveland.
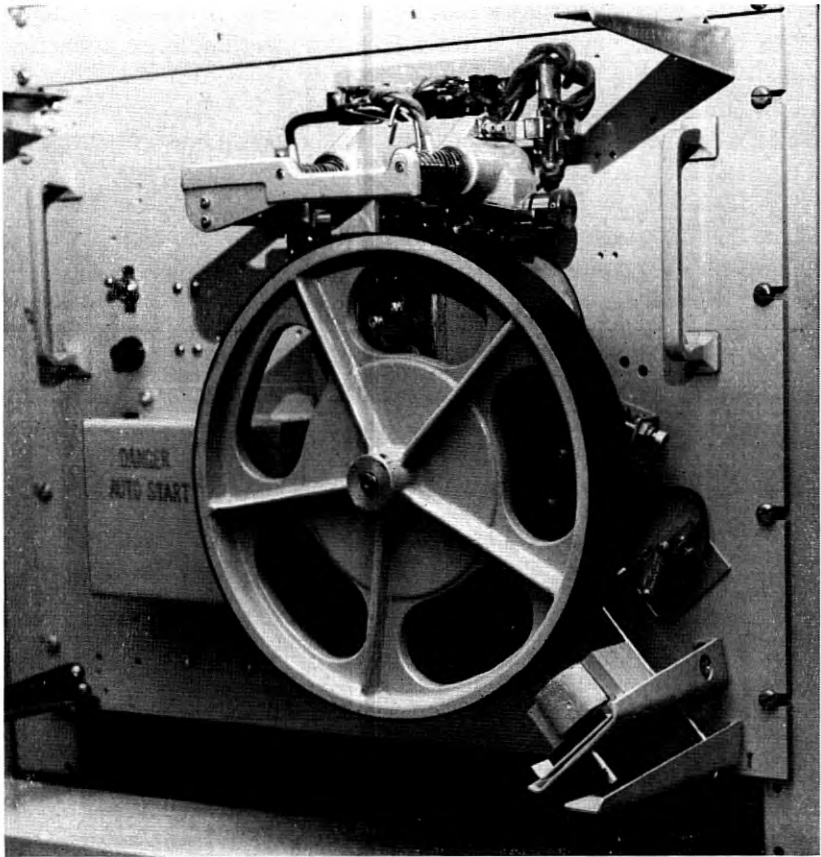
Fig. 6—Closeup of recording machine in 3A announcement system at Cleveland.

The first installation of transcribed message equipment employing this new medium was in the 3A announcement system at Cleveland, Ohio, to supply weather announcement service.

The magnetic recording equipment in this installation is a cylinder-type mechanism with associated recording-reproducing amplifier. The mechanism uses bands $\frac{1}{16}$ inch thick, $1\frac{5}{8}$ inches wide and $7\frac{13}{16}$ inches in diameter, stretched over a cylinder 9 inches in diameter. A single record-reproduce head in a pivoted mounting is cam-controlled to trace a helix on the cylinder. The cam is coupled to the cylinder via a quick-change gear train which gives a choice of a three-turn, a five-turn or an eight-turn helix, and the cylinder is driven from a gear-reducer which allows a choice of two slightly different operating speeds. Six different cycle times, ranging from about ten seconds to about 45 seconds, are provided

by the two operating speeds and the three cam ratios. Approximately 90 per cent of any cycle time is available for recording or reproduction, and the remaining 10 per cent is occupied by the return of the head to the beginning of the helix.

The recorded track is 0.100 inches wide, and when an eight-turn helix is used, there is a separation of 0.025 inches between tracks. The previously described low-frequency alternating current erase is used.

The 3A announcement system employs three channels of this recording equipment in a complex control circuit which provides facilities for erasing, recording, monitoring and automatic switchover to stand-by channels in event of failure. Figs. 5 and 6 show the recording equipment in the Cleveland installation.

Other equipments using this recording medium have been designed to furnish transcribed message service for intercept of calls to vacant, changed and unassigned numbers, to quote delays on long distance calls, and to furnish stock quotation service. Some of these equipments are now undergoing service trials preparatory to standardization for Bell System use.

This new recording medium has been developed to provide the maximum attainable life and reliability in applications requiring an enormous number of repetitions of voice messages. Equipment for such applications is usually located in central offices where the temperature range and other operating conditions are fairly well stabilized. These favorable conditions have facilitated the development of a recording medium which has made it possible to design simple and economical magnetic recorders which are sufficiently versatile and reliable to stimulate the use of transcribed message services to an extent hitherto unrealizable.

There are a number of potential Bell System applications for transcribed message services which do not require an extreme number of message repetitions, but put a premium on low initial cost and trouble-free operation in intermittent service under wide extremes of environment. It may prove desirable to meet the life requirements for applications of this type with a different approach to the lubrication problem, with an unlubricated compound, or with a coated medium which would have some transmission advantages. It is expected that further work in these fields will produce improved recording media for applications of this nature, to expand the field of use in the telephone plant.

Introduction to Formal Realizability Theory—II

By BROCKWAY McMILLAN

This part of the paper exhibits a network to realize a given positive real impedance matrix.

I. INTRODUCTION TO PART II

1.0 In this part of the paper we prove the following theorem:

1.1 *Theorem:* Let $Z(p)$ be an $n \times n$ matrix whose elements are $Z_{rs}(p)$, $1 \leq r, s \leq n$, where

   (i) Each $Z_{rs}(p)$ is a rational function

   (ii) $\overline{Z_{rs}(p)} = Z_{rs}(\bar{p})$

   (iii) $Z_{rs}(p) = Z_{sr}(p)$

   (iv) For each set of real constants $k_1, \cdots, k_n$, the function

$$\varphi_Z(p) = \sum_{r,s=1}^{n} Z_{rs}(p) k_r k_s$$

has a non-negative real part whenever $Re(p) > 0$.

Then there exists a finite passive network, a $2n$-pole, which has the impedance matrix $Z(p)$. A dual result holds for admittance matrices $Y(p)$.

1.2 The converse of this theorem was proved in Part I: that if a finite passive $2n$-pole has an impedance matrix $Z(p)$, then this matrix has properties (i) through (iv) of 1.1.

1.3 We recall that in Part I matrices satisfying the conditions of 1.1 were called *positive real* (PR).

1.4 The proof of 1.1 is a direct generalization to matrices of the Brune process[2] for realizing a two-pole impedance function $f(p)$. For this proof we shall require from Part I certain specific properties of positive real operators and matrices. These will be summarized in Section 2 below. Further than this, the present part is almost independent of Part I,

although in terminology, notation, and method a direct continuation of it. References to sections or paragraphs in Part I will be made thus: (I, 6) or (I, 6.23).

1.5 The distinction emphasized in Part I between operators, as abstract geometrical objects, and matrices as concrete arrays of numbers representing these geometrical objects, is not one which we have now to maintain with any strictness. We shall generally preserve it verbally but not use the bracket notation for matrices introduced in Part I.

II. PROPERTIES OF POSITIVE REAL OPERATORS AND MATRICES

2.0 We recall that an impedance operator $Z(p)$ is a linear function from the linear space $\mathbf{K}$ of current vectors k to the linear space $\mathbf{V}$ of voltage vectors v. A positive real operator $Z(p)$ is one whose matrix in any real coordinate frame is positive real. In Section 16 of Part I the following properties of a PR operator $Z(p)$ were established:

2.01 $Z(p)$ has no poles in Γ_+.*

2.02 If $Re(Z(p)k, k) = 0$ for some $p \in \Gamma_+$, then $Z(p)k \equiv 0$ for all p.

2.03 If it exists, $Z^{-1}(p) = Y(p)$ is PR.

2.04 If $Z(p)$ has a pole at $p = p_0$, it has one at $p = \bar{p}_0$.

2.05 If $Z(p)$ has a pole at $p = i\omega_0$, that pole is simple and

$$Z(p) = \frac{2p}{p^2 + \omega_0^2} R + Z_1(p),$$

where R is real, symmetric, semidefinite, and not zero, and $Z_1(p)$ is PR·

2.06 If $Z(p)$ has a pole at $p = \infty$, that pole is simple and

$$Z(p) = pR + Z_1(p)$$

where R and $Z_1(p)$ are as in 2.05.

2.07 It was emphasized at several points in Part I that the fact of possessing an impedance matrix, and that of possessing an admittance matrix, are each restrictions on a $2n$-pole $\mathbf{N}$. It is readily verified from (I, 6.3) and (I, 6.31)—and, indeed, well known—that if $\mathbf{N}$ has both an impedance matrix $Z(p)$ and an admittance matrix $Y(p)$, then

$$Y(p) = Z^{-1}(p).$$

---

* Γ_+ is the open right half plane: all finite p such that $Re(p) > 0$.

That is, if the impedance matrix of a $2n$-pole $\mathbf{N}$ is non-singular, then its admittance matrix exists, and conversely.

2.08 It was proved by Cauer[5], and in (I, 16.8), that if $Z(p)$ is PR and of rank $m < n$, then there exists a real, constant, non-singular matrix W such that

$$Z(p) = W'Z^{B}(p)W \tag{1}$$

where $Z^{B}(p)$ is a non-singular $m \times m$ PR matrix bordered by zeros.

2.09 Properties (i) through (iv) of 1.1 define the PR property for a matrix $Z(p)$. A convenient equivalent definition is that

  (i) $Z(p)$ is symmetric,

  (ii) For each $k \, \epsilon \, \mathbf{K}$, the function

$$\varphi(p) = (Z(p)k, \, k)$$

is a PR function of p.

This equivalent definition was established in (I, 16.13).

2.1 In Section 16 of Part I it was also mentioned that there exists for any rational operator $Z(p)$ (PR or not) a numerical function $\delta(Z)$ which generalizes to operators the usual definition of the degree of a rational function. We list here the properties of this degree $\delta(Z)$. They will be established in Section 7.

2.11 $\delta(Z)$ is an integer ≥ 0.

2.12 If $\delta(Z) = 0$, then $Z(p)$ is a constant—that is, does not depend upon p.

2.13 If $Z^{-1}(p)$ exists, then $\delta(Z) = \delta(Z^{-1})$.

2.14 If $Z(p) = Z_1(p) + Z_2(p)$, where $Z_1(p)$ is finite at every pole of $Z_2(p)$, and $Z_2(p)$ is finite at every pole of $Z_1(p)$, then

$$\delta(Z) = \delta(Z_1) + \delta(Z_2).$$

2.15 If $Z(p) = f(p)R$, where $f(p)$ is a scalar and R is a constant operator, then

$$\delta(Z) = [\text{degree of } f] \cdot [\text{rank of } R].$$

Here the degree of f is the sum

$$\sum_{p_0} [\text{order of the pole of } f(p) \text{ at } p_0]$$

where p_0 runs over all poles of $f(p)$, including ∞.

2.16 If A and B are constant non-singular matrices, then

$$\delta(Z) = \delta(AZB).$$

It is evident then that $\delta(Z)$ is a geometrical property, being constant over the usual equivalence classes

$$W'Z(p)W$$

or

$$W^{-1}Z(p)W$$

of matrices. Hence we may speak of the degree $\delta(Z)$ of an operator $Z(p)$.

2.17 If $Z(p)$ is formed from an $m \times m$ matrix $Z_1(p)$ by bordering the latter with zeros, then

$$\delta(Z) = \delta(Z_1).$$

2.18 Concerning the degree $\delta(Z)$ we here state a fundamental theorem:

Theorem: The $2n$-pole whose existence is asserted by 1.1 can be constructed with $\delta(Z)$ reactive elements, and no fewer.

The proof of this theorem will be distributed through Sections 4 and 6. In fact, we must even define exactly the phrase "can be constructed with x reactive elements." This will be done in Section 3.

2.2 *Lemma:* If $Z_1(p)$ and $Z_2(p)$ are PR operators or matrices, then

$$Z(p) = Z_1(p) + Z_2(p)$$

is also PR. If either of $Z_1(p)$ or $Z_2(p)$ is non-singular, then $Z(p)$ is.

Proof: Clearly $Z(p)$ is symmetric. By 2.09, therefore, $Z(p)$ is PR if the function

$$(Z(p)k, k) = (Z_1(p)k, k) + (Z_2(p)k, k) \tag{1}$$

is PR for each $k \in \mathbf{K}$. The right hand side is obviously PR by hypothesis.

If either of $Z_i(p)$ is non-singular, the function (1) cannot vanish in Γ_+ unless $k = 0$ (this is 2.02). Hence in this case $Z(p)$ also is non-singular.

2.21 Clearly 2.2 is independent of the implication, tacit in the notation, that the operators involved are impedances. The lemma holds for PR operators, whether interpreted as operating from $\mathbf{K}$ to $\mathbf{V}$ (impedances) or from $\mathbf{V}$ to $\mathbf{K}$ (admittances).

2.3 In (I, 6.21) and (I, 6.3) it was noted that any $n \times n$ impedance matrix $Z(p)$ defines by fiat a general $2n$-pole $\mathbf{N}$ whose impedance matrix is that $Z(p)$. Such is the generality of the notion of general $2n$-pole (I, 4).

Given $2n$-poles $\mathbf{N}_1$ and $\mathbf{N}_2$, with impedance matrices respectively $Z_1(p)$ and $Z_2(p)$, we know then that there is a general $2n$-pole $\mathbf{N}$ whose impedance matrix is

$$Z(p) = Z_1(p) + Z_2(p).$$

We call this $\mathbf{N}$ the series combination of $\mathbf{N}_1$ and $\mathbf{N}_2$.

2.31 Designate the terminal pairs of $\mathbf{N}_1$ by (S_r, S_r'), those of $\mathbf{N}_2$ by (T_r, T_r'), $1 \leq r \leq n$. It is evident that if $\mathbf{N}_1$ and $\mathbf{N}_2$ appear in a diagram so connected that

(i) S_r' is connected to T_r, $1 \leq r \leq n$;

(ii) No other connections are made to these nodes;
then the device with terminals S_r, T_r' is $\mathbf{N}$. This follows at once from Kirchoff's laws applied to the ideal graph (I, 4.11).

2.32 Dually, if $\mathbf{N}_1$ and $\mathbf{N}_2$ have admittance matrices $Y_1(p)$, $Y_2(p)$, then

$$Y(p) = Y_1(p) + Y_2(p)$$

is the matrix of a $2n$-pole $\mathbf{N}$ defined as the parallel connection of $\mathbf{N}_1$ and $\mathbf{N}_2$. $\mathbf{N}$ is the device whose terminal pairs are formed by joining S_r, T_r and also S_r', T_r', $1 \leq r \leq n$.

2.33 Fig. 1 shows the conventions to be used in indicating $2n$-poles ($n = 4$ in the Figure) with, respectively, impedance matrices and admittance matrices. Fig. 2 then shows the series connection of two impedance devices and the parallel connection of two admittance devices. In each case the terminals on the left are those of the composite device.

2.4 The series and parallel connections just described are special ways of combining $2n$-poles needed for the generalized Brune process for matrices. They have been introduced here on their merits, as new op-
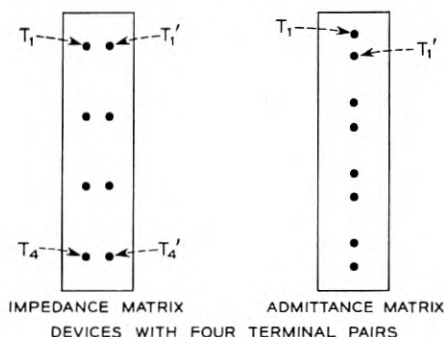
IMPEDANCE MATRIX   ADMITTANCE MATRIX
DEVICES WITH FOUR TERMINAL PAIRS
Fig. 1—Conventions used in representing 2N poles.

erations. They are, however, expressible in terms of the basic operations of juxtaposition (I, 17) and restriction (I, 18).

For example, the series connection of $\mathbf{N}_1$ and $\mathbf{N}_2$ is formed by first juxtaposing $\mathbf{N}_1$ and $\mathbf{N}_2$, to get a $2 \times 2n$-pole $\bar{\mathbf{N}}$. Let $\mathbf{J}$ be the $2n$ dimensional space of $2n$-tuples

$$j = [j_1, \cdots, j_n, \ell_1, \cdots, \ell_n].$$

We interpret this j as a $2n$-tuple of currents in the $2 \times 2n$-pole $\bar{\mathbf{N}}$, where j_r is the current in the rth terminal pair of $\mathbf{N}_1$ and ℓ_r that in the rth pair of $\mathbf{N}_2$, $1 \leq r \leq n$. Let $\mathbf{K}$ be an n-dimensional space. Given an n-tuple $k \in \mathbf{K}$, say

$$k = [k_1, \cdots, k_n],$$

we define the operator C from $\mathbf{K}$ to $\mathbf{J}$ by

$$j = Ck = [k_1, \cdots, k_n, k_1, \cdots, k_n].$$

Restricting $\bar{\mathbf{N}}$ by C gives the series combination $\mathbf{N}$ of $\mathbf{N}_1$ and $\mathbf{N}_2$. The details may easily be supplied by the interested reader.

2.41 Representing the series and parallel connections in terms of juxtaposition and restriction makes the lemma, 2.2, an immediate consequence of the lemma of (I, 17.2) and the theorems of (I, 17.3, 18.3).

2.5 We report here for record a curious property of PR operators which has so far found no application:

Lemma: If $Z(p)$ is a PR impedance operator from $\mathbf{K}$ to $\mathbf{V} = \mathbf{K}^*$, and $Y(p)$ any PR admittance operator from $\mathbf{V}$ to $\mathbf{K}$, then the operator

$$1 + Y(p)Z(p)$$

SERIES CONNECTION OF N_1 AND N_2 PARALLEL CONNECTION OF N_1 AND N_2
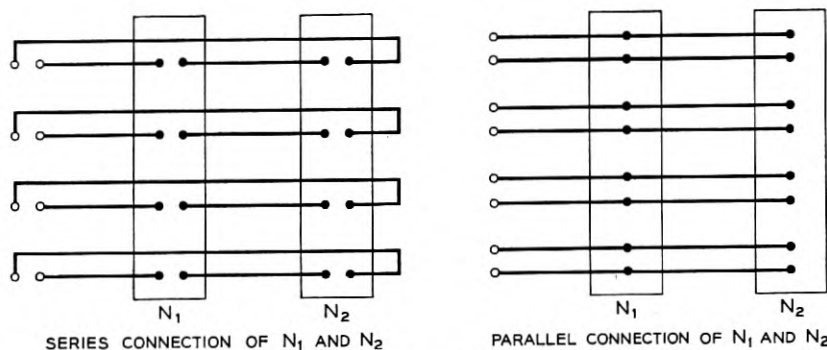
Fig. 2—Series and parallel connection of 2N poles: Series, left, and parallel, right.

in **K** is non-singular. Dually

$$1 + Z(p)Y(p)$$

in **V** is non-singular.

Proof: Suppose that $k \, \epsilon \, \mathbf{K}$ is such that

$$(1 + Y(p)Z(p))k = 0 \tag{1}$$

for all p. Then

$$0 = Z(\bar{p})(1 + Y(p)Z(p))k = Z(\bar{p})k + Z(\bar{p})Y(p)Z(p)k$$

for all p. Then, however,

$$(Z(\bar{p})k, \, k) + (Z(\bar{p})Y(p)Z(p)k, \, k) = 0. \tag{2}$$

We may write the second term as

$$\overline{(Z^*(\bar{p})k, \, Y(p)Z(p)k)} = (Z(p)k, \, Y^*(p)Z^*(\bar{p})k) \tag{3}$$

by (I, 14.0) applied twice. Now $Z(p)$ is PR, in particular real and symmetric, so

$$Z^*(\bar{p}) = \overline{Z^*(p)} = Z'(p) = Z(p).$$

Using a similar calculation with $Y(p)$, the quantity (3) becomes

$$(Z(p)k, \, Y(\bar{p})Z(p)k). \tag{4}$$

For each $p \, \epsilon \, \Gamma_+$, we have $\bar{p} \, \epsilon \, \Gamma_+$ and the first term of (2) has a non-negative real part. But for $\bar{p} \, \epsilon \, \Gamma_+$, (4) is the conjugate of

$$\overline{(v, \, Y(\bar{p})v)} \tag{5}$$

where $v = Z(p)k$. Now (5) is a PR function of $\bar{p}$, hence has a non-negative real part for $\bar{p} \, \epsilon \, \Gamma_+$, for any v. In particular therefore this is true for the v which, at p, makes (5) the conjugate of (4). Therefore (4) has a non-negative real part throughout Γ_+. It follows from (2) then that

$$Re(Z(\bar{p})k, \, k) = 0$$

for all $\bar{p} \, \epsilon \, \Gamma_+$. By 2.02, then,

$$Z(p)k \equiv 0.$$

By (1), then

$$1k = k = 0.$$

Hence (1) implies $k = 0$. Therefore the operator in (1) has an inverse

III. A SIMPLE REALIZABILITY THEOREM

3.0 The following theorem is contained in Cauer[5]. Since it provides the basic step in our realizability process, we shall prove it here.

3.1 *Theorem:* Let $f(p)$ be any one of the four functions

(i) $f(p) \equiv 1$,

(ii) $f(p) \equiv p$,

(iii) $f(p) = \dfrac{1}{p}$,

(iv) $f(p) = \dfrac{2p}{p^2 + \omega_0^2}$, $\omega_0^2 > 0$.

Let R be a real, constant, symmetric semidefinite $n \times n$ matrix of rank r. Then:

(A) The matrix

$$Z(p) = f(p)R$$

is PR and there exists a finite passive $2n$-pole **N** with the impedance matrix $Z(p)$.

(B) The $2n$-pole **N** can be realized with ideal transformers and, respectively,

   (i) with r resistors,
   (ii) with r coils,
   (iii) with r capacitors,
   (iv) with r coils and r capacitors.

(C) The dual statements to (A) and (B) are true.

Proof: That $Z(p)$ in PR is easily verified directly. It will follow also from the results of Part I when we exhibit a (finite passive) network whose matrix is $Z(p)$. To construct this latter, let D be a diagonal matrix such that

$$R = WDW'$$

where W is a real, constant, non-singular matrix. That D and W always exist is the analog for impedance operators of the result of Halmos[9], par. 41, for dimensionless operators. In fact, W can be taken to be orthogonal ($W^{-1} = W'$, cf. Halmos[9], par. 63). If R is of rank r, D has r non-vanishing diagonal elements, say d_{11}, d_{22}, $\cdots$, d_{rr}.

Since R is semidefinite, each $d_{ii}f(p)$, $1 \leq i \leq r$, is the impedance of an obviously passive two pole. Call this two-pole $\mathbf{M}_i$. Let $\mathbf{M}_{r+1}$, $\cdots$, $\mathbf{M}_n$ be two poles consisting of short circuits. Consider the $2n$-pole $\mathbf{N}_1$

made by connecting $\mathbf{M}_s$ between T_s and T'_s, $1 \leq s \leq n$. This $2n$-pole has the impedance matrix

$$Z_1(p) = f(p)D.$$

Then

$$Z(p) = f(p)WDW' = WZ_1(p)W'$$

is the matrix of a $2n$-pole $\mathbf{N}$ which can be obtained from $\mathbf{N}_1$ by the use of ideal transformers. Clearly $\mathbf{N}_1$, and therefore $\mathbf{N}$, contains exactly the elements claimed in (B) of the theorem.

The dual theorem (C) needs no comment.

3.11 *Corollary:* The conclusion (A) of 3.1 holds if the hypotheses on $f(p)$ are replaced by "$f(p)$ is PR." The same method of proof applies but one must use the Brune theory to realize the impedances $d_{ii}f(p)$, $1 \leq i \leq r$.

3.2 The case (ii) of 3.1 shows that any physical system of coupled coils can be realized with a set of isolated (i.e., not coupled) coils, with ideal transformers to supply the coupling [Cf. (I, 19.12)]. With this fact in mind, we see that the method of network synthesis used in (I, 19) can be simplified to the following: one starts with a finite collection of two-poles: each one is a resistor, capacitor, or coil (inductor). These are then appropriately connected to suitable ideal transformers. Viewed from certain selected terminals of these transformers, this network is a $2n$-pole equivalent to the desired one.

The difference between this process and that of (I, 19) is the minor one that coupled coils have been eliminated. We may then, however, regard any finite passive network as made up solely of simple two-poles (resistors, capacitors, coils) and ideal transformers.

It is readily verified from (I, 19.2) that open and short circuits are special cases of ideal transformers.

If a network made up in this way uses ℓ coils and c capacitors, we shall call $\ell + c$ the number of reactive elements in the network (or used by, or used in, the network).*

3.21 *Lemma:* The network described in the proof of 3.1 uses $\delta(Z)$ reactive elements. This is obvious from 2.12, 2.15, and 2.16.

IV. THE BRUNE PROCESS FOR A POSITIVE REAL MATRIX

4.0 Let $Z(p)$ be an $n \times n$ PR matrix. We can regard it as the impedance matrix of a general $2n$-pole $\mathbf{N}$. In this section we shall describe the

---

* By this definition, a reactive element is an energy storage element. Ideal transformers are not reactive, by the very fact of their ideality.

construction of a finite passive network which, as a $2n$-pole, has the impedance matrix $Z(p)$—i.e. is a $2n$-pole equivalent to $\mathbf{N}$. We call such a network a (physical) realization of $\mathbf{N}$, or of $Z(p)$. The dual problem, that of realizing a PR admittance matrix, can be handled dually.

Let $Z_0(p) = Z(p)$, $\mathbf{N}_0 = \mathbf{N}$, $n_0 = n$. We describe an inductive procedure which, given a $2n_r$-pole $\mathbf{N}_r$, $r \geq 0$, either

(i) Constructs a physical realization of $\mathbf{N}_r$, or

(ii) Constructs a $2n_{r+1}$-pole $\mathbf{N}_{r+1}$ such that if $\mathbf{N}_{r+1}$ is physically realizable, then $\mathbf{N}_r$ is.

To show that this induction actually gives a realization of any PR matrix $Z_0(p)$ we must demonstrate that, first, it is effective—i.e. that at any stage $\mathbf{N}_r$ at least one of (i) and (ii) is possible. Second, we must show that the process terminates with the construction of a finite network. The details of these demonstrations are given in the paragraphs 4.1 et seq. of this section. In the paragraphs 4.01 to 4.07 we describe the logical pattern into which these details are to be fit when they are established.

4.01 There are nine basic operations by which the networks $\mathbf{N}_r$ are constructed. We name the operations here, in order to give a clearer picture of the logic of the process, but their mathematical treatment is deferred to later paragraphs.

IP: A PR impedance matrix $Z_r(p)$ which has poles on $p = i\omega$ is represented as

$$Z_r(p) = pR_\infty + \frac{1}{p} R_0 + \sum_k \frac{2p}{p^2 + \omega_k^2} R_k + Z_{r+1}(p),$$

where $Z_{r+1}(p)$ is PR and has no poles on $p = i\omega$.

AP: A PR admittance matrix $Y_r(p)$ is represented dually:

$$Y_r(p) = pG_\infty + \frac{1}{p} G_0 + \sum_k \frac{2p}{p^2 + \omega_k^2} G_k + Y_{r+1}(p).$$

ID: A PR impedance matrix $Z_r(p)$ is represented as $W'Z_{r+1}^B(p)W$, where $Z_{r+1}^B(p)$ is a non-singular $Z_{r+1}(p)$ bordered by zeros.

AD: Dual to ID.

Res: A PR matrix $Z_r(p)$ is represented as

$$Z_r(p) = aS + Z_{r+1}(p),$$

where S is real, constant, symmetric, and positive definite, and $a \geq 0$ is the largest a for which $Z_{r+1}(p)$ is PR.

Con: The dual to Res.

IB: This is the analog of the step in the Brune process for scalars in which the reactance of a minimum resistance structure is tuned out to create a zero. The details are intricate in the generalization to $2n$-poles.

AB: This is the dual operation to IB.

F: A $2n_r$-pole $\mathbf{N}_r$ which has a constant PR matrix (admittance or impedance) is realizable at once, by 3.1. The operation F denotes this realization.

To each $\mathbf{N}_r$, one of these nine operations is to be applied. The effect of the last (F) is clearly salutary. That of each of the others is to split off a realizable piece of $\mathbf{N}_r$ and leave a $2n_{r+1}$-pole $\mathbf{N}_{r+1}$ to which again some one of the operations is to be applicable.

Exactly which of these operations to apply at any stage depends upon the properties of the $\mathbf{N}_r$ in question. We shall first devise a notation for describing the relevant properties of $\mathbf{N}_r$, and then in 4.04 present a table which summarizes what is to be proved in the paragraphs 4.1 et seq.

4.02 Definition: We say that $Z(p)$ has a zero of its real part at $p = i\omega_0$ if for some $k \,\epsilon\, \mathbf{K}$, $k \neq 0$, we have

$$[Z(i\omega_0) + Z(-i\omega_0)]k = 0.$$

4.03 Let I be an integer describing a $2n$-pole $\mathbf{N}$ as follows:

$I = 0$ if $\mathbf{N}$ has no impedance matrix.

$I = 1$ if $\mathbf{N}$ has a non-constant impedance matrix which has no poles on $p = i\omega$, and no zeros of its real part on $p = i\omega$.

$I = 2$ if $\mathbf{N}$ has a non-constant impedance matrix with a zero of its real part on $p = i\omega$, but no poles on $p = i\omega$.

$I = 3$ if $\mathbf{N}$ has an impedance matrix with a pole or poles on $p = i\omega$.

Let A be an integer describing the admittance category of $\mathbf{N}$ in a dual way (e.g., $A = 0$ if $\mathbf{N}$ has no admittance matrix, etc.).

Let (I, A) denote the category of $2n$-poles $\mathbf{N}$ for which the indicated values of both I and A are true. Let

$$(I_1 + I_2, \qquad A_1 + A_2) \tag{1}$$

denote the category of $2n$-poles $\mathbf{N}$ for which either I_1 or I_2 is true and, simultaneously, either A_1 or A_2 is true, with a similar definition for more summands. Then for example the category (1) above consists of the logical union of the following:

$$(I_1, A_1), \qquad (I_1, A_2), \qquad (I_2, A_1), \qquad (I_2, A_2).$$

Let C denote the category of $2n$-poles $\mathbf{N}$ which have a constant matrix, impedance or admittance.

It is clear that any $2n$-pole $\mathbf{N}$ belongs in C or in exactly one of the sixteen elementary categories whose union is $(0 + 1 + 2 + 3, 0 + 1 + 2 + 3)$.

Table 4.04 shows for each category of $\mathbf{N}_r$, except $(0, 0)$, which operations may be applied, and the possible categories of the resulting $\mathbf{N}_{r+1}$.

A $2n$-pole $\mathbf{N}$ not in $(0, 0)$ has at least one matrix, and if it has two these are of the same degree $(2.07, 2.13)$. We may then denote the degree of whatever matrix $\mathbf{N}$ has simply by $\delta(\mathbf{N})$. The fourth and fifth columns of Table 4.04 show the relations of $\delta(\mathbf{N}_r)$ to $\delta(\mathbf{N}_{r+1})$, and of n_r to n_{r+1}.

4.05 Table 4.04 summarizes facts to be proved in 4.1 et seq. Assuming now that the assertions in this table are true, we can show that the inductive procedure is effective.

We observe first that the category C and every possible elementary category (I, A) except $(0, 0)$ is contained in at least one of the categories listed in the first column. Hence to any $2n$-pole not in $(0, 0)$ there is at least one operation applicable. Further we note that the category $(0, 0)$ does not appear in the third column. Since by hypothesis $\mathbf{N}_0$ is not in $(0, 0)$, it follows by induction that no $\mathbf{N}_r$ will be. Therefore the process can stop only by the operation F: completion.

Second, we notice that if $\mathbf{N}_r$ is not in the category $(1, 1)$, then an applicable operation can be found which actually reduces one of the two numbers $\delta(\mathbf{N}_r)$, n_r. Furthermore, if $\mathbf{N}_r$ is in $(1, 1)$, a sequence of two operations can be found which reduces one of $\delta(\mathbf{N}_r)$, n_r. Therefore before the realization process terminates (with F),

(i) There are not more operations chosen from the list IP, AP, IB, AB, than the integer $\delta(\mathbf{N}_0)$;

(ii) There are not more operations chosen from the list ID, AD, than the integer $n_0 - 1$ (since after these, still $n_{r+1} > 0$);

TABLE 4.04

Category of $\mathbf{N}_r$	Operation	Category of $\mathbf{N}_{r+1}$	$\delta(\mathbf{N}_r) -$ $\delta(\mathbf{N}_{r+1})$	$n_r -$ n_{r+1}
$(3, 0 + 1 + 2 + 3)$	IP	$C + (1 + 2, 0 + 1 + 2 + 3)$	>0	0
$(0 + 1 + 2 + 3, 3)$	AP	$C + (0 + 1 + 2 + 3, 1 + 2)$	>0	0
$(1 + 2, 0)$	ID	$(1 + 2, 1 + 2 + 3)$	0	$>0*$
$(0, 1 + 2)$	AD	$(1 + 2 + 3, 1 + 2)$	0	$>0*$
$(1, 1)$	Res	$(2, 0 + 1 + 2 + 3)$	0	0
$(1, 1)$	Con	$(0 + 1 + 2 + 3, 2)$	0	0
$(2, 1 + 2)$	IB	$C + (1 + 2 + 3, 0 + 1 + 2 + 3)$	>0	0
$(1 + 2, 2)$	AB	$C + (0 + 1 + 2 + 3, 1 + 2 + 3)$	>0	0
C	F	—	—	—

* But $n_{r+1} > 0$.

(iii) There are not more operations chosen from the list Res, Con, than the integer $\delta(\mathbf{N}_0) + n_0 - 1$.

Finally, then, the process must terminate after at most $2\delta(\mathbf{N}_0) + 2n_0 - 1$ operations.

4.06 Besides the data in 4.04, one other fact must be established about each operation: that $\mathbf{N}_r$ is physically realizable if $\mathbf{N}_{r+1}$ is. This will be done as we discuss each operation. When it is established, we reason back from the result of operation F, which provides a physical realization of some $\mathbf{N}_m$ ($m \leq 2\delta(\mathbf{N}_0) + n_0 - 1$), through $\mathbf{N}_{m-1}$ to $\mathbf{N}_0 = \mathbf{N}$, and obtain a realization of $\mathbf{N}$ in finitely many steps.

4.07 Finally, we shall prove about each step that:

If $\mathbf{N}_{r+1}$ can be realized with x_{r+1} reactive elements, then $\mathbf{N}_r$ can be realized with

$$x_{r+1} + \delta(\mathbf{N}_r) - \delta(\mathbf{N}_{r+1})$$

reactive elements. This observation will provide the basis for proving the theorem of 2.18. For if $\mathbf{N}_m$ is the network with which the process terminates, then by 3.21 $\mathbf{N}_m$ can be realized with $\delta(\mathbf{N}_m)$ reactive elements. Reading back through the construction, each increment of degree that is encountered is balanced by an equal increment in the total number of reactive elements, so that, finally, $\delta(\mathbf{N})$ is the total number of reactive elements used. That no construction using fewer reactive elements can succeed will be shown in Section 6.

We now turn to IP, ID, Res, and IB, omitting the dual considerations. In each case, notation is simplified by writing Z, Y, $\mathbf{N}$, n respectively for Z_r, Y_r, $\mathbf{N}_r$, n_r, and Z_1, Y_1, $\mathbf{N}_1$, n_1 for Z_{r+1}, Y_{r+1}, $\mathbf{N}_{r+1}$, n_{r+1}.

4.1 Given a $2n$-pole $\mathbf{N}$ in any category for which $I = 3$, its impedance matrix $Z(p)$ exists by hypothesis and has poles on $p = i\omega$. These can be removed successively by 2.05 and 2.06, giving

$$Z(p) = pR_\infty + \frac{1}{p} R_0 + \sum_{k=1}^{K} \frac{2p}{p^2 + \omega_k^2} R_k + Z_1(p). \tag{1}$$

In this expansion, either of R_0, R_∞ may of course be absent, and all the R_k are real, symmetric, constant and semidefinite, for $k = 0, 1, \cdots, K, \infty$. Furthermore, $Z_1(p)$ is PR and has no poles on $p = i\omega$, by 2.05, 2.06 and construction.

Let $\mathbf{N}_1$ be the $2n_1$-pole whose impedance matrix is $Z_1(p)$. We define IP to be the operation giving $\mathbf{N}_1$ from $\mathbf{N}$. Either $\mathbf{N}_1 \, \epsilon \, C$, or $I = 1$ or 2

for $\mathbf{N}_1$, since at least $Z_1(p)$ exists. Furthermore, by construction $Z_1(p)$ is again an $n \times n$ matrix, so $n_1 = n$.

By 2.14 and 2.15,

$$\delta(Z) = \text{rank } (R_\infty) + \text{rank } (R_0) + 2 \sum_{k=1}^{K} \text{rank } (R_k) + \delta(Z_1). \quad (2)$$

Since $\delta(Z)$ is finite, this shows that K is finite. Indeed, $2K \leq \delta(Z)$. Furthermore, $\delta(Z) > \delta(Z_1)$, because a matrix of rank zero is itself zero, and by hypothesis $Z(p)$ has a pole on $p = i\omega$. Therefore we have established the claims in the first line of the Table 4.04, and by a dual argument those in the second line.

We must yet show that if $\mathbf{N}_1$ is physically realizable, then $\mathbf{N}$ is. Each term in (1), save $Z_1(p)$, is the matrix of a physically realizable $2n$-pole, by 3.1. There are at most $K + 2$ such terms. The series combination of their respective $2n$-poles is therefore physically realizable and $\mathbf{N}$ results from the series connection of these and $\mathbf{N}_1$ (2.2). Therefore if $\mathbf{N}_1$ is realizable, so is $\mathbf{N}$.

Fig. 3 shows the relation of $\mathbf{N}$ and $\mathbf{N}_1$ under IP, and the dual relation under AP. Here we have shown $n = 3$. The boxes labelled 0, ∞, $\cdots$, K are the devices corresponding to the poles at 0, ∞, $\cdots$, $i\omega_K$, the terminals on the extreme left are those of $\mathbf{N}$, and $\mathbf{N}_1$ is on the right.

4.11 From (2), and (B) of 3.1, we see that the number of reactive elements used in the realization of the network between $\mathbf{N}_1$ and $\mathbf{N}$ is exactly

$$\delta(Z) - \delta(Z_1) = \delta(\mathbf{N}) - \delta(\mathbf{N}_1).$$

Clearly the dual result holds for AP. This verifies 4.07 for IP and AP.

4.2 Consider a $2n$-pole $\mathbf{N}$ in $(1 + 2, 0)$. In particular, then, the impedance matrix $Z(p)$ of $\mathbf{N}$ exists and is not constant, but $Z(p)$ has no inverse. Then 2.08 applies, and we have

$$Z(p) = W'Z_1^B(p)W, \quad (1)$$

where W is real, constant, and non-singular, and $Z_1^B(p)$ is a non-singular matrix $Z_1(p)$ bordered by zeros. Let $\mathbf{N}_1$ be the $2n_1$-pole whose impedance matrix is $Z_1(p)$. We define ID as the operation which gives $\mathbf{N}_1$ from $\mathbf{N}$. Now $n_1 < n$, because $Z(p)$ is singular and $Z_1(p)$ is not. Also, $Z_1(p)$ is not constant, because $Z(p)$ is not, and $\delta(Z_1) = \delta(Z)$, by 2.17. Therefore $n_1 \neq 0$, also $\mathbf{N}_1$ is not in C. Because $Z_1(p)^{-1}$ exists, $\mathbf{N}_1$ is in $A = 1, 2$ or 3. Because $Z(p)$ has no poles on $p = i\omega$, neither has $Z_1(p)$, so $\mathbf{N}_1 \in (1 +$

2, $1 + 2 + 3$). This verifies the statements on the third line of the
Table 4.04, and the fourth by duality.

That **N** is physically realizable if $\mathbf{N}_1$ is, is the gist of (I, 8.11) and (I,
8.4). We prove it here by noting that $Z_1^B(p)$ is the matrix of a $2n$-pole
$\mathbf{N}_2$ which obtains by adjoining $n - n_1 > 0$ pairs of shorted terminals
to $\mathbf{N}_1$. Then (1) shows that **N** obtains from $\mathbf{N}_2$ by the use of ideal trans-
formers (I, 9.1).

Fig. 4 shows in schematic form the effects of the operation ID and
AD. In each case, it is emphasized that $\mathbf{N}_1$ has a matrix dual to that of
N. We have shown $n = 5$, $n_1 = 3$.

4.21 No reactive elements are used in this construction, so 4.07 is
satisfied.

4.3 Consider now a $2n$-pole **N** in (1, 1). Then its impedance matrix
$Z(p)$ is finite for every $p = i\omega$, and not constant.

Let $R(p)$, $I(p)$, respectively, be the real and imaginary parts of $Z(p)$:

$$2R(p) = Z(p) + \overline{Z(p)} = Z(p) + Z(\bar{p}) = Z(p) + Z^*(p);$$

$$2iI(p) = Z(p) - \overline{Z(p)} = Z(p) - Z(\bar{p}) = Z(p) - Z^*(p);$$

$$Z(p) = R(p) + iI(p).$$
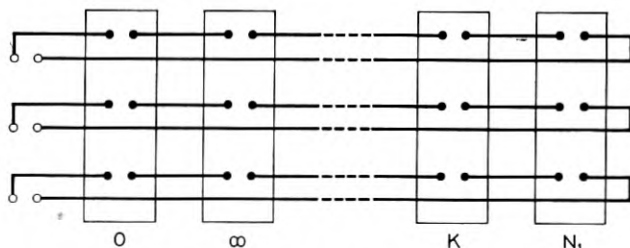
STRUCTURE RESULTING FROM IP
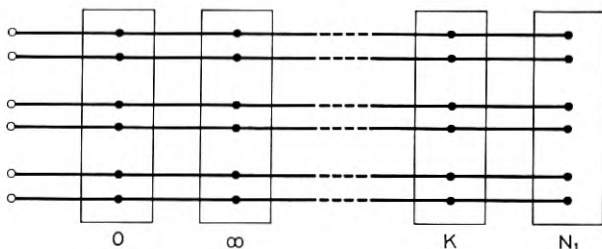
STRUCTURE RESULTING FROM AP

Fig. 3—Structure resulting from IP, above and AP, below.

Then $R(p) = R^*(p)$, $I(p) = I^*(p)$, and both are real and symmetric. If k is any vector,

$$(Z(p)k, k) = (R(p)k, k) + i(I(p)k, k),$$

and the self-adjoint property of R and I imply that each scalar product on the right is real. Therefore

$$\begin{aligned} Re(Z(p)k, k) &= (R(p)k, k), \\ Im(Z(p)k, k) &= (I(p)k, k). \end{aligned} \tag{1}$$

We note that

$$2iI(\bar{p}) = Z(\bar{p}) - Z^*(\bar{p}) = Z^*(p) - Z(p) = -2iI(p)$$

so that, in particular, $I(i\omega)$ is an odd function of ω.

4.31 *Lemma:* Let S be a given real, constant, symmetric, and positive *definite* matrix. Then there exists a unique number $a > 0$ such that

(i) The matrix

$$R(i\omega) - aS$$

is semidefinite for every ω,

(ii) For some $\omega_0 \geq 0$, possibly $+\infty$,

$$R(i\omega_0) - aS$$

is singular.

Proof: We first show how the number a would be calculated, and then reduce the claims of the lemma to a well-known and basic theorem in
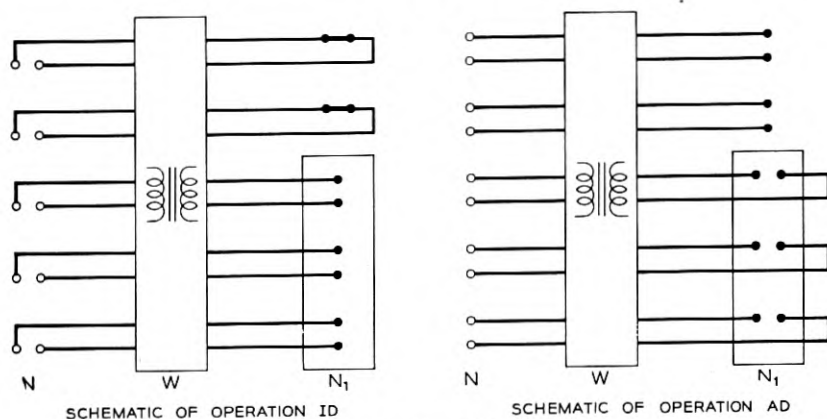
Fig. 4—Schematic of operation ID, left and AD, right.

the theory of quadratic forms. Fix ω and consider the matrix

$$R(i\omega) - \lambda S$$

as a function of λ. Its determinant,

$$\Delta_\omega(\lambda) = |R(i\omega) - \lambda S|,$$

is an nth degree polynomial in λ with the following two properties:

(α) The coefficient of λ^n in $\Delta_\omega(\lambda)$ is not zero and is independent of ω,

(β) The n roots of

$$\Delta_\omega(\lambda) = 0 \tag{2}$$

are real and positive.

Now $R(i\omega)$ is rational, hence continuous, and finite for all ω, including $\omega = \infty$, by the hypothesis that $\mathbf{N}$ is in $(1, 1)$. By (α) above, therefore, each root of (2) is a continuous function of ω on the compact set $-\infty \leq \omega \leq \infty$. Let $a(\omega)$ denote the least root of (2). Then $a(\omega)$ is again bounded and continuous for all ω. There is, therefore, an ω_0 where $a(\omega)$ takes its least value. This is the ω_0 referred to in the lemma, and

$$a = a(\omega_0).$$

We see that this calculation requires solving an nth degree polynomial equation containing a parameter (ω), and then minimizing the least root by varying the parameter. Though some properties of $R(i\omega)$ are available to assist in the process, and the choice of S is somewhat free to us, this is scarcely a feasible calculation in practice. Even when one reduces the minimizing problem to finding the roots of a derivative, there remains a prodigious calculation in all but the simplest cases.

Since by its definition $R(i\omega) = R(-i\omega)$, we may take $\omega_0 \geq 0$.

The relation (1) above implies that

$$(R(i\omega)k, k) \geq 0$$

for all real ω and all $k \in \mathbf{K}$, because $Z(p)$ is PR. That is, $R(i\omega)$ is semi-definite. The hypothesis that $Z(p)$ has no zero of its real part $R(p)$ on $p = i\omega$ then implies that $R(i\omega)$ is positive definite. All of (i), (ii), (α), and (β) then follow from well-known properties of definite quadratic forms. They may, for example, all be deduced from Halmos[9], paragraphs 62, 63, and 74, by choosing a coordinate frame in which the operator corresponding to S above is represented by the unit matrix. A more elegant reduction to the cited results of Halmos[9] can also be constructed.

4.32 *Lemma:* Given $\mathbf{N}$ in $(1, 1)$, we choose any real constant symmetric

and positive definite matrix S and find the a described in 4.31. Then the matrix

$$Z_1(p) = Z(p) - aS$$

is PR and has a zero of its real part at $p = i\omega_0$.

Proof: Clearly $Z_1(p)$ is symmetric. By 2.09, then, $Z_1(p)$ is PR if the function

$$\varphi_1(p) = (Z_1(p)k, k) = (Z(p)k, k) - a(Sk, k) \tag{3}$$

is PR for each k. Clearly this function is rational and has no singularities in Γ_+. It suffices then to show that its real part is non-negative on $p = i\omega$. By (1) of 4.3

$$Re \varphi_1(i\omega) = (R(i\omega)k, k) - a(Sk, k)$$

and this is non-negative by (i) of 4.31.

That $Z_1(p)$ has a zero of its real part at $p = i\omega_0$ is (ii) of 4.31.

4.33 Let $\mathbf{N}_1$ be the $2n$-pole whose impedance matrix is the $Z_1(p)$ of 4.32. We define the operation Res as that which produces $\mathbf{N}_1$ from $\mathbf{N}$. It is evident from (3) above that the poles of $Z_1(p)$ are exactly those of $Z(p)$, hence $I = 2$ for $\mathbf{N}_1$. Nothing can be said of the admittance matrix for $\mathbf{N}_1$. $\delta(Z_1) = \delta(Z)$ by 2.14 and 2.15, and $n_1 = n$ by construction. The claims in 4.04 are now established for Res, and dually for Con.

The relation

$$Z(p) = Z_1(p) + aS$$

shows that $\mathbf{N}$ is a series combination of $\mathbf{N}_1$ and a device with the impedance matrix aS. Since $a > 0$, this latter is a realizable resistance network (3.1). Hence $\mathbf{N}$ is realizable if $\mathbf{N}_1$ is.

4.34 We observe that no reactive elements are used in the network between $\mathbf{N}_1$ and $\mathbf{N}$ (2.12, 3.12). This verifies 4.07 for Res and Con.

4.4 We now turn to the *piece de resistance* of the generalized Brune process, the operation IB and its dual. Consider a $2n$-pole $\mathbf{N}$ in the category $(2, 1 + 2)$—i.e., its impedance matrix $Z(p)$ exists, is not constant, is non-singular on $p = i\omega$, and has a zero of its real part at some $p = i\omega_0$. We have for some $k \in \mathbf{K}$ such that $k \neq 0$,

$$R(i\omega_0)k = 0. \tag{1}$$

Here, $R(p)$ is as defined in 4.3.

4.41 We now assert that we may assume that $0 < \omega_0$, and $i\omega_0 \neq \infty$ in

(1). Certainly we may take $\omega_0 \geq 0$, because $R(i\omega) = R(-i\omega)$. Furthermore, by (1),

$$Z(i\omega_0)k = iI(i\omega_0)k. \tag{2}$$

$I(i\omega)$, being odd, and finite everywhere on $p = i\omega$, must vanish at $\omega = 0$, and at $i\omega = \infty$. Hence if $\omega_0 = 0$ or $i\omega_0 = \infty$, $Z(i\omega_0)k = 0$ and $Z(p)$ is singular on $p = i\omega$. This denies our hypothesis that $\mathbf{N} \ \epsilon \ (2, 1 + 2)$.

4.42 Let $\mathbf{J}$ be the set of all vectors $k \ \epsilon \ \mathbf{K}$ such that (1) holds: the null space of $R(i\omega_0)$. Then clearly $\mathbf{J}$ is a linear manifold. Furthermore, $\mathbf{J}$ is real, because, if (1) holds then

$$\overline{R(i\omega_0)k} = \overline{R(i\omega_0)}\bar{k} = R(i\omega_0)\bar{k} = \bar{0} = 0$$

and $\bar{k}$ also is in $\mathbf{J}$.

Relations (1) and (2) hold for all $k \ \epsilon \ \mathbf{J}$.

4.43 By its construction, $I(i\omega_0)$ is real and symmetric, but not necessarily definite. There does however exist a real diagonal matrix D and a real non-singular W such that $I(i\omega_0) = W'DW$. Let D_+ be the (diagonal) matrix obtained from D by replacing all negative elements of D by zero, and define D_- by

$$D = D_+ - D_- . \tag{3}$$

Then D_+ and D_- are real, symmetric, and non-negative semidefinite. Define

$$A = \omega_0 W' D_+ W,$$
$$B = \frac{1}{\omega_0} W' D_- W. \tag{4}$$

We have chosen $\omega_0 > 0$, so A and B are both real, symmetric and non-negative. Certainly therefore

$$Z^{(2)}(p) = Z(p) + \frac{1}{p} A + pB \tag{5}$$

is PR. Also $Z^{(2)}(p)$ has an inverse, because $Z(p)$ has one by hypothesis and 2.2 applies.

4.431 Let $v \ \epsilon \ \mathbf{V}$ be such that for some $k_1 \ \epsilon \ \mathbf{K}$

$$v = Ak_1$$

and for some $k_2 \ \epsilon \ \mathbf{K}$

$$v = Bk_2 .$$

Then $v = 0$.

Proof: We may assume that the first r diagonal elements of D are the non-zero elements of D_+, the next s those of $-D_-$. By (4),

$$(W')^{-1}v = \omega_0 D_+ W k_1,$$

$$(W')^{-1}v = \frac{1}{\omega_0} D_- W k_2.$$

The first of these relations exhibits $(W')^{-1}v$ as an n-tuple with non-zero components at most among the first r, the second as an n-tuple with non-zero components at most among the last $n - r$. Hence all components of $(W')^{-1}v$ are zero. Hence v itself is zero.

4.44 Define

$$X(p) = -\frac{1}{p} A - pB, \tag{6}$$

and let $\mathbf{N}_x$ be the $2n$-pole whose impedance matrix is $X(p)$. $\mathbf{N}_x$ is not physically realizable, since it is made up of negative reactances.

Let $\mathbf{N}^{(2)}$ be the $2n$-pole whose impedance matrix is $Z^{(2)}(p)$. Then by (5) $\mathbf{N}$ obtains from $\mathbf{N}^{(2)}$ and $\mathbf{N}_x$ by connecting them in series.

We have the following relation holding on $p = i\omega$, but only thereon since it is only there that $X(p)$ is a pure imaginary:

$$Z^{(2)}(i\omega) = R(i\omega) + i\left[I(i\omega) - \frac{1}{\omega} A + \omega B\right].$$

In particular, at $i\omega_0$,

$$Z^{(2)}(i\omega_0) = R(i\omega_0) + i[I(i\omega_0) - W'D_+W + W'D_-W]$$

$$= R(i\omega_0),$$

by (3) and (4). Since $\mathbf{J}$ is the null space of $R(i\omega_0)$ by definition, $\mathbf{J}$ is the null space of $Z^{(2)}(i\omega_0)$.

4.45 Now $Y^{(2)}(p) = [Z^{(2)}(p)]^{-1}$ exists and is PR. Since $Z^{(2)}(i\omega_0)$ annihilates every element of $\mathbf{J}$, it follows that $Y^{(2)}(p)$ does not exist at $p = i\omega_0$—therefore $Y^{(2)}(p)$ has a pole at $i\omega_0$. Hence we may apply AP and represent $Y^{(2)}(p)$ as a reactance network, with admittance matrix

$$G(p) = \frac{2p}{p^2 + \omega_0^2} G, \tag{7}$$

in parallel with a $2n$-pole $\mathbf{N}^{(3)}$ which has an admittance matrix, say

$$Y^{(2)}(p) = G(p) + Y^{(3)}(p), \tag{8}$$

where $Y^{(3)}(p)$ is finite at $p = i\omega_0$.

4.46 Multiplying (8) on either side by $Z^{(2)}(p)$,

$$\frac{2p}{p^2 + \omega_0^2} GZ^{(2)}(p) + Y^{(3)}(p)Z^{(2)}(p) = 1$$

$$= \frac{2p}{p^2 + \omega_0^2} Z^{(2)}(p)G + Z^{(2)}(p)Y^{(3)}(p).$$

(9)

Here, to be strictly correct, we should write two separate equations, interpreting 1 as the identity operator in **K** for, here, the left equality, and as the identity operator in **V** for the right equality. Multiplying (9) through by $p - i\omega_0$ and letting $p \rightarrow i\omega_0$, we obtain

$$GZ^{(2)}(i\omega_0) = 0 = Z^{(2)}(i\omega_0)G.$$

Here, as in (9), we have condensed two dimensionally incompatible equalities. From this it follows that each of G and $Z^{(2)}(i\omega_0)$ has its range in the null space of the other. In particular, therefore, the range of G is contained in **J**.

4.47 Consider now a v such that $Gv = 0$. Then, by (7) and (8),

$$v \equiv Z^{(2)}(p)Y^{(2)}(p)v \equiv Z^{(2)}(p)Y^{(3)}(p)v$$

so, at $i\omega_0$,

$$v = Z^{(2)}(i\omega_0)Y^{(3)}(i\omega_0)v = Z^{(2)}(i\omega_0)k$$

for some finite vector $k = Y^{(3)}(i\omega_0)v$. Since $Z^{(2)}(i\omega_0)$ is finite, $v \neq 0$ implies that $k \neq 0$. Then, however, v lies in the range of $Z^{(2)}(i\omega_0)$. Combining this fact with the result of 4.46, we see that for $Gv = 0$ it is necessary and sufficient that v lie in the range of $Z^{(2)}(i\omega_0)$: the range of $Z^{(2)}(i\omega_0)$ is exactly the null space of G.

4.48 Now in Halmos[9], par. 37, it is shown that for any dimensionless operator in an n-space the dimensionality of its range space (its *rank*) and the dimensionality of its null space (its *nullity*) add up to n. A similar result and proof hold for operators between **V** and **K**. Let m be the dimensionality of **J**. Then $n - m$ is the rank of $Z^{(2)}(i\omega_0)$, and therefore the dimensionality of the range of $Z^{(2)}(i\omega_0)$, and by 4.47 the dimensionality of the null space of G. Hence, finally,

$$\text{rank } (G) = n - (n - m) = m.$$

By 4.46, therefore, **J** is exactly the range of G.

4.49 Now $\mathbf{N}^{(3)}$, whose admittance matrix is $Y^{(3)}(p)$, might not be ex-

pected to have an impedance matrix. The following reasoning shows that it does have, however:

Consider a $v \, \epsilon \, \mathbf{V}$ for which $Y^{(3)}(p)v \equiv 0$. Then from the right side of (9), with (5),

$$v = \frac{2p}{p^2 + \omega_0^2} \, Z(p)Gv + \frac{2}{p^2 + \omega_0^2} \, AGv + \frac{2p^2}{p^2 + \omega_0^2} \, BGv. \qquad (10)$$

We have by hypothesis that $Z(p)$ is finite on $p = i\omega$. Therefore we may calculate, by letting $p \to 0$ in (10), that

$$v = \frac{2}{\omega_0^2} \, AGv,$$

and, by letting $p \to \infty$ in (10), that

$$v = 2BGv.$$

These two equations exhibit v as an element in the range of A and also an element in the range of B. The only possible such v is $v = 0$, by 4.43. Therefore there is no non-zero v such that $Y^{(3)}(p)v \equiv 0$. Then $Z^{(3)}(p) = Y^{(3)}(p)^{-1}$ exists as a PR operator.

4.491 Let

$$L(p) = \frac{1}{p} \, H + pF \qquad (11)$$

be the matrix whose poles at $p = 0$ and $p = \infty$ are those of $Z^{(3)}(p)$. That is, let

$$Z^{(3)}(p) = L(p) + Z^{(4)}(p), \qquad (12)$$

where $Z^{(4)}(p)$ is PR and finite at 0 and ∞. Because $Z^{(3)}(p)$ is PR, H and F are both real, symmetric, and semidefinite. Let $\mathbf{N}_L$ be the $2n$-pole whose impedance matrix is $L(p)$, and $\mathbf{N}^{(4)}$ the $2n$-pole with matrix $Z^{(4)}(p)$. In fact, $\mathbf{N}_L$ is realizable. $\mathbf{N}^{(3)}$ is the series combination of $\mathbf{N}_L$ and $\mathbf{N}^{(4)}$, by (12).

4.5 Equations (5), (7), (8), and (12) above are statements about matrices in a particular coordinate frame—that frame appropriate to the given $\mathbf{N}$. We can interpret them as operator relations by simple decree. We wish now to draw a circuit diagram illustrating these relations. To do so, we introduce a suitable new coordinate frame.

Because $G(p)$ is PR and of rank m, we know that a frame can be found in which the matrix for $G(p)$ is an $m \times m$ non-singular matrix bordered by zeros (2.08, or (I, 16.8)). By (7) and the result of 4.48, we

may take the first m current vectors, k_1, k_2, $\cdots$, k_m, specifying this frame, to span $\mathbf{J}$. It follows from the matrix form of G then that the corresponding dual vectors v_1, $\cdots$, v_m span the range of G—i.e., the null space of $Z^{(2)}(i\omega_0)$. We shall adopt such a frame for the further discussion.

Let $\mathbf{K}_1$ be the space spanned by k_{m+1}, $\cdots$, k_n, and $\mathbf{V}_1$ that spanned by v_{m+1}, $\cdots$, v_n, in this frame. Then

$$\mathbf{K} = \mathbf{J} \oplus \mathbf{K}_1$$
$$\mathbf{V} = \mathbf{U} \oplus \mathbf{V}_1, \tag{1}$$

say, where $\mathbf{U} = \mathbf{J}^*$, $\mathbf{V}_1 = \mathbf{K}_1^*$ [Cf. (I, 10.6)].

If $\mathbf{M}$ is the name of any given $2n$-pole discussed in the paragraphs 4.4 to date, we let $\overline{\mathbf{M}}$ denote the Cauer equivalent of $\mathbf{M}$ in this new frame.

4.51 Let $\overline{\mathbf{N}}_G$ be the $2m$-pole whose matrix in the new frame is the $m \times m$ non-singular admittance matrix which, when bordered, gives the matrix of the operator

$$G(p) = \frac{2p}{p^2 + \omega_0^2} G.$$

The $2n$-pole whose matrix is $G(p)$ then obtains by adjoining $n-m$ open circuits to $\overline{\mathbf{N}}_G$. The matrix of $\overline{\mathbf{N}}_G$ operates from $\mathbf{U}$ to $\mathbf{J}$ and has an inverse.

4.52 Fig. 5 shows a diagram, which $n = 5$, $m = 3$, of the manner in which we now have $\mathbf{N}$ represented. The terminals on the extreme left are those of $\mathbf{N}$. $\mathbf{N}$ is obtained from $\overline{\mathbf{N}}$ by a transformer. The horizontal current paths cut the dotted section A-A at points which may be interpreted as the terminals of $\overline{\mathbf{N}}$. Ideal transformers, as in Fig. 1 of I, can be introduced here as needed. Putting them in the diagram merely complicates the picture.

$\overline{\mathbf{N}}$ is the series connection of $\overline{\mathbf{N}}_X$ and $\mathbf{N}^{(2)}$. The terminals of the latter are on B-B. $\mathbf{N}^{(2)}$, again, is the parallel connection of a $2n$-pole obtained from $\overline{\mathbf{N}}_G$ by the adjunction of open circuits, and $\overline{\mathbf{N}}^{(3)}$. The latter has its terminals on C-C. Again, $\overline{\mathbf{N}}^{(3)}$ is the series connection of $\overline{\mathbf{N}}_L$ and $\overline{\mathbf{N}}^{(4)}$.

4.53 Let $\mathbf{M}_{AD}$ be the device between A-A and D-D of Fig. 5. This device has n terminal pairs on A-A and n more on D-D. We may suppose that ideal transformers are attached at each terminal pair as in Fig. 1 of I, since including them in the construction of $\overline{\mathbf{N}}$ would not alter its behavior. Then $\mathbf{M}_{AD}$ is a $2(2n)$-pole.

$\mathbf{M}_{AD}$ is constructed from certain $2r$ poles (with various r) as indicated in the diagram of Fig. 5. The ideal graph* of this diagram (rather, of

---

* Cf. (I, 4.1).

the relevant part of it between A-A and D-D) obtains from Fig. 5 by inserting ideal branches—two poles—across each terminal pair of each box, and neglecting the outlines of the boxes. The upper m channels of this ideal graph are then T sections, and the lower n-m are degenerate T sections with no shunt arm. This ideal graph is shown in Fig. 6. The ideal branches are shown as small boxes.

The program of the next few paragraphs is to demonstrate that $\mathbf{M}_{AD}$ is a physically realizable $2(2n)$-pole.

4.54 Let us designate the terminal pairs of $\mathbf{M}_{AD}$ on the section A-A by T_1, T_1', $\cdots$; T_n, T_n', where the rth pair is the intersection with A-A of the leads to the rth terminal pair of $\bar{\mathbf{N}}$. We designate the pairs on
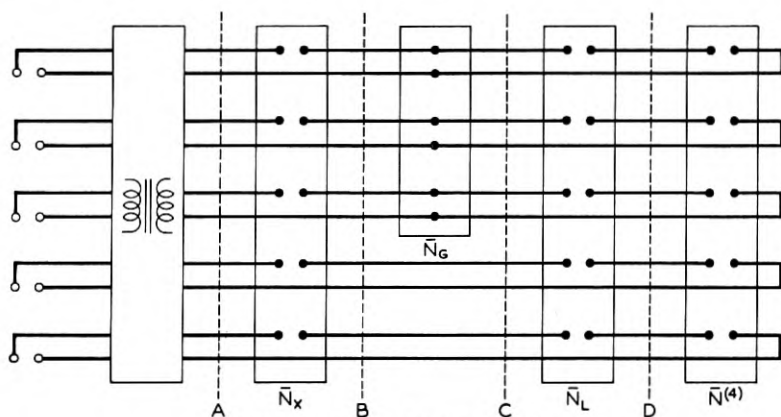
Fig. 5—Original form for $\mathbf{N}$.
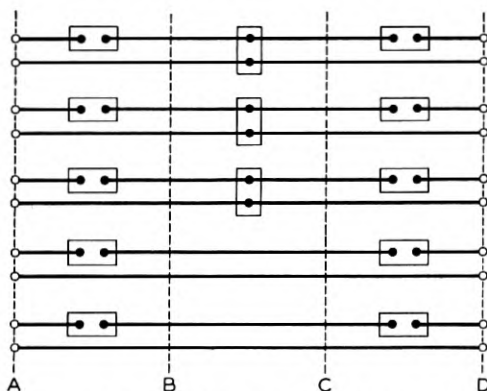
Fig. 6—Ideal graph of $\mathbf{M}_{AD}$.

D-D by S_1, S_1'; $\cdots$; S_n, S_n', where here the rth pair is the intersection with D-D of the leads to the rth terminal pair of $\bar{\mathbf{N}}^{(4)}$. In each case we orient the pair T, T' or S, S' so that the primed (negative) terminal is on the lead to the primed terminal of $\bar{\mathbf{N}}$ or $\bar{\mathbf{N}}^{(4)}$.

Let the $2n$-tuple

$$[a_1, a_2, \cdots, a_n, b_1, b_2, \cdots, b_n] \tag{2}$$

represent the currents into the terminals of $\mathbf{M}_{\text{AD}}$ in the order

$$T_1, T_2, \cdots, T_n, S_1, \cdots, S_n.$$

Then we may interpret

$$[a_1, \cdots, a_n] \tag{3}$$

as a vector in $\mathbf{K}$ expressed in the coordinate frame introduced for Fig. 5, and also

$$[b_1, \cdots, b_n] \tag{4}$$

as a vector in $\mathbf{K}$ in the same frame. That is, any current vector into $\mathbf{M}_{\text{AD}}$ can be written as an ordered pair

$$k_1, k_2 \tag{5}$$

where each $k_i \in \mathbf{K}$, with the convention that such a pair determines a $2n$-tuple (2) from the n-tuples (3) of k_1 and (4) of k_2.

We shall write the ordered pair (5) in the form

$$k_1 \oplus k_2. \tag{6}$$

Because we have $\mathbf{K}$ represented in the special way

$$\mathbf{K} = \mathbf{J} \oplus \mathbf{K}_1,$$

where $\mathbf{J}$ is the subspace spanned by n-tuples (3) in which the last n - m components vanish (this is (1) of 4.5) we can further split the $2n$-tuple (2) into

$$(j_1 \oplus \ell_1) \oplus (j_2 \oplus \ell_2), \tag{7}$$

where $j_i \in \mathbf{J}$, $\ell_i \in \mathbf{K}_1$, $i = 1, 2$, and in (6)

$$k_i = j_i \oplus \ell_i. \tag{8}$$

Formulas dual to those of (2) through (8) of course hold for voltage $(2n)$-tuples. Let $\mathbf{K}^2$ be the space of current $2n$-tuples (2) (or (7)) and $\mathbf{V}^2$ the space of voltage $(2n)$-tuples

$$[e_1, e_2, \cdots, e_n, f_1, \cdots, f_n] = (u_1 \oplus v_1) \oplus (u_2 \oplus v_2)$$

analogous to (2) and (7), with the scalar product

$$\sum_{r=1}^{n} e_r \bar{a}_r + \sum_{r=1}^{n} f_r \bar{b}_r. \tag{9}$$

It is a common and convenient malpractice in vector algebra to use, for example, the symbol j both for an m-tuple in $\mathbf{J}$ and for the n-tuple

$$j \oplus 0 \, \epsilon \, \mathbf{J} \oplus \mathbf{K}_1$$

of the form (8). Taking this advantage, we can see that (9) is simply

$$(u_1 + v_1, j_1 + \ell_1) + (u_2 + v_2, j_2 + \ell_2) \tag{9'}$$

where here the parentheses denote scalar products between $\mathbf{V}$ and $\mathbf{K}$. The form (9') can also be derived directly from (1), (7), and (I, 10.6).

4.55 We now wish to compute the voltage-current pairs admitted by $\mathbf{M}_{AD}$. Referring to Fig. 5, we observe that $\bar{\mathbf{N}}_X$ and $\bar{\mathbf{N}}_L$ both have impedance matrices ($X(p)$ and $L(p)$ respectively, or, rather, the matrix forms of these in the frame of present interest) finite at all p except $p = 0$, $p = \infty$. Each will, therefore, admit any current n-tuple into its terminals, i.e., through its ideal branches, at any but these exceptional frequencies. By construction, $\bar{\mathbf{N}}_G$ has a *non-singular* admittance matrix and therefore also will admit any current m-tuple into its terminals (2.07), except at most at certain isolated frequencies. It is evident by Kirchoff's laws applied to Fig. 6 then that $\mathbf{M}_{AD}$ will admit any current $2n$-tuple of the form

$$(j_1 \oplus k) \oplus (j_2 \oplus (-k)) \tag{10}$$

where $j_i \, \epsilon \, \mathbf{J}$, $i = 1, 2$, and $k \, \epsilon \, \mathbf{K}_1$, except at most at finitely many exceptional frequencies. Conversely, if the current $2n$-tuple specified by (7) is that in $\mathbf{M}_{AD}$, conservation at the absent shunt arms of the lower degenerate T-sections implies that, as elements of $\mathbf{K}$,

$$k_1 + k_2 = 0,$$

that is, the current is of the form (10). Hence $2n$-tuples of the form (10) span the space of currents admitted by $\mathbf{M}_{AD}$. Let us call this space $\mathbf{K}_M^2$. It is a proper subspace of $\mathbf{K}^2$ unless $m = n$.

4.56 Let $G^{-1}(p)$ denote the $m \times m$ impedance matrix of $\bar{\mathbf{N}}_G$. Then by (7) of 4.4, interpreted as an operator equation,

$$G^{-1}(p) = \left(\frac{1}{2} p + \frac{\omega_0^2}{2p} \right) G^{-1} \tag{11}$$

where G^{-1} is a real, constant, symmetric, non-singular $m \times m$ matrix.

We can now compute the voltage across $\mathbf{M}_{AD}$ corresponding to the current (10). Let w be the n-tuple of voltages appearing at the section B-B or C-C of Fig. 6, with its components listed in the appropriate order. Then we may interpret w as a vector in $\mathbf{V}$, and write it

$$w = u_0 \oplus v_0 \tag{12}$$

where $u_0 \, \epsilon \, \mathbf{U}$, $v_0 \, \epsilon \, V_1$. Now by Kirchoff's current law applied to the shunt arms in the upper channels of Fig. 6, the current into $\mathbf{\bar{N}}_G$ is

$$j_1 + j_2 ,$$

and therefore

$$u_0 = G^{-1}(p)(j_1 + j_2). \tag{13}$$

By Kirchoff's voltage law applied to a typical mesh which begins on A-A, goes through $\mathbf{N}_x$ to B-B, and then through a shunt arm and returns to A-A, the voltage n-tuple appearing at A-A is

$$X(p)(j_1 + k) + w.$$

Referring to (12), let us use u_0 also to denote the vector

$$u_0 \oplus 0 \, \epsilon \, \mathbf{V},$$

and v_0 to denote

$$0 \oplus v_0 \, \epsilon \, \mathbf{V}.$$

Interpreting (13) in this way we get

$$X(p)(j_1 + k) + G^{-1}(p)(j_1 + j_2) + v_0 \tag{14}$$

as the voltage n-tuple on A-A.

A similar calculation gives

$$L(p)(j_2 - k) + G^{-1}(p)(j_1 + j_2) + v_0 \tag{15}$$

as the voltage n-tuple on D-D. The ordered pair (14), (15) then gives the voltage $2n$-tuple corresponding to (10), in the notation analogous to (5).

4.57 $X(p)$, $L(p)$, and $G^{-1}(p)$, respectively, are defined in (6) of 4.44, (11) of 4.491, and (11) of 4.56. Each one is finite except at $p = 0$ and $p = \infty$. Let $\Gamma_\mathbf{M}$ be the complex plane from which these two points are deleted. It is now possible to show that the linear correspondence whose pairs, for each $p \, \epsilon \, \Gamma_\mathbf{M}$, are the voltages (14), (15) $\epsilon \, \mathbf{V}^2$ and the currents (10) $\epsilon \, \mathbf{K}^2$, satisfies P1 through P7 of $(I, 6, 7)$—that is, is PR $(I, 16.71)$.

In the present special circumstances it is almost as easy to study $\mathbf{M}_{AD}$ in a slightly different way than this. Since fewer direct references to I are involved, we shall take the alternative path.

We first calculate the scalar product between the voltage (14), (15) and an arbitrary current of the form (10), say the current

$$(h_1 \oplus \ell) \oplus (h_2 \oplus (-\ell)) \epsilon \mathbf{K}_M^2 .$$

To do so, we consider the form (9') for such a product. In the first writing, then, this scalar product is

$$(X(p)(j_1 + k) + G^{-1}(p)(j_1 + j_2) + v_0 , h_1 + \ell)$$
$$+ (L(p)(j_2 - k) + G^{-1}(p)(j_1 + j_2) + v_0 , h_2 - \ell).$$

Each of these scalar products has three voltages appearing in it. Distributing the products over these voltages, and using the facts that the range of $G^{-1}(p)$ is $\mathbf{J}$ and that $v_0 \epsilon \mathbf{V}_1 = (\mathbf{J})^0$ we get a second form:

$$(X(p)(j_1 + k), h_1 + \ell) + (G^{-1}(p)(j_1 + j_2), h_1) + (v_0 , \ell)$$
$$+ (L(p)(j_2 - k), h_2 - \ell) + (G^{-1}(p)(j_1 + j_2), h_2) + (v_0 , -\ell).$$

The terms involving v_0 go out and we can collect to

$$(X(p)(j_1 + k), h_1 + \ell) + (G^{-1}(p)(j_1 + j_2), h_1 + h_2)$$
$$+ (L(p)(j_2 - k), h_2 - \ell). \tag{16}$$

This is the desired scalar product.

4.58 Let us now consider the $(n + m)$-tuples

$$[a_1 , a_2 , \cdots , a_n , b_1 , \cdots , b_m] = j_1 \oplus k \oplus j_2 \tag{17}$$

obtained from (2) by deleting the $b_{m+1} , \cdots , b_n$. We still interpret these as currents into the relevant terminals of $\mathbf{M}_{AD}$. We also observe that when the current (17) is given, (2) can be determined, because by (10)

$$a_{m+s} + b_{m+s} = 0, \qquad s = 1, 2, \cdots , n - m.$$

Given (17), and therefore (2) or (10), we can determine the voltages (14) and (15), where v_0 is an arbitrary element of $\mathbf{V}_1$. Let us agree now always so to choose v_0 that the component of (15) in the subspace $\mathbf{V}_1$ vanishes. This means that, in (17), we have specified arbitrarily the currents into the left-hand terminals of $\mathbf{M}_{AD}$ (on A-A) and into the upper m of the right-hand terminals. We have also agreed that the voltages across the lower n-m terminals on D-D shall be zero, so that (15) is an

n-tuple of the form

$$u \oplus 0 \tag{18}$$

where $u \in \mathbf{U}$. Regarding (15), with this determination of v_0, as simply an m-tuple u (ignoring its last $n - m$ zero components), we see that (17) and the ordered pair (14), (15) are now currents and voltages in a $2(n + m)$-pole $\mathbf{M}_{AD}^*$ obtained from $\mathbf{M}_{AD}$ by shorting and thereafter ignoring the lower $n - m$ terminals on D-D.

4.59 Now (17) is unrestricted. Given it, the corresponding voltages can be computed from (14) and (15) by determining v_0 so that (15) lies in $\mathbf{U}$. Hence $\mathbf{M}_{AD}^*$ has an impedance matrix, since any single valued linear mapping from (17) to voltages can be described by a matrix. Our job is now to show that this matrix comes under 3.1. Before doing this, however, we shall point out that a realization of $\mathbf{M}_{AD}^*$ provides one for $\mathbf{M}_{AD}$.

Fig. 7 shows how a $2(2n)$-pole equivalent to $\mathbf{M}_{AD}$ would be constructed from $\mathbf{M}_{AD}^*$. The equivalence is evident almost at once: The pairs of $\mathbf{M}_{AD}^*$ are the currents (17) and the voltages (14) and (15) with a special determination of v_0, where (15) is regarded as an m-tuple. The current (10) is clearly that which flows in the $2(2n)$-pole of Fig. 7 when (17) flows in $\mathbf{M}_{AD}^*$. Furthermore, regarding (15) as an n-tuple of the form (18), we see that the voltages in Fig. 7 can be obtained from (14), (15) by adding an arbitrary voltage of the form

$$(0 \oplus v) \oplus (0 \oplus v),$$

where $v \in \mathbf{V}_1$ of course. This arbitrary added voltage eliminates the special role played by v_0 in (14) and (15). Hence therein v_0 itself may be considered to be an arbitrary element of $\mathbf{V}_1$, and (14), (15) represent the voltages in Fig. 7. The pairs admitted by the $2(2n)$-pole of Fig. 7 are therefore exactly those admitted by $\mathbf{M}_{AD}$, Q.E.D.

4.60 We have now established that $\mathbf{M}_{AD}^*$ has an impedance matrix, say $M(p)$. $M(p)$ operates from an $(n + m)$ space of currents (17) of 4.58 to an $(n + m)$ space of voltages (14), (15) of 4.56, where in (15) we properly choose v_0 so that the last $(n - m)$ components are zero and can be ignored.

Now any impedance matrix $\hat{Z}(p)$ is completely determined when we know for each two currents m_1 and m_2 the scalar product

$$(\hat{Z}(p)m_1, m_2) \tag{1}$$

(Cf. Halmos[9], par. 53). We shall make this computation for $M(p)$. The

currents (17) of 4.58 may be regarded as elements of the subspace (10) of 4.55. We have called this subspace $\mathbf{K_M^2}$. The voltages (14), (15), with v_0 chosen to make (15) an n-tuple of the form (18) (4.58), are elements of a subspace $\mathbf{V_M^2}$ of $\mathbf{V}^2$.

It is evident at once that the scalar product between a current $(n + m)$-tuple (17) and the $(n + m)$-tuple (14), (15) (v_0 properly chosen!) is exactly the same as the scalar product between the current $(2n)$-tuple (10) and the $(2n)$-tuple formed from the $(n + m)$-tuple (14), (15) by adjoining $(n - m)$ zeros to expand (15) to an n-tuple of the form (18).
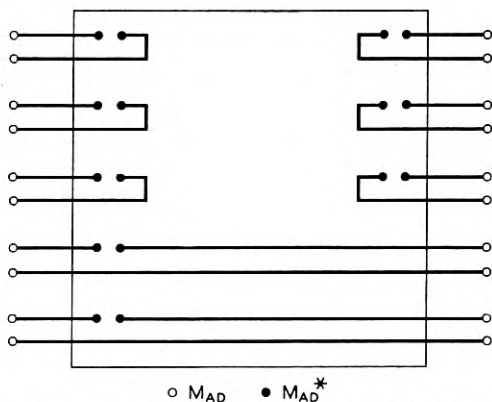
Fig. 7 = Construction of $\mathbf{M_{AD}}$ from $\mathbf{M_{AD}}^*$. The solid terminals are those of $\mathbf{M_{AD}}^*$, the open circles those of $\mathbf{M_{AD}}$.

Now we know that we may regard (15) as an n-tuple of the form (18) by a suitable choice of v_0. But we calculated in 4.57 the scalar product between an arbitrary $(2n)$-tuple and (14), (15) with an arbitrary v_0. The answer was (16) of 4.57. By proper choice of v_0, then, (16) represents the bilinear form (1) above for $M(p)$. Since (16) is independent* of v_0, it contains in itself the whole of the properties of $M(p)$.

4.61 To show that $M(p)$ is PR, we need show only that $M(p)$ is symmetric and that is *quadratic* form ($j_i = h_i$ and $k = \ell$ in (16)) is a PR function of p (2.09).

By their definitions, $X(p)$, $L(p)$, and $G^{-1}(p)$ are all symmetric. Hence if all currents are real, the value of (16) is unchanged by interchanging j_i with h_i, $i = 1, 2$, and k with ℓ. Therefore $M(p)$ is symmetric.

4.62 Henceforth we consider the quadratic from

---

* This is the gist of P3 of (I, 7.4). Use of the results of I here would have given a more direct but much less constructive representation of $\mathbf{M_{AD}}$.

$$(X(p)(j_1 + k), j_1 + k) + (\mathrm{G}^{-1}(p)(j_1 + j_2), j_1 + j_2)$$
$$+ (L(p)(j_2 - k), j_2 - k) \tag{2}$$

obtained from (16). By the definitions of $X(p)$, $L(p)$, and $\mathrm{G}^{-1}(p)$ this is a rational function taking real values for real p. Hence we need only show of (2) that its real part is non-negative when $Re(p) > 0$ to show that it and $M(p)$ are PR.

Referring to (6) and (11) of paragraph 4.4 and (11) of 4.56 for the definitions, we see that (2) can be written

$$\frac{1}{p}\Big[- (A(j_1 + k), j_1 + k) + \frac{\omega_0^2}{2}(G^{-1}(j_1 + j_2), j_1 + j_2)$$
$$+ (H(j_2 - k), j_2 - k)\Big] \tag{3}$$
$$+ p\Big[- (B(j_1 + k), j_1 + k) + \frac{1}{2}(G^{-1}(j_1 + j_2), j_1 + j_2)$$
$$+ (F(j_2 - k), j_2 - k)\Big].$$

That is, the quadratic form in question has poles, simple ones, only at 0 and ∞, and has no constant term. If we can show that the residues at these poles are non-negative, then it will follow not only that $M(p)$ is PR but that $M(p)$ is of the form

$$\frac{1}{p} M_0 + p M_\infty$$

where each of these summands is realizable by 3.1.

Unfortunately, there still remains some computation to verify that the residues of (3) are non-negative.

4.62 We first recapitulate some relations obtained earlier:

$$Z^{(2)}(p) = Z(p) + \frac{1}{p} A + pB; \tag{4}$$

this is (5) of 4.42.

$$Y^{(2)}(p) = \frac{2p}{p^2 + \omega_0^2} G + Y^{(3)}(p); \tag{5}$$

this is (7) and (8) of 4.45.

$$Z^{(3)}(p) = \frac{1}{p} H + pF + Z^{(4)}(p); \tag{6}$$

this is (11) and (12) of 4.491.

By their definitions,

$$Z^{(i)}(p) = [Y^{(i)}(p)]^{-1}$$

for $i = 2, 3$. By hypothesis, $Z(p)$ and

$$Z(p)^{-1} = Y(p)$$

are both finite everywhere on $p = i\omega$. By its construction, $Z^{(4)}(p)$ is finite at $p = 0$ and $p = \infty$.

4.63 We claim now that each $Y^{(i)}(p)$ is finite at $p = 0$ and ∞, $i = 2, 3$.

Proof: We need consider only $Y^{(2)}(p)$ since $Y^{(3)}(p)$ differs from it by something which vanishes at $p = 0$ and $p = \infty$ ((5) above). Let

$$Y^{(2)}(p) = \tilde{Y}(p) + \frac{1}{p} E + pQ$$

where $\tilde{Y}(p)$ is finite at $p = 0$ and $p = \infty$. Since $Y^{(2)}(p)$ is PR (4.43), E and Q are real and symmetric.

Using the form (4) above for $Z^{(2)}(p)$,

$$
\begin{aligned}
1 = Z^{(2)}(p)Y^{(2)}(p) = {}& Z(p)\tilde{Y}(p) + BE + AQ \\
& + p(Z(p)Q + B\tilde{Y}(p)) + p^2 BQ \\
& + \frac{1}{p}(Z(p)E + A\tilde{Y}(p)) + \frac{1}{p^2} AE.
\end{aligned}
\tag{7}
$$

Multiplying through by $p^2, p, \dfrac{1}{p^2}, \dfrac{1}{p}$ and taking limits as $p \to 0, 0, \infty, \infty$, respectively, we obtain

$$
\begin{aligned}
AE &= 0 \\
Z(0)E + A\tilde{Y}(0) &= 0, \\
BQ &= 0, \\
Z(\infty)Q + B\tilde{Y}(\infty) &= 0.
\end{aligned}
\tag{8}
$$

We can also write a formula like (7) with the factors in reverse order, and obtain the analogous forms to (8) in which the factors are commuted. Let us call these commuted relations (8'). Multiply the second relation (8) on the left by E and use the first relation of (8'). We obtain

$$EZ(0)E = 0. \tag{9}$$

Working similarly with the last two relations in (8) and (8'), we get

$$QZ(\infty)Q = 0. \tag{10}$$

Now let v be an arbitrary voltage in **V** and let

$$w = Z(0)Ev.$$

Then $w \, \epsilon \, \mathbf{V}$, and by (9) the current

$$Ew = 0$$

for any v. Hence

$$
\begin{aligned}
0 = (v, Ew) &= \overline{(w, E^*v)} = (\overline{w}, \bar{E}^*\bar{v}) \\
&= (\bar{Z}(0)\bar{E}\bar{v}, E'\bar{v})
\end{aligned}
\tag{11}
$$

by (I, 7.2, 14.0). Now E is real and symmetric, as noted above. Hence $E = \bar{E} = E'$. Furthermore, $Z(0)$ is real, so (11) becomes

$$(Z(0)Eu, Eu) = 0 \tag{12}$$

where $u = \bar{v}$ is any element of **V**. Now $Z(p)$ is non-singular on $p = i\omega$, and its real part is semidefinite there. At $p = 0$, $Z(0)$ is its own real part, hence semidefinite and non-singular, hence definite. Then (12) implies that $Eu = 0$. This being true for all $u \, \epsilon \, \mathbf{V}$, $E = 0$.

The proof that $Q = 0$ follows similarly from (10).

4.64 With $Y^{(2)}(p)$ and $Y^{(3)}(p)$ simplified at $p = 0$ and ∞, we can go back and compute

$$
\begin{aligned}
1 = Z^{(2)}(p)Y^{(2)}(p) \\
= \left(Z(p) + \frac{1}{p}A + pB\right)\left(\frac{2p}{p^2 + \omega_0^2}G + Y^{(3)}(p)\right).
\end{aligned}
\tag{13}
$$

Of the six terms obtained on expanding this exactly one, namely

$$\frac{1}{p}AY^{(3)}(p)$$

is not obviously finite at $p = 0$, and another,

$$pBY^{(3)}(p)$$

is not *a priori* finite at $p = \infty$. We conclude by multiplying through by p and letting $p \to 0$, and dually at $p = \infty$, that

$$
\begin{aligned}
AY^{(3)}(0) &= 0 = Y^{(3)}(0)A \\
BY^{(3)}(\infty) &= 0 = Y^{(3)}(\infty)B,
\end{aligned}
\tag{14}
$$

where the commuted form can be established by a new calculation from $1 = Y^2(p)Z^2(p)$, or by taking transposes.

In a similar way, we compute from

$$1 = Z^{(3)}(p)Y^{(3)}(p) = Z^{(4)}(p)Y^{(3)}(p) + \frac{1}{p} HY^{(3)}(p) + pFY^{(3)}(p) \quad (15)$$

that

$$
\begin{aligned}
HY^{(3)}(0) &= 0 = Y^{(3)}(0)H, \\
FY^{(3)}(\infty) &= 0 = Y^{(3)}(\infty)F.
\end{aligned}
\quad (16)
$$

Now $Y^{(3)}(p)$ is finite at 0 and ∞, so we may expand it in a power series about either point. Let these be

$$
\begin{aligned}
Y^{(3)}(p) &= Y^{(3)}(0) + pY_1^{(3)}(0) + O(p^2), \\
Y^{(3)}(p) &= Y^{(3)}(\infty) + \frac{1}{p} Y_1^{(3)}(\infty) + O\left(\frac{1}{p^2}\right).
\end{aligned}
\quad (17)
$$

Putting the appropriate one of these into (13) and taking a limit at 0 or ∞ we get, by using (14), that

$$
\begin{aligned}
1 &= \frac{1}{\omega_0^2} AG + AY_1^{(3)}(0) + Z(0)Y^{(3)}(0), \\
1 &= 2BG + BY_1^{(3)}(\infty) + Z(\infty)Y^{(3)}(\infty).
\end{aligned}
\quad (18)
$$

A relation (18') with factors commuted is also true.

We may also put (17) into (15) and get

$$
\begin{aligned}
1 &= Z^{(4)}(0)Y^{(3)}(0) + HY_1^{(3)}(0), \\
1 &= Z^{(4)}(\infty)Y^{(3)}(\infty) + FY_1^{(3)}(\infty),
\end{aligned}
\quad (19)
$$

and also a commuted form (19').

Right multiply the first line of (19) by A and the second by B, and use (14). This gives

$$
\begin{aligned}
A &= HY_1^{(3)}(0)A, \\
B &= FY_1^{(3)}(\infty)B.
\end{aligned}
\quad (20)
$$

Left multiply the first line of (18') by H and the second by F. This gives, by (16),

$$
\begin{aligned}
H &= \frac{2}{\omega_0^2} HGA + HY_1^{(3)}(0)A, \\
F &= 2FGB + FY_1^{(3)}(\infty)B.
\end{aligned}
\quad (21)
$$

Using (20) in (21), we have the relations

$$\frac{2}{\omega_0^2} HGA = H - A,$$

$$2FGB = F - B. \tag{22}$$

These are fundamental to the evaluation of the residues of (3). Before calculating these residues, we draw a further important conclusion from the formulas just developed.

Relation (20) exhibits A as a product of H and a possibly singular matrix (viz., $Y_1^{(3)}(0)A$). Hence

$$\text{rank } (A) \leq \text{rank } (H).$$

But relation (21) shows H as a product of A by

$$\frac{2}{\omega_0^2} HG + HY_1^{(3)}(0).$$

Hence

$$\text{rank } (H) \leq \text{rank } (A).$$

That is,

$$\text{rank } (A) = \text{rank } (H),$$

$$\text{rank } (B) = \text{rank } (F), \tag{23}$$

the latter being established in the same way.

4.65 The formulas developed in 4.64 are all quite symmetric as between relations obtained at $p = \infty$ and those at $p = 0$. We shall now continue to the evaluation of the residue of (3) at $p = \infty$. The evaluation at $p = 0$ proceeds in an exactly similar manner.

The residue in question is, from (3),

$$-(B(j_1 + k), j_1 + k) + \tfrac{1}{2}(G^{-1}(j_1 + j_2), j_1 + j_2)$$
$$+ (F(j_2 - k), j_2 - k). \tag{24}$$

Here j_1 and j_2 are any elements of $\mathbf{J}$ and k any element of $\mathbf{K}_1$. The range of G is $\mathbf{J}$ and the operator G^{-1} operates from $\mathbf{J}$ to $\mathbf{U} = \mathbf{J}^*$, representing the inverse to the operation G from $\mathbf{U}$ to $\mathbf{J}$.

Let us define h and eliminate j_2 by the relation

$$j_2 = 2h + 2GB(j_1 + k) - j_1. \tag{25}$$

Since the range of G is $\mathbf{J}$, $h \in \mathbf{J}$.

The definition analogous to (25) for the other pole of (3) is

$$j_2 = \frac{2}{\omega_0^2} h + \frac{2}{\omega_0^2} GA(j_1 + k) - j_1.$$

We shall now say no more about this pole.

Putting (25) into (24) we get at once the form

$$-(B(j_1 + k), j_1 + k) + (G^{-1}h + G^{-1}GB(j_1 + k), 2h + 2GB(j_1 + k))$$

$$+ (2Fh + 2FGB(j_1 + k) - Fj_1 - Fk, 2h + 2GB(j_1 + k) - j_1 - k).$$

Here we cannot at once put $G^{-1}G = 1$, because this is only true in **U**. We expand in the following way: The first product is left intact, the second is expanded by distributivity into four terms, and in the third we use (22) and expand into five terms by distributivity. The ten resulting terms are:

$$-(B(j_1 + k), j_1 + k) + 2(G^{-1}h, h)$$

$$+ 2(G^{-1}GB(j_1 + k), h) + 2(G^{-1}h, GB(j_1 + k))$$

$$+ 2(G^{-1}GB(j_1 + k), GB(j_1 + k))$$

$$+ 4(Fh, h) - 2(B(j_1 + k), h)$$

$$+ 2(Fh, 2GB(j_1 + k) - j_1 - k)$$

$$- 2(B(j_1 + k), GB(j_1 + k)) + (B(j_1 + k), j_1 + k).$$

Enumerate these terms $1, 2, \cdots, 10$ in the order written. We shall show by combining that only 2 and 6 remain.

Clearly 1 and 10 cancel.

Consider the operator $G^{-1}G$ as we have defined it. If $v \in \mathbf{V}$, we can put

$$v = u + v_1$$

where $u \in \mathbf{U}, v_1 \in \mathbf{V}_1$. Then

$$Gv = Gu + Gv_1 = Gu,$$

because of the matrix form for G in the coordinate system chosen in 4.5. By definition of G^{-1} (in 4.56), since $u \in \mathbf{U}$,

$$G^{-1}Gu = u.$$

Hence, combining the last three relations,

$$G^{-1}Gv = v - v_1 \tag{26}$$

for any $v \in \mathbf{V}$, where v_1 is a suitable element of $\mathbf{V}_1$ (depending on v of course).

Using (26) in term 3, we get for this term

$$2(B(j_1 + k), h) - 2(v_1, h)$$

for some $v_1 \in \mathbf{V}_1$. But $h \in \mathbf{J} = (\mathbf{V}_1)^0$ ((1) of 4.5). Hence the second term here vanishes and term 3 cancels term 7. By an exactly similar argument, since $GB(j_1 + k) \in \mathbf{J}$, we find that term 5 cancels term 9.

Consider term 4, and write it in the form

$$2(G^{-1}h, k_1) = \overline{2((G^{-1})^*k_1, h)}$$
$$= 2((\bar{G}^{-1})^*\bar{k}_1, \bar{h}) = 2(G^{-1}\bar{k}_1, \bar{h}).$$

This follows by (I, 7.2, 14.0) and the fact that G^{-1} is symmetric. Putting in the definition of k_1, and using the fact that G and B are real, we get

$$2(G^{-1}\bar{k}_1, \bar{h}) = 2(G^{-1}\overline{GB}(\bar{j}_1 + \bar{k}), \bar{h})$$
$$= 2(G^{-1}GB(j_1 + \bar{k}), \bar{h}).$$

Now $\mathbf{J}$ is real (4.42) so $\bar{h} \in \mathbf{J}$. Therefore the reasoning used on term 3 yields finally

$$2(B(\bar{j}_1 + \bar{k}), \bar{h})$$

as the value of term 4.

We now write term 8 as

$$2(Fh, k_2)$$

and transform it to

$$2(F\bar{k}_2, \bar{h}),$$

by the reasoning just used on 4. Putting in what k_2 is, this is

$$2(2F\overline{GB}(\bar{j}_1 + \bar{k}) - Fj_1 - F\bar{k}, \bar{h}).$$

Using the reality of G and B, and (22), this is

$$- 2(B(\bar{j}_1 + \bar{k}), \bar{h}).$$

This cancels term 4 and all terms save 2 and 6 are accounted for. Finally, then, the residue of (3) at $p = \infty$ is

$$2(G^{-1}h, h) + 4(Fh, h). \tag{27}$$

Since G^{-1} is definite in $\mathbf{J}$ and F is semidefinite, this residue is non-negative, and indeed not zero if $h \neq 0$ and $h \in \mathbf{J}$.

4.7 We have established the non-negativity of the residue of (3) at $p = \infty$. A similar argument (exactly parallel, in fact) will establish the same for the residue at $p = 0$. Each term in the representation

$$M(p) = \frac{1}{p} M_0 + pM_\infty$$

of 4.61 is then realizable by 3.1. Hence $\mathbf{M}_{AD}^{*}$ is a realizable reactance $2(n + m)$-pole, and so therefore is $\mathbf{M}_{AD}$, as we noted in discussing Figure 7 (4.59). Therefore, if $\bar{\mathbf{N}}^{(4)}$ of Figure 5 is physically realizable, so also is $\bar{\mathbf{N}}$ and therefore $\mathbf{N}$. We denote by $\mathbf{N}_1$ the $\bar{\mathbf{N}}^{(4)}$ obtained in this way from $\mathbf{N}$, and define IB as the operation which constructs $\mathbf{N}_1$ from $\mathbf{N}$.

We must still establish the claims made in 4.04 for IB. No properties of $\bar{\mathbf{N}}^{(4)} = \mathbf{N}_1$ have been proved beyond the existence of its impedance matrix, $Z^{(4)}(p)$, but this is all that is claimed in the third column of 4.04. The fifth column is also established. We must now however compare the degree of $\mathbf{N}_1$, i.e., of $Z^{(4)}(p)$, with that of $Z(p)$.

By 2.13, 2.14 and 2.15 applied to (4), (5), and (6) of 4.62,

$$\delta(Z^{(2)}) = \delta(Z) + \text{rank } (A) + \text{rank } (B),$$

$$\delta(Z^{(2)}) = \delta(Y^{(2)}) = \delta(Y^{(3)}) + 2 \text{ rank } (G),$$

$$\delta(Y^{(3)}) = \delta(Z^{(3)}) = \delta(Z^{(4)}) + \text{rank } (H) + \text{rank } (F).$$

We know $m = \text{rank } (G) \geq 1$. Let

$$r = \text{rank } (A) + \text{rank } (B).$$

Then from (23), and the relations above in order,

$$\delta(Z) = \delta(Z^{(2)}) - r = (\delta(Z^{(3)}) + 2m) - r$$
$$= (\delta(Z^{(4)}) + r) + 2m - r$$
$$= \delta(Z^{(4)}) + 2m.$$

Hence $\delta(Z) - \delta(Z^{(4)}) = \delta(\mathbf{N}) - \delta(\mathbf{N}_1) = 2m > 0$. The claims of 4.04 are then established.

4.71 We must yet verify 4.07 for IB. Let $\delta(M)$ be the degree of

$$M(p) = \frac{1}{p} M_0 + p M_\infty.$$

Then by 3.21, $\mathbf{M}_{AD}^{*}$, whose matrix is $M(p)$, can be realized with $\delta(M)$ reactive elements. By Figure 7, then $\mathbf{M}_{AD}$ can be so realized, and it follows that exactly $\delta(M)$ reactive elements are comprised between $\mathbf{N}$ and $\mathbf{N}_1$ under IB.

Now by 2.14 and 2.15,

$$\delta(M) = \text{rank } (M_0) + \text{rank } (M_\infty).$$

We shall compute the second term. The first is obtained by an exactly parallel calculation.

Using the fact that $M(p)$ is determined by its quadratic form, we see that M_∞ is the matrix whose form is the residue of that of $M(p)$ at $p = \infty$. This residue was computed in (27) of 4.65 to be

$$2(G^{-1}h, h) + 4(Fh, h) \tag{1}$$

when the current vector, (17) of 4.58, is

$$j_1 \oplus k \oplus j_2, \tag{2}$$

and, (25) of 4.65,

$$2h = j_1 + j_2 - 2GB(j_1 + k). \tag{3}$$

Here j_1, $j_2 \in \mathbf{J}$ and $k \in \mathbf{K}_1$.

Now M_∞ is an $(n + m) \times (n + m)$ matrix by construction. Then

$$\nu = n + m - \text{rank} (M_\infty) \tag{4}$$

is its nullity, the dimension of its null space. This is proved in Halmos[9], par. 37, for dimensionless operators, and a similar proof applies to impedance operators.

Now for any symmetric and semidefinite impedance operator $\hat{Z}$, the null space of $\hat{Z}$ is exactly the aggregate of currents k such that the quadratic form

$$(\hat{Z}k, k) = 0.$$

This may be seen at once by choosing a coordinate frame in which the matrix of $\hat{Z}$ is diagonal. Since we know from 4.65 that M_∞ is symmetric and semidefinite, we can compute ν as the dimensionality of the space of vectors (2) above for which (1) vanishes.

As noted in 4.65, $h \in \mathbf{J}$, and (1) vanishes if and only if $h = 0$, because G^{-1}, as an operator from $\mathbf{J}$ to $\mathbf{U}$, is definite (semidefinite and non-singular). Hence ν is the maximum number of linearly independent vectors (2) for which, from (3),

$$(1 - 2GB)j_1 + j_2 - 2GBk = 0. \tag{5}$$

The left member of (5) is a vector in $\mathbf{J}$ depending linearly and homogeneously on the vector (2). Hence, regarding $\mathbf{J}$ as a subspace of the space $\mathbf{J} \oplus \mathbf{K}_1 \oplus \mathbf{J}$ in which (2) lies, the left member of (5) is the value in $\mathbf{J} \oplus \mathbf{K}_1 \oplus \mathbf{J}$ of a certain linear operation applied to the vector (2). Let us call this operator P. The number ν, by definition the number of linearly independent vectors (2) for which (5) holds, is the nullity of P. The dimension of P is $n + m$, and its rank is clearly m because the left member of (5)—a typical element in the range of P—lies in $\mathbf{J}$ and by

suitable choice of j_2 can be made to be any element of **J**. Hence the nullity of P is $(n + m) - m = n$ (Halmos[9], par. 37). That is

$$\nu = n,$$

and, by (4)

$$\text{rank } (M_\infty) = m.$$

A parallel argument will establish the same result for M_0. Hence

$$\delta(M) = 2m = \delta(\mathbf{N}) - \delta(\mathbf{N}_1)$$

by a result of 4.7. Therefore $\mathbf{M}_{AD}^*$ and $\mathbf{M}_{AD}$ can be realized with

$$\delta(\mathbf{N}) - \delta(\mathbf{N}_1)$$

reactive elements and 4.07 holds for IB.

V. THE DEGREE OF A RATIONAL MATRIX

5.0 In this section we consider arbitrary $n \times n$ matrices $Z(p)$ whose elements are rational functions of the complex variable p. They are treated, generally, as arrays of functions with certain rules for addition, multiplication, and reciprocation, without geometric interpretation. A geometric development is possible, but would be cumbrous. Related ideas may be found, geometrically developed, in Appendix I of Halmos[9].

This section deals wholly with concepts well known in the algebraic theory of matrices over an arbitrary field—in this case the field of rational functions. I have not found, however, any place where the particular developments which seem to be needed here are made sufficiently explicitly for reference. Accordingly, the presentation here is somewhat detailed. The particular path of argument followed is only one of many possible; it was chosen to lead easily to results needed in Section 6, and to parallel generally the rest of the paper.

This section could be abbreviated somewhat if one restricted himself to PR matrices $Z(p)$. We prefer not to limit the applicability of these results, however, since they may well be useful in non-passive realizability theory.

5.01 *Definition:* If $R(p)$ is a rational function of the form

$$R(p) = (p - p_0)^m R_1(p),$$

where $R_1(p)$ is finite and not zero at p_0, and m may be of any sign, we call m the exponent of $(p - p_0)$ in $R(p)$. The number

$$r = \sup (-m, 0)$$

is called the order of the pole of $R(p)$ at p_0, even if $r = 0$.

5.1 Let $Z(p)$ be an $n \times n$ matrix whose elements $Z_{rs}(p)$ are rational functions of the complex variable p. We write

$$Z_{rs}(p) = \frac{N_{rs}(p)}{D_{rs}(p)},$$

where N_{rs} and D_{rs} are relatively prime polynomials. Let $\Psi_Z(p)$ be the least common multiple of all $D_{rs}(p)$, $(1 \leq r, s \leq n)$, so normalized that the coefficient of the highest power of p appearing in $\Psi_Z(p)$, (the *leading coefficient*) is unity. Then $\Psi_Z(p)$ is uniquely determined by $Z(p)$.

The matrix $\Psi_Z(p)Z(p)$ has polynomial elements. Its *Smith normal form* is a diagonal matrix $E(p)$,

$$E(p) = \begin{bmatrix} E_1(p) & 0 & \cdot & \cdot & \cdot & 0 \\ 0 & E_2(p) & & & & \\ \vdots & & \ddots & & & \\ \vdots & & & E_R(p) & & \\ 0 & & & & 0 \cdot & \\ & & & & & \cdot 0 \end{bmatrix} = A(p)\Psi_Z(p)Z(p)B(p), \quad (1)$$

with the following properties:
  (a) R is the rank of $\Psi_Z(p)Z(p)$.
  (b) Each $E_i(p)$, $1 \leq i \leq R$, is a polynomial with unit leading coefficient.
  (c) Each $E_i(p)$ is a factor of $E_{i+1}(p)$, $1 \leq i \leq R - 1$.
  (d) $A(p)$ and $B(p)$ are polynomial matrices, each with a constant non-vanishing determinant.
  (e) $E_1(p)E_2(p) \cdots E_k(p)$ is the normalized (and therefore unique) highest common factor of all k-rowed minor determinants of $\Psi_Z(p)Z(p)$.

These properties of $E(p)$ are developed for example, in Bocher[15], Theorems 2 and 3 of paragraph 91 and Theorem 1 of paragraph 94. A simple variation of this last cited theorem will also prove the following uniqueness lemma.

5.11 *Lemma:* If some $E^0(p)$ satisfies (1) and (a), (b), (c) and (d) above, all written with superscripts on each E, and on A and B, then $E^0(p) = E(p)$.

  Proof: $E^0(p)$ is equivalent to $E(p)$ in the sense of paragraph 94 of

Bocher[15], for

$$E^0(p) = A^0(p)A^{-1}(p)E(p)B^{-1}(p)B^0(p).$$

Therefore it is also equivalent in the sense of par. 91 of Bocher[15], (for this is Theorem 1 of paragraph 94). Hence the normalized greatest common factor of all k-rowed minors of $E^0(p)$ is the same as that of $E(p)$, that is, $E_1(p) \cdots E_k(p)$. But the greatest common factor of all k rowed minors of $E^0(p)$ is $E_1^0(p) \cdots E_k^0(p)$, because of property (c). In particular then $E_1(p) = E_1^0(p)$, and consequently $E_k(p) = E_k^0(p)$ by induction for $1 \leq k \leq R$.   Q.E.D.

5.12 *Definition:* The normal form $W(p)$ of $Z(p)$ is the matrix $\Psi_z^{-1}(p)E(p)$. We write the elements of $W(p)$ in their lowest terms,

$$W(p) = A(p)Z(p)B(p) = \begin{bmatrix} \dfrac{e_1(p)}{\Psi_1(p)} & 0 & \cdot & \cdot & \cdot & 0 \\ 0 & \dfrac{e_2(p)}{\Psi_2(p)} \cdot \\ \cdot & & \cdot \dfrac{e_R(p)}{\Psi_R(p)} \\ \cdot & & & 0 \cdot \\ \cdot & & & & \cdot 0 \\ 0 & & & & & \end{bmatrix} \quad (2)$$

with the polynomials $e_k(p)$, $\Psi_k(p)$ each having unit leading coefficients.

5.13 *Theorem:* The normal form $W(p)$ of $Z(p)$, as given by (2), has the properties (a′), (b′), (c′), (d′), and (e′) listed below. Furthermore, any $W^0(p)$, given by (2) with superscripts on W, A, B, e_k, and $\Psi_k(1 \leq k \leq R)$, which satisfies (a′), (b′), (c′), and (d′) with corresponding superscripts, is in fact $W(p)$.

(a′) R is the rank of $Z(p)$

(b′) For each k, $1 \leq k \leq R$, $e_k(p)$ and $\Psi_k(p)$ are relatively prime polynomials with unit leading coefficients.

(c′) Each $e_k(p)$ is a factor of $e_{k+1}(p)$, $1 \leq k \leq R - 1$, and each $\Psi_j(p)$ is a factor of $\Psi_{j-1}(p)$, $2 \leq j \leq R$.

(d′) $A(p)$ and $B(p)$ are polynomial matrices each with a constant non-vanishing determinant

(e′) $\Psi_1(p) = \Psi_z(p)$.

Proof: (a′) and (d′) follow immediately from (a) and (d) of 5.1. (b′) is a matter of definition. (c′) follows from (c) of 5.1 and the definition, 5.12, since the effect of cancelling common factors in each fraction of the sequence

$$\frac{E_1(p)}{\Psi_z(p)}, \frac{E_2(p)}{\Psi_z(p)}, \cdots, \frac{E_R(p)}{\Psi_z(p)}$$

cannot remove from any $E_k(p)$ a factor which was present in earlier $E_j(p)(j < k)$ but was not cancelled therefrom (treat each linear factor of Ψ_z and of E_1 as distinct, and each linear factor of $\dfrac{E_{k+1}(p)}{E_k(p)}$ as distinct to see this easily).

Property (e′) is best proved by a reductio ad absurdum. We recall that $E_1(p)$ is the highest common factor of all elements of $\Psi_z(p)Z(p)$. Suppose now that $E_1(p)$ contained a factor φ in common with $\Psi_z(p)$. Then every non-zero element of $\Psi_z(p)Z(p)$ contains the factor φ. Hence no denominator in $Z(p)$ cancels φ from $\Psi_z(p)$. Hence no denominator contains φ as a factor, but this denies its presence in their least common multiple, $\Psi_z(p)$.

The uniqueness of $W(p)$ follows at once from the uniqueness lemma, 5.11. Multiply (2) by $\Psi_z(p)$. Then

$$\Psi_z(p)W^0(p) = A^0(p)\Psi_z(p)Z(p)B^0(p) \tag{3}$$

has diagonal elements of the form

$$\frac{\Psi_z(p)e_k(p)}{\Psi_k(p)}, \qquad 1 \leq k \leq R. \tag{4}$$

But by (3) and (d′), these are the result of polynomial operations on the polynomial matrix $\Psi_z(p)Z(p)$. Hence the elements (4) are polynomials, and each has unit leading coefficient. $\Psi_z(p)W^0(p)$ then clearly satisfies (a), (b), (c), and (d) of 5.1. Therefore by 5.11, $\Psi_z(p)W^0(p) = E(p) = \Psi_z(p)W(p)$. Therefore $W^0(p) = W(p)$.   Q.E.D.

5.14 *Corollary:* $W(p)$ is its own normal form.

5.15 *Corollary:* Let $\varphi(p)$ be a rational function and

$$Z_1(p) = \varphi(p)Z(p).$$

Let $W(p)$ be the normal form of $Z(p)$ and $W_1(p)$ the normal form of $Z_1(p)$. Then, when written in normalized lowest terms,

$$W_1(p) = \varphi(p)W(p).$$

Proof: Supposing that (2) above holds for W and Z, we have

$$\varphi(p)W(p) = A(p)Z_1(p)B(p).$$

Call the left side of this equation $W_1^0(p)$. We must identify this with $W_1(p)$. We have just showed that it satisfies (d′) of 5.13. It clearly satisfies (a′), (b′) and (c′), with Z_1 written for Z. Hence 5.13 implies the desired equality.

5.16 *Corollary:* If $C(p)$ and $D(p)$ are polynomial matrices with constant non-vanishing determinants, then the normal forms of $Z(p)$ and $C(p)Z(p)D(p)$ are the same.

Proof:

$$AZB = (AC^{-1})CZD(D^{-1}B)$$

and the bracketed factors are again polynomial matrices with constant non-vanishing determinants.

5.2 *Definition:* The point p_0 is a pole of $Z(p)$ if some element of $Z(p)$ has a pole at $p = p_0$. If p_0 is not a pole of $Z(p)$, we say that $Z(p_0)$ is finite, or that $Z(p)$ is finite at p_0.

5.21 If p_0 is a pole of $Z(p)$, we may expand each element of Z in partial fractions and collect those terms having poles at p_0, obtaining, when $p_0 \neq \infty$,

$$Z(p) = (p - p_0)^{-r}Z_r + (p - p_0)^{-r+1}Z_{r-1} \\ + \cdots + (p - p_0)^{-1}Z_1 + Z_0(p), \tag{1}$$

where $Z_0(p_0)$ is finite, $Z_r \neq 0$, and the Z_k, $1 \leq k \leq r$, are matrices of constants. If $p_0 = \infty$, we read p^ℓ for $(p - p_0)^{-\ell}$ in (1), $1 \leq \ell \leq r$. All of $Z_0(p)$, Z_1, $\cdots$, Z_r are uniquely defined by their construction from $Z(p)$.

5.22 *Definition:* If $Z(p)$ is given by (1) above, then r is the order of the pole of $Z(p)$ at p_0.

5.23 Clearly, if $Z(p)$ has the form (1) at $p_0 \neq \infty$, some non-vanishing element of $Z(p)$ has a denominator containing the factor $(p - p_0)^r$, and no element has a pole of order higher than r at p_0. Hence $(p - p_0)^r$ divides $\Psi_z(p)$, but no higher power of $(p - p_0)$ does. Therefore, by (e$'$) of 5.13, the normal form $W(p)$ of $Z(p)$ has a first element with an rth order pole at p_0. In particular, then, $p_0 \neq \infty$ is a pole of order r of $Z(p)$ if and only if it is a pole of order r of $W(p)$.

5.24 *Definition:* Consider a pole of order r of $Z(p)$, say p_0, with $p_0 \neq \infty$. In the normal form $W(p)$ of $Z(p)$, (2) of 5.12, let γ_k be the order of the pole of the kth diagonal element

$$\frac{e_k(p)}{\Psi_k(p)}$$

at the point $p = p_0$. Then $\gamma_k \geq \gamma_{k+1}$, and $\gamma_1 = r$. We write the γ_k in an ordered array

$$S(Z, p_0) = [\gamma_1, \gamma_2, \cdots, \gamma_n].$$

5.25 *Definition:* Consider two matrices $Z(p)$ and $Z_1(p)$, with

$$S(Z, p_0) = [\gamma_1, \gamma_2, \cdots, \gamma_n],$$
$$S(Z_1, p_0) = [\gamma_1', \gamma_2', \cdots, \gamma_n'].$$

We say

$$S(Z, p_0) \geq S(Z_1, p_0) \tag{2}$$

if and only if

$$\gamma_1 + \gamma_2 + \cdots + \gamma_k \geq \gamma_1' + \gamma_2' + \cdots + \gamma_k'$$

for every $k = 1, 2, \cdots, n$. We say

$$S(Z, p_0) = S(Z_1, p_0) \tag{3}$$

if

$$\gamma_k = \gamma_k'$$

for $k = 1, 2, \cdots, n$. It is easy to see that (3) is equivalent to the simultaneous validity of (2) and the reverse inequality.

5.26 *Theorem:* Let $p_0 \neq \infty$ be a pole of $Z(p)$. Let $F(p)$ be a rational $n \times n$ matrix which is finite at p_0. Then

$$S(Z, p_0) \geq S(FZ, p_0).$$

In particular, if $F(p)$ is also non-singular at p_0, then

$$S(Z, p_0) = S(FZ, p_0).$$

Proof: Let $\psi_F(p)$ and $\psi_Z(p)$ be the least common denominators of the elements of $F(p)$ and $Z(p)$, respectively. Then the exponent of $(p - p_0)$ in $\psi_Z(p)$ is r, while in $\psi_F(p)$ it is zero by 5.23.

Let $-\varepsilon_k$ be the exponent of $(p - p_0)$ in the kth diagonal element of the normal form of Z, and $-\varepsilon_k'$ the similar quantity for FZ. Then

$$\varepsilon_1 \geq \varepsilon_2 \geq \cdots \geq \varepsilon_n,$$
$$\varepsilon_1' \geq \varepsilon_2' \geq \cdots \geq \varepsilon_n', \tag{3}$$

by (c') of 5.13. Let

$$\gamma_k = \sup(\varepsilon_k, 0),$$
$$\gamma_k' = \sup(\varepsilon_k', 0),$$

Then $\gamma_k \geq \varepsilon_k$, $\gamma_k' \geq \varepsilon_k'$, and

$$S(Z, p_0) = [\gamma_1, \gamma_2, \cdots, \gamma_n],$$
$$S(FZ, p_0) = [\gamma_1', \gamma_2', \cdots, \gamma_n'].$$

By 5.15, the normal form of FZ is

$$(\psi_F\psi_Z)^{-1} \cdot (\text{normal form of } \psi_F\psi_Z FZ).$$

Hence the exponent of $(p - p_0)$ in the kth diagonal element of the normal form of $\psi_F\psi_Z FZ$ is $r - \varepsilon'_k$. By a similar argument, the exponent of $(p - p_0)$ in the kth diagonal element of the normal form of $\psi_Z Z$ is $r - \varepsilon_k$. Hence, by (e) of 5.1,

$$(r - \varepsilon'_1) + \cdots + (r - \varepsilon'_b)$$

is the exponent of $(p - p_0)$ in the highest common factor of all b-rowed minor determinants of $\psi_F\psi_Z FZ$. Similarly

$$(r - \varepsilon_1) + \cdots + (r - \varepsilon_b)$$

is the exponent of $(p - p_0)$ in the highest common factor of all b-rowed minor determinants of $\psi_Z Z$.

Now $\psi_F\psi_Z FZ$ is a polynomial matrix. A typical b-rowed determinant of this matrix is of the form

$$\psi_F^b\psi_Z^b \sum M_b N_b , \tag{4}$$

where the summation is over certain products $M_b N_b$ of b-rowed minors M_b of F and b-rowed minors N_b of Z. For a proof of this, see MacDuffee[16], Theorem 99.1. The expression (4) is the same as

$$\sum (\psi_F^b M_b)(\psi_Z^b N_b) \tag{5}$$

where the factors $(\psi_Z^b N_b)$ are now b-rowed minors of $\psi_Z Z$. If φ is a factor common to all b-rowed minors of $\psi_Z Z$, it certainly is a factor common to all expressions (4) or (5). Hence the highest common factor of all b-rowed minor determinants of $\psi_F\psi_Z FZ$—i.e., of all expressions (4) or (5),—has an exponent for $(p - p_0)$ no lower than that in the highest common factor of all b-rowed minor determinants of $\psi_Z Z$. Hence for any b,

$$(r - \varepsilon'_1) + \cdots + (r - \varepsilon'_b) \geq (r - \varepsilon_1) + \cdots + (r - \varepsilon_b),$$

or

$$\varepsilon_1 + \cdots + \varepsilon_b \geq \varepsilon'_1 + \cdots + \varepsilon'_b .$$

It follows that

$$\gamma_1 + \cdots + \gamma_b \geq \varepsilon'_1 + \cdots + \varepsilon'_b .$$

This being true for every b, it is certainly true for every b such that all terms on the right are ≥ 0 (cf. (2)). This means that for $b = 1$, and for

every successive $b > 1$ such that $\varepsilon'_b \geq 0$,

$$\gamma_1 + \cdots + \gamma_b \geq \gamma'_1 + \cdots + \gamma'_b .$$

This inequality is now not altered if non-negative numbers are added to its left member and zeros to its right member. Hence it holds for all b, $1 \leq b \leq n$, and

$$S(Z, p_0) \geq S(FZ, p_0). \tag{6}$$

This is the first claim of the theorem.

Now if $F(p)$ is non-singular at p_0, then $F^{-1}(p)$ is rational, and finite at p_0. Hence by what is already proved,

$$S(FZ, p_0) \geq S(F^{-1}(FZ), p_0).$$

This last array is just $S(Z, p_0)$. Hence we have (6) and its reverse, and the theorem is proved.

5.27 *Theorem:* If $p_0 \neq \infty$ and

$$Z(p) = Z_1(p) + Z_2(p),$$

where $Z_2(p)$ is finite at p_0, then

$$S(Z, p_0) = S(Z_1, p_0).$$

The proof of this depends upon the following lemma.

5.28 *Lemma:* Let $Z^*(p)$ be such that at $p = p_0 \neq \infty$ its only elements having poles are on the main diagonal. Let $-\varepsilon'_1, -\varepsilon'_2, \cdots$ be the exponents of $(p - p_0)$ in the diagonal elements of $Z^*(p)$, so enumerated that

$$+ \varepsilon'_1 \geq + \varepsilon'_2 \geq \cdots \geq + \varepsilon'_n .$$

Let $-\varepsilon_1, -\varepsilon_2, \cdots, -\varepsilon_n$ be the exponents of $(p - p_0)$ in the successive diagonal elements of the normal form of $Z^*(p)$. Then if $\varepsilon'_b \geq 0$ we have

$$\varepsilon'_1 + \cdots + \varepsilon'_b \geq \varepsilon_1 + \cdots + \varepsilon_b .$$

Proof: There exist constant non-singular matrices F, G such that FZ^*G has the same rows and columns as Z^* so permuted that the diagonal elements of FZ^*G are arranged in the order of ascending powers of $(p - p_0)$, the highest order pole being in the first position. Since the normal forms of Z^* and FZ^*G are identical, it suffices to consider Z^* itself to be in this form.

Let $\psi = \psi_{Z^*}(p)$. Now ψZ^* has its diagonal elements in the order of increasing positive power of $(p - p_0)$. Furthermore, any off-diagonal element of ψZ^* has $(p - p_0)^r$ as a factor.

Let b be such that $\varepsilon_b' \geq 0$. Any b-rowed minor of ψZ^* is a sum of products of b elements of ψZ^*. That b-rowed minor which has in it a term with a lowest possible exponent of $(p - p_0)$ is the upper left b-rowed minor. Even this minor has a term with exponent

$$(r - \varepsilon_1') + \cdots + (r - \varepsilon_b') \tag{7}$$

for $(p - p_0)$, this term being the product of the main diagonal elements. Hence the highest common factor of all b-rowed minors of ψZ^* has an exponent for $(p - p_0)$ not less than (7). Hence

$$(r - \varepsilon_1) + \cdots + (r - \varepsilon_b) \tag{8}$$

is not less than (7), since this is the exponent of $(p - p_0)$ in the product of the first b diagonal elements of the normal form of ψZ^*. The inequality between (8) and (7) is just the conclusion claimed in the lemma.

5.281 *Proof* of 5.27: Let

$$W(p) = A(p)Z(p)B(p)$$

be the normal form of $Z(p)$. Then

$$W = AZ_1B + AZ_2B. \tag{9}$$

If we expand all three terms here in Laurent series about p_0, the term AZ_2B contributes no negative powers. It follows then from the diagonal form of W that the matrix

$$Z^* = AZ_1B$$

satisfies the conditions of 5.28. The ε_k' of that lemma are, from (9), just the exponents of $(p - p_0)$ in the successive diagonal elements of W, the normal form of Z, and the ε_k of 5.28 are the similar quantities for the normal form of $Z^* = AZ_1B$. But the normal form of AZ_1B is the same as that of Z_1 (5.16). Therefore in the inequality of 5.28 we may interpret all of the ε's as exponents in the respective normal forms of Z and Z_1.

Now

$$Z_1(p) = Z(p) + (-Z_2(p))$$

and $-Z_2(p)$ is again finite at p_0. Hence we may conclude by the argument just used that if $\varepsilon_b \geq 0$ also

$$\varepsilon_1 + \cdots + \varepsilon_b \geq \varepsilon_1' + \cdots + \varepsilon_b'.$$

Hence if either of ε_b or ε_b' is non-negative

$$\varepsilon_1 + \cdots + \varepsilon_b = \varepsilon_1' + \cdots + \varepsilon_b'.$$

By induction on b, then,

$$\varepsilon_k = \varepsilon_k'$$

for $k = 1, 2$, etc. until such k that both are negative. Therefore

$$\gamma_k = \sup\,(\varepsilon_k\,,\,0) = \gamma_k' = \sup\,(\varepsilon_k'\,,\,0)$$

for all $k = 1, 2, \cdots, n$. That is,

$$S(Z, p_0) = S(Z_1\,,\,p_0),$$

Q.E.D.

5.29 *Theorem:* Let $Z(p)$ be such that at $p = p_0 \neq \infty$ its only elements having poles lie on the main diagonal. Let $\sigma_1\,,\,\sigma_2\,,\,\cdots,\,\sigma_n$ be the orders of these poles, so enumerated that

$$\sigma_1 \geq \sigma_2 \geq \cdots \geq \sigma_n\,.$$

Then

$$S(Z, p_0) = [\sigma_1\,,\,\sigma_2\,,\,\cdots,\,\sigma_n].$$

Proof: We write

$$Z(p) = Z^*(p) + Z_2(p),$$

where $Z^*(p)$ is diagonal, having exactly the diagonal elements of $Z(p)$. By 5.27,

$$S(Z, p_0) = S(Z^*, p_0).$$

Now $Z^*(p)$ falls under 5.28, but is diagonal in addition. In the proof of 5.28, therefore, it is exactly the principal minors of ψZ^* which have the lowest exponents for $(p - p_0)$, since all non-principal minors vanish and have zeros of arbitrary order at $p = p_0$. Furthermore, (7) is exactly the least exponent of $(p - p_0)$ in any b-rowed minor of ψZ^* since the principal minors are simple products. Hence (7) and (8) are equal, for any $b = 1, 2, \cdots, n$. Therefore the exponents in the normal form of Z^* are exactly those of Z^* and

$$S(Z, p_0) = S(Z^*, p_0) = [\sigma_1\,,\,\sigma_2\,,\,\cdots,\,\sigma_n].$$

Q.E.D.

5.3. *Definition:* Let

$$p = T(q) = \frac{\alpha q + \beta}{\gamma q + \delta}$$

be a non-singular bi-rational transformation from the q-sphere to the

p-sphere. Denote its inverse by

$$q = T^{-1}(p).$$

Given a rational $Z(p)$ the matrix

$$Z_1(q) = Z(T(q))$$

is rational in q.

For any p_0 such that $T^{-1}(p_0) \neq \infty$, we define

$$S_T(Z, p_0) = S(Z_1, T^{-1}(p_0)).$$

5.31 *Theorem:* If p_0 and $T^{-1}(p_0)$ are both finite,

$$S_T(Z, p_0) = S(Z, p_0).$$

Proof: Let $W_1(q)$ be the normal form of

$$Z_1(q) = Z(T(q)).$$

We have

$$W_1(q) = A(q)Z_1(q)B(q).$$

Consider

$$W_2(p) = W_1(T^{-1}(p)) = A(T^{-1}(p))Z(p)B(T^{-1}(p)).$$

Here the pre- and post factors of $Z(p)$ are rational, finite, and non-singular at p_0. Hence by 5.26

$$S(W_2, p_0) = S(Z, p_0). \tag{1}$$

Let $q_0 = T^{-1}(p_0)$. It is then easily computed that the inverse transformation $T^{-1}(p)$ takes the form

$$q - q_0 = \frac{a(p - p_0)}{b(p - p_0) + 1}, \qquad a \neq 0.$$

Any given diagonal element of $W_1(q)$ is of the form

$$(q - q_0)^\epsilon R(q),$$

where ε may have any sign, and $R(q)$ is rational, finite, and not zero at q_0. The corresponding diagonal element of $W_2(p)$ is then

$$(p - p_0)^\epsilon \left(\frac{a}{b(p - p_0) + 1} \right)^\epsilon R_1(p),$$

where $R_1(p) = R(T^{-1}(p))$, and the factor multiplying $(p - p_0)^\epsilon$ is again

finite and not zero at p_0. The exponents of $(p - p_0)$ in the elements of $W_2(p)$ are therefore exactly the exponents of $q - q_0$ in the elements of $W_1(q)$. From 5.29, then

$$S(W_2, p_0) = S(W_1, q_0).$$

This with (1) and the definition 5.3 proves the theorem.

5.32 *Definition*: Given any p_0, let $p = T(q)$ be a non-singular bi-rational transformation such that $q_0 = T^{-1}(p_0) \neq \infty$. We define $S^*(Z, p_0)$ by

$$S^*(Z, p_0) = S_T(Z, p_0).$$

5.33 *Lemma*: $S^*(Z, p_0)$ is independent of the T chosen to define it.

Proof: Consider $q = T^{-1}(p)$ and $r = U^{-1}(p)$, each such that p_0 is mapped on a finite point. Then by definition

$$S_T(Z, p_0) = S(Z_1, q_0),$$

$$S_U(Z, p_0) = S(Z_2, r_0),$$

where

$$q_0 = T^{-1}(p_0), \qquad r_0 = U^{-1}(p_0),$$

$$Z_1(q) = Z(T(q)),$$

$$Z_2(r) = Z(U(r)).$$

Now $r = U^{-1}(T(q)) = V(q)$, say, and r_0 and q_0 are finite. Hence by 5.31

$$S_V(Z_2, r_0) = S(Z_2, r_0) = S_U(Z, p_0). \tag{2}$$

But by definition

$$S_V(Z_2, r_0) = S(Z_3, V^{-1}(r_0)) = S(Z_3, q_0) \tag{3}$$

where

$$Z_3(q) = Z_2(V(q))$$

But

$$Z_2(V(q)) = Z(U(U^{-1}(T(q)))) = Z(T(q)) = Z_1(q).$$

Hence

$$S(Z_3, q_0) = S(Z_1, q_0) = S_T(Z, p_0).$$

This, with (2) and (3), proves the lemma.

5.34 *Theorem*: Theorems 5.26, 5.27, and 5.29 hold for S^* without the restriction that p_0 be finite.

Proof: Let $q_0 = T^{-1}(p_0) \neq \infty$. For 5.26 we have

$$S^*(Z, p_0) = S(Z_1, q_0) \geq S(F_1Z_1, q_0) = S^*(FZ, p_0)$$

where the equalities are by definition and the inequality is 5.26 applied to matrices rational in q, since

$$F_1(q) = F(T(q))$$

is by hypothesis finite at q_0. The remaining conclusion of 5.26 follows similarly. The proofs of 5.27 and 5.29 are equally simple.

5.35 *Theorem:* If we extend 5.3 to S^* by defining

$$S_T^*(Z, p_0) = S^*(Z_1, T^{-1}(p_0)),$$

then 5.31 holds for S^* with no restrictions on p_0 or $T^{-1}(p_0)$.

Proof: By their definitions,

$$S_T^*(Z, p_0) = S^*(Z_1, T^{-1}(p_0)) = S_U(Z_1, T^{-1}(p_0)), \tag{4}$$

where U is such that $U^{-1}(T^{-1}(p_0))$ is finite. But

$$S_U(Z_1, T^{-1}(p_0)) = S(Z_2, U^{-1}(T^{-1}(p_0))) \tag{5}$$

where

$$Z_2(r) = Z_1(U(r)) = Z(T(U(r))).$$

Let $V(r) = T(U(r))$. Then, by definitions,

$$S(Z_2, U^{-1}(T^{-1}(p_0))) = S_V(Z, p_0) = S^*(Z, p_0), \tag{6}$$

since $V^{-1}(p_0) = U^{-1}(T^{-1}(p_0))$ is finite. The theorem follows from (4), (5), and (6).

5.4 *Definition:* Let

$$S^*(Z, p_0) = [\gamma_1, \gamma_2, \cdots, \gamma_n].$$

Define

$$\delta(Z, p_0) = \gamma_1 + \gamma_2 + \cdots + \gamma_n,$$

$$\delta(Z) = \sum \delta(Z, p_0),$$

where the latter summation is over all poles p_0 of $Z(p)$, including $p_0 = \infty$. This $\delta(Z)$ is the degree of Z for which we must establish the properties claimed in 2.11 through 2.17. These properties will be demonstrated in 5.41 through 5.45, in numerical order, saving 2.13, which is deferred to 5.46.

5.41 Clearly $\delta(Z)$ is an integer and non-negative. If $\delta(Z) = 0$, then every γ at every p_0 is zero. Hence no p_0, not even ∞, is a pole of Z. Hence each element of $Z(p)$ is a constant. This establishes 2.11 and 2.12.

5.42 Suppose

$$Z(p) = Z_1(p) + Z_2(p)$$

where each $Z_i(p)$ is finite at every pole of the other. The poles of $Z(p)$ are then exactly the poles $p_0^{(1)}$ of Z_1 and those $p_0^{(2)}$ of Z_2. At each pole, 5.27 applies in the enlarged sense of 5.34, so

$$\delta(Z, p_0^{(i)}) = \delta(Z_i, p_0^{(i)}).$$

Breaking the sum defining $\delta(Z)$ into sums over the $p_0^{(1)}$ and $p_0^{(2)}$ proves that

$$\delta(Z) = \delta(Z_1) + \delta(Z_2).$$

This is 2.14.

5.43 If

$$Z(p) = f(p)R,$$

where R is a constant matrix, then the normal form of $Z(p)$ is $f(p)$ times a diagonal matrix of the same rank as R (5.15). 2.15 then follows at once.

5.44 If

$$Z_1(p) = AZ(p)B,$$

where A and B are constant and non-singular, the poles of $Z_1(p)$ and $Z(p)$ are the same. At each, 5.26 applies in the enlarged sense of 5.34. Therefore $\delta(Z_1) = \delta(Z)$. This is 2.16.

5.45 If $Z_1(p)$ is $Z(p)$ bordered by zeros, they have the same poles. One verifies at once from 5.11 that the normal form of $Z_1(p)$ is that of $Z(p)$ bordered by zeros. Since also $Z_1(T(q))$ is $Z(T(q))$ bordered by zeros, it follows that

$$S^*(Z_1, p_0) = S^*(Z, p_0)$$

at every pole, whence $\delta(Z_1) = \delta(Z)$. This is 2.17.

5.46 We must prove that if $Z(p)$ is non-singular, then

$$\delta(Z) = \delta(Z^{-1})$$

Proof: Choose a bi-rational transformation $p = T(q)$ such that at

$p = T(\infty)$ both of $Z(p)$ and $Z^{-1}(p)$ are finite. Let

$$Z_1(q) = Z(T(q)).$$

Then

$$Z_1^{-1}(q) = Z^{-1}(T(q)).$$

Let $W_1(q)$ be the normal form of $Z_1(q)$, with diagonal elements

$$\frac{e_k(q)}{\psi_k(q)}$$

in lowest terms. Since $Z_1(q)$ is of rank n, none of these vanish identically.

We first claim that $\delta(Z) = \delta(Z_1)$. The poles p_0 of Z are exactly the points

$$p_0 = T(q_0)$$

where q_0 runs over the poles of Z_1. At each pole,

$$S^*(Z, p_0) = S_T^*(Z, p_0) = S^*(Z_1, q_0)$$

by 5.35. Hence $\delta(Z, p_0) = \delta(Z_1, q_0)$ and the result follows by addition. Similarly, then, $\delta(Z^{-1}) = \delta(Z_1^{-1})$.

Next we assert that $\delta(Z_1)$ is just the degree of the polynomial

$$\psi_1(q)\psi_2(q) \cdots \psi_n(q).$$

For $\delta(Z_1, q_0)$ is the exponent of $(q - q_0)$ in this polynomial, and the zeros of this polynomial are exactly the poles of $Z_1(q)$.

We observe that if

$$W_1(q) = A(q)Z_1(q)B(q),$$

then

$$W_1^{-1}(q) = B^{-1}(q)Z_1^{-1}(q)A^{-1}(q).$$

This then is the result of polynomial operations on $Z_1^{-1}(q)$, and has diagonal elements

$$\frac{\psi_k(q)}{e_k(q)}. \tag{1}$$

Clearly by arranging these in reverse order, we have a normal form. This is 5.13. Hence the functions (1) are the diagonal elements of the normal form of $Z_1^{-1}(q)$. The argument above applied to $Z_1^{-1}(q)$ then shows that $\delta(Z_1^{-1})$ is the degree of

$$e_1(q) \cdots e_n(q).$$

Finally, we note the determinant relation

$$| W_1(q) | = | A(q) || Z_1(q) || B(q) | = (\text{constant}) \times | Z_1(q) | ,$$

since the determinants of A and B are constant. Now $Z_1(q)$ has no pole at $q = \infty$, hence its determinant is finite there. The same is true of $Z_1^{-1}(q)$, so indeed

$$| Z_1(\infty) | = 0.$$

Now by direct calculation

$$| W_1(q) | = \frac{e_1(q) \cdots e_n(q)}{\psi_1(q) \cdots \psi_n(q)}.$$

Since this is finite and not zero at $q = \infty$, the numerator and denominator are of the same degree. Hence

$$\delta(Z) = \delta(Z_1) = \text{degree } (\Pi\psi_k) = \text{degree } (\Pi e_k) = \delta(Z_1^{-1}) = \delta(Z^{-1}).$$

VI. THE EXACT COUNT OF REACTIVE ELEMENTS

6.0 We showed in the inductive argument of 4.07 that the Brune process constructs a realization for a given $Z(p)$ which uses exactly $\delta(Z)$ reactive elements. To establish 2.18, we must still show that no network with fewer than $\delta(Z)$ reactive elements can do this. To prove this, we shall show that if $Z(p)$ is the impedance matrix of a network containing x reactive elements, then

$$\delta(Z) \leq x. \tag{1}$$

We shall, in fact, in this Section show somewhat more than (1). The demonstration of (1) requires enough calculation that is as easy to prove the following extension of 2.18.

6.01 *Theorem:* Given any linear correspondence L, (I, 6.2), which PR, (I, 16.71), there exists a number $\delta(L)$ such that
  (i) The realization process outlined in (I, 8) and 4.07 of this Part constructs with $\delta(L)$ reactive elements a network realizing a member of the Cauer class of L.
  (ii) If L is the correspondence established by the Cauer class of a physical network which contains x reactive elements, then

$$\delta(L) \leq x.$$

The proof is divided among the remaining paragraphs of this Section. We maintain here a strict distinction between geometric objects and their concrete coordinate representations.

6.02 We observe at once that if a $\delta(L)$ exists satisfying (i) and (ii), then it must be unique because it is exactly the minimum number of reactive elements required to realize any representative of the Cauer class L. No particular pains then need be taken as we go along to verify that the value of $\delta(L)$ arrived at is in fact independent of the mode of defining it.

6.1 Given a PR geometrical linear correspondence L between $\mathbf{V}$ and $\mathbf{K}$, there is a frame which reduces L in the sense of (I, 13.02). In this frame we have the dual decomposition

$$\mathbf{V} = \mathbf{V}_{L0} \oplus \mathbf{V}_2 \oplus \mathbf{V}_1$$

$$\mathbf{K} = \mathbf{K}_1 \oplus \mathbf{K}_2 \oplus \mathbf{K}_{L0}$$

in which each subspace is real and spanned by selected basis vectors. Furthermore,

$$\mathbf{V}_L = \mathbf{V}_{L0} \oplus \mathbf{V}_2 ,$$

$$\mathbf{K}_L = \mathbf{K}_2 \oplus \mathbf{K}_{L0} ,$$

Finally, if r is the dimension of $\mathbf{V}_2$ and $\mathbf{K}_2$, there is an $r \times r$ PR matrix $[Z_1(p)]$ such that, when

$$[v_2 , k_2] \ \epsilon \ L(p)$$

and

$$v_2 \ \epsilon \ \mathbf{V}_2 , \qquad k_2 \ \epsilon \ \mathbf{K}_2 ,$$

then

$$[v_2] = [Z_1(p)][k_2].$$

Here the r-tuples are those representing v_2 and k_2 as elements of $\mathbf{V}_2$ and $\mathbf{K}_2$ in the chosen frame.

6.11 *Definition:* We define $\delta(L)$ by

$$\delta(L) = \delta([Z_1]),$$

where $[Z_1(p)]$ is the matrix described above.

6.12 This number $\delta(L)$ is the number of reactive elements used when the Brune process is applied to realize $[Z_1(p)]$. (This is 4.07). Then, however, by the argument of (I, 8.5), the representative $[L]$ of L in the particular frame in question can be realized by adjoining open and short circuits to a realization of $[Z_1(p)]$. This operation adds no new reactive elements. Neither does the operation of converting $[L]$ to any

Cauer equivalent $[L]_1$ by the use of ideal transformers. Therefore the particular $\delta(L)$ we have defined—which depends for its definition upon a somewhat arbitrary choice of coordinate frame—satisfies (i) of 6.01.

6.2 *Lemma:* Let L be a PR geometrical linear correspondence between $\mathbf{K}$ and $\mathbf{V}$, and M another between spaces $\mathbf{J}$ and $\mathbf{U} = \mathbf{J}^*$ obtained by restricting L as in (I, 18). Then

$$\delta(M) \leq \delta(L).$$

Proof: We use the results and notation of (I, 18). In particular, C is a real constant operator from $\mathbf{J}$ to $\mathbf{K}$, C^* its adjoint from $\mathbf{V}$ to $\mathbf{U}$, and the pairs of $M(p)$ are those pairs

$$[u, j]$$

such that

$$u = C^*v \qquad \text{and} \qquad [v, Cj] \ \epsilon \ L(p).$$

Choose a frame in $\mathbf{V}$ and $\mathbf{K}$ which reduces L as in 6.1. We recall that $\mathbf{J}_M$ consists of all vectors $j \ \epsilon \ \mathbf{J}$ such that $Cj \ \epsilon \ \mathbf{K}_L$ (I, 18.31). Let $\mathbf{J}_2$ consist of all $j \ \epsilon \ \mathbf{J}$ such that

$$Cj \ \epsilon \ \mathbf{K}_2 \,.$$

Let $\mathbf{J}_3$ consist of all $j \ \epsilon \ \mathbf{J}$ such that

$$Cj \ \epsilon \ \mathbf{K}_{L0} \,.$$

Then $\mathbf{J}_2$ and $\mathbf{J}_3$ are disjoint and both are subspaces of $\mathbf{J}_M$. We can therefore write

$$\mathbf{J}_M = \mathbf{J}_2 \oplus \mathbf{J}_3 \oplus \mathbf{J}_4 \,,$$

after a suitable choice of $\mathbf{J}_4$.

We now claim that

$$\mathbf{J}_3 \oplus \mathbf{J}_4 \subset \mathbf{J}_{M0} \,. \tag{1}$$

For we have if $j \ \epsilon \ \mathbf{J}_M$ that, uniquely,

$$j = j_2 + j_3 + j_4 \,,$$

where $j_i \ \epsilon \ \mathbf{J}_i$. Therefore

$$Cj = Cj_2 + Cj_3 + Cj_4$$

where by construction $Cj_2 \ \epsilon \ \mathbf{K}_2$, $Cj_3 \ \epsilon \ \mathbf{K}_{L0}$, and, necessarily, then $Cj_4 = 0$. If $j_2 = 0$, therefore, $Cj \ \epsilon \ \mathbf{K}_{L0}$ and

$$[0, Cj] \ \epsilon \ L(p).$$

Therefore

$$[C^*0, j] = [0, j] \,\epsilon\, M(p).$$

this proves (1).

We can now write

$$\mathbf{J}_M = \mathbf{J}_{21} \oplus \mathbf{J}_{20} \oplus \mathbf{J}_0 \qquad (2)$$

where

$$
\begin{aligned}
\mathbf{J}_2 &= \mathbf{J}_{21} \oplus \mathbf{J}_{20}, \\
\mathbf{J}_{20} &= \mathbf{J}_2 \cap \mathbf{J}_{M0}, \\
\mathbf{J}_0 &= \mathbf{J}_3 \oplus \mathbf{J}_4, \\
\mathbf{J}_{M0} &= \mathbf{J}_{20} \oplus \mathbf{J}_0.
\end{aligned}
\qquad (3)
$$

Choosing an arbitrary $\mathbf{J}_5$ disjoint from $\mathbf{J}_M$, we can write, using (2) and (3),

$$\mathbf{J} = \mathbf{J}_5 \oplus \mathbf{J}_{21} \oplus \mathbf{J}_{M0}, \qquad (4)$$

where

$$\mathbf{J}_M = \mathbf{J}_{21} \oplus \mathbf{J}_{M0}.$$

Using the arguments of (I, 12.3), we find that the decomposition of $\mathbf{U}$ dual to (4) is, because M is PR,

$$\mathbf{U} = \mathbf{U}_{M0} \oplus \mathbf{U}_{21} \oplus \mathbf{U}_3 \qquad (5)$$

where

$$\mathbf{U}_M = \mathbf{U}_{M0} \oplus \mathbf{U}_{21}.$$

As in (I, 12.3) we can now introduce a frame appropriate to the decomposition indicated in (4) and (5) and obtain a matrix $[Z_{21}(p)]$ describing the correspondence between $\mathbf{J}_{21}$ and $\mathbf{U}_{21}$. Say this is an $m \times m$ matrix, m being the dimension of $\mathbf{J}_{21}$. We can define

$$\delta(M) = \delta([Z_{21}]).$$

Let $\mathbf{J}_2$ have dimension m_1. By (3), if we border $[Z_{21}(p)]$ by $m_1 - m$ rows and columns of zeros, to obtain an $m_1 \times m_1$ matrix $[Z_2(p)]$, we can interpret $[Z_2(p)]$ as follows:

Given $j \,\epsilon\, \mathbf{J}_2$, it can be represented by an m_1-tuple $[j]$ in the basis in that subspace. Then the m_1-tuple

$$[u] = [Z_2(p)][j] \qquad (6)$$

represents in the dual basis in $(\mathbf{J}_2)^0$ a vector $u \in \mathbf{U}_{21}$ such that

$$[u, j] \in M(p).$$

Now this u necessarily is of the form

$$u = C^*v, \tag{7}$$

where

$$[v, Cj] \in L(p).$$

But $j \in \mathbf{J}_2$, so $Cj \in \mathbf{K}_2$, so v may be taken to be an element of $\mathbf{V}_2$, with components

$$[v] = [Z_1(p)][Cj] \tag{8}$$

in the basis therein.

We have bases now in $\mathbf{V}$, $\mathbf{K}$, $\mathbf{U}$, and $\mathbf{J}$, each of which has a set of basis vectors spanning, respectively, $\mathbf{V}_2$, $\mathbf{K}_2$, $(\mathbf{J}_2)^0$, and $\mathbf{J}_2$. By definition of $\mathbf{J}_2$, and by (7) and (8), C operates from $\mathbf{J}_2$ to $\mathbf{K}_2$, and C^* from $\mathbf{V}_2$ to $(\mathbf{J}_2)^0$. Hence in these respective bases C and C^* may be represented by $m_1 \times m_1$ matrices. In these bases then, from (7) and (8),

$$[u] = [C^*][v] = [C^*][Z_1(p)][C][j].$$

Comparing this with (6), we have

$$[Z_2(p)] = [C^*][Z_1(p)][C].$$

Hence by definitions and 5.26,

$$\delta(M) = \delta([Z_2]) \leq \delta([Z_1]) = \delta(L).$$

This is the assertion to be proved.

6.3 We can now turn to (ii) of 6.01. We follow the synthesis procedure of (I, 19), as modified in the remarks of 3.2.

Consider a network constructed from x reactive elements, r resistors, and some ideal transformers. As in (I, 19.2), the synthesis of this network begins by juxtaposing the $r + x$ two poles and the ideal transformers, all as separate devices. The correspondence $[L]$ established by this juxtaposition is exhibited in (I, 19.2) as one described by a diagonal matrix $[Z_d(p)]$ juxtaposed with one described by certain ideal transformers. A frame which reduces this correspondence as in 6.1 can be found by a change of basis wholly within those subspaces in which the ideal transformers operate. Hence the degree $\delta(L)$ of this correspondence in exactly $\delta([Z_d])$ which, by 5.29, is x.

Now let $[M]$ be the concrete linear correspondence established by the

network to be synthesized. Then (I, 19.3, 19.4) show that $[M]$ is obtained by two successive restrictions upon $[L]$. Hence by 6.2

$$\delta(M) \le \delta(L) = x.$$

Q.E.D.

BIBLIOGRAPHY

1. M. Bayard, "Synthèse des Réseaux Passifs a un Nombre Quelconque de Paires de Bornes Connaissant Leurs Matrices d'Impedance ou d'Admitance," *Bulletin, Société Francaise des Electriciens,* **9,** 6 series, Sept. 1949.
2. O. Brune, *Jour. Math. and Phys., M.I.T.,* **10,** Oct. 1931, pp. 191–235.
3. W. Cauer, *Ein Reaktanztheorem, Sitzungsberichte Preuss. Akad. Wissenschaft,* Heft 30/32, 1931.
4. W. Cauer, "Die Verwirklichung von Wechselstromswiderständen vorgeschriebener Frequenzabhängigkeit," *Archiv für Elektrotechnik,* **17,** 1926.
5. W. Cauer, "Ideale Transformatoren und Lineare Transformationen," *Elektrische Nachrichten-Technik,* **9,** May, 1932.
6. S. Darlington, *Journal of Mathematics and Physics, M.I.T.,* **18,** No. 4, Sept. pp. 257–353.
7. R. M. Foster, *Bell System Tech. J.,* April, 1924, pp. 259–267.
8. C. M. Gewertz, *Network Synthesis,* Baltimore, 1933.
9. P. R. Halmos, *Finite Dimensional Vector Spaces,* Princeton, 1942.
10. Y. Oono, "Synthesis of a Finite 2n-Terminal Network by a Group of Networks Each of Which Contains Only One Ohmic Resistance," *Jour. Inst. Elec. Comm. Eng. of Japan,* March, 1946. Reprinted in English in the *Jour. Math. and Phys., M.I.T.,* **29,** Apr., 1950.
11. Y. Oono, "Synthesis of a Finite 2n-Terminal Network as the Extension of Brune's Theory of Two-Terminal Network Synthesis," *Jour. Inst. Elec. Comm. Eng. of Japan,* Aug., 1948.
12. J. L. Synge, "The Fundamental Theorem of Electrical Networks," *Quarterly of Applied Mathematics,* **9,** No. 2, July, 1951.
13. R. Bott, and R. J. Duffin, "Impedance Synthesis without the Use of Transformers," *Jour. Appl. Phys.,* **20,** Aug., 1949, p. 816.
14. H. W. Bode, *Network Analysis and Feedback Amplifier Design,* New York, 1945.
15. M. Bôcher, *Introduction to Higher Algebra,* New York, 1930.
16. C. C. MacDuffee, *An Introduction to Abstract Algebra,* New York, 1940.

Abstracts of Bell System Technical Papers*
Not Published in This Journal

The Effect of Inhomogeneities on the Electrical Properties of Diamond.
A. J. Ahearn[1]. *Phys. Rev.*, **84**, pp. 798–802, Nov. 15, 1951.

To account for the non-uniformities in the electrical properties of diamond, particularly those observed in bombardment conduction, the proposal is made that the well-known lattice imperfections are not distributed homogeneously in the physical crystal, and that the resulting fluctuations in the height of the energy bands relative to the Fermi level might produce interspersed "pools of mobile charge" separated by barriers within the diamond. These pools and barriers should lead to dielectric losses at high frequencies. A single conducting channel, in series with a barrier, could be represented by a series resistance R_s and capacity C_s or by the equivalent parallel resistance R_p and capacity C_p.

With some, but not all, diamonds measurable dielectric losses at 70 mc/sec were observed. R_p varied from 5×10^6 ohms, the limit of measurement, to 4×10^5 ohms. Furthermore, the proposed model suggests that, in some cases, these barriers might be sufficiently lowered to establish a dc conducting channel all the way through a crystal. With a few of the lossy diamonds precisely this phenomenon of "high conduction" has been observed, in which a resistance of the order of a megohm is obtained with a dc voltage applied. This current appears abruptly in time but it lags behind the application of the voltage. This lag is influenced by irradiation with light or alpha-particles or by previous treatment.

The proposed pools of mobile charge are a sufficient but not necessary description of the dielectric loss observations, but the high conduction phenomenon lends further support to this idea of conducting channels with barriers in lossy diamonds. Such localized conducting channels would introduce inhomogeneities into an otherwise uniform electric field applied across an insulator. In bombardment conduction, measurements of counting efficiency could be very sensitive to field inhomogeneities.

Under alpha-particle bombardment a large variation in counting efficiency over the surface of typical diamonds is shown. In a group of 20 diamonds, most of those that exhibited definite losses also had high (≥ 25 per cent) counting efficiencies in some region, and the majority of the remainder had low counting efficiencies. These experiments lend further support to the suggestion that in-

---

homogeneous fields at least partially account for the inhomogeneities in bombardment conduction.

Serious errors in the normal estimates of range and mobility of electrons or holes in insulators can be introduced by neglecting these field inhomogeneities.

Diffusion in Alloys and the Kirkendall Effect. J. BARDEEN[1] and C. HERRING[1]. Pp. 87–111. *Am. Soc. for Metals.* Atom movements; a seminar ... held during the thirty-second National Metal Congress and Exposition, Chicago, Oct. 21–27, 1950. Cleveland, Ohio, Am. Soc. for Metals, 1951. 240 p.

Some Roots of an Equation Involving Bessel Functions. B. P. BOGERT[1]. *Jl. Math. Phys.*, **30,** pp. 102–105, July, 1951. (Monograph 1903).

Creep Test Methods for Determining Cracking Sensitivity of Polyethylene Polymers. W. C. ELLIS[1] and J. D. CUMMINGS[1]. *A.S.T.M. Bull.*, No. 178, pp. 47–49, Dec., 1951.

Conventional creep testing methods for evaluating the cracking sensitivity of polyethylene polymers are described. The tests show that sensitivity to cracking in the presence of an active agent decreases with increasing average molecular weight of the polymer. For a given stress condition and environment, there appears to be a threshold value of stress and strain for the occurrence of cracking.

Observer Reaction to Video Crosstalk. A. D. FOWLER[1]. *J. Soc. Motion Picture and Television Engrs.*, **57,** pp. 416–424, Nov., 1951. (Monograph 1928).

Presented here are results of tests to determine how much video crosstalk can be tolerated in black-and-white television pictures. Experienced observers viewed a television picture and rated the disturbing effects of controlled amounts of crosstalk from another video system. Crosstalk coupling was simulated by a network which permitted changes in frequency characteristic as well as in coupling loss. Tolerable limits for crosstalk coupling are derived from the test results.

Mass Spectrometric Studies of Molecular Ions in the Noble Gases. J. A. HORNBECK[1] and J. P. MOLNAR[1]. *Phys. Rev.*, **84,** pp. 621–625, Nov. 15, 1951.

Molecular ions of the rare gases (He_2^+, Ne_2^+, A_2^+, Kr_2^+, and Xe_2^+) produced by electron impact at gas pressures from 10^{-4} to 10^{-2} mm Hg have been studied with a small mass spectrometer. The ion intensity increased linearly with electron current and with the square of the gas pressure. The form of the ionization versus electron energy curves resembles closely curves of excitation probability by electron collision. The appearance potentials of the molecular ions were less

---

[1] Bell Telephone Laboratories

than those of the atomic ions by $1.4^{+0.7}_{-0.2}$ volts in He, $0.7^{±0.7}_{0.3}$ volt in Ne, $0.7^{±0.7}_{0.2}$ volt in A, $0.7^{+0.7}_{-0.3}$ volt in Kr. These results can be interpreted, we believe, only by assuming that the process of formation of the molecular ions observed in this experiment is, using helium as an example, an excitation by electron impact, He + e + K.E. → He* + e, followed by the collision process, He* + He → He_2^+ + e, where He* stands for a helium atom raised to a high-lying excited state. Our results differ from those of Arnot and M'Ewen on helium particularly in that they reported the appearance potential low enough to permit metastable atoms to form molecular ions.

The Drift Velocities of Molecular and Atomic Ions in Helium, Neon, and Argon. J. A. HORNBECK[1]. *Phys. Rev.*, **84**, pp. 615–620, Nov. 15, 1951.

Drift velocity measurements as a function of E/p_0, the ratio of field strength to normalized gas pressure, are presented for atomic and molecular ions of He, Ne, and A in their respective parent gases. Identification of the molecular ions is based upon the time resolution of the apparatus and the dependence of ion concentration on pressure, applied voltage, and gas purity. Extrapolation of the low field measurements to zero field yields mobility values for atomic ions, μ_0 (He$^+$) = 10.8 cm^2/volt sec, μ_0 (Ne$^+$) = 4.4, and μ_0 (A$^+$) = 1.63 in good agreement with theory: Massey and Mohr compute μ_0 (He$^+$) = 11, and Holstein gives μ_0 (Ne$^+$) = 4.1 and μ_0 (A$^+$) = 1.64. Drift velocity data at low field for the molecular ions agree within experimental error with data of Tyndall and Powell (He), and Munson and Tyndall (Ne and A), which they assigned to atomic ions. A qualitative description in terms of ion-atom interaction forces is given for the observed field variation of the atomic ion drift velocities up to high E/p_0.

Checking Analogue Computer Solutions. E. LAKATOS[1]. *Proc. Inst. Radio Engrs.*, **39**, p. 1571, Dec., 1951.

Experimental Heat Contents of SrO, BaO, CaO, BaCO₃ and SrCO₃ at High Temperatures. Dissociation Pressures of BaCO₃ and SrCO₃. J. J. LANDER[1]. *J. Am. Chem. Soc.*, **73**, pp. 5794–5797, Dec., 1951. (Monograph 1930).

The high temperature heat contents of SrO, BaO, CaO, BaCO₃ and SrCO₃ have been measured using the "drop" method. Values have been obtained for the heats of the transitions of the carbonates. The dissociation pressures of the carbonates have been measured to pressures below 0.1 mm and values calculated for lower pressures from the observed heat contents and observed dissociation pressures at higher temperatures.

Electron-Hole Production in Germanium by Alpha-Particles. K. G. McKAY[1]. *Phys. Rev.*, **84**, pp. 829–832, Nov. 15, 1951.

The number of electron-hole pairs produced in germanium by alpha-particle

---

[1] Bell Telephone Laboratories

bombardment has been determined by collecting the internally produced carriers across a reverse-biased *n-p* junction. No evidence is found for trapping of carriers in the barrier region. Studies of individual pulses show that the carriers are swept across the barrier in a time of less than 2×10^{-8} sec. The counting efficiency is 100 per cent. The energy lost by an alpha-particle per internally produced electron-hole pair is 3.0 ± 0.4 ev. The difference between this and the energy gap is attributed to losses to the lattice by the internal carriers. It is concluded that recombination due to columnar ionization is negligible in germanium.

The n-p-n *Junction as a Model for Secondary Photoconductivity.* K. G. McKay[1]. *Phys. Rev.*, **84**, pp. 833–835, Nov. 15, 1951.

A germanium *n-p-n* junction with the *p* region floating, has been subjected to alpha-particle bombardment. The transient currents resulting from individual incident alphas have been studied. This enables one to study the rate of decay of excess holes in the *p*-region. This decay time appears to increase with applied bias, pass through a maximum, and eventually approach a constant value. The total charge flowing across the unit, as a result of the bombardment by a single alpha-particle, may become large; quantum yields of greater than 60 have been observed. The unit possesses many of the important characteristics of materials which exhibit "secondary photoconductivity." It is concluded that various forms of *n-p-n* barriers must therefore play an important role in such materials and that their understanding can be greatly facilitated by studies of *n-p-n* barriers in germanium.

Frequency Detection and Speech Formants. E. Peterson[1]. *Acoustical Soc. Am., Jl.*, **23**, pp. 668–674, Nov., 1951.

This study is aimed primarily at evaluating the utility of axis-crossing detectors in tracking speech formants. Detectors of the usual type are found subject to an error, fundamental in nature. To remove this source of error speech is modulated up in frequency as a single sideband before limiting and detecting processes are applied. Experimental results with this carrier type of detector on a small number of speech samples are presented, and compared with spectrograms. Conclusions are that the average axis-crossing rates cannot be trusted in general to follow specific formants, whether the speech is normal or differentiated. But when the formants are sufficiently localized by frequency selectivity, prospects of tracking the lower formants look promising.

Transistor Circuit Design. G. Raisbeck[1]. *Electronics*, **24**, pp. 128–132, 134, Dec., 1951. (Monograph 1932).

How to derive amplifier, oscillator, modulator and multi-vibrator transistor circuits from known vacuum-tube circuits. Technique, known as duality, is explained in detail and may be applied to any complex vacuum-tube circuit to find the corresponding transistor circuit.

Communication Theory—Exposition of Fundamentals. C. E. Shannon[1]. Pp. 44–47. General treatment of the problem of Coding. Pp. 102–104.

---

[1] Bell Telephone Laboratories

Great Britain. Ministry of Supply. Symposium on Information Theory. Report of Proceedings held . . . Royal Soc., Burlington House, Lond., Sept. 26–29, 1950.

On the Relation Between the Sound Fields Radiated and Diffracted by Plane Obstacles. F. M. WIENER[1]. *J. Acoust. Soc. Am.*, **23,** pp. 697–700, Nov., 1951.

In the past, acoustic diffraction and radiation problems have often been treated separately, although their intimate connection is clear from theory. In the case of plane piston radiators and plane rigid scatterers exposed to a perpendicularly incident plane wave, this connection becomes particularly simple and useful. It is easy to show that the radiated sound field is everywhere the same as the field scattered (diffracted) in the diffraction case, except for a factor of proportionality. It is also shown that the reaction of the medium on the radiator, as expressed by the mechanical radiation impedance, is equal to the force per unit incident pressure exerted on the same obstacle, held rigid as a scatterer, except for a factor of proportionality. By way of illustration, the foregoing principles are applied to the important case of the circular disk.

Magnetic Modulators. E. P. FELCH[1], V. E. LEGG[1], and F. G. MERRILL[1]. References. *Electronics*, **25,** pp. 113–117, Feb., 1952.

Conversion of low-level, low-frequency or dc signals to ac signals capable of being amplified by conventional means is accomplished by magnetic-amplifier-type device that combines high efficiency and reliability with extreme ruggedness.

Conservation of Nickel. G. R. GOHN[1]. *A.S.T.M., Bull.*, No. 179, p. 32, Jan., 1952.

The Mechanism of Electrolytic Rectification. H. E. HARING[1]. *Electrochem. Soc., Jl.*, **99,** pp. 30–37, Jan., 1952. (Monograph 1929).

An electrochemical theory is proposed for rectification, as exemplified by the tantalum (or aluminum) electrolytic rectifier and capacitor. A detailed consideration of the mechanism of formation of the oxide film which constitutes the rectification barrier leads to the conclusion that this barrier consists of an electrolytic polarization, in the form of a concentration gradient of excess metal ions, permanently fixed or "frozen" in position in an otherwise insulating matrix of electrolytically-formed oxide. The physical structure which has been described functions as (a) a current-blocking ionic space charge or (b) a current-passing electronic semiconductor, depending solely upon the direction of the applied voltage. The movement of electrons only is required. An explanation for breakdown of the barrier at excessively high voltages is suggested. This explanation may be applicable to dielectric breakdown of other kinds.

---

[1] Bell Telephone Laboratories

Nullification of Space-Charge Effects in a Converging Electron Beam by a Magnetic Field. M. E. HINES[1]. *Proc. Inst. Radio Engrs.*, **40**, pp. 61–64, Jan., 1952. (Monograph 1935).

This paper presents the conditions necessary for maintaining a uniformly converging conical electron beam in the presence of space charge. It is an extension of the Brillouin focusing condition to conical flow, requiring a converging rather than a uniform magnetic field. In this type of electron flow, the diverging effects of space charge are balanced against magnetic reaction forces for reasonably small cone angles of convergence. Though the balance of forces is exact only for infinitesimal angles, it is reasonably accurate for cones of half-angle as great as 10 degrees. The minimum beam size will be limited only by the effects of thermal velocities, by gun aberrations, and by the magnetic field obtainable.

Continuous Motion Picture Projector for Use in Television Film Scanning. A. G. JENSEN[1], R. E. GRAHAM[1], and C. F. MATTKE[1]. Bibliography. *J. Soc. Motion Picture and Television Engrs.*, **58**, pp. 1–21, Jan., 1952.

The projector used for this equipment drives a 35-mm motion picture film at the standard (nonintermittent) speed of 24 frame/sec and produces a television signal of 525 lines and 30 frames interlaced 2 to 1. The projector utilizes a system of movable plane mirrors mounted on a rotating drum and controlled by a single stationary cam. Vertical jitter in the television image is minimized by means of an electronic servo system operating on the film sprocket holes, resulting in a residual vertical motion of about 1/2000 of a picture height. A second electronic servo system is incorporated to suppress flicker. The combination of this scanner and a high-grade monitor is capable of producing a television picture with a resolution corresponding to about 8 mc and with good tone rendition over a range up to 200 to 1.

Low Temperature Polymorphic Transformation in WO_3. B. T. MATTHIAS[1] and E. A. WOOD[1]. *Phys. Rev.*, **84**, p. 1255, Dec. 15, 1951.

The Concentration of Molecules on Internal Surfaces in Ice. E. J. MURPHY[1]. *J. Chem. Phys.*, **19**, pp. 1516–1518, Dec., 1951.

In this paper the experimental expression for the "local conductivity" of ice is given. This expression has two terms, one of which has already been discussed and brought into close relation with the structure of ice, that is, with its heat of sublimation and its lattice constant. This paper brings out another relation, deriving it from the second term of the experimental expression. It is concluded from an analysis outlined here that the second term of the local conductivity gives the concentration of molecules in "internal surfaces". For the specimen of ice to which this method was applied the concentration of molecules on internal surfaces comes out as 1.03×10^{17} molecules/cc. This is proposed as a new method of studying imperfections (internal surfaces) in dielectric crystals, and one which seems to be well suited to this purpose. It gains its advantages from

---

[1] Bell Telephone Laboratories

the fact that it is not dependent upon the regularity of the imperfections, as in x-ray diffraction methods, or upon the connectivity of the system of internal surfaces, as in direct current condution.

Meditations on Physics Today. J. R. PIERCE[1]. *Phy. Today,* **5,** p. 3, Jan., 1952.

Stabilization of Dielectrics Operating Under Direct Current Potential. H. A. SAUER[1], D. A. McLEAN[1], and L. EGERTON[1]. *Ind. Eng. Chem.,* **44,** pp. 135–140, Jan., 1952.

[1] Bell Telephone Laboratories.

Contributors to this Issue

E. N. GILBERT, B.S., Queens College, 1943; Ph.D., Massachusetts Institute of Technology, 1948. M.I.T. Radiation Laboratory, 1944–46. Bell Telephone Laboratories, 1948–. Dr. Gilbert's first assignment was in a group studying information theory, and in 1949 he joined a group concerned with switching theory. Member of the American Mathematical Society.

I. L. HOPKINS, B.S., Massachusetts Institute of Technology, 1927; Bell Telephone Laboratories, 1927–. For eighteen years, Mr. Hopkins designed testing equipment and tested insulating materials. Right after World War II, he tested and developed special-purpose rubber compounds, and since 1948 he has been conducting research in the physical properties of polymers.

W. A. MALTHANER, B.E.E., Rensselaer Polytechnic Institute, 1937. Bell Telephone Laboratories, 1937–. Mr. Malthaner is currently engaged in research on new automatic telephone central-office systems, interoffice signaling systems, and subscriber dialing and supervisory arrangements. Until World War II, when he worked on the development of automatic fire control systems and fire control radar, Mr. Malthaner tested and developed central office circuits and switching systems. Associate of the American Institute of Electrical Engineers. Member of the Institute of Radio Engineers, Tau Beta Pi and Sigma Xi.

WARREN P. MASON, B.S. in E.E., University of Kansas, 1921; M.A., Ph.D., Columbia, 1928. Bell Telephone Laboratories, 1921–. Dr. Mason has been engaged in investigating the properties and applications of piezoelectric crystals, in the study of ultrasonics, and in mechanics. Fellow of the American Physical Society, Acoustical Society of America and Institute of Radio Engineers and member of Sigma Xi and Tau Beta Pi.

BROCKWAY MCMILLAN, B.S., Massachusetts Institute of Technology, 1936; Ph.D., Massachusetts Institute of Technology, 1939; Instructor of Mathematics, Massachusetts Institute of Technology, 1936–39; Procter

Fellow and Henry B. Fine Instructor in Mathematics, Princeton University, 1939–42; U.S.N.R., 1942–46, studying exterior ballistics of guns and rockets; Los Alamos Laboratory, spring 1946; Bell Telephone Laboratories, 1946–. Dr. McMillan has been engaged in mathematical research and consultation work. Member of American Mathematical Society, Institute of Mathematical Statistics, and A.A.A.S.

JAMES Z. MENARD, B.S., Arkansas State Teachers College, 1941. U. S. Army, 1941–46. Bell Telephone Laboratories, 1946–. Mr. Menard has been engaged in the development of magnetic recording equipment and audio equipment for telephone plant applications.

J. A. MORTON, B.S. in E.E., Wayne University, 1935; M.S., University of Michigan, 1936. Bell Telephone Laboratories, 1936–. Mr. Morton is currently in charge of the development of the transistor and other semi-conductor devices. In the past he has been concerned with research on coaxial cables, microwave amplifier circuits, radar receivers, and with vacuum tube development. He designed a microwave tube used in the New York-San Francisco microwave relay system. Member of the I.R.E., Eta Kappa Nu, Alpha Delta Psi, Mackenzie Honor Society, Phi Kappa Phi, and Sigma Xi.

H. EARLE VAUGHAN, B.S. in C.E., Cooper Union, 1933. Bell Telephone Laboratories, 1928–. Since World War II, Mr. Vaughan has been investigating switching systems and high speed signaling means. In the past he studied voice operated devices and fundamental effects of speech and noise on voice-frequency signaling systems. During World War II, he was engaged in government projects, conducting research on anti-aircraft computers and fire control radars.

SAMUEL D. WHITE, B.S. in E.E., Rutgers University, 1927; E.E., Rutgers University, 1932; Bell Telephone Laboratories, 1927–. Until 1939, Mr. White was a member of the acoustical research department. He then entered the switching apparatus development group and is currently studying some aspects of relay problems. Member of I.R.E., Acoustical Society of America, and Sigma Xi.